

Topics in Stereochemistry, Volume 17

Editors
Ernest L. Eliel
Samuel H. Wilen

JOHN WILEY & SONS

**TOPICS IN
STEREOCHEMISTRY**

VOLUME 17

ADVISORY BOARD

STEPHEN J. ANGYAL, *University of New South Wales, Sydney, Australia*

ALAN R. BATTERSBY, *Cambridge University, Cambridge, England*

GIANCARLO BERTI, *University of Pisa, Pisa, Italy*

F. ALBERT COTTON, *Texas A. & M University, College Station, Texas*

JOHANNES DALE, *University of Oslo, Oslo, Norway*

DAVID GINSBURG, *Technion, Israel Institute of Technology, Haifa, Israel*

JEAN-MARIE LEHN, *Collège de France, Paris, France*

JAN MICHALSKI, *Centre of Molecular and Macromolecular Studies,
Polish Academy of Sciences, Lodz, Poland*

KURT MISLOW, *Princeton University, Princeton, New Jersey*

MICHINORI ŌKI, *Tokyo University, Tokyo, Japan*

VLADIMIR PRELOG, *Eidgenössische Technische Hochschule, Zurich,
Switzerland*

GÜNTHER SNATZKE, *Ruhruniversität, Bochum, Federal Republic of
Germany*

JOHN B. STOTHERS, *University of Western Ontario, London, Ontario,
Canada*

HANS WYNBERG, *University of Groningen, Groningen, The Netherlands*

TOPICS IN

STEREOCHEMISTRY

EDITORS

ERNEST L. ELIEL

*Professor of Chemistry
University of North Carolina
Chapel Hill, North Carolina*

SAMUEL H. WILEN

*Professor of Chemistry
City College, City University of New York
New York, New York*

VOLUME 17

AN INTERSCIENCE® PUBLICATION

JOHN WILEY & SONS

New York • Chichester • Brisbane • Toronto • Singapore

An Interscience® Publication
Copyright © 1987 by John Wiley & Sons, Inc.

All rights reserved. Published simultaneously in Canada.

Reproduction or translation of any part of this work beyond that permitted by Section 107 or 108 of the 1976 United States Copyright Act without the permission of the copyright owner is unlawful. Requests for permission or further information should be addressed to the Permissions Department, John Wiley & Sons, Inc.

Library of Congress Catalog Card Number: 67-13943

ISBN 0-471-85282-1

Printed in the United States of America

10 9 8 7 6 5 4 3 2 1

INTRODUCTION TO THE SERIES

It is patently impossible for any individual to read enough of the journal literature so as to be aware of all significant developments that may impinge on his or her work, particularly in an area such as stereochemistry, which knows no topical boundaries. Stereochemical investigations may have relevance to an understanding of a wide range of phenomena and findings irrespective of their provenance. Because stereochemistry is important in many areas of chemistry, comprehensive reviews of high quality play a special role in educating and alerting the chemical community to new stereochemical developments.

The above considerations were reason enough for initiating a series such as this. In addition to updating information found in such standard monographs as *Stereochemistry of Carbon Compounds* (Eliel, McGraw-Hill, 1962) and *Conformational Analysis* (Eliel, Allinger, Angyal, and Morrison, Interscience, 1965; reprinted by American Chemical Society, 1981) as well as others published more recently, the series is intended also to deal in greater detail with some of the topics summarized in such texts. It is for this reason that we have selected the title *Topics in Stereochemistry* for this series.

The series is intended for the advanced student, the teacher, and the active researcher. A background of the basic knowledge in the field of stereochemistry is assumed. Each chapter is written by an expert in the field and, hopefully, covers its subject in depth. We have tried to choose topics of fundamental importance aimed primarily at an audience of inorganic and organic chemists but involved frequently with basic principles of physical chemistry and molecular physics, and dealing also with certain stereochemical aspects of biochemistry.

It is our intention to produce future volumes at intervals of one to two years. The editors will welcome suggestions as to suitable topics.

We are fortunate in having been able to secure the help of an international board of editorial advisors who have been of great assistance by suggesting topics and authors for several chapters and by helping us avoid, in so far as possible, duplication of topics appearing in other, related monograph series. We are grateful to the editorial advisors for this assistance, but the editors and authors alone must assume the responsibility for any shortcomings of *Topics in Stereochemistry*.

E. L. ELIEL
S. H. WILEN

PREFACE

In contrast to previous volumes, Volume 17 contains only three chapters. We shall not bore the reader with the circumstances that led to such brevity; it certainly is not because there is a lack of suitable material or an absence of activity in the field of stereochemistry. We hope that the quality of the chapters will make up for their lesser quantity.

The first chapter, by Mario Farina of the city of Milan, Italy, the former home of Giulio Natta and the place of gestation of many ideas in polymer stereochemistry, treats this subject in a comprehensive manner. There are other books dealing with the unraveling of the configuration of stereoregular polymers by nuclear magnetic resonance spectroscopy and there are edited collections dealing with the synthesis of optically active polymers. However, to the best of our knowledge, there is no other text where all these subjects relating to polymer stereochemistry are treated collectively. At a time when polymer chemistry is experiencing a resurgence, this collection of valuable information should be welcomed by practicing chemists from a wide variety of fields other than polymer science.

The second chapter, by T. B. Freedman and L. A. Nafie, on the stereochemical aspects of vibrational optical activity, deals with a subject that is just beginning to come of age. In contrast to the previous chapter, which reviews a mature field, this chapter is designed to introduce chemists at large to a relatively new stereochemical technique, which will probably become very useful for the determination of configuration and conformation.

The third chapter, by J. F. Stoddart, is concerned with a very "hot" subject, namely, the stereochemical aspects of crown ether chemistry. Many chapters have been written on this topic; Stoddart's concentrates on the synthesis of a variety of chiral crown ethers and surveys some of their uses in different areas of physical, chemical, and biological science.

Even though we continue to enjoy the help of an excellent group of editorial advisors, we invite our readers to send us suggestions for future chapters and authors.

ERNEST L. ELIEL
SAMUEL H. WILEN

*Chapel Hill, North Carolina
New York, New York
January 1987*

CONTENTS

THE STEREOCHEMISTRY OF LINEAR MACROMOLECULES	1
<i>by Mario Farina, Dipartimento di Chimica Organica e Industriale, Università di Milano, Milan, Italy</i>	
STEREOCHEMICAL ASPECTS OF VIBRATIONAL OPTICAL ACTIVITY	113
<i>by Teresa B. Freedman and Laurence A. Nafie, Department of Chemistry, Syracuse University, Syracuse, New York</i>	
CHIRAL CROWN ETHERS	207
<i>by J. Fraser Stoddart, Department of Chemistry, The University, Sheffield, United Kingdom</i>	
SUBJECT INDEX	289
CUMULATIVE INDEX, VOLUMES 1-17	301

**TOPICS IN
STEREOCHEMISTRY**

VOLUME 17

The Stereochemistry of Linear Macromolecules

MARIO FARINA

*Dipartimento di Chimica Organica e Industriale
Università di Milano
Milano, Italy*

I. Introduction	1
II. Stereoisomerism of Macromolecular Chains	3
A. Isotactic and Syndiotactic Polymers	4
B. Other Stereoregular Polymers	8
C. Nonconventional Structures	14
D. Microtacticity	18
III. The Contribution of NMR Spectroscopy to Macromolecular Stereochemistry	27
A. A Pioneering Research Problem: Poly(methyl methacrylate)	31
B. The Present Level of Spectral Analysis	34
IV. Conformational Analysis	42
A. Conformations of Crystalline Polymers	46
B. Disordered Conformations	52
C. New Methods and New Problems	59
V. Chirality in Polymers	66
A. Prediction of Chirality in Flexible Macromolecular Systems	67
B. Synthesis of Optically Active Polymers from Chiral Monomers	72
C. Asymmetric Polymerization	78
D. Properties and Uses of Optically Active Polymers	84
VI. Stereochemical Control During Polymerization	87
VII. Conclusions	93
Addendum	94
Acknowledgments	96
References	96

I. INTRODUCTION

The discovery of the polymerization processes promoted by transition metal catalysts and the foundation of macromolecular stereochemistry represents a major breakthrough in chemistry in the second half of this century. Since the first discoveries by Ziegler in Mülheim and Natta in Milan there has been an enormous development of fundamental and applied research that still continues

after more than 30 years (1). This is not the place to deliberate on the role played by this research in the development of the petrochemical and plastics industry during the 1960s and 1970s, nor is it the place to illustrate all the resultant benefits of scientific knowledge produced in many fields of chemistry (organometallic and coordination chemistry, homogeneous and heterogeneous catalysis, etc.). In the following pages I shall try to shed some light on only one aspect of this subject, namely, the impact that polymer chemistry has had on classic organic stereochemistry.

In brief, we can say that the study of macromolecular compounds has introduced a new dimension into organic stereochemistry. This is true not only in the spatial sense if one considers the shape of the macromolecule, but also in the time sense if one examines the process of polymerization and the transmission of stereoregularity and chirality within each macromolecule. Finally, the study of macromolecules has necessitated the introduction of concepts and methods (e.g., the statistical approach), which are usually not pertinent to the stereochemistry of low molecular weight compounds (4).

The aim of these pages is twofold: first, to fill the gap existing between the language and the experience of organic stereochemists and polymer chemists and second, to show how macromolecular stereochemistry can be discussed and defined using the concepts and criteria of fundamental stereochemistry. I shall also try to illustrate the role of the conformational analysis of polymers as a nodal point in determining structure-property relationships. From among the experimental techniques, greatest emphasis will be given to NMR spectroscopy, particularly ^{13}C NMR, in its most recent developments.

The reader will find no description of the many individual polymers studied. I have preferred to give major emphasis to the general aspects of the subject, illustrated in each instance by a few chosen examples.

Given the vastness of the subject matter I have limited myself to dealing with the structural (or static) aspects of macromolecular stereochemistry. An adequate treatment of the stereochemistry of polymerization, with specific regard to the polymerization of olefins and conjugated diolefins, would have occupied so much space and called for such a variety of additional information as to make this article excessively long and complex. I trust that others will successfully dedicate themselves to this task. However, the connection between polymer structure and polymerization mechanism is so important that the fundamentals of dynamic macromolecular stereochemistry cannot be completely ignored in this chapter.

Macromolecular stereochemistry has been treated in this series only once, more than 15 years ago, in a chapter by Goodman (6). Reference may be made to this review and to a contemporary treatise on the same subject, edited by Ketley (7), to know the state of the art at the end of the 1960s, at the end, that is, of the most creative era in the development of this field.

More recent books have been cited in the bibliography and may be useful to consult (8-19). Discussions of several stereochemical concepts are reported in the various editions of the IUPAC nomenclature rules (20, 21).

II. STEREOISOMERISM OF MACROMOLECULAR CHAINS

Among the points that distinguish macromolecular from low molecular weight compounds are the nonhomogeneity of their molecular dimension and structure. If two compounds of low molecular weight have different numbers of atoms or a different connectivity they inevitably constitute two different chemical entities. To the contrary, in a polymer sample, it is common to find molecules of varying sizes, some up to 10-20 times larger than others, or molecules equal in molecular weight but differing in detailed structure; this does not necessarily mean that they should be considered as different compounds.

With the exception of some compounds of biological origin, macromolecular compounds should be considered as mixtures of very similar but not identical molecules and are characterized by the average values of the molecular parameters of all the species present in the sample. Consequently, any discussion and definition concerning macromolecular substances implies a statistical character. This peculiarity derives from the nature of the polymerization reaction itself, which involves numerous successive stages without purification of intermediate products, and from the impossibility of separating macromolecules differing only in minor details. The macromolecules contained in a macroscopic sample display, besides a more or less wide molecular weight distribution, different types of terminal groups and a different number and distribution of structural defects. One of the more common defects consists in the presence of short or long branching or inverted monomer units. Thus, in a vinyl polymer formed by $-\text{CH}_2-\text{CHR}-$ units, there may be found, besides the normal head-to-tail ($-\text{CH}_2-\text{CHR}-\text{CH}_2-\text{CHR}-$) structure, a number of head-to-head ($-\text{CH}_2-\text{CHR}-\text{CHR}-\text{CH}_2-$) and tail-to-tail ($-\text{CHR}-\text{CH}_2-\text{CH}_2-\text{CHR}-$) sequences. Other kinds of defects may be present when a single monomer is able to give rise to two different monomer units; for example, butadiene polymers may contain 1,2[$-\text{CH}_2-\text{CH}(\text{CH}=\text{CH}_2)-$] or 1,4($-\text{CH}_2-\text{CH}=\text{CH}-\text{CH}_2-$) monomer units. These units succeed each other according to statistical rules that depend on the polymerization mechanism.

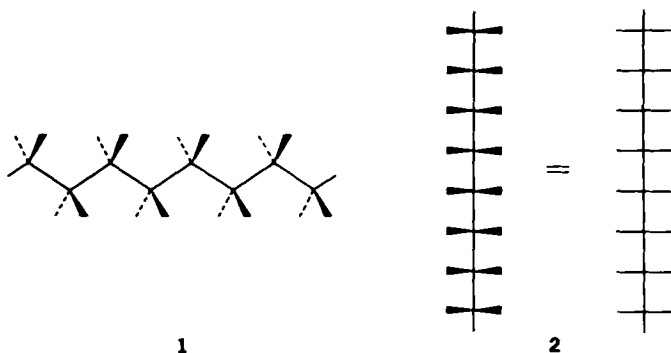
But even when the constitution of the polymer may be regarded as essentially homogeneous, considerations analogous to the previous ones may apply at the stereochemical level. For this reason the study of macromolecular stereoisomerism calls for a twofold approach. On the one hand, one must turn to ideal models that permit the identification of the type of structure existing in the polymer; on the other, statistical criteria must be used to determine to what

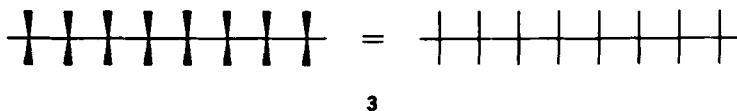
degree the real polymer differs from the ideal structure. We shall begin with the first of these problems, that is, with the determination of the most common structures observed in the macromolecular field and then move on to examination of real polymers. First to be discussed will be the structures of vinyl polymers that are, inherently and historically, the most important.

A. Isotactic and Syndiotactic Polymers

Given the high conformational mobility possessed by linear macromolecules (a few exceptions will be referred to later) their molecular structure may be discussed in terms of conventional stereoformulas that stress their essential configurational features. Among such graphic representations, the zigzag, **1**, and Fischer, **2**, projections are the most used; only occasionally, and in particular cases, other representations have been employed, as in **30** and **77** and **78**. Although representation **1** has real physical significance (it corresponds to the minimum energy conformation of a polymethylene chain) the Fischer projection is generally preferred because it is easy to print and because it permits immediate recognition of the steric relationship among the substituents bound to the chain, regardless of their distance and, in particular, regardless of whether such substituents are separated by an odd or even number of bonds. This advantage derives from the different intrinsic repetition period of the two representations, which is equal to only one bond in the Fischer projection but to two bonds in the zigzag projection, and from the different ways by which the successive angles along the chain are observed: in **2** they are seen in a homogeneous way while in **1** there is an alternation of concave and convex angles. As a consequence, misunderstandings arise when a simplified representation with the zigzag plane perpendicular to the page is used: The resultant figure is indistinguishable from a horizontal Fischer projection but has a different meaning.

The IUPAC Commission on macromolecular nomenclature recommends the



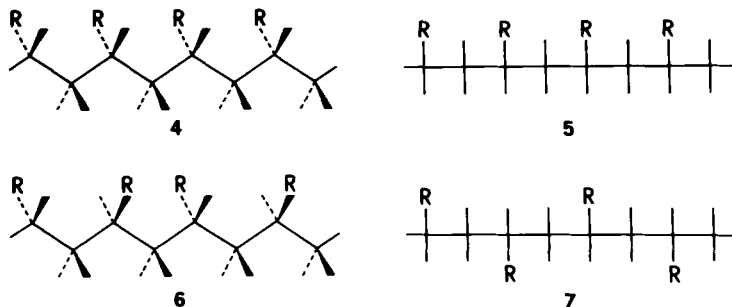


use of the zigzag formulas, as in 1, or of the horizontal Fischer projections, 3 (21). The latter are obtained from 2 by a rigid 90° rotation in the plane: Contrary to the usual rules the horizontal lines represent bonds extending behind the plane while the vertical lines are projected in front of the plane. Consequently the absolute configuration of any asymmetric carbon atom is inverted with respect to normal use. Fortunately, as will be better explained later, in the majority of cases ideal linear macromolecules may be considered as nonchiral and only diastereoisomeric relations are of interest, with no reference to the absolute configurations of the single centers.

In this article the use of formula 3 will always refer to rotated Fischer projections. In any case, the formulas must represent a section of chain long enough to illustrate the structural features excluding, unless explicitly required, the terminal groups. This representation corresponds to the use of a macromolecular model with an infinite chain length.

As is well known, the most simple head-to-tail stereoregular vinyl polymers were called isotactic (22–24) and syndiotactic (25) by Natta. The first compounds to be recognized as such were polypropylene and 1,2-polybutadiene, respectively (26). Ideal isotactic vinyl polymers (4, 5, Scheme 1) have all the substituents on the same side of the chain while in syndiotactic polymers (6, 7) the substituents regularly alternate between the two sides of the chain (27).

A fundamental characteristic of isotactic polymers is the presence of translational symmetry with periodicity equal to a single monomer unit: In the representation 4 and 5 successive monomer units can be superimposed by simple translation (30–32). In a syndiotactic structure this superimposition is not possible for two successive groups. The corresponding symmetry operator, if one



Scheme 1

excepts the case of chiral substituents (33), is the mirror glide plane (32). As a consequence, an isotactic polymer contains sequences of monomeric units (or of substituted carbon atoms) having an identical configuration, while a syndiotactic polymer contains successive monomer units (or substituted carbon atoms) of opposite configuration (22–25).

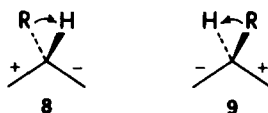
Tertiary carbon atoms along the chain have been defined as “asymmetric” (22–25, 34–37), “pseudoasymmetric” (6, 10, 38–40), “stereoisomeric centers” (30, 31), and “diastereic centers” (41). The first two terms put the accent on chirality and are linked to the use of models of finite and infinite length, respectively; the last two consider only phenomena of stereoisomerism. Note the relationship between these last definitions and Mislow’s and Siegel’s recent discussion (42), where the two concepts—stereoisomerism (or stereogenicity) and chirality—are clearly distinguished. The tertiary carbon atoms of vinyl polymers are always stereogenic; whether they are chirotopic or achirotopic (42) depends on structural features and also on the type of model chosen (43).

However, even when the absolute configuration of each atom is of little significance, there remains the problem of defining the relative configuration of tertiary atoms, that is, the relative position of the substituents. For this purpose various notations have been adopted in the macromolecular literature: *d*, *l* (22, 28, 37), *b*, *p* or *d*, *q* (44), *0*, *l* (11, 45), *r*, *s* (46), where the designation is purely conventional. A simple expedient to clarify the problem consists in imagining an observer who walks along the chain: If a given substituent is seen from one side, for example, from the right, a particular symbol is used, if observed from the left the opposite symbol is employed (30). Note that on reversing the direction of observation the symbols must be reversed also.

These same considerations were expressed in a manner only seemingly different by Corradini (47, 48), who introduced a representation widely used in conformational analysis of vinyl polymers. He defined the chain bonds adjacent to the tertiary carbon atom as + or – according to the clockwise or counterclockwise sequence of the two substituents in the Cahn–Ingold–Prelog sense, as shown in 8 and 9, as one proceeds along the chain.

A polymer is defined as isotactic when the bonds issuing from the successive stereoisomeric centers (conventionally indicated by a vertical line) always have the same disposition when observed in the same direction: $+|-+|-+|-+|-+|-*$ or $-|+|-+|-+|-+|-+|+$; it is defined as syndiotactic when the disposition of the signs is inverted at each stage: $+|- -|+|+|- -|+|+|-$. An isotactic sequence is, therefore, represented by

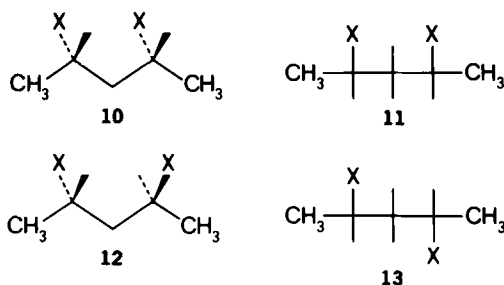
*Editor's comment: The meaning here is $+|-+|-+|-+|-+|-$; that is, in five successive stereogenic centers the + arrangement is seen first as one proceeds along the chain. When the gap between the stereogenic centers is closed in the notation, the signs between the lines then reveal the nature of the sequence.



two bonds of opposite sign $|+ -|$ or $|- +|$ and a syndiotactic sequence can be represented by two of equal sign $|+ +|$ or $|- -|$. Flory (40) uses a different convention, the letters *d* and *l* corresponding to $-$ and $+$, respectively.

This representation fits into the more general treatment of prochirality and prostereoisomerism (42, 50–52). Using the infinite chain model the $+$ and $-$ bonds must be considered enantiotopic (53) because they are related by a mirror plane perpendicular to the chain axis and passing through every tertiary carbon atom.

To resolve any ambiguity regarding the configurational notation and to adapt the vinyl polymer treatment to the kind of information obtainable by NMR spectroscopy, Bovey and co-workers proposed a different nomenclature (10, 17, 44, 54, 55). Using model compounds of low molecular weight as a starting point, they considered the arrangement of the substituents in an isotactic polymer analogous to that existing in a *meso*-2,4-disubstituted pentane, **10** and **11**, and that existing in a syndiotactic polymer analogous to the disposition in one of the enantiomers of a *racemic*-2,4-disubstituted pentane, **12** and **13** (Scheme 2). The polymer segment comprising two successive homologous substituents was called dyad, the letters *m* (*meso*) being assigned to the isotactic and *r* (*racemic*) to the syndiotactic dyads. Consequently an ideal isotactic polymer contains only *m* dyads ($\dots mmmmm \dots$) and a syndiotactic only *r* ($\dots rrrrr \dots$). Although the choice of the terms “*meso*” and “*racemic*” can cause confusion, their common meaning not being retained in the macromolecular field (21), the use of the letters *m* and *r* greatly facilitates the examination of the polymer structure. This is particularly true for nonstereoregular structures, especially in the study of short sequences (microtacticity) and in NMR spectral interpretation. Nevertheless, even this type of description has its limitations as will be shown later.

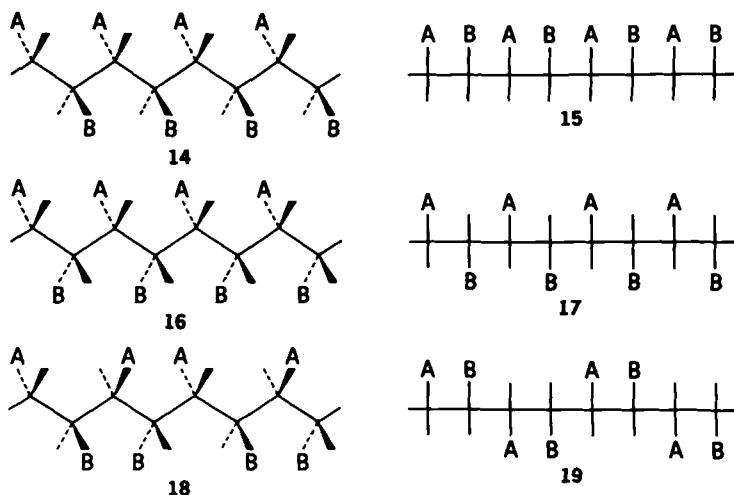


Scheme 2

The term "atactic" was introduced in 1956 to indicate a polymer with no steric regularity (56). It was first used to indicate a behavior opposite to that of isotactic and syndiotactic polymers [in early articles the term anisotactic was employed (23)]. Its meaning is sometimes restricted to polymers having an equal number of randomly distributed substituents on both sides of the chain (21); deviations from this random disposition are interpreted in terms of microtacticity.

B. Other Stereoregular Polymers

Polymers with a double isotactic structure were first obtained from *cis*- and *trans*-propylene-1-*d*₁, $\text{CH}_3-\text{CH}=\text{CHD}$ (57). Generally speaking, pure *cis*- or *trans*-1,2-disubstituted ethylenes, $\text{CHA}=\text{CHB}$, can give rise to three simple stereoregular polymers, two diisotactic and one disyndiotactic (31, 58); their formulas are shown as 14–19 (Scheme 3). The arrangement of two adjacent nonequivalent substituents A and B, may be defined as erythro and threo according to the conventional definition (59). It should be observed that for each of the two diisotactic polymers the zigzag and Fischer projections do not coincide: In 14 (zigzag representation of an erythro-diisotactic polymer), for example, all the substituents A are on one side of the chain and substituents B are on the other, whereas in the Fischer projection 15, which represents the same chain, substituents A and B are all on the same side; for threo-diisotactic polymers, 16 or 17, the opposite situation obtains.

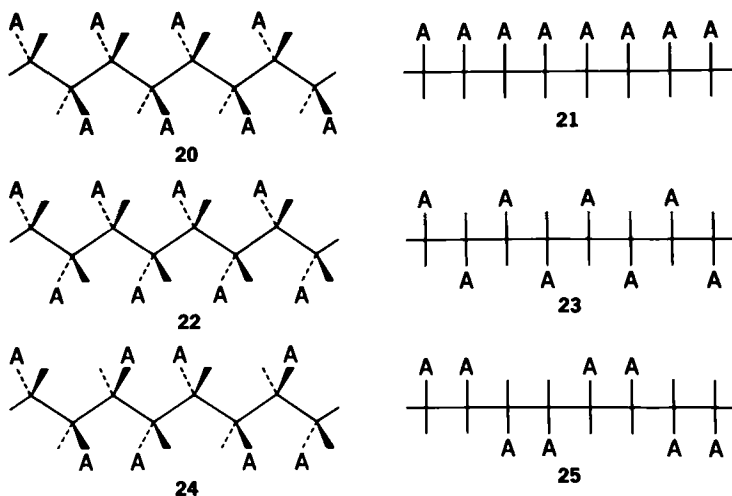


Scheme 3

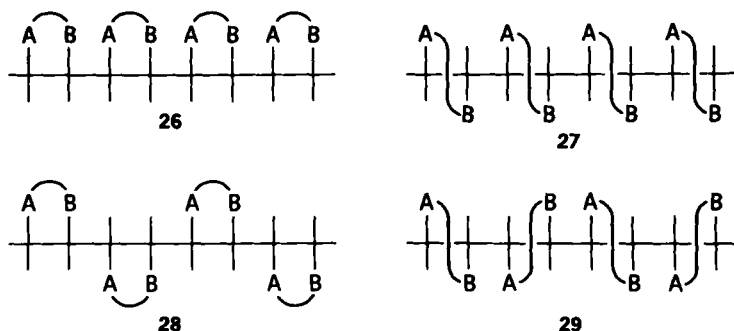
These monomers produce a single disyndiotactic polymer characterized by alternating erythro and threo relationships between adjacent substituents, **18** or **19**. In such a polymer it is not possible—unless one turns to selective isotopic labeling—to determine whether the erythro and threo relationship refers to the substituents A and B of the same monomer unit or to those of two successive monomeric units.

1,2-Disubstituted ethylene monomers with equal substituents, $\text{CHA}=\text{CHA}$, similarly give rise to three stereoregular structures analogous to the preceding (**20–25**) (Scheme 4), for which the same nomenclature is valid. However, they can also be considered as formed by $-\text{CHA}-$ structural units (31): For $\text{A} = \text{CH}_3$ we have three different polyethylenes. Generalizing these definitions, **20** or **21** could be called isotactic polyethylidene, **22** or **23** syndiotactic polyethylidene, and **24** or **25** heterotactic polyethylidene [heterotactic being a term that has been used to characterize the *mr* triads in vinyl polymers (44, 54, 55)]. The microtacticity of a polymer of this type, polyfluoromethylene ($\text{A}=\text{F}$), has recently been discussed (17, 60).

The contrast between formulas **20** and **21**, both pertaining to isotactic polyethylidene, should be noted: This contrast occurs because the polymer repeating unit has only one carbon atom in the chain and thus there is no correspondence between such periodicity and that of the zigzag representation. The classical definition of an isotactic polymer (as one in which all substituents are on the same side of the chain) holds true, in general terms, only if the polymer is represented in the Fischer projection. Analogous considerations pertain to syndiotactic polyethylidene **22** and **23**.



Scheme 4

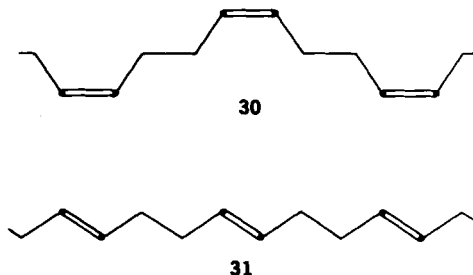


Scheme 5

Cyclic olefin monomers such as indene, benzofuran, and so on, can give rise to two diisotactic polymers erythro and threo, illustrated in the Fischer projection in **26** and **27**, and to two different disyndiotactic polymers **28** and **29** (Scheme 5), as each monomeric unit is clearly defined and quite distinct from its neighbors (**58**, **61**). For polymers of this type the terminology erythro and threo is used also.

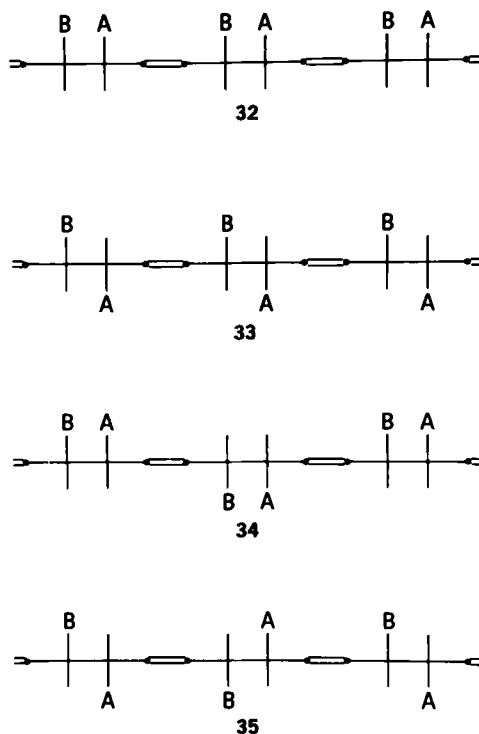
The butadiene polymers represent another cornerstone of macromolecular stereochemistry. Butadiene gives rise to four different types of stereoregular polymers: two with 1,2 linkage and two with 1,4. The first two, isotactic (**62**) and syndiotactic (**25**), conform to the definitions given for vinyl polymers, while the latter have, for every monomer unit, a disubstituted double bond that can exist in the two different, *cis* and *trans*, configurations (these terms are defined with reference to the polymer chain). If the monomer units all have the same *cis* or *trans* configuration the polymers are called *cis*- or *trans*-tactic (**30** and **31**). The first examples of these stereoisomers were cited in the patent literature as early as 1955–1956 (**63**). Structural and mechanistic studies in the field have been made by Natta, Porri, Corradini, and associates (**65**–**68**).

The same type of stereoisomerism was observed a long time ago in the



polyisoprenes of vegetable origin: Natural rubber is, in fact, a *cis*-tactic 1,4-polyisoprene (or simply a *cis*-1,4-polyisoprene), whereas balata and gutta-percha are *trans*-tactic 1,4-polyisoprene (69–71).

The combination of *cis*–*trans* isomerism with *iso*–*syndio* and *erythro*–*threo* dispositions gives complex structures as exemplified by the 1,4 polymers of 1- or 4-monosubstituted butadienes, such as 1,3-pentadiene (72, 73), and 2,4-pentadienoic acid (74, 75) and of 1,4-disubstituted butadienes, for example, sorbic acid (76). This last example is described in 32–35 (Scheme 6, rotated Fischer projection). Due to the presence of three elements of stereoisomerism for each monomer unit (two tertiary carbons and the double bond) these polymers have been classed as *tritactic*. Ignoring optical antipodes, eight stereoregular 1,4 structures are possible, four *cis*-tactic and four *trans*-tactic. In each series (*cis*, *trans*) we have two *diisotactic* and two *disyndiotactic* polymers characterized by the terms *erythro* and *threo* in accordance with the preceding explanation. It should be noted that here the *erythro*–*threo* relationship refers to adjacent substituents that belong to two successive monomer units.



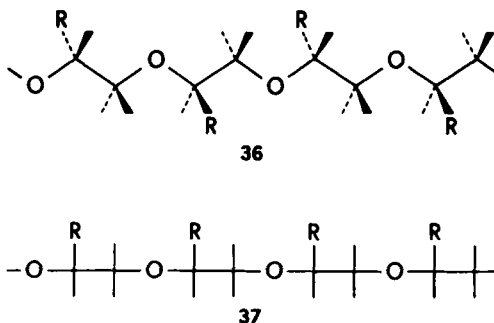
Scheme 6

Until now the discussion has centered on the addition polymers obtained from unsaturated monomers by reaction of the $C=C$ or $C=O$ double bond. However, polymers obtained by other methods (ring-opening polymerization, polycondensation, etc.) offer interesting stereochemical phenomena also. As a rule, in these classes of macromolecular compounds the monomer units are clearly defined, the direction of the chain is often distinguishable and the stereoisomeric elements present in the chain already preexist in the monomer. There are, however, numerous exceptions and further clarification is called for.

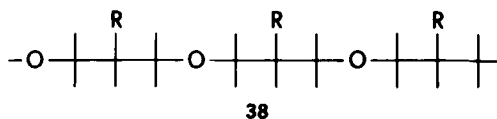
The extension of the term isotactic to condensation polymers was made by Natta in his first article discussing poly-L- α -amino acids (22). In itself the term isotactic is redundant here as the configuration of the repeating unit is sufficient to identify the macromolecular structure. It is, however, useful to distinguish a system, racemic or not, in which each macromolecule is composed of only L or only D residues from a mixture of macromolecules made up of random or alternate sequences of L or D units. Similarly the term syndiotactic serves in the identification of oligopeptides or polypeptides composed of alternate sequences of D and L units, like those synthesized by Lorenzi and Tomasic (77).

Similarly the term isotactic was applied by Price and Osgan (78) to the crystalline polymer obtained from optically active and racemic propylene oxide. The zigzag and Fischer representations of an isotactic poly(propylene oxide) are shown in **36** and **37** (Scheme 7). Their different appearance is due, as already explained in a similar case, to the odd number of chain bonds existing in each monomer unit. Formula **36** presents alternately substituents on both sides of the chain and is very similar to the actual structure observed in the crystal state (79).

There is a very close resemblance between the vinyl polymers and those derived from symmetric monomers like 3-methyloxetane, **38**, (80) or from the condensation of 3-methylglutaric acid with ethylene glycol or ethylenediamine.

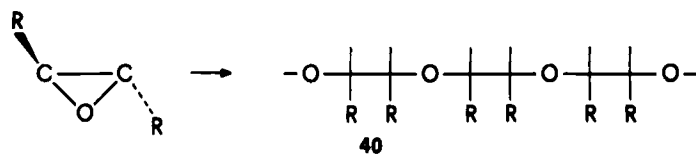
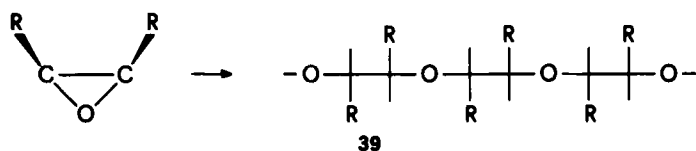


Scheme 7

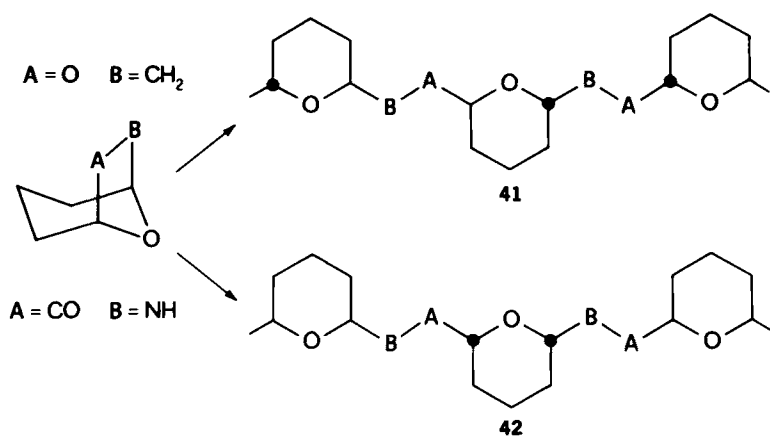


If, during ring opening polymerization a tertiary carbon is involved in the reaction, a configurational inversion may occur in which case a change in the stereochemistry of the monomer unit with respect to the monomer will be observed. Thus, the *cis*-2,3-epoxybutane gives rise to a polymer with threo monomer units, **39**, whereas the *trans* isomer is transformed into erythro or meso units, **40** (Scheme 8) (81, 82).

More complex cases may be found in bicyclic compounds like those studied by Kops (83, 84) and Sumitomo and co-workers (85, 86) **41**, **42** (Scheme 9).



Scheme 8

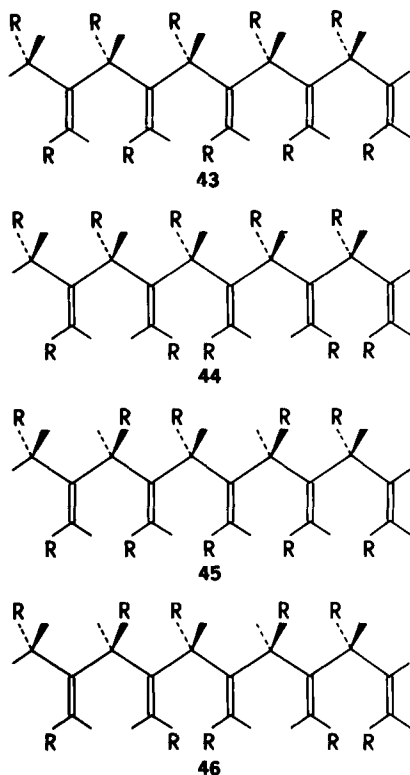


Scheme 9

C. Nonconventional Structures

This section illustrates some recent research concerning novel macromolecular stereoisomers. It differs from previous research because of the use of uncommon monomers, of particular methods of polymerization, or of chemical transformations of preformed polymers.

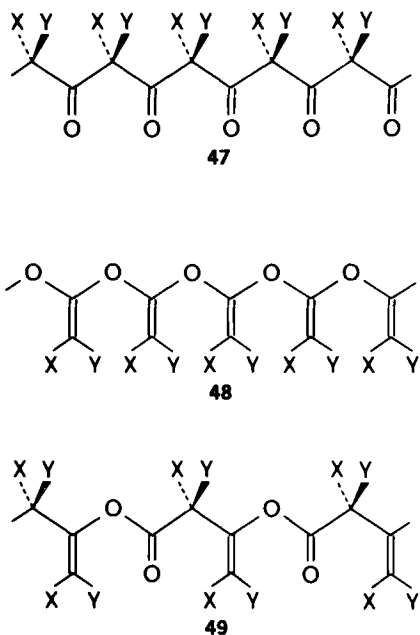
Monomers with cumulated double bonds, such as substituted allenes and ketenes, produce a great variety of structures. Stereoisomerism is found both at the saturated (iso- or syndiotacticity) and at the unsaturated carbons where the substituents in the plane of the chain can be oriented in either direction (forward or backward). With regard to 1,3-disubstituted allenes, four stereoregular structures, **43–46** (Scheme 10), are predicted. Porri, Rossi, and Ingrosso succeeded in polymerizing 2,3-pentadiene (1,3-dimethylallene) samples of different optical purity (87). In their experiments they recognized the existence of sequences **43**.



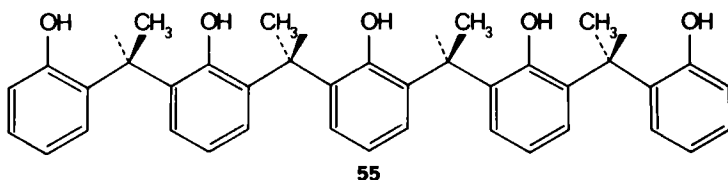
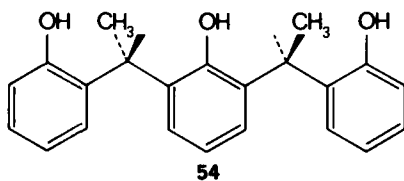
Scheme 10

It has been known for some time that dimethylketene produces three different types of polymers with polyketonic (**47**, $X = Y$), polyacetalic, **48**, and polyester, **49**, structures (88–90) (Scheme 11). The use of nonsymmetric ketenes like methylisopropylketene should produce an iso-syndio stereoisomerism in the ketonic form (**47**, $X \neq Y$, only one of the possible stereoisomers is shown) and an orientational isomerism in the polyacetalic form, **48**; in the polyester form, **49**, there would be a combination of the two possibilities, analogous to those described for polyallenes. 4-Methylpentamethyleneketene offers the reverse possibilities: iso-syndio isomerism in the polyacetalic form, **50**, orientational isomerism in the polyketonic form, **51**, and the combination of the two in the polyester form, **52** (Scheme 12). The three polymeric forms (ester, acetal, ketone) of 2- and 3-methylpentamethyleneketene each show both of these types of isomerism, one along and the other perpendicular to the chain.

Experimentally obtained were an ester polymer from methylisopropylketene, two polymers from pentamethyleneketene (one with the ester the other with ketonic structure), and an ester polymer from 4-methylpentamethyleneketene (91). Their stereochemistry has not yet been definitely determined. From the last monomer two cyclic dimers of ketonic structure, cis and trans (92) were obtained; they possess a close analogy to the aforementioned polymers.

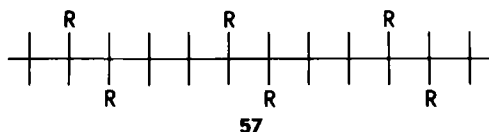
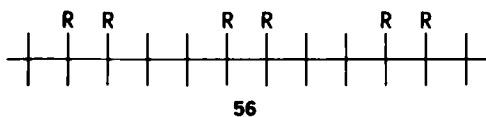


Scheme 11



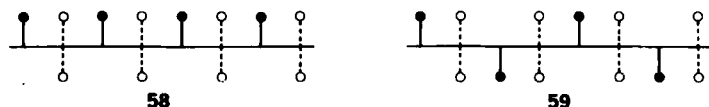
Formation of stereogenic atoms by polycondensation reaction was recently reported by Casiraghi et al. (94) during his research on regular phenol-formaldehyde polymers. Through careful selection of conditions, this reaction can be directed exclusively to the *ortho* positions (95). Substituting acetaldehyde for formaldehyde and using phenoxymagnesium bromide as the catalyst, a series of all-*ortho* diastereomeric oligomers is obtained, several of which were characterized by X-ray diffraction. The reaction is strongly biased towards the production of the syndiotactic dimer and tetramer, **54** and **55**.

A line of research that has aroused much interest in recent years is the study of head-to-head, tail-to-tail polymers (96-98). Their direct synthesis has little likelihood of being successful as head-to-tail sequences usually predominate in vinyl polymerization. One possibility for their preparation is through the chemical modification of suitable preformed polymers. In the case of the head-to-head, tail-to-tail polypropylene, different stereoisomeric forms have been isolated, depending on the method of preparation. In the general scheme, the precursor is an unsaturated polymer obtained by polymerization of the disubstituted butadiene (2,3-dimethylbutadiene or 2,4-hexadiene); then, by chemical or catalytic reduction, this polymer is converted into the desired polypropylene, whose structure can then be examined by NMR spectra. Head-to-head, tail-to-



tail erythro-diisotactic, **56**, threo-diisotactic, **57**, erythro-diatactic, and threo-diatactic polypropylenes, as well as a wholly atactic sample were thus obtained.

An analogous method was used to obtain a new class of macromolecular stereoisomers: The hemitactic polymers (99–101). This term refers to a head-to-tail vinyl polymer in which the tertiary carbon atoms constitute two distinct series: one, which includes monomer units 1, 3, 5, 7, . . . , possesses strict steric regularity, whereas the other, with monomer units 2, 4, 6, 8, . . . , is completely at random. In such polymers only one in every two tertiary atoms is influenced by an ordering rule: **58** and **59** show the schematic structure of the hemiisotactic and hemisyndiotactic polymers where the white circles indicate the positions of disordered substituents. The hemiisotactic polypropylene was obtained by Farina, Di Silvestro, Sozzani and Savaré (99, 101) by nonstereoselective reduction of isotactic *trans*-1,4-poly-2-methylpentadiene.


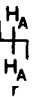
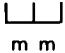
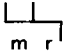
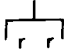
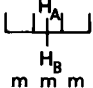

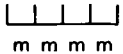
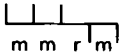
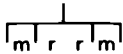
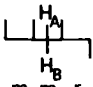
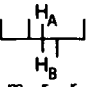
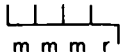
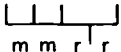
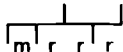
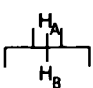
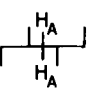
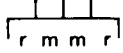
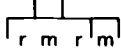
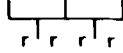
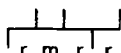


D. Microtacticity

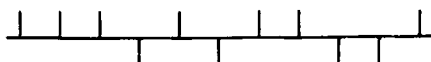
This term describes the phenomena of stereoisomerism observable in short chain segments. Microtacticity considerations can be applied to stereoregular polymers, to sequences of partially regular polymers, and to highly disordered polymers, both from the qualitative and quantitative points of view. This approach is the most appropriate and complete for the structural study of real polymers.

The common method of representing head-to-tail vinyl stereosequences is by the use of a two-letter alphabet, *m* and *r*, already mentioned in a preceding section. The letters refer to the dyads indicated in Table 1 (horizontal Fischer projection) (102). Segments of chain containing three centers of stereoisomerism are called triads (10, 17, 44, 54, 55): They result from the succession of two dyads and are indicated by the letters *mm*, *mr*, *rm*, and *rr*, respectively. In vinyl polymers the sequences *mr* and *rm* are indistinguishable and the independent triads are reduced to three. The terms isotactic (*i* = *mm*), heterotactic (*h* = *mr* + *rm*), and syndiotactic (*s* = *rr*) (54, 55) have also been proposed. Longer sequences are called tetrad, pentad, hexad . . . and are described by 3, 4, 5, . . . letters (Table 1). The longest sequence recognized until now is the undecad, corresponding to a chain segment with 20 bonds, observed in hemiisotactic polypropylene (101).

Table 1
Nomenclature and Symmetry of Stereosequences in Vinyl Polymers

DYADS		TRIADS		
				
TETRAADS		PENTADS		
				
				
				
				

An alternative way of describing microtacticity, already used in earlier papers and advocated by Price (45, 103) and by Randall (11) takes into consideration the configuration of the individual tertiary atoms and uses the symbols *d*, *l* or *0*, *1*. This nomenclature seems preferable in particular cases, for example, when dealing with optically active polymers or when examining polymerization processes, such as in the Ziegler-Natta polymerization of propylene carried out in a chiral environment. In this case the probability of the occurrence, within a single chain, of a *dd* (*00*) sequence can be different from that of *ll* (*11*) even though both are indicated by *m* in Bovey's nomenclature. Given the interchangeability of the representations it is useful to be familiar with both terminologies and to be able to convert the stereosequence into either form: As an example the undecad **60** may be read as *00010100110* (or the equivalent *11101011001*) or as *mmrrrrmmr*.



In the absence of degeneracy the number of possible stereosequences is equal to 2^{n-1} (n being the number of stereogenic centers present in the sequence). In vinyl polymers, because of the equivalence of the two directions of the chain, many sequences differ only in the way they are observed (e.g., *rrmr* and *rmrr*) and must, therefore, be considered only once. The number of independent sequences, calculated by the Frisch, Mallows, and Bovey formula (10, 44) is shown in Table 2. In hemiisotactic polymers, where strict selection criteria exist, this number is drastically reduced (100).

In stereoregular polymers there is only one type of sequence, or, at the most, a very limited number (in a regular heterotactic . . . *mrmmrrmr* . . . polymer both *mr**m* and *rmr* tetrads are present) (44).

The central methylene group of several even sequences of vinyl polymers presents interesting properties of symmetry (10, 54, 55) (Table 1). The dyad *r* has a twofold symmetry axis perpendicular to the chain projection and passing through the CH₂ carbon. This axis interchanges the two hydrogens that are, therefore, homotopic (equivalent) (104). In contrast, in the dyad *m* no symmetry exists to relate the two hydrogen atoms; these are, therefore, diastereotopic and may display different chemical and spectroscopic behavior. The methylene hydrogen atoms are found to be homotopic only in two tetrads (*rrr* and *mr**m*) and in four hexads (*rrrrr*, *mrrrm*, *rmrmr* and *mmrmm*), that is, in *r*-centered palindromic sequences of any length (as far as the NMR can sense). These properties find a natural application in the analysis of the NMR spectra and have been shown to be most useful in determining the type of stereoregularity (e.g., it is possible to ascertain if a polymer is isotactic or syndiotactic without resorting to X-ray analysis).

Other results, perhaps even more important, have been achieved by using the

Table 2
Number of Stereosequences

Sequences	Nonvinyl Polymers ^a	Vinyl Polymers	Hemiisotactic Polymers
Dyads	2	2	2
Triads	4	3	3
Tetrads	8	6	4
Pentads	16	10	7
Hexads	32	20	8
Heptads	64	36	14
Octads	128	72	16
Nonads	256	136	28

^aFor example, polymers from monoalkyloxiranes and thiiranes, 1- (or 4)-monosubstituted butadienes, α -substituted- β -propiolactones, α -amino acids, and so on.

concept of microtacticity in a quantitative way: primarily the determination of the degree of stereoregularity and the identification of some stereochemical aspects of the polymerization mechanism. From kinetic and mechanistic assumptions it is possible to develop a series of probability schemes which may then be compared with the experimental concentration of the various stereosequences: dyads, triads, tetrads. All conditions being equal, the simplest mechanism is generally accepted that is in reasonable agreement with experimental data at the highest accessible level.

Two types of quantitative relationships among the sequence probabilities must be considered. Some relationships are of a general character as they derive from considerations of stoichiometry and chain continuity. They might be called "necessary quantitative relations" (10, 44). With regard to the vinyl polymers and up to the pentad level, they are summarized in Table 3. Such relationships serve for qualitative and quantitative testing of experimental data. Other relationships depend on the kind of sequence distribution and, therefore, on the mechanism of polymerization. If the distribution can be expressed as a function of a single parameter the generation of the chain is a "Bernoulli trial" process (10, 11, 103) in which each event is independent of the preceding one. If p_m is the probability of formation of an m dyad, the equations given in Table 4, column 2 are obtained. These expressions are fully analogous to those for the ideal copolymerization between two pseudomonomers m and r .

Table 3
Necessary Relationships Among Stereosequences in Vinyl Polymers^a

Dyad-triad	$m = mm + \frac{1}{2} mr$ $r = rr + \frac{1}{2} mr$
Triad-tetrad	$mm = mmm + \frac{1}{2} mmr$ $mr = mmr + 2rmm$ $mr = mrr + 2mrm$ $rr = rrr + \frac{1}{2} mrr$
Tetrad-tetrad	$mmr + 2rmm = mrr + 2mrm$
Tetrad-pentad	$mmm = mmmm + \frac{1}{2} mmmr$ $mmr = mmmr + 2rmmr = mmrm + mmrr$ $rmr = \frac{1}{2} mrmr + \frac{1}{2} rmrr$ $mrm = \frac{1}{2} mrmr + \frac{1}{2} mrrm$ $rrm = 2mrrm + mrrr = mmrr + rmrr$ $rrr = rrrr + \frac{1}{2} mrrr$
Pentad-pentad	$mmmr + 2rmmr = mmrm + mmrr$ $mrrr + 2mrrm = rrmr + rrrm$

^aThe symbols m , mm , and so on, are used for the frequency (or analytical concentration) of the corresponding stereosequences, normalized over all the sequences of the same length.

Table 4
Sequence Distribution for Vinyl Polymers According to Different Stereochemical Rules

Sequence	Chain End Control		Enantiomeric Site Control Two-Parameter Nonsym- metric Chains ^{a,d}	Hemiotactic Polymers ^{a,e}
	Symmetric Ber- noulli Chains ^{a,b}	Symmetric First-Order Markov Chains ^{a,c}		
<i>m</i>	<i>p</i>	<i>b/S</i>	$(x\bar{y} + y\bar{x})/M$	α
<i>r</i>	\bar{p}	<i>a/S</i>	$2xy/M$	$\bar{\alpha}$
<i>mm</i>	<i>p</i> ²	$\bar{a}b/S$	$(xy^2 + y\bar{x}^2)/M$	$\frac{1}{2}(\alpha^2 + \alpha)$
<i>mr</i>	$2p\bar{p}$	$2ab/S$	$2xy(\bar{x} + \bar{y})/M$	—
<i>rr</i>	\bar{p}^2	$\bar{a}b/S$	$(x^2y + xy^2)/M$	$\frac{1}{2}(\bar{\alpha}^2 + \bar{\alpha})$
<i>mmm</i>	<i>p</i> ³	\bar{a}^2b/S	$(x\bar{y}^3 + y\bar{x}^3)/M$	α^2
<i>mmr</i>	$2p\bar{p}^2$	$2aab/S$	$2xy(\bar{x}^2 + \bar{y}^2)/M$	$\alpha\bar{\alpha}$
<i>mr</i>	$p\bar{p}^2$	a^2b/S	$xy(x\bar{x} + y\bar{y})/M$	—
<i>rrm</i>	$p^2\bar{p}$	$\bar{a}b^2/S$	$2xy\bar{xy}/M$	—
<i>rrr</i>	$2p\bar{p}^2$	$2abb/S$	$2xy(x\bar{y} + y\bar{x})/M$	$\alpha\bar{\alpha}$
	\bar{p}^3	$\bar{a}b^2/S$	$2x^2y^2/M$	$\bar{\alpha}^2$
<i>mmmm</i>	<i>p</i> ⁴	\bar{a}^3b/S	$(x\bar{y}^4 + y\bar{x}^4)/M$	$\frac{1}{2}(\alpha^3 + \alpha^2)$
<i>mmmr</i>	$2p^3\bar{p}$	$2a\bar{a}^2b/S$	$2xy(\bar{x}^3 + \bar{y}^3)/M$	$\alpha^2\bar{\alpha}$
<i>mrmm</i>	$p^3\bar{p}^2$	a^2ab/S	$xy(x\bar{x}^2 + y\bar{y}^2)/M$	$\frac{1}{2}\alpha\bar{\alpha}^2$
<i>mmrm</i>	$2p^2\bar{p}$	$2a\bar{a}b^2/S$	$2xy\bar{xy}(\bar{x} + \bar{y})/M$	—
<i>mmrr</i>	$2p^2\bar{p}^2$	$2a\bar{a}bb/S$	$2xy(xy^2 + y\bar{x}^2)/M$	$\alpha\bar{\alpha}$
<i>rmrm</i>	$2p^2\bar{p}^2$	$2a^2b^2/S$	$2xy\bar{xy}(x + y)/M$	—
<i>rmrr</i>	$2p\bar{p}^3$	$2a^2bb/S$	$2x^2y^2(\bar{x} + \bar{y})/M$	—
<i>mrmm</i>	$p^2\bar{p}^2$	$\bar{a}b^2b/S$	$xy(xy^2 + y\bar{x}^2)/M$	$\frac{1}{2}\alpha^2\bar{\alpha}$
<i>mrmm</i>	$2p\bar{p}^3$	$2abb^2/S$	$2x^2y^2(x + y)/M$	$\alpha\bar{\alpha}^2$
<i>rrrr</i>	\bar{p}^4	$\bar{a}b^3/S$	$x^2y^2(x + y)/M$	$\frac{1}{2}(\bar{\alpha}^3 + \bar{\alpha}^2)$

^a $\bar{p} = 1 - p$; $\bar{a} = 1 - a$; $\bar{x} = 1 - x$; $\bar{\alpha} = 1 - \alpha$.

^b $p = P_m$.

^c $a = P_{mr}$; $b = P_{mm}$; $S = a + b$; this distribution reduces to a Bernoulli process when $S = 1$ (or $a = \bar{b}$).

^d $\bar{x} = P_{oi}$; $y = P_{io}$ (at the same catalytic site); $M = x + y$; this distribution reduces to a nonsymmetric Bernoulli process when $M = 1$ or $(x = \bar{y})$ and to a symmetric Bernoulli process when $x = y$;

^e α = probability of a *mm* triad centered on a disordered methine carbon.

If, instead, the dyad probability depends on the nature (m or r) of the preceding dyad, the distribution follows a first-order Markov process, with two independent statistical parameters p_{mr} and p_{rm} , (the probability that after a m dyad a r dyad follows and vice versa, respectively). The corresponding equations are listed in Table 4, column 3. They correspond to those of a nonideal copolymerization and are reduced to the previous case when $p_{rm} + p_{mr} = 1$.

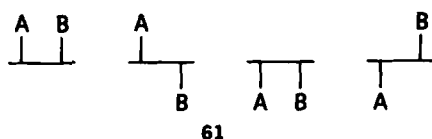
In many cases the equations for the longer sequences (tetrads, pentads, etc.) are markedly simplified if they are normalized not on the totality of the sequences but only on those centered on the same letter or group of letters. For example, the reduced frequency of the mmm tetrad with respect to all the m centered tetrads or that of the $mmrr$ pentad with respect to all the mr centered pentads is expressed by quadratic expressions for both the Bernoulli and Markov processes.

More complex schemes have been proposed, such as second-order Markov chains with four independent parameters (corresponding to a copolymerization with "penultimate effect," that is, an effect of the penultimate member of the growing chain), the nonsymmetric Bernoulli or Markov chains, or even non-Markov models; a few of these will be examined in a later section. Verification of these models calls for the knowledge of the distribution of sequences that become longer, the more complex the proposed mechanism. Considering only Bernoulli and Markov processes it may be said that at the dyad level all models fit the experimental data and hence none can be verified; at the triad level the Bernoulli process can be verified or rejected, while all Markov processes fit; at the tetrad level the validity of a first-order Markov chain can be confirmed, at the pentad level that of a second-order Markov chain, and so on (10).

Statistical criteria and selection rules can also be applied to polymers obtained by reactions of preformed polymers; to this class belong both the stereoirregular polymers obtained by epimerization of isotactic or syndiotactic samples (105, 106) and the hemitactic polymers already cited, 58 and 59. With particular regard to the hemiisotactic polymers their structure may be considered as a statistical succession of nonsuperimposed triads mm and rr (100). As a consequence, all sequences containing an odd number of equal dyads terminated on each side by different dyads are precluded. The number of these precluded sequences varies with the level of observation (Tables 2 and 5). With the only exceptions of the homosteric sequences . . . mmm . . . and . . . rrr . . . the capacity of the sequences to give rise to three or four sequences of a higher order is not uniform along each branch but appears only once in every two generations. The mr triad, for example, gives rise only to the $mmrr$ pentad, all other mr -centered pentads being forbidden because they contain isolated m or r dyads ($mmrm$, $rmrm$, $rmrr$). Selection rules do not operate on the $mmrr$ pentad (ending on the two sides with a pair of identical letters); as a consequence such a pentad can split into four heptads. In turn each heptad gives a single nonad, which separates into four undecads, and so on.

Table 5
Generation of Stereosequences in Atactic (*Left*) and Hemiisotactic (*Right*) Vinyl Polymers

		Generation of Stereosequences in Atactic (<i>Left</i>) and Hemiisotactic (<i>Right</i>) Vinyl Polymers		
<i>mm</i>	{ <i>mmmm</i>	3 heptads	
	 <i>mmmr</i>	4 heptads	
	 <i>rmrr</i>	3 heptads	
	 <i>mmrm</i>	4 heptads	
<i>mr</i>	{ <i>mmrr</i>	4 heptads	
	 <i>rmrr</i>	4 heptads	
	 <i>rmrr</i>	4 heptads	
	 <i>mmrm</i>	3 heptads	
<i>rr</i>	{ <i>mmrr</i>	4 heptads	
	 <i>mmrr</i>	4 heptads	
	 <i>rrrr</i>	3 heptads	
		10 pentads	36 heptads	
<i>mm</i>	{ <i>mmmm</i>	3 nonads	
	 <i>mmmmr</i>	1 nonad	
	 <i>rmmmr</i>	1 nonad	
	 <i>mmmmrr</i>	4 nonads	
<i>mr</i>	{ <i>rmmmr</i>	3 nonads	
	 <i>mmmmrr</i>	1 nonad	
	 <i>mmmmrrr</i>	1 nonad	
	 <i>rmmmrr</i>	1 nonad	
<i>rr</i>	{ <i>mmmmrr</i>	3 nonads	
	 <i>mmmmrrr</i>	4 nonads	
	 <i>mmmmrrrr</i>	1 nonad	
	 <i>mmmmrrrrr</i>	1 nonad	
		7 pentads	14 heptads	
		7 pentads	28 nonads	

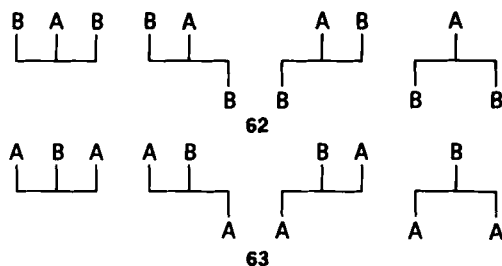


The statistical treatment of a hemiisotactic polymer can be made on the basis of a single parameter α ; the corresponding formulas are reported in Table 4, last column. For extreme values of α the polymer is no longer hemiisotactic but syndiotactic (for $\alpha = 0$) or isotactic (for $\alpha = 1$). The particular distribution existing in the hemiisotactic polymer is not reproducible with either the Bernoulli or the Markov processes expressed in m/r terms.

The microstructural approach can be extended to the polymers of 1,2-disubstituted ethylenes, to diene polymers, and to those obtained by ring-opening polymerization and by polycondensation. Differences with regard to vinyl and vinylidene polymers are observed in the type and number of the sequences, their nomenclature and the statistic model for the quantitative interpretation of their distribution.

For polymers obtained from disubstituted ethylenes $\text{CHA}=\text{CHB}$, Price (45, 103) considered four elementary states and developed a statistical scheme with eight conditional probabilities. The four elementary states correspond to the monomer units *00*, *01*, *11*, *10*, the first digit referring to substituent A, the second to B, **61**. The knowledge of the sequences of two monomer units (four-center sequences) is required for the testing of such a scheme.

Frisch, Mallows, and Bovey (44), and later Chujo, Kamei, and Nishioka (107) examined the same class of polymers and pointed out the existence of two series of three-center sequences that are intrinsically different, one centered on substituent A, **62**, the other on B, **63** (Scheme 13). They were distinguished by different symbols, for example, by small and capital letters (108). Six three-center stereosequences and 20 five-center sequences are possible, due to the

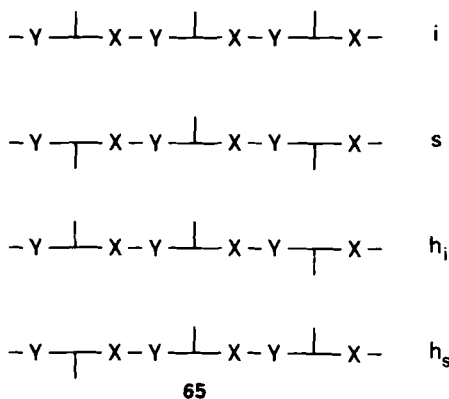
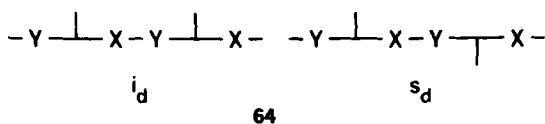


Scheme 13

occurrence of some degeneracy (e.g., note that the second and third sequence are equivalent in **62** and in **63**). Various simplified probabilistic schemes were proposed, and applied to the study of the polymers obtained from methyl 3,*d*₁-methacrylate (44) and from methyl propenyl ether (107). The difference from the Price scheme is that the probabilities here refer to the configurational relations between adjacent centers and not to the succession of the monomer units. The models just examined can also be applied to polymers of CHA=CHA type olefins: a recent example is that of polyfluoromethylene (60).

Stereosequences in polymers having the general formula $-\text{CHR}-\text{X}-\text{Y}-$ [e.g., poly- α -amino acids, polymers derived from substituted oxiranes, thiranes, aziridines, lactones or lactams, and 1,4 polymers of 1- (or 4) monosubstituted butadienes] are not affected by the degeneracy phenomena existing in vinyl polymers. Their number is indicated in the first column of Table 2.

Audisio studied the microtacticity of the 1,4-*trans*-polypentadiene $[-\text{CH}_2-\text{CH}=\text{CH}-\text{CH}(\text{CH}_3)-]$ in connection with that of the poly(methyltetramethylene) $[-\text{CH}_2-\text{CH}_2-\text{CH}_2-\text{CH}(\text{CH}_3)-]$ obtained from the preceding compound by reduction (109, 110), and succeeded in evaluating the distribution of the triads *mm*, *mr*, and *rr*. He has proposed an interpretation according to a one-parameter model based on enantiomorphic catalyst sites (111) (see Table 4, column 4, $M = 1$).



Scheme 14

In a recent study on poly(α -methyl- α -ethyl-propiolactone) and poly(α -methyl- α -propyl-propiolactone) (112) Spassky et al. extended the earlier examination carried out on oxiranes and thiranes (113) to the tetrad and pentad level. Because of the chirality of these polymers, Spassky avoids the use of the terms *m* and *r* as being inapplicable (21). To indicate the dyads *RR* (or *SS*) and *RS* (or *SR*) **64** he used the symbols i_d and s_d where the indices stand for dyad. In their turn the triads *RRR* (or *SSS*) are indicated with *i*, *RSR* (or *SRS*) with *s*, *RRS* (or *SRR*) with h_i (heterotactic triad beginning with an i_d dyad) and *RSS* (or *SRR*) with h_s (heterotactic triad beginning with a s_d dyad), **65** (Scheme 14) (114).

Until now, the most complex microstructural investigation has probably been that on the polysorbates (115, 116), which have sequences $-\text{CHA}-\text{CH}=\text{CH}-\text{CHB}-\text{CHA}-\text{CH}=\text{CH}-\text{CHB}-$. The hydrogenated polymers may analogously be considered $-\text{CHA}-\text{CH}_2-\text{CH}_2-\text{CHB}-\text{CHA}-\text{CH}_2-\text{CH}_2-\text{CHB}-$. In these cases the complexity of the disubstituted polymer adds to that of the polymers in which the two chain directions are different. In principle 4 two-center, 8 three-center, and 16 four-center sequences must be considered.

III. THE CONTRIBUTION OF NMR SPECTROSCOPY TO MACROMOLECULAR STEREOCHEMISTRY

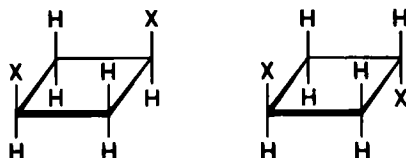
For several years after Natta's discovery, attention was devoted almost exclusively to stereoregular polymers. Among the many reasons for this was the fact that stereoregular polymers constituted a new class of compounds offering ample research opportunities and having wide practical application. Many were crystalline and this, in addition to influencing their physical properties, made it possible to determine their structure by X-ray diffraction. All the investigators were well aware that crystallinity and stereoregularity were incomplete and that diffractometric analysis fathomed only sections of the chain and only a fraction of the macromolecules in the polymer sample. At that time experimental techniques revealing the structure of *all* sections of the macromolecules, be they regular or defective, were lacking. Even IR spectroscopy, which in principle could resolve the problem, was of help only in a few cases due to the complexity of interpretation and the limited possibilities of spectral calculation existing at that time.

This gap was filled by the development of NMR spectroscopy. It is Bovey's merit to have demonstrated the potentiality of this technique in the macromolecular field and, in particular, its sensitivity to the stereochemical environment. The applications of this technique, the methods of investigation, and the type of problem that can be solved are closely connected with the progress made in NMR instrumentation in the last quarter century. From low magnetic field spec-

trometers, capable of observing only high abundance nuclei (H, F) we have passed to high field instruments equipped with devices able to increase the signal-to-noise ratio and to enhance sensitivity, thus permitting the recording of the first carbon spectra. Pulse Fourier transform instruments, able to collect and to elaborate spectral data obtained with different pulse sequences, and spectrometers for solid samples, which use the technique of rotation at the magic angle, have come into use more recently. The application of NMR spectroscopy to the structural analysis of polymers has been reviewed and discussed on numerous occasions (10, 11, 17, 117, 118).

It is well known that nuclei situated in the same constitutional and stereochemical environment are isochronous. Molecular nonhomogeneity and the fact that symmetry equivalence is created by translation (the validity of this assumption is tied to the infinite chain model) make the application of this principle in the macromolecular field rather complex. Near the chain end, nuclei of the same type (e.g., the methyl carbons of polypropylene) resonate at different frequencies; but, as one moves toward the center of the chain the chemical shift of such nuclei tends to an asymptotic value. With present day instrumentation the chain end effect is no longer visible beyond four to six monomer units: It may thus be assumed that a regular polymer of high molecular weight gives rise to one single resonance for each type of nucleus present in the repeating unit [three carbons and four (or three) hydrogens for each monomer unit of polypropylene, six carbons and six (or five) hydrogens in polystyrene, five carbons and four (or three) hydrogens in poly(methyl methacrylate), and so on: The alternate numbers for hydrogen atoms relate to a possible symmetry equivalence of methylene hydrogens existing in certain sequences].

The case of not strictly regular polymers is different. Nuclei at the center of identical sequences have, necessarily, the same chemical shift, but there exists the problem of just how long the sequence must be for this to hold true (119). In principle it should correspond to the entire macromolecule; in practice the answer depends on the individual case. For example, the 100-MHz ^1H NMR spectrum of methyl groups directly bonded to the chain in atactic poly(methyl methacrylate) consists of three slightly broad singlets, corresponding to the triads *mm*, *mr*, and *rr*. This last signal shows signs of further splitting. In fact, the spectrum of the same sample registered in a higher magnetic field shows resolution at the pentad level (8 signals—including the shoulders—out of 10 possible signals). Under these conditions the pentad is the longest detectable sequence (10). In the 50.3-MHz ^{13}C NMR spectrum of polypropylene, a structural variation at the extremes of a nonad produces palpable effects of different magnitude for the different sequences (101): The difference in the CH_3 chemical shift between the *mmmmrrmmmm* and *mmmmrrmmmr* sequences is 0.06 ppm, that between *mmmmmmmmmm* and *mmmmmmmmmr* is 0.03 ppm, while that between sequences *rrrrrrrrrr* and *rrrrrrrrrm* is <0.005 ppm. If the difference is sufficiently great and the intensity ratio between the sequences is favorable, different signals for each



66

sequence can be observed; otherwise, due to the superimposition of slightly displaced resonances, the peaks are merely broadened. It is important to distinguish this phenomenon from the other well-known causes of signal broadening.

The NMR spectra of polymers are further complicated by the presence of sizeable homonuclear and heteronuclear spin-spin couplings. In the case of the proton spectra of vinyl polymers it is necessary to consider geminal, vicinal, and also virtual couplings between the isochronous protons. Because of these couplings the spectrum cannot be interpreted by a first-order approximation (117). A useful approximation for $-\text{CH}_2-\text{CHX}-$ polymers, where X is a substituent whose nuclei do not couple with those of the chain, is that of considering them as six-spin systems related to the cyclic dimers such as 66 (120). Polymers having a high degree of stereoregularity show excellent agreement between calculated and experimental spectra. More difficult is the treatment of irregular polymers. In this case the spectrum is the sum of a series of multispin systems related to all the possible stereochemical arrangements. When the substituent X is able to couple with main chain nuclei, as in polypropylene, the spectrum is even more complicated. The vinylidene polymers $-\text{CH}_2-\text{CXY}-$ represent a happy exception being interpreted as a series of two-spin AB systems. In fact the development of NMR spectroscopy of polymers began with poly(methyl methacrylate) (54).

Simplification of complex spectra can be obtained either with the preparation of suitable polymer samples or by means of instrumental techniques. Examples are the wide use of ^2H or ^{13}C labeled monomers, of homo- or heteronuclear decoupling, of off-resonance decoupling, and of a variety of pulse sequence techniques. Because of the time scale of the NMR experiment, what is observed is an averaged spectrum with respect to the conformational transformations and to exchange reactions with low activation energy.* In particular both the chemical shift and the coupling constants are average values weighted over all the accessible conformations and consequently are dependent on temperature (10).

Because of the close connection between stereosequence distribution and

*The kinetics of conformational changes in macromolecular chains has been investigated by Liao and Morawetz (*Macromolecules*, 1980, 13, 1228) who compared the behavior of polymers containing suitable probes with that of low-molecular weight analogs. Activation energy was the same in both cases and differences in absolute values of rate constants did not exceed 30%. This finding, however, does not exclude the existence of restrictions of the motion of large chain segments in a viscous medium.

polymerization mechanism, a most important problem in polymer NMR spectroscopy is the evaluation of the degree of reliability of the quantitative measurements. Two distinct difficulties exist in this respect: The first is the correct evaluation of signal intensity, the second concerns the effective correspondence between the relative area of a signal and the concentration of the respective sequence in the sample.

In the first case there is no difficulty for well-separated signals, but when complex multiplets or partially overlapping signals are encountered, the normal techniques of integration or area measurement become inadequate. In such a case the best solution consists in simulating the spectrum, allowing one or more independent parameters—number, position, shape, height, and width of peaks—to vary. The Lorentzian line shape is considered to be the most correct theoretically (10, 11) but sometimes it is more convenient to use a Gaussian line shape, especially should there exist many overlapping quasicoincident signals. A refinement of this process is the application of line shape analysis, based on best-fitting procedures, to the whole spectrum or to its individual parts.

The second difficulty is not encountered in proton spectroscopy, where proportionality between peak area and concentration of the respective sequence is virtually guaranteed, but is present in carbon spectroscopy where one works under heteronuclear broad-band decoupling conditions. Under such conditions, both the nuclear Overhauser effect (NOE) and the differences in spin-lattice relaxation time T_1 can alter the intensity. In this connection, however, Schaefer showed that for the different ^{13}C nuclei inside the polymer chain, because of the restricted molecular movement, there are no large differences in NOE (121).

As regards T_1 , which can vary from some tenths of a second to some seconds depending on the degree of substitution of the atom in question and on its position, its effect can be eliminated by an appropriate choice of experimental conditions. To obtain correct quantitative measurements it is desirable to introduce a delay between successive pulses up to five times the longest relaxation time of the observed nuclei (in many cases the delay amounts to 8–10 s) (11). Another important factor is the acquisition time, which must be long enough to give a high resolution spectrum.

As a consequence a quantitative ^{13}C NMR spectrum calls for 5–10 times the instrument time of a purely qualitative one. It is not feasible to increase the concentration of the polymer in solution excessively because this involves an increase in linewidth and the gain in time (considering the lower number of transients required) is accompanied by a poorer quality of the spectrum. The planning of a high quality ^{13}C NMR experiment requires a fine balance between results, time, and costs.

In the following pages we shall treat, in detail, the NMR analysis of two polymers, poly(methyl methacrylate) and polypropylene, which have epitomized, in consecutive epochs, the most classical and fruitful examples of interaction between NMR spectroscopy and macromolecular stereochemistry.

A. A Pioneering Research Problem: Poly(methyl methacrylate)

The first NMR investigation of this polymer goes back as far as 1960 to an article that may be considered the birth of a new chapter in macromolecular chemistry. Bovey and Tiers examined two samples of poly(methyl methacrylate), one (a) obtained by anionic polymerization at low temperature, the other (b) by radical polymerization (54). The ^1H NMR spectra of the polymers run at 40 MHz, and even more those recorded at higher field, showed clear differences, both in the region of the methylene protons and in that of the methyl protons (Figure 1). The former presents, between 1.5 and 2.5 δ (CH_2 subspectrum), a well-separated doublet of doublets and around 1.3 δ (CH_3 subspectrum) a singlet accompanied by two minor peaks at a slightly higher field. The second, instead, presents a rather broad singlet around 2 δ (CH_2), sometimes split into two peaks, and another singlet at 1.1 δ (CH_3) with two minor peaks at a lower field.

The first point of the stereochemical analysis is in the recognition of the sequence to which a given nucleus is sensitive; the problem seems rather obvious for vinyl or vinylidene polymers where the sequence must extend equally from the two sides of the nucleus in question; but for diene polymers or those containing heteroatoms, the problem is not so simple. In the present case, the methylene protons are sensitive to the structure of the even sequences, dyads and tetrads, whereas the methyl protons are sensitive to the odd sequences, triads, and pentads.

As seen in Table 1, in the *m* dyad the methylene protons are diastereotopic and consequently their spectrum consists of an AB doublet of doublets with a geminal coupling constant $J_{AB} = -15$ Hz. In contrast, in the *r* dyad the two protons are equivalent and, therefore, a singlet is observed in the spectrum.

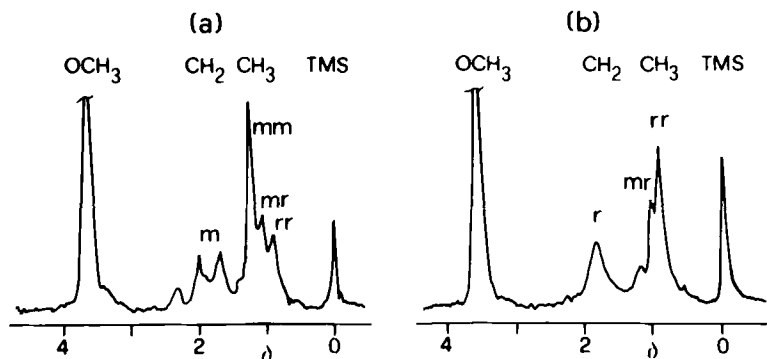


Figure 1. 40 MHz ^1H NMR spectrum of isotactic (a) and syndiotactic (b) poly(methyl methacrylate). From ref. (54); Copyright John Wiley & Sons.

From this observation the structural assignment was made as follows: Isotactic (or prevailing isotactic) to the first polymer and syndiotactic to the second. As a consequence the most intense methyl singlet in the two spectra must be attributed to the *mm* and *rr* triads, respectively. The presence of additional peaks in both the methyl and methylene spectral regions indicates that the polymers are not sterically pure and that the spectra are sensitive to longer sequences. The presence of a third methyl signal in both samples indicates the presence of *mr* triads. This, in turn, implies the presence of *mmr*, *rmr*, *mrr*, and *mrmm* tetrads in addition to the sterically pure *mmm* and *rrr* tetrads. The first two *m*-centered tetrads give rise to two well-spaced doublets of doublets similar to those of *mmm*, while *mrmm* gives rise to a singlet (like *rrr*) and *mrrr* to a not well-defined doublet of doublets. The complete analysis of tetrads is easily effected if the spectrum is recorded at a higher magnetic field. Under these conditions, even

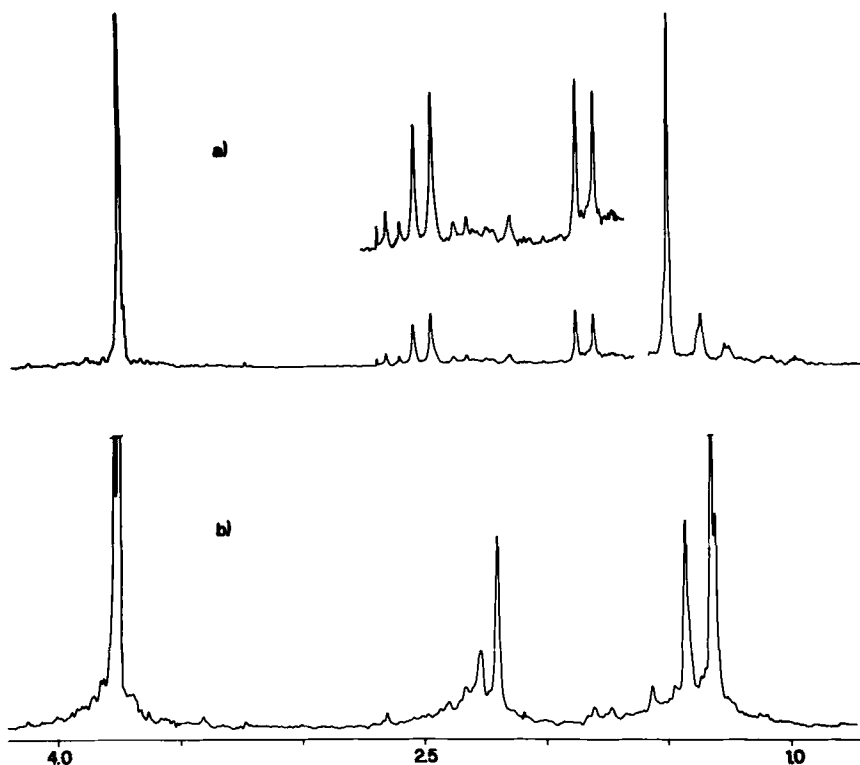


Figure 2. 200 MHz ^1H NMR spectrum of isotactic (a) and syndiotactic (b) poly(methyl methacrylate).

the methyl spectrum shows a splitting of triad into pentad signals (8 signals corresponding to the 10 pentads; Figure 2).

To prove the correctness of this analysis we shall try to look for alternative explanations. A stereoregular heterotactic polymer . . . *mrmrmr* . . . could also explain the presence of a methyl singlet and a well-separated doublet of doublets for methylene protons, in agreement with the spectrum of the first sample; in fact, there would be present the *mr* triad and the *mrmr* tetrad with diastereotopic protons. However, in addition, an equal amount of the *mrm* tetrad should be present, yet the corresponding singlet is not visible with the required intensity. In the same way other hypothetical structures can be rejected.

In favorable cases therefore, ^1H NMR spectroscopy constitutes an absolute method for the determination of the stereoisomeric structure of polymers. This affirmation holds true not only in the sense that the spectrum is in agreement with the proposed structure (isotactic for the first polymer, syndiotactic for the second) but also because a detailed examination of the whole spectrum permits the exclusion of other hypotheses that might reasonably be put forward.

The integration of the methyl singlets allows for easy determination of the triad content and assesses their distribution according to different statistical models. In Figure 3 the distribution of the triads obtained in a series of radical and anionic polymerizations of methyl methacrylate is shown as a function of p_m . The curves represent the distribution expected for a Bernoulli trial process. Points with a low p_m value, corresponding to samples obtained by radical polymerization, fit the theoretical curve well while those with high p_m values, corresponding to samples obtained by anionic polymerization, have a higher content of *rr* triads than that calculated. A Bernoulli model is, therefore, sufficient to explain the distribution of the stereosequences in a relatively simple process like radical polymerization, whereas more complex schemes, involving higher-order Markov chains or even non-Markov processes, are needed (10, 122) to explain polymerization carried out in the presence of metallic counterions (Li or MgBr). It must be made clear however that the verification of these hypotheses cannot simply be done at the triad level but requires knowledge of the distribution of longer sequences.

The above analysis represented the first example of the combined use of spectroscopic results and statistical calculations to define the polymerization mechanism, a combination which, today, is the norm for those who work in polymer stereochemistry.

The passage from proton to carbon spectroscopy has led to few new significant results for poly(methyl methacrylate). The ^{13}C NMR spectrum at 25.2 MHz presents a degree of structural resolution analogous to that of the high-field proton spectrum (123). Curiously, the highest sensitivity to the stereochemical sequences is observed in the CO group that appears to divide into eight signals corresponding to single pentads or groups of pentads. Better results,

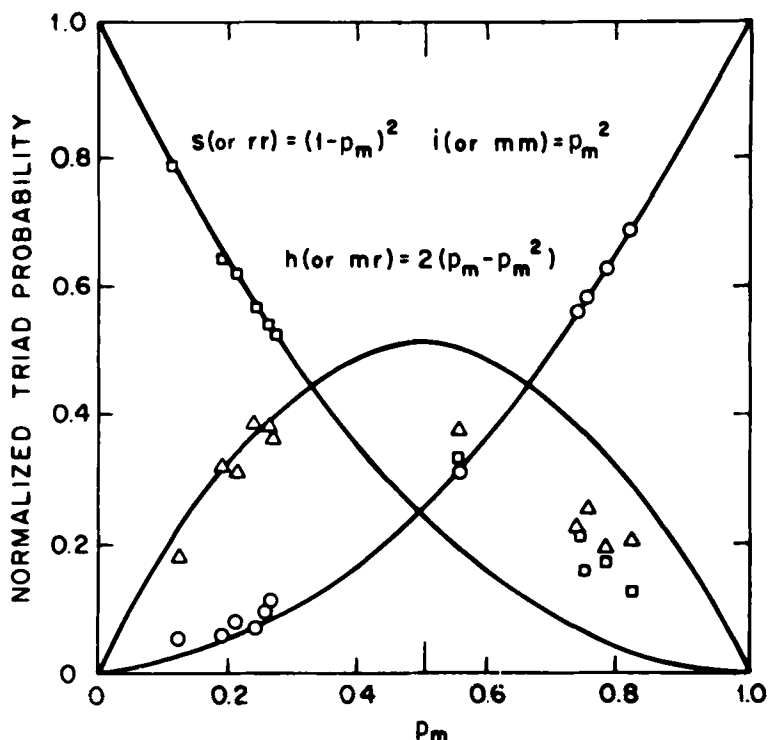


Figure 3. Triad distribution in poly(methyl methacrylate) as a function of p_m . Points at $p_m < 0.5$ are obtained by radical polymerization, those at $p_m > 0.5$ by anionic polymerization (10). Copyright Academic Press.

however, have been obtained with spectrometers operating at a higher magnetic field. Thus the spectrum recorded at 90 MHz shows approximately a dozen peaks in the CO region revealing a sensitivity up to the heptad level (124).

B. The Present Level of Spectral Analysis

As in many other aspects of polymer stereochemistry, polypropylene also plays a central role in NMR spectroscopy. Since 1962 numerous articles have dealt with the interpretation of its proton spectrum (125–128); the state of knowledge at the end of that decade has been well described by Woodbrey (117). The difficulty in this study stems from two factors: The narrow frequency range comprising the entire spectrum and the large homonuclear coupling between CH_2 , CH , and CH_3 protons. The whole spectrum is within a range of <1.5

ppm, with a marked overlap of signals. For example, one of the diastereotopic methylene protons in the isotactic polymer has a chemical shift practically coincident with that of the methyl signal (0.87δ compared with 0.86); furthermore, the resonances due to any particular pair of methylene protons, which are affected by the spin couplings to the methine proton, may be further affected by couplings of the methine protons to methyl and other methylene protons. In this sense, all the protons of a polypropylene molecule can be mutually or virtually coupled (117). This is particularly deleterious when the spectra are recorded at low magnetic field, as was done in the early studies.

Under analogous conditions the spectrum of syndiotactic polypropylene is clearly distinguishable from that of the isotactic polymer but it, also, suffers from the same limitations. In both polymers it is difficult to determine the degree of stereoregularity with any accuracy.

Substantial progress has been made with the synthesis of polymer samples obtained from deuterated monomers, as, for example, from propylene-2,3,3,3- d_4 $\text{CH}_2=\text{CD}-\text{CD}_3$. In this way the spectrum reduces to that of an AB (isotactic polymer) or A_2 (syndiotactic polymer) system, analogous to that of the polymethacrylate. At the same time, the accidental overlap of methyl with methylene signals is eliminated. The isotactic polymer gives the expected doublet of doublets (126–128) (Figure 4) while the syndiotactic polymer gives a singlet. The simplicity of the spectrum has made evident several features, previously never observed in the polymer field. Segre, for example, was able to record a spectrum at 100 MHz with deuterium decoupling achieving a linewidth <0.5 Hz (130). In this experiment most of the structural and instrumental conditions contributing to the broadening of the signal are eliminated and the linewidth is comparable with that in low molecular weight compounds.

An even simpler spectrum (a single resonance for sterically pure samples) was obtained from polymers of the two [(Z) and (E)] isomers of propylene-1,2,3,3,3- d_5 , **67** and **68** (Scheme 15), respectively. The isotactic polymer of the

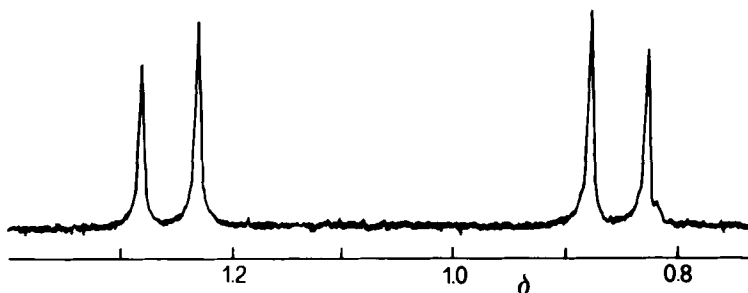
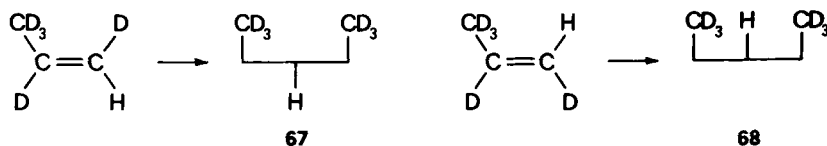


Figure 4. Deuterium decoupled 270 MHz ^1H NMR spectrum of isotactic polypropylene 2,3,3,3,3- d_5 . From ref. (129): Copyright Pacini Editore, S.R.I., Pisa.



Scheme 15

first monomer displays a singlet at 0.87 ppm and that of the second a singlet at 1.26 ppm. On the basis of the known stereochemistry of polymerization (see later) the signal at the higher field (0.87 ppm) must be attributed to the hydrogen which, in the Fischer projection, appears on the side opposite the methyl group. Such a proton was called *syn* by Zambelli et al. (131) because the zigzag projection was used as a reference, and *anti* by Bovey (17). Analogously the singlet at 1.26 ppm was attributed to the proton *anti* according to Zambelli and *syn* according to Bovey. The syndiotactic polymer of both monomers gives a singlet with the same chemical shift (1.03 ppm).

When nonstereoregular deuterated polymers are examined with deuterium decoupling, it is possible to observe fine structure revealing resolution at the tetrad level. The spectrum of the substantially atactic polymers obtained from each stereoisomer of pentadeuteropropylene presents 6 singlets, 3 of which coincide in both spectra, making a total of 9 signals for the two combined polymers. This number must be compared with that of the distinct anisochronous hydrogens present in the 6 possible tetrads, which is equal to 10. Therefore, it is possible to perform an almost complete analysis of the sequences [only the tetrads *rrr* and *mmm* have, by chance, the same chemical shift (132, 133); several authors, however, did not, at the time, agree with this assignment (119, 134–136)].

A further improvement in the spectrum of propylene polymers has been achieved through use of a high magnetic field spectrometer (figure 5). Ferguson reported 220-MHz proton spectra of nondeuterated polypropylenes in which the signals are clearly separated (137). In particular the two diastereotopic methylene hydrogens of isotactic polypropylene give two well-separated multiplets (one of which coincides with the methyl doublet) while those of syndiotactic polypropylene appear as a pseudotriplet. Further studies on deuterated samples led to the observation of a splitting of signals attributable to the hexads (138).

This highly sophisticated investigation has been superseded by ^{13}C spectroscopy, which is more sensitive to the stereochemical environment and does not require the preparation of deuterated polymers. ^{13}C NMR analysis of steric purity and sequence distribution can, therefore, be directly carried out on commercially available polymers. Thus, any doubt regarding the previous conclusions about laboratory-produced polymers obtained under necessarily different

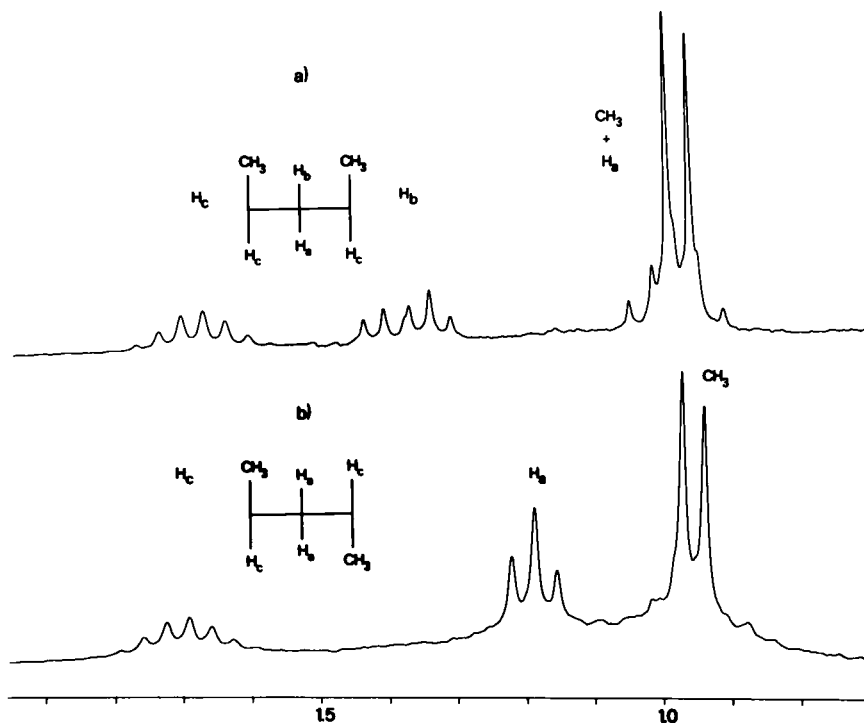


Figure 5. 200 MHz ^1H NMR spectrum of isotactic (a) and syndiotactic (b) polypropylene.

conditions (due to possible isotope effects and the poor reproducibility of the actual polymerization conditions) is eliminated.

Today, carbon spectra registered in continuous wave mode (139, 140) are only of historical interest. The Fourier transform spectrometers operating between 20 and 100 MHz under standard conditions (5–10% w/v of polymer in *o*-dichlorobenzene or 1,2,4-trichlorobenzene solvent at 100–140°C) allow quantitative analysis of pentads, more than sufficient for routine testing and for obtaining information on the polymerization mechanism (11, 17, 141–143). In several cases, the choice of optimum experimental conditions gives spectra with higher resolution and sensitive to longer sequences (17, 101). ^{13}C spectra of isotactic and syndiotactic polypropylene (Figure 6c and 6b) show only three signals each, one around 44–48 ppm (CH_2 subspectrum), one near 28–29 ppm (CH) and one in the 19–22 ppm region (CH_3). The two spectra differ notably in the value of these chemical shifts (up to 1.5 ppm). In atactic polypropylene (Figure 6a) the three signals present a complex structure due to their sensitivity

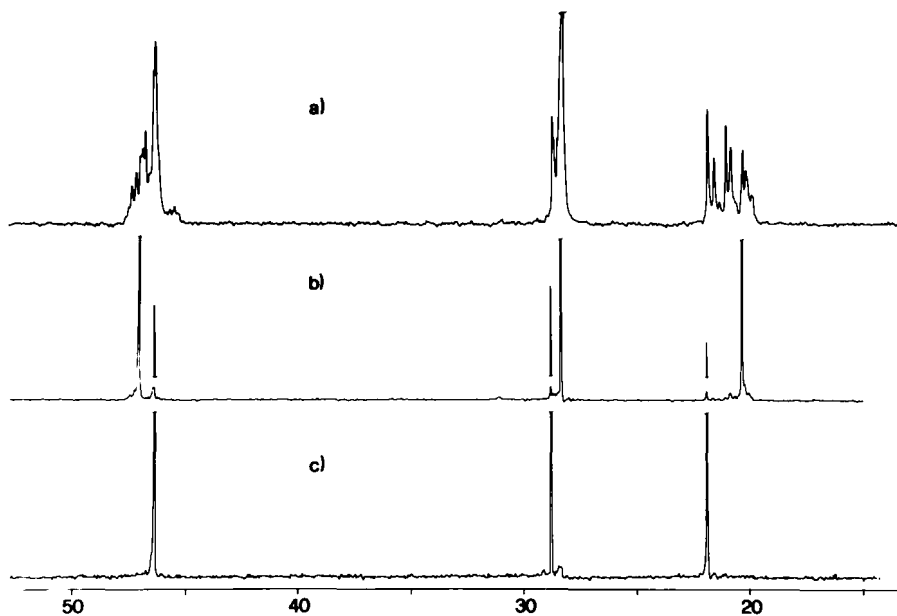


Figure 6. 50.3 MHz ^{13}C NMR spectrum of atactic (a) syndiotactic (b) and isotactic (c) polypropylene run at 100°C .

to the steric environment, particularly in the high field region (CH_3) where at least 9 signals, corresponding to the 10 pentads, are visible [Figures 6a and 7].

Interpretation of the spectrum has been accomplished very neatly by two different methods. Stehling and Knox (105) examined samples of both isotactic and syndiotactic polypropylenes that had been slightly epimerized by a radical

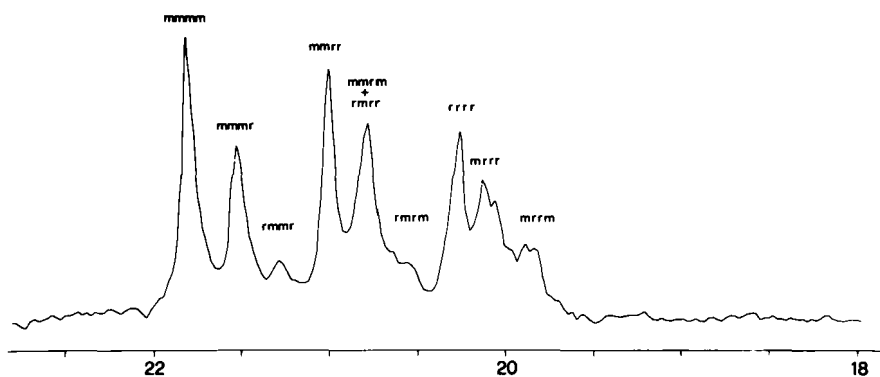


Figure 7. Methyl region of 50.3 MHz ^{13}C NMR spectrum of atactic polypropylene run at 100°C .

reaction, which inverts the configuration of the carbon atoms one at a time. In the former case next to the intense *mmmm* (e.g., *11111*) signal, three signals related to the presence of a single configurational inversion in a 2:2:1 ratio are observed. The third is unequivocally assigned to the *mrrm* (*11011*) sequence, while the first two derive from the pentads *mmmr* (*11110*) and *mmrr* (*11101*). The factor two in the intensity ratios derives from the lack of symmetry of the corresponding sequences, which can be realized in two different ways (e.g., *mmmr* and *rmmm*). On isomerizing the syndiotactic polymer (e.g., *10101*) three new signals still with the 2:2:1 ratio are observed, the third being due to the pentad *rmmr* (*10001*) and the others to *mrrr* (*00101*) and *mmrr* (*11101*). The peak common to both polymers is thereby identified as *mmrr*, and thus the remaining signals (*mmmr*, *mrrr*) can be assigned by default. The missing pentads were tentatively assigned on the basis of the so-called "necessary" pentad intensity relationships (cf., Section II-D).

Zambelli, Locatelli, Bajo, and Bovey (143) proposed assignment of the pentads by comparison with the spectra of two diastereomeric mixtures of the 3,5,7,9,11,13,15-heptamethylheptadecane enriched in ^{13}C on the 9-methyl. In the synthesis, which started from optically active precursors of known configuration, a selection of the stereoisomers occurred, which permitted the assignments to be made by means of intensity criteria. These authors reached the same conclusions as Stehling and Knox. A parallel analysis was effected with the methylene subspectrum by using 2,4,6,8,10,12-hexamethyltridecane enriched in ^{13}C at position seven (144, 145).

These assignments were rationalized according to two different schemes that consider only configurational or only conformational contributions. The latter will be discussed in Section IV-B. With regard to the former, an upfield shift was attributed to the presence of methyl groups having the opposite notation—in the Price sense—with respect to the observed methyl (placed at the center of the sequence) and in its close proximity. In fact, the signal at lowest field in the methyl region belongs to the *11111* (*mmmm*) pentad and that at highest field to *00100* (*mrrm*). This regularity is followed by all the pentads; the order of appearance is *11111* > *11110* > *01110* > *11101* > *11100* \approx *01101* > *01100* > *10101* > *10100* > *00100*. In terms of *m/r* nomenclature the order is *mmmm* > *mmmr* > *rmmr* > *mmrr* > *mmrm* \approx *rmrr* > *rmrm* > *rrrr* > *mrrr* > *mrrm* (146). It should, however, be noted that this prediction is valid only within a limited range of experimental conditions—in particular when the NMR spectrum is recorded at high temperatures (130–140°C).

A deeper understanding of the ^{13}C NMR spectrum of polypropylene was obtained through the use of hemiisotactic polypropylene, **58**, already mentioned (101). The strictly limited number of sequences (see Tables 2 and 5) greatly simplifies the spectrum, eliminating the major part of peak overlapping, especially in the methyl region; furthermore, its high solubility permits the use of

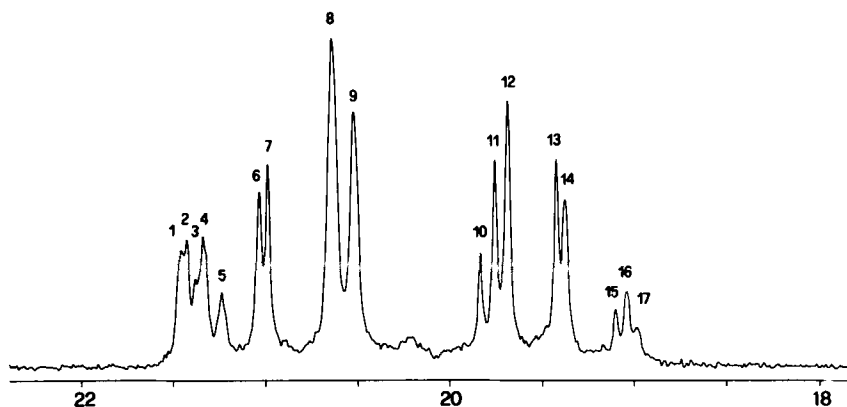


Figure 8. Methyl region of 50.3 MHz ^{13}C NMR spectrum of hemiisotactic polypropylene run at room temperature.

better resolution conditions, different from those generally used for conventional polypropylenes.

The CH_3 subspectrum recorded at 50.3 MHz at room temperature consists of 17 signals between 19 and 21.9 ppm from TMS (Figure 8), thus indicating a sensitivity towards sequences longer than heptads, (of which there are only 14, cf. Table 2). The assignment of the signals was carried out on the basis of the intensity ratios (see Table 4, column 5, $\alpha = 0.5$) and by comparison with the heptad chemical shifts calculated by Schilling and Tonelli (147). For the present purpose, attention should be focused on the signals 15–17. All three are derived from the *mrrm* pentad: On applying the selection rules valid for this polymer as discussed in Sect. II-D, it can be shown that this pentad gives rise to only three undecads (cf. Table 5). Consequently the three signals must be assigned to the *rrmmrrmmrr*, *mmmmrrmmrr*, and *mmmmrrmmmm* undecads. Similarly, signal 2 is attributed to *mmmmmmmmrr* and signal 3 to *rrmmmmmmrr*. At this moment these are the longest nonhomosteric sequences conclusively determined in a macromolecular compound.

Stereosequence analysis of common vinyl polymers both by ^1H NMR (or ^{19}F NMR for the fluorinated analogs) and by ^{13}C NMR have been reported and discussed on several occasions (11, 17, 118). Among the more detailed studies in this field attention is drawn to the 100.6-MHz ^{13}C NMR spectrum of atactic poly(vinyl alcohol) reported by Ovenall (148). The spectrum of the methine carbon observed in $\text{Me}_2\text{SO}-d_6$, presents 21 signals in the 64 to 68-ppm region (Figure 9) and thus shows a clear differential sensitivity towards the microstructural environment. Starting at high field, one finds 3 well-separated signals corresponding to the 3 *rr*-centered pentads, then a set of 8 signals due to the 16 *mr*-centered heptads, and lastly 10 signals due to the 10 *mm*-centered heptads,

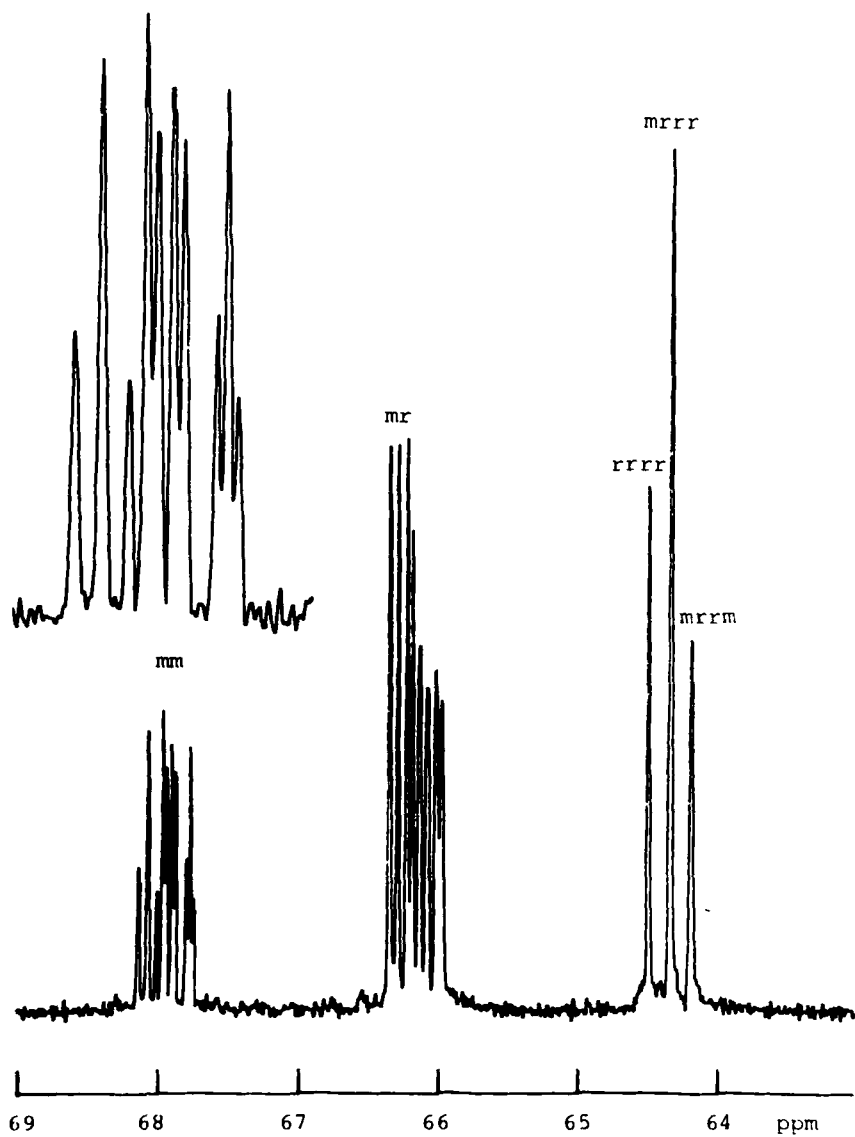


Figure 9. 90 MHz ^{13}C NMR spectrum of atactic poly(vinyl alcohol) (148). From Ovenall, D.W. *Macromolecules* **1984**, *17*, 1458. Copyright (1984) American Chemical Society.

6 of which have been assigned. The methylene spectrum recorded in D_2O is also very detailed: Of the 15 signals 12 have been assigned to single hexads or groups of hexads.

Stereochemical analysis of 1H and ^{13}C NMR has been accomplished for the polymers of butadiene, isoprene, and other dienes, for polymers containing heteroatoms in the main chain, and for vinyl and diene copolymers; lack of space precludes discussion of these interesting studies (11, 118).

In recent years new NMR techniques offering broad applications in stereochemical analysis have come into use. A prominent example is 2D-NMR (both 2D-resolved and 2D-correlated spectroscopy), which has been extensively applied to biopolymers (149–151). Its use with synthetic polymers has, until now, been limited to but a few cases (152, 153). A further technique, cross-polarization magic-angle spinning spectroscopy (CP-MAS NMR) will be discussed in the section on conformational analysis of solid polymers.

Among recent results obtained in this field, the 2D spectra of poly(methyl methacrylate) reported by Schilling et al. (153a), and which pertain to a polymer discussed extensively in the present article, should be mentioned. COSY (proton chemical shift correlation) and NOESY (proton NOE correlation) 2D spectra were recorded at 500 MHz on samples of isotactic and atactic (prevailing syndiotactic) poly(methyl methacrylate). Previous peak assignments were confirmed by this technique; in addition, a long range coupling constant—not detectable in the 1D spectrum—was observed between the CH_3 protons and one of the protons of the adjacent methylene groups, in particular to the proton that is erythro to methyl. Such a coupling constant should arise from a W-shaped four-bond arrangement of the coupled nuclei or, in other words, from a transplanar three-bond disposition of the methyl group with respect to the methylene hydrogen. This finding is consistent with a trans zigzag, or nearly trans, conformation of the main chain, similar to that observed by Tadokoro and co-workers in the crystalline state (153b).

IV. CONFORMATIONAL ANALYSIS

In stereochemical language the term conformation indicates every arrangement of atoms in space compatible with a given connectivity and configuration. Specification of each conformation is expressed in terms of internal coordinates: bond distances, bond angles, and dihedral angles (or torsion angles or rotation angles around single bonds). Torsion angles are the parameters that most directly determine molecular shape and, as a consequence, conformations are usually described as a function of torsion angle. Conformational analysis permits the determination, experimentally or by calculation, of the relation between structure and energy and, hence, of the relation between structure and chemical and physical behavior.

All this is true both for low molecular weight compounds and for polymers. However, relevant differences are found not only in specific structural features, but also in the different intent with which the analysis is carried out. In common organic stereochemistry, attention is essentially on reactivity: Many aspects of regio- or stereoselectivity, as well as reaction rate, can be explained or predicted in terms of conformation. In contrast, in polymers, the focus of interest is almost always on the physical (or mechanical) properties. It should not be forgotten that polymers are principally used as materials (plastics, fibers, elastomers, etc.) and that their properties are sometimes modified during fabrication. The fabrication process may induce the formation of particular structures at the molecular and supermolecular level, which can often be traced back to conformational factors.

Experimental evidence of the presence of certain local conformations is generally not readily available (it is quite rare, in polymers, to find cases where torsion angle values can be obtained from vicinal coupling constants) and it is not even easy to experimentally determine the energy differences among different conformations, because of the enormous number of states to be considered. Consequently, the most common way to investigate macromolecular conformations is to identify a structural model by calculation and then to verify its validity by suitable experiments. In addition to the typical structural methods (X-ray, electron and neutron diffraction, IR and NMR spectroscopy, chiroptical methods, etc.) other physical methods can be used that allow the determination of overall properties of the macromolecule: I refer here particularly to the measurement of the average dimensions of the molecule obtained by hydrodynamic methods or by light scattering.

The calculations are usually made using methods of molecular mechanics applied to an appropriate segment of chain. In its most general form conformational energy is calculated as the sum of contributions from bond stretching (E_b), bond angle deformation (E_r), rotation around single bonds (E_θ),* interactions between nonbonded atoms or van der Waals interactions (E_{nb}), hydrogen bonds, dipolar interactions, electrostatic factors, and so on.

For hydrocarbon and hydrocarbonlike polymers usually only four terms are considered

$$E_{\text{conf}} = E_b + E_r + E_\theta + E_{nb}$$

and, in some cases, only the rotational (E_θ) and van der Waals (E_{nb}) contributions. The E_b contribution is almost always negligible; E_r assumes importance only in highly crowded polymers [polyisobutene, poly(methyl methacrylate)].

*Editors' footnote: The convention adopted in polymer chemistry (21)— τ for bond angle, θ for torsion angle—will be used in this article. It is opposite to the usage commonly adopted by crystallographers and others in the description of small molecules.

When introduced into calculations these two terms are treated according to a harmonic approximation (b = bond distance, τ = bond angle; see footnote on p. 43):

$$E_b = \frac{1}{2} k_b \Delta b^2 \quad \text{and} \quad E_\tau = \frac{1}{2} k_\tau \Delta \tau^2$$

The rotational contribution is expressed in Pitzer's classical form (θ = torsion angle; see footnote on page 43.):

$$E_\theta = \frac{1}{2} E_0 (1 + \cos 3\theta)$$

while for the interaction between the nonbonded atoms either Lennard-Jones or Buckingham's expressions are applied (r = distance between nonbonded atoms):

$$E_{nb} = A/r^{12} - B/r^6 \quad \text{or} \quad E_{nb} = A \exp(-Cr) - B/r^6$$

(This energetic contribution must be considered for all pairs of atoms in the system.)

According to the IUPAC recommendations (21) the torsion angle θ in an A-B-C-D sequence is considered positive when, with the system being observed along the central B-C bond, the rear atom D is rotated clockwise with respect to the front atom A. The value $\theta = 0^\circ$ is chosen for the completely eclipsed conformation (154). Conformations where atoms A and D form an angle near 60° are indicated by the letter G (gauche) or G^+ , those having $\theta \approx 180^\circ$ by T (trans), and those where $\theta \approx 300^\circ$ (or -60°) by \bar{G} or G^- . (Properly speaking, G and \bar{G} are enantiomeric gauche conformations of unspecified sign.)

Examination of models easily convinces one that, even for simple molecules such as linear hydrocarbons, there exists a strong correlation among the rotations about two adjacent C-C bonds and that the energy cannot always be considered the sum of the contributions corresponding to each rotation. For this reason simple diagrams of E vs. θ , like that often seen for butane, are not used in the macromolecular field. It is preferable to represent the state of the system by square maps in which the values of the variables θ_1 and θ_2 are placed on the axes and the energy is represented by a series of contour lines.

In Figure 10 is shown the conformational map of n -pentane from energy level 0 ($\theta_1 = \theta_2 = 180^\circ$, conformation TT) to 6 kcal mol $^{-1}$. The representation is not symmetrical with respect to the median lines: For $\theta_1 = 60^\circ$ and $\theta_2 = 60^\circ$ (conformation G^+G^+) a well is observed whereas for $\theta_1 = 300^\circ$ and $\theta_2 = 60^\circ$ (G^-G^+) the molecule has a high energy content corresponding to the approach of the two methyls within a distance of $< 3 \text{ \AA}$ (157).

In a macroscopic sample the molecules are arranged inside the boundary line

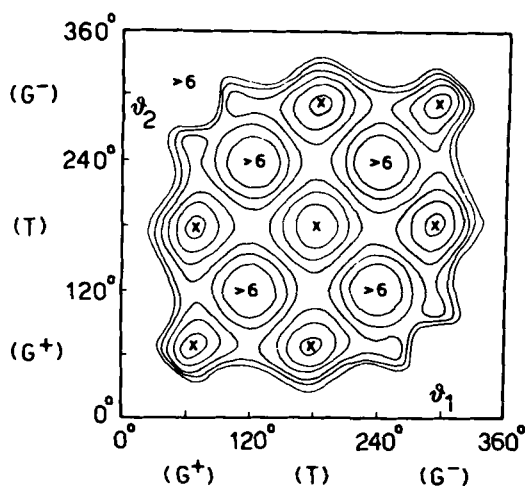


Figure 10. Conformational map of *n*-pentane. Energy unit: kcal mol⁻¹. From ref. (156): Copyright Hühig and Wepf, Basel.

of the map in a nonuniform way. The highest concentrations correspond to the energy minima according to Boltzmann's distribution [$x_i \propto \exp(-E_i/RT)$]. In an equivalent manner, one can say that a molecule of *n*-pentane resides in the various conformations for lengths of time proportional to Boltzmann's statistical weights for the pertinent energy contours.

A very common approximation goes by the name of "rotational isomeric state model" (RIS). With such a model it is assumed that the molecular population is placed exclusively in a few energy minima, always according to the Boltzmann distribution. The conformations corresponding to the minima are called conformers, or rotational isomers, and are indicated by one or more letters (G, T): for butane three conformers are considered (G⁺, T, G⁻), for pentane five (TT, G⁺T, TG⁻, G⁺G⁺, G⁻G⁻). A more detailed examination of pentane reveals the existence of two further wells ($\theta_1 = 65^\circ$, $\theta_2 = 260^\circ$ and $\theta_1 = 100^\circ$, $\theta_2 = 295^\circ$), sometimes indicated by G⁺G^{*-} and G^{*+}G⁻, respectively, close to the forbidden G⁺G⁻ conformation, but with a much lower energy (157, 158).

It should be observed that theoretical conformational analysis refers to an isolated molecule that has no interaction with the adjacent ones. This assumption is appropriate for low molecular weight compounds in the gas phase. For macromolecular compounds particular conditions are known under which the interactions with the environment are minimized. In any case, such interactions are considered to be of higher order, to be introduced into calculations only where necessary.

The two main fields of application of conformational analysis concern the

prediction of the crystalline structure of stereoregular polymers and the determination of the conformational equilibrium of polymers in the amorphous state, in the melt or in solution. Given the different methodology in the two fields, the two situations will be described separately.

A. Conformations of Crystalline Polymers

The most relevant property of stereoregular polymers is their ability to crystallize. This fact became evident through the work of Natta and his school, as the result of the simultaneous development of new synthetic methods and of extensive structural investigations. Previously, the presence of crystalline order had been ascertained only in a few natural polymers (cellulose, natural rubber, balata, etc.) and in synthetic polymers devoid of stereogenic centers (polyethylene, polytetrafluoroethylene, polyamids, polyesters, etc.). After the pioneering work of Meyer and Mark (70), important theoretical and experimental contributions to the study of crystalline polymers were made by Bunn (159–161), who predicted the most probable chain conformation of linear polymers and determined the crystalline structure of several macromolecular compounds.

Except in globular proteins, the unit cell of a crystalline polymer has relatively reduced dimensions and contains only a small portion of the macromolecule. Hence the chain should extend across numerous unit cells (along the *c* axis), repeating for each cell a structural disposition identical (or isomorphous) to that observed in the adjacent cells. Inside each cell there can be elements of symmetry that further reduce the structural possibilities of the single chains. These considerations, together with a wide examination of the existing structures, led Natta and Corradini to the formulation of the principle of equivalence (32, 47): The conformation of the chain in the crystalline state is defined by a succession of equivalent structural units. The structural unit in general coincides with one or with one half of a monomer unit; successive structural units occupy geometrically equivalent positions with respect to a crystallographic axis. It should be pointed out that this principle of equivalence is often verified but is not necessary to ensure order along the chain; it may be considered as a very useful working hypothesis in determining the crystalline structure of polymers.

The second guideline in this field is the principle of minimum conformational energy: In the crystal state the polymer conformation coincides or almost coincides with the most stable conformation predicted for an isolated macromolecule. This principle is reached by a series of successive approximations, the first of which consists in ignoring the *PV* and *TS* factors and in relating the stability of the crystal to its internal energy; the second in ignoring chain-chain interactions, and in considering the macromolecular conformation under the restrictions imposed by the equivalence principle. These approximations are valid when only one well-defined energy minimum exists. If the minimum is

wide and flat or if two or more minima with comparable energy exist, packing factors can change the chain conformation in the crystal from that predicted for the isolated chain.

Crystalline stereoregular polymers have been discussed several times by Natta and Corradini (3, 32, 47). More recently they have been reviewed by Wunderlich (162) and Tadokoro (163).

In 1960, extending the earlier study done by Klug, Crick, and Wyckoff (164), Corradini singled out the linear repetition groups within which the chains of crystalline polymers may be classified (47, 165). He took into consideration only those symmetry operations that leave the chain axis unchanged, with the exception of r , the rotation around the same axis. The corresponding elements of symmetry are t , axis of translation coincident with the chain axis; i , inversion center; m and d , mirror planes perpendicular and parallel, respectively, to the chain axis; 2 , binary axis perpendicular to the chain axis; c , mirror glide plane along the chain axis; $s(M/N)$, helical axis corresponding to a rotation of $2\pi N/M$ around the chain axis combined with a translation along the axis equal to $1/M$ of the repetition period. Only 13 combinations of these elements [or 15 if one considers as independent groups the particular cases $t\ 1$ and $t\ 2$ obtained from $s(M/N)\ 1$ and $s(M/N)\ 2$ when $(M/N) = 1$] are possible. They are summarized in Table 6.

In the crystal state most stereoregular polymers have helical conformations. Group $s(M/N)\ 1$ comprises all the isotactic vinyl polymers [polypropylene, polybutene, polystyrene, etc., $M/N = 3/1$; poly-*o*-methylstyrene, etc., $4/1$;

Table 6
Line Repetition Groups for Crystalline Polymers

Line Group	Examples
$t1$	<i>1,4-Trans</i> -polyisoprene
$s(M/N)1$	Isotactic polypropylene ($M/N = 3/1$)
$t2$	—
$s(M/N)2$	Syndiotactic polypropylene (helical form)
tm	Nylon 77
tc	Poly(1,1-difluoroethylene) (form 2)
ti	Erythro-diisotactic poly(ethylene- <i>alt</i> -2-butene)
td	—
$s(2/1)m$	Poly(1-pentenylene) (or polypentenamer)
$s(2/1)d$	Nylon 66
tdm	—
tid	—
tcm	Syndiotactic 1,2-polybutadiene
tic	1,4- <i>Cis</i> -polybutadiene
$s(2/1)dm$	Polyethylene

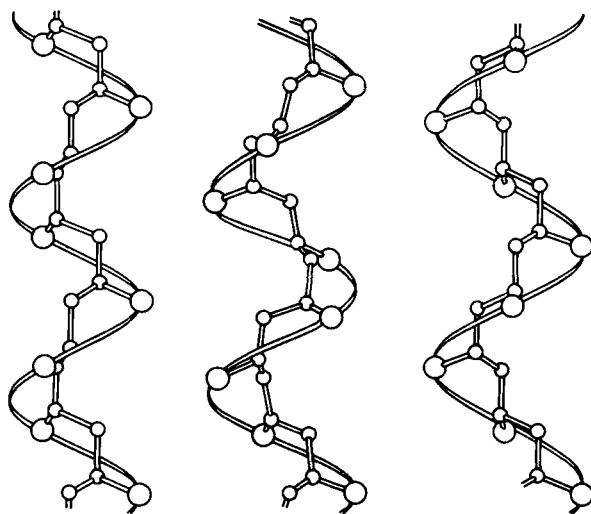


Figure 11. 3/1, 7/2, and 4/1 helical conformations of isotactic polymers in the crystalline state. From ref. (166): Copyright Soc. Chim. Ital.

poly-4-methylpentene, 7/2; poly-*m*-methylstyrene, 11/3; poly(*iso*-propyl vinyl ether) 17/5] (32, 47, 166) (Figure 11) and is also represented by the conformation of many important natural polymers such as the α -helix of proteins ($M/N = 18/5$) (167). In their turn, groups *t c*, *t c m e s* ($M/N = 2$) are compatible with syndiotactic vinyl structures (47, 168): Syndiotactic polypropylene is dimorphic and its crystalline modifications have a zigzag planar conformation (*t c m*) (169) or a twofold helix with a perpendicular symmetry axis [*s*(2/1) 2] (170) (Figure 12).

The importance of the helix in polymer organization in space requires a more detailed examination of the relation among the geometrical parameters of the helix (h : unit height, *i.e.*, the translation along the helix axis per repeating unit, $h = \vec{c}/M$, where \vec{c} is identity period; t : unit twist, *i.e.*, the angle of rotation about the helix axis per repeating unit, $t = 2\pi N/M$) and the conformational parameters (b , τ , θ). Beginning with the work of Shimanouchi and Mizushima (171) and Hughes and Lauer (172) various authors have proposed formulas valid for the different cases (47, 163, 173, 174).

The relationship for an isotactic vinyl chain characterized by two chain bonds b_1 and b_2 , two valency angles τ_1 and τ_2 , and two dihedral angles θ_1 and θ_2 under helical symmetry conditions [*s*(M/N) 1] is

$$h = \frac{b_1(A - \cos t - B \cos \theta_1)^{1/2} - b_2(A - \cos t - B \cos \theta_2)^{1/2}}{2^{1/2} \sin(t/2)}$$

$$1 + 2 \cos t = A(1 + \cos \theta_1 \cos \theta_2) - B(\cos \theta_1 + \cos \theta_2) \\ - (\cos \tau_1 + \cos \tau_2) \sin \theta_1 \sin \theta_2 + \cos \theta_1 \cos \theta_2$$

where $A = \cos \tau_1 \cos \tau_2$ and $B = \sin \tau_1 \sin \tau_2$.

Assuming $b_1 = b_2 = 1.54 \text{ \AA}$, $\tau_1 = \tau_2 = 114^\circ$, $\theta_1 = 180^\circ$ (T) and $\theta_2 = 60^\circ$ (G^+) [or $\theta_1 = 300^\circ$ (G^-) and $\theta_2 = 180^\circ$ (T)], then $t = 120^\circ$ is obtained in agreement with the presence of a $3/1$ helix (left or counterclockwise in the first case, right or clockwise in the second) and $h = 2.17 \text{ \AA}$ identical to that found in the fiber spectrum of isotactic polypropylene. The left helix can, therefore, be represented by $G^+T|G^+T|G^+T|G^+T|$ and the right by $|TG^-|TG^-|TG^-|TG^-|$ where the vertical lines indicate the position of the tertiary atom.

Calculations of conformational energy made by means of molecular mechanics fully confirm these conclusions. Such calculations were first introduced into the examination of synthetic crystalline polymers by Liquori and co-workers (175, 176) and were extensively used by Natta, Corradini, Allegra, Ganis, and co-workers (168, 177-179). The conformational energy map of isotactic poly-

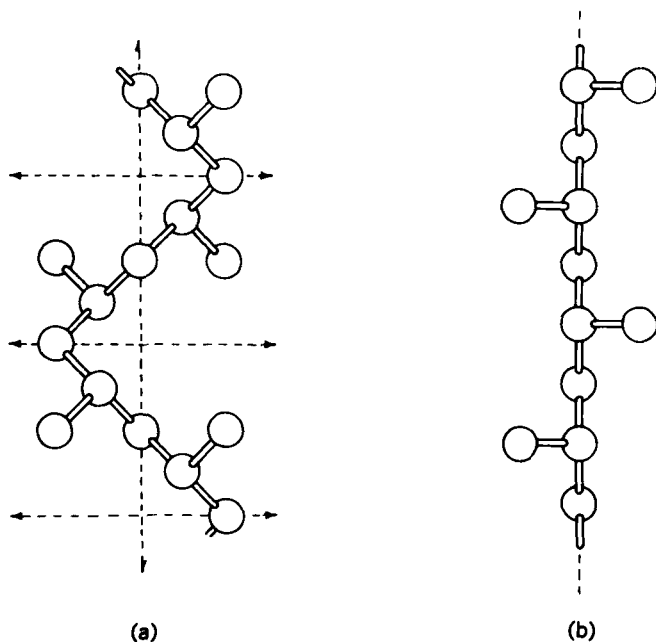


Figure 12. Helical (a) and zigzag (b) conformations of crystalline syndiotactic polypropylene. From ref. (168); Copyright Accad. Naz. Lincei.

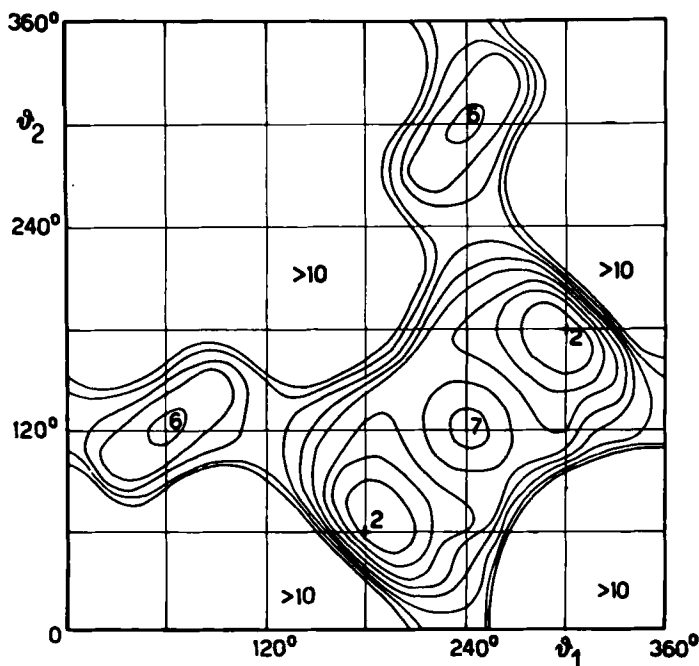


Figure 13. Conformational map of isotactic polypropylene in the crystalline state. Energy unit: kcal per mole of monomer units. From ref. 177: Copyright Hüthig and Wepf, Basel.

propylene, under the constraint of the equivalence principle (which in this case is expressed by imposing a succession of a pair of torsion angles $\theta_1, \theta_2, \theta_1, \theta_2$, etc.) is shown in Figure 13. The two minima of equal depth visible in the figure coincide with the torsion angles described previously. Analogous maps are obtained for a wide series of poly- α -olefins having substituents different from methyl. Sometimes rather wide energy wells are observed, in other cases two very close minima (180) exist. The low energy region is placed at θ_1 and θ_2 values compatible with one or even more types of helices (3/1, 7/2, 4/1, etc.). This fact justifies the presence of different crystalline modifications sometimes observed for the same polymer (e.g., poly-1-butene).

For syndiotactic polypropylene, the structural repeating unit should contain at least two monomer units. The equivalence principle leads to the following relation between the torsion angle: $\theta_1, \theta_2, \theta_2, \theta_1$, and so on. The energy map calculated is shown in Figure 14 (177). Angles θ_1 and θ_2 refer to the two bonds emanating from the group $-\text{CH}(\text{CH}_3)-$. Three almost equivalent energy minima are observed: two ($\theta_1 \approx 180^\circ, \theta_2 \approx 60^\circ$ and $\theta_1 \approx 300^\circ, \theta_2 \approx 180^\circ$) correspond to the two enantiomorphous helices with symmetry $s(2/1) 2$

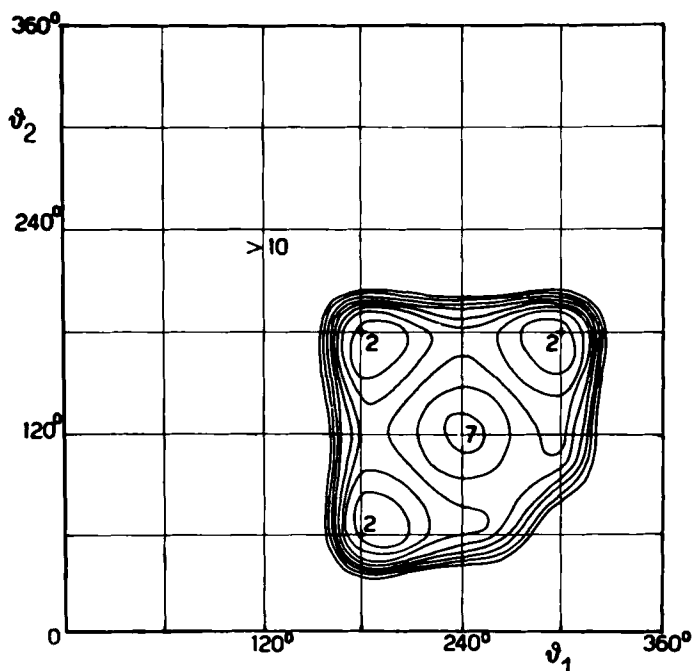


Figure 14. Conformational map of syndiotactic polypropylene in the crystalline state. Energy unit: kcal per mole of monomer units. From ref. (177): Copyright Hüthig and Wepf, Basel.

$|\text{TT}|\text{G}^+\text{G}^+|\text{TT}|\text{G}^+\text{G}^+|\text{TT}|$ and $|\text{G}^-\text{G}^-|\text{TT}|\text{G}^-\text{G}^-|\text{TT}|\text{G}^-\text{G}^-|$; the third ($\theta_1 = \theta_2 = 180^\circ$) to the zigzag planar form $|\text{TT}|\text{TT}|\text{TT}|\text{TT}|$ (symmetry tcm) (Figure 12). The dimorphism of syndiotactic polypropylene, therefore, finds an adequate explanation on a conformational basis: It is interesting to observe that this phenomenon was first recognized theoretically (173) and only later verified experimentally (169, 170).

It might be argued that a simple principle like that of staggered bonds, which takes into consideration only T and G conformations (32, 159) might be sufficient to explain the structure of synthetic crystalline polymers. This is true if one considers macromolecules with moderate steric hindrance where the torsional term is the determining factor for the position of energy minima; but on examining vinylidene polymers, $-\text{CH}_2-\text{CR}_1\text{R}_2-$, or in general polymers with bulky substituents, the energy term due to nonbonded interactions can have a very large value in the staggered conformations and can thereby provoke a displacement of the preferred geometry from the classical 60 and 180° angles. In such a case a concomitant strong variation of the valency angles $\text{C}-\text{CH}_2-\text{C}$ is observed. An accurate analysis of a situation of this type was undertaken for

polyisobutene by Allegra, Benedetti, and Pedone (181), using conformational calculations and crystallographic data from low molecular weight models. This polymer has a very long repetition period along the chain axis (18.6 Å) and contains eight monomer units per cell. The best model from the conformational point of view is a 8/3 helix with the valency angle C—CH₂—C equal to 124° and torsion angles of $\theta_1 = 23.3^\circ$, $\theta_2 = 132.5^\circ$.

Tanaka, Chatani, and Tadokoro improved this model by refining the crystal structure of polyisobutene (182). The resulting structure is a 2/1 helix in which the structural unit contains four nonequivalent monomer units. In the crystal cell there are always eight monomer units arranged in three turns but the 8/3 helical symmetry is no longer retained. This example represents one of the most notable exceptions to the equivalence principle. Displacement from the exact helical conformation is small, however, and all the pairs of torsion angles fall inside the same energy well.

Isotactic poly(methyl methacrylate), also, is an intricate case, resolved only after a 20-year debate. The repetition period along the chain axis is 10.40 Å corresponding to 5 monomer units; the entire cell contains 20 monomer units (four chains). At first, the structure was resolved as a 5/1 helix (183) with $\theta_1 = 180^\circ$ and $\theta_2 = -108^\circ$ but no reasonable packing was found using this assumption. Further conformational calculations showed that helices like 10/1 or 12/1 should be more stable than the 5/1 helix. The structure was solved by Tadokoro and co-workers (153b) who proposed the presence of a double helix. Two chains, with the same helical sense and the same direction but displaced by 10.40 Å one from the other are wound on each other, each chain having 10 monomer units per turn [$s(10/1)$] and a 20.80-Å repeat period. As a result, the double helix has a 10.40-Å translational identity period, identical to that found in the fiber spectrum. The conformational parameters are $\theta_1 = 179^\circ$ and $\theta_2 = -148^\circ$. Energy calculations indicate that the double helix is more stable by 4.4 kcal per mole of monomer units than two isolated 10/1 helices, a result that is in line with the well-known capacity of this polymer to form complexes in solution (184).

Among the uncommon structures of stereoregular polymers determined in recent times, is that of isotactic polystyrene first observed by Keller and co-workers in crystalline gels (185) and later studied by Corradini et al. (186). In this case too, a highly stretched helix [$s(6/1)$] is observed, with unit height $h = 5.1$ Å and unit twist $t = 60^\circ$. The repeating unit contains two independent monomer units with rotation angles close to 180°.

B. Disordered Conformations

Most linear polymers have a flexible chain in which every monomer unit is able to assume more than one low energy conformation by rotation around single

bonds. When the structural defects of the polymer or the thermodynamic or kinetic factors (linked, for example, to the temperature or to the presence of a solvent) inhibit crystallization, all these states are populated and the chain assumes a disordered form, described as a random coil. In solution, or in the fluid state in general, every macromolecule unceasingly changes its form, going from one conformation to another, the whole system consisting of a mixture of macromolecules of different conformation, the composition of which corresponds to that of the free energy minimum. One should refer to this description when discussing the properties of polymers in the amorphous state, in the melt, or in solution. For example, rubber elasticity can be interpreted as a transition from totally disordered to partially oriented conformations involving essentially only an entropy change. All this explains the importance that this subject has assumed within polymer science.

The theoretical and methodological aspects of conformational analysis of macromolecular chains in the disordered state were discussed by Flory in his classic book (155, 187). The literature on the subject includes a large number of books and reviews (37, 39, 188-190); extensive discussions may also be found in general textbooks of macromolecular science (9, 12, 13, 191).

The principal aim of research in this area is that of relating the local conformation of the chain with the average overall properties of the macromolecule, in particular with its mean-square radius of gyration $\langle s^2 \rangle$ or with its mean-square end-to-end distance $\langle r^2 \rangle$, and of their temperature coefficients. $\langle s^2 \rangle$ is experimentally accessible through measurements of viscosity in solution or through light scattering. To a traditional stereochemist, used to dealing with molecules having an exactly defined structure or endowed with a low degree of freedom, this treatment appears, to a certain extent, arbitrary and devoid of checks for self-consistency. Apart from the approximations introduced (limited number of states under consideration, elimination of interactions beyond those of the first and second order, etc.) the relatively high number of adjustable parameters might suggest that the method has been adapted to fit the desired aims and that it has no general validity. This objection is, however, gradually overcome as verification from different sources accumulates. For example, the same treatment with the same parameters can be successfully used for the prediction of $\langle s^2 \rangle$, of the mean-square dipolar moment $\langle \mu^2 \rangle$, of the epimerization equilibrium, of the ^{13}C chemical shift, and so on.

It is generally recognized that the average dimensions of a macromolecule are dependent on two factors: one related to short distance interactions, those to which conformational analysis is applied, and one concerned with long distance interactions that are often considered in terms of excluded volume effects or covolume effects. One may, therefore, put:

$$\langle r^2 \rangle = \alpha^2 \langle r^2 \rangle_0$$

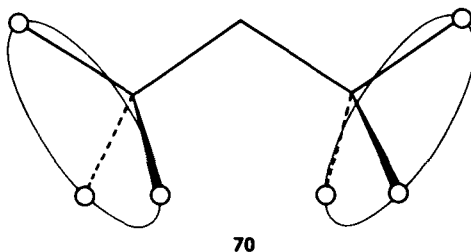
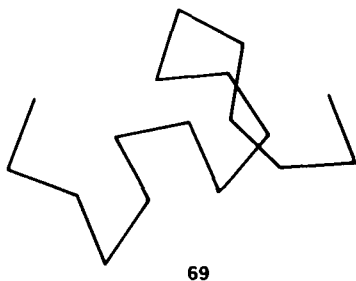
where $\langle r^2 \rangle_0$ is the unperturbed mean-square end-to-end distance and α is a perturbation coefficient that takes into account both the polymer volume itself and the interactions with the solvent, which effect is particularly important in dilute solution and with "good" solvents.

It is however possible to find conditions, called unperturbed or theta conditions (because for each polymer-solvent pair they correspond to a well-defined temperature called θ temperature) in which α tends to 1 and the mean-square distance reduces to $\langle r^2 \rangle_0$. In θ conditions well-separated chain segments experience neither attraction nor repulsion. In other words, there are no long-range interactions and the conformational statistics of the macromolecule may be derived from the energy of interaction between neighboring monomer units. For a high molecular weight chain in unperturbed conditions there is a simple relationship between the mean-square end-to-end distance $\langle r^2 \rangle_0$ and the mean-square radius of gyration $\langle s^2 \rangle_0$, both being proportional to the molecular weight (or to the molecular length). Following current symbolism we may write

$$\langle s^2 \rangle_0 = \frac{1}{6} \langle r^2 \rangle_0 \quad \text{and} \quad \langle r^2 \rangle_0 = C_\infty N b^2$$

where b is the bond length (or the root-mean-square value of different bond lengths occurring along the chain), N is the number of bonds and C_∞ is the asymptotic value of the so-called characteristic ratio containing the conformational information. C_∞ is generally comprised between 4 and 15 and changes smoothly with temperature.

The problem of conformational analysis of a chain is, therefore, that of calculating C_∞ . The approximation of the freely jointed chain, with no correlation between successive bonds, **69**, gives a value of $C_\infty = 1$. If one introduces into the model a constant value for the bond angles, but permits free rotation around the bonds (in the formula **70** all points of the base circumferences of the



two cones are equally probable), the value of C_∞ is between 2 and 2.2 depending on the τ value (109.47 or 112°) in accord with the equation:

$$C_\infty = \frac{1 - \cos \tau}{1 + \cos \tau}$$

A further expansion of the average dimensions of the coil results when one assumes that rotation around single bonds is not free but is still independent of the rotation around the adjacent bonds. Let us take as an example a polyethylene chain: On the base of each of the two cones of formula 70, three positions are identified, T, G^+ , and G^- , differently populated according to the energy difference $E = E_G - E_T$ and the temperature. The characteristic ratio is then written:

$$C_\infty = \frac{1 - \cos \tau}{1 + \cos \tau} \frac{1 - \langle \cos \theta \rangle}{1 + \langle \cos \theta \rangle}$$

where $\langle \cos \theta \rangle$ is the average value of $\cos \theta$ weighed proportionally to the population of each state:

$$\langle \cos \theta \rangle = \Sigma w_i \cos \theta_i$$

where $w_i = \exp(-E_i/RT)/\Sigma \exp(-E_i/RT)$.

Placing $E_T = 0$, $E_G = 500 \text{ cal mol}^{-1}$, $T = 413 \text{ K}$, $G^+ = 60^\circ$, $G^- = 300^\circ$ and $T = 180^\circ$, one obtains $C_\infty = 3.1\text{--}3.4$, still far from the experimental value ($C_\infty = 6.7$).

This model is, in any case, unacceptable: Examination of formula 70 shows that, according to what was previously stated regarding the *n*-pentane, in the G^+G^- conformation two carbon atoms approach to about 2.5 Å and consequently this conformation has little probability of existence. The introduction of correlation between adjacent rotation angles entails the use of a mathematical formulation (the matrix multiplication method) which will not be discussed here; the reader is referred to the texts cited and to the specialized literature for details.

From a stereochemical point of view the physical problem to be resolved (which antecedes that of calculation) consists in the identification of the rotational isomeric states to be considered and in the evaluation of their statistical weight, that is, their relative energy.

In a first approximation, interdependence among the rotations around successive bonds is expressed for polyethylene by putting the statistical weight of the G^+G^- sequences equal to zero. With respect to the preceding model a further increase in the value of C_∞ is then observed. A more detailed analysis (157)

considers the presence of the gauche distorted conformation G^* ($\theta = \pm 100^\circ$) already cited for the *n*-pentane. For the G^+G^{*-} sequence an energy of 3200 cal mol⁻¹ with respect to TT and a resulting small (but nonzero) statistical weight have been proposed. Calculations carried out on this basis allow the reproduction of the experimental C_∞ value as well as of its temperature coefficient.

The problem is further complicated for vinyl polymers with their problems of stereoisomerism. The first descriptions of the conformational state of isotactic polypropylene in solution go back 25 years (178, 179, 192, 193). Corradini, Allegra, and Ganis proposed a model, still essentially valid today, according to which macromolecules possess a local helical structure analogous to that observed in the crystalline state. The helix segments are rather short, only a few monomer units, after which an inversion of the helix sense occurs, with simultaneous alteration of its direction (Figure 15). As a whole this disordered con-

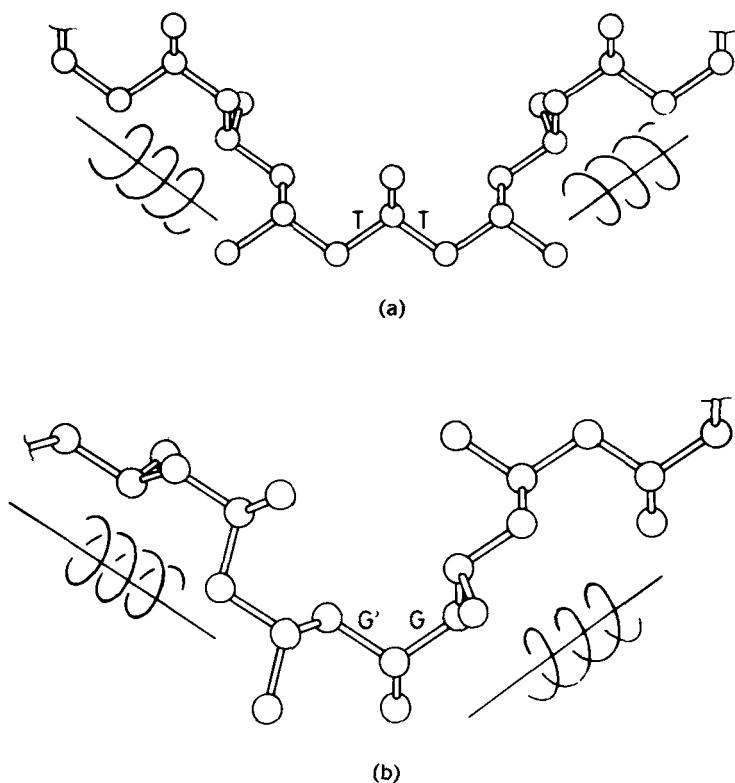
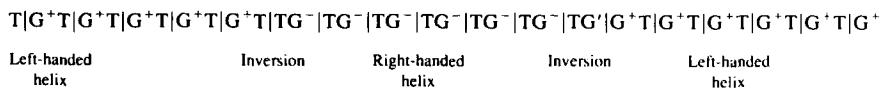
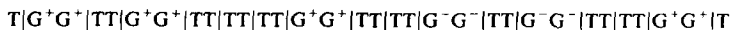


Figure 15. Models of helix inversion in isotactic polypropylene: (a) TT conformation; (b) G'G conformation. From ref. (178); Copyright Accad. Naz. Lincei.

formation may still be considered a random coil. For a single chain, the passage from clockwise to counterclockwise helix is not equivalent to the opposite passage due to the different orientation of the substituents with respect to the helical axis: In one case the inversion can be realized with a low energy barrier through a conformation close to TT; in the other case the passage requires high energy conformations, indicated as G', with θ values near $\pm 120^\circ$. Schematically the macromolecule may be shown as



For syndiotactic polypropylene analogous reasoning leads to a model characterized by zigzag chain segments bound on the two sides to right and left helical conformations, like those existing in its crystalline form (Figure 16) (179):



Flory, Mark, and Abe (194) carried out a statistical mechanics analysis of vinyl polymers on the basis of a three rotational state model. Energy maps have been calculated both for *m* and *r* dyads as a function of the rotation angles around the bonds astride the methylene groups (CHR—CH₂—CHR). These maps differ from those examined for crystalline polymers where rotations around

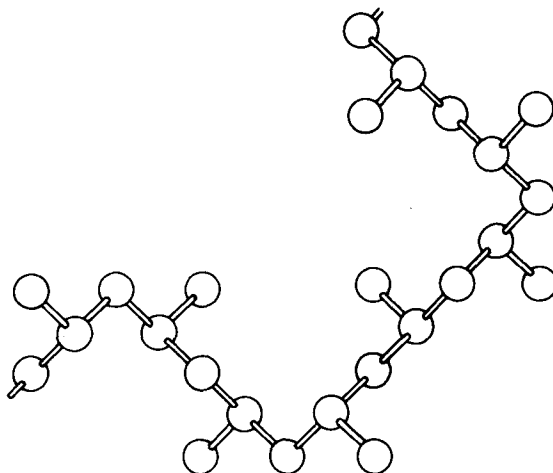


Figure 16. Model of a segment of syndiotactic polypropylene in a disordered conformation. From ref. (179); Copyright Hüthig and Wepf, Basel.

the bond astride the —CHR— group were considered and where a regular sequence, dictated by the equivalence principle, was imposed. The 3×3 matrix, which represents the statistical weights, is not symmetric due to the presence of the substituents and is different for m and r dyads.

The conformation of atactic polymers, with any value of the m/r ratio, must be treated as that of a copolymer, wherein the monomer unit statistics are compounded with those of the rotational states. In this case we may either refer to Monte-Carlo type procedures, as done by Flory, Mark, and Abe (194), or to the pseudostereochemical equilibrium method used by Allegra (195) and Brückner (196). In the latter case the atactic polymer is formally considered as a homopolymer that may assume the conformations of either the m or r dyads, with suitable adjusted statistical weights.

The value of C_∞ obtained by Flory, Mark, and Abe (194) for the perfectly isotactic polypropylene is far greater than the experimental estimate. Their conformational model is very rigid and gives a much larger preference to helical conformations than is actually found. This prompted the authors to postulate stereoirregular units in isotactic chains, the presence of which disrupts the predicted perpetuation of the preferred conformation through long sequences of units. Configurational defects in the chain should have been around 5–10% (expressed as r dyads). This assertion is not compatible with the most commonly accepted ^1H NMR results on the steric purity of isotactic polypropylene (197). It should be pointed out that using the simpler analysis proposed earlier by Allegra, Ganis, and Corradini (179) a much lower value of C_∞ is obtained (198).

The controversy was resolved on the basis of firm experimental data on the steric purity of polypropylene samples, mainly obtained by ^{13}C NMR spectroscopy (according to which the r dyad content does not exceed 2%) and of new conformational approaches due to Boyd and Breitling (200), Allegra, Calligaris, Randaccio, and Moraglio (201), and Suter and Flory (202). Boyd and Breitling derived the isomeric rotational states from minimization of the conformational energy of 2,4,6-trimethylheptane, conceived as a propylene trimer, thus accounting in detail for interactions between atoms separated by more than four bonds. Allegra and coworkers evaluated the full conformational integral in the continuum of the rotational states. The inherent limitations of the RIS method, especially when the energy minima are broad, are thus overcome, at least in principle. The calculations are carried out through a double Fourier transformation of the statistical weight of rotational pairs, followed by a matrix algorithm strictly isomorphous to that utilized in the RIS method (203). The continuum approach may be used in conjunction with that of a pseudostereochemical equilibrium to evaluate C_∞ for polypropylenes with varying degrees of stereoregularity (196).

Suter and Flory carried out their calculations taking into account the structure of the methyl substituent and identified 10 energy minima both for the m and r

dyad (202). Geometry and energy values were averaged within extended regions of the conformational map around each minimum. In this way, a model was proposed with 5 (no longer 3) rotational states around each bond, having $\theta = 75^\circ$ (G^+), 110° (G^*), 130° (T^*), 165° (T) and 295° (G^-), respectively. In the 5×5 matrix of the statistical weights, 10 nonzero values are introduced, corresponding to the 10 energetically allowed combinations of rotation angles. This matrix is multiplied by a second matrix, to account for the higher-order interactions. A more flexible model results that gives good agreement with the experimental value of C_∞ and of its temperature coefficient for isotactic polypropylene.

The Suter-Flory model was successfully used to interpret the results of the epimerization reaction carried out on propylene oligomers (204) and on polypropylene itself (106, 205). In both cases a slight prevalence of the r dyad over the m (52/48) is observed. The epimerized polypropylene has a microstructure almost coincident with a Bernoulli distribution and represents the polymer sample closest to an ideal atactic polymer so far obtained.

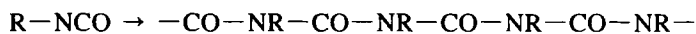
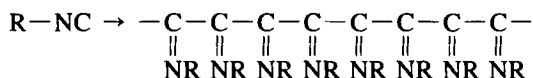
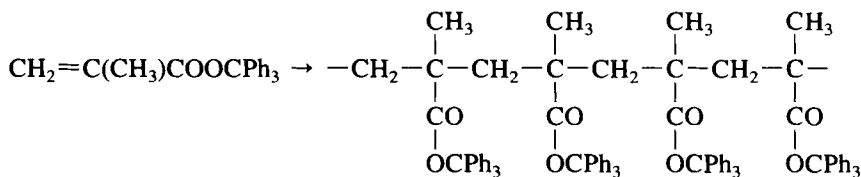
In Section III-B we showed that the chemical shift of methyl carbons in polypropylene can be calculated considering the relative position of the adjacent substituents, expressed in configurational terms (m or r , 0 or 1). An alternative interpretation, with a better physical basis, takes into account only conformational aspects. Experimental evidence from hydrocarbon spectra has established that the presence of a gauche conformation between carbon atoms separated by three bonds causes an upfield shift (γ effect) (206). For flexible molecules the magnitude of this shift depends on the fraction of conformers having gauche interactions with the observed carbons (207).

Earlier studies had shown that the chemical shift of the methyl carbons of mm , mr , and rr triads could actually be predicted by evaluating, in a semi-quantitative way, the number of gauche $CH_3 \dots CH$ three-bond interactions in each sequence (208). Extensive calculations regarding both the methyl carbon in odd sequences and the methylene carbon in even sequences, were made by Ferro and co-workers (144, 145, 209) and by Tonelli (147, 210) using different conformational models. For each stereochemical sequence the conformational equilibrium was determined and the chemical shift was calculated by means of the γ effect without applying any additional configurational information. Their results are almost coincident and are in excellent agreement with independent signal attributions. This method was also applied to predict the ^{13}C NMR spectrum of polymers other than polypropylene (211, 212).

C. New Methods and New Problems

Until now I have described the classical approach to polymer conformation. In today's research, however, new interests arise and novel methodologies are applied, both calling for further comments.

Not all polymers in solution assume the mobile disordered conformation broadly defined as random coil; some can be compared to a rigid rod. Their structural features are fairly easily predicted: The presence of cyclic units in the main chain, a limited number of single bonds around which rotation is possible, high energy barriers that further limit conformational mobility. Typical examples are the aromatic polyamides (Aramide polymers), which have a practical use as ultrahigh module fibers (213). This type of polymer often forms mesophases in a limited temperature range (thermotropic liquid crystals) or in the presence of solvents (lyotropic liquid crystals); in both cases a marked molecular orientation is maintained. The use of preoriented liquid crystals in the spinning process is a favorable condition for oriented crystallization and for obtaining fibers with outstanding mechanical properties. Polyalkylisocyanates may be considered very simple rodlike polymers (214–217) **71**. Their structure corresponds to that of a *N*-substituted Nylon-1. Distortion from planarity has been postulated for these polymers. The conformation in the crystal can be described as 8/3 helix; the same conformation, at least in part, persists in solution. The rigid character of polyalkylisocyanates is particularly evident in low molecular weight fractions: By increasing the molecular weight hydrodynamic behavior changes to that of semirigid polymers and finally to that of random-coil polymers (217a). Among the polymers that exist in solution as rigid helices, of notable interest are polymers whose chirality is of purely conformational origin, such as polyimino-methylenes, **72**, and poly(trityl methacrylate) **73** (Scheme 16). Polymerization of the isonitriles was extensively studied by Millich (218) and by Drenth, Nolte, and Van Beijnen (219–221) and co-workers (222). The main chain consists of

**71****72****73**

Scheme 16

a succession of sp^2 trigonal carbon atoms in a nearly syn planar (eclipsed) conformation: The impenetrability of atoms imposes a small deviation from planarity and leads to the formation of a helix analogous to that of hexahelicene. The presence and the stability of a chiral conformation was demonstrated by chromatographic resolution on a chiral support of the two enantiomers of poly*tert*-butyliminomethylene.

A quite different example was reported by Okamoto et al. (223) in the polymerization of trityl methacrylate; from the configurational point of view the resulting isotactic vinylidene polymer is unable to exist in enantiomeric forms, as we shall see in the following chapter. Nonetheless, if polymerization takes place in the presence of a chiral initiator (the complex between butyllithium and sparteine) very high optical activity is observed, both during polymerization and in the purified polymer. The phenomenon was attributed to the presence of two unusual factors: The existence of a "conformational" asymmetric induction and high conformational rigidity due to the presence of very bulky substituents. During polymerization each monomer enters the chain in a preordered way resulting from the reciprocal interplay of the chirality of the catalytic complex and of the bulkiness of substituents, thus initiating helical chains all having the same screw sense. Once formed, the helices are stable in solution for an indefinite period even at high temperatures because the trityl substituents hinder conformational transitions involving the main chain.

The general shape of a macromolecule is sometimes referred to as macroconformation—in contrast to microconformation, which concerns the succession of torsion angles about a limited number of consecutive bonds. The random coil, rigid rod, and rigid helix represent examples of macroconformations. The same term is used to specify the molecular shape in semicrystalline polymers, one of the most important and still open problems in the field of polymer morphology.

Polyethylene samples crystallized from very dilute solutions form lamellar lozenge-shaped monocrystals, with base dimensions of the order of several micrometers and with a thickness of a few hundred angstroms, which can be studied by electron microscopy (162,224). The polymer chain crosses the monocrystal along its shortest length after which it folds on itself. In a perfect crystal one can assume that the folding occurs with a regular adjacent reentry (Figure 17). If the same polymer is crystallized from the melt at normal pressure a lamellar morphology is still observed, similar to that of the monocrystals but much less perfect. The thickness of the lamellae is always of the order of hundreds of angstroms. If, finally, the polymer is crystallized from the melt under extremely high pressure (200–500 MPa or 2000–5000 atm) the crystalline domain increases its thickness to several thousand angstroms: The polymer is said to have an "extended chain macroconformation." The extended chain and the folded chain with regular reentry represent two ideal states of crystalline

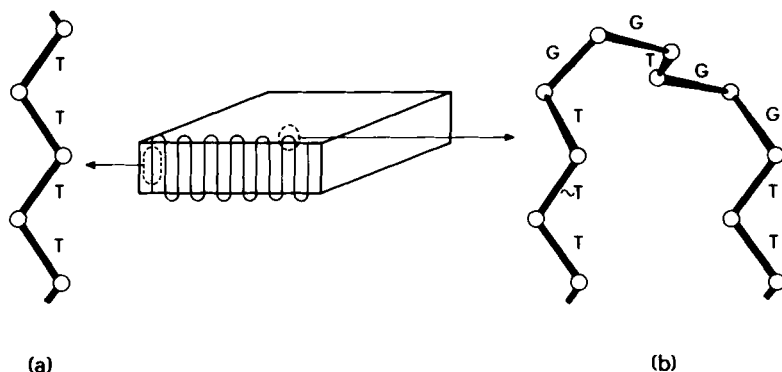


Figure 17. Schematic representation of a lamellar polyethylene single crystal. (a) and (b) show enlarged features of its structure: in (a) the zigzag conformation of the macromolecular chain inside the crystal; in (b) a hypothetical model for the regular folding, drawn according to the calculation reported in ref. 224a.

polymer macroconformation, whereas the random coil represents the chain conformation in the disordered amorphous state. A real semicrystalline polymer will be in an intermediate situation, more or less near one of the ideal models according to the conditions of crystallization and the nature of the sample (molecular weight, stereochemical purity, chain mobility, number and distribution of defects, etc.).

There has been a sharp debate for many years on the best description of the real macroconformation. Much experimental research has been carried out on pure polymers using different techniques (225) [small angle and intermediate angle neutron scattering (226), electron microscopy, IR, etc.]. Yoon and Flory (40, 228–231) and Gawrisch et al. (232) held the view that the probability of adjacent reentry in polymeric lamella is rather low (<50%) and does not justify the validity of such a model. The trajectory of the chain extends across numerous lamellae and its macroconformation is not far from that of the random coil. In the view of Keller and co-workers (224, 233–236) the adjacent reentry, although not complete (3:1 with respect to other possibilities) largely prevails.

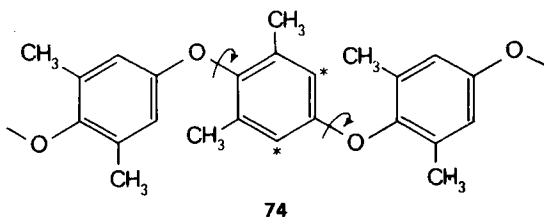
The close connection that exists between polymer morphology and mechanical properties stimulated extensive research in this field. In amorphous polymers, elastic neutron scattering led to important results. Using mixtures of conventional and deuterated macromolecules, the mean square radius of gyration $\langle s^2 \rangle$ of several amorphous polymers in bulk has been determined (237). This quantity is related to the mean square end-to-end distance $\langle r^2 \rangle$ and to the characteristic ratio C_∞ , already discussed in the preceding section. The C_∞ value is practically coincident with that observed in θ solvents. It may be deduced that in an amorphous polymer the macroconformation is essentially random coil and

that the effect of the excluded volume (which produces an increase in dimensions) balances the attractive interaction between nearby chain segments so that the chains are in an unperturbed condition (238).

An increasingly common technique in this field is high resolution NMR spectroscopy of solid polymers. It is well known that an organic solid substance gives rise to a very weak and poorly defined ^{13}C NMR spectrum for several reasons: Large line broadening due to static dipole-dipole interactions, chemical shift anisotropy due to the different nuclear orientations with respect to the magnetic field, and long spin-lattice ^{13}C relaxation time T_1 . These drawbacks can be overcome by using a particular spectral technique, the so-called CP-MAS spectroscopy (240-242), which requires high power proton decoupling, fast rotation of the sample around an axis forming a 54.7° angle with respect to the magnetic field ("magic angle spinning"), and the use of ^1H - ^{13}C cross polarization pulse sequences.

First introduced to polymer chemistry by Schaefer and collaborators, CP-MAS spectroscopy has already yielded interesting results in both structural and dynamic studies. The comparison of spectra in solution and in bulk permits identification of frozen conformations, distinction between spectra of crystalline and amorphous phases and measurement of the rate of several conformational transitions. For example, the ^{13}C spectrum of the poly(phenylene oxide), **74**, in solution consists of five signals while the CP-MAS spectrum displays six. In the solid state the resonance of the aromatic CH appears split into two components. The phenomenon is attributed to the forbidden rotation of the benzene ring around the O . . . O axis, which makes the two carbon atoms indicated with an asterisk no longer equivalent.

In Sect. IV-A the helical conformation $s(2/1)_2$ of syndiotactic polypropylene was described (see Figure 12). Unlike the methyl and methine carbons, the methylene carbons occupy two distinct positions along the helix, hence the three-signal spectrum of syndiotactic polypropylene in solution should change to a four-signal spectrum when recorded on a crystalline sample. That is exactly what happens (Figure 18) (243); the splitting between the two CH_2 signals is that expected on the basis of the different γ effects observed in the two specific positions.



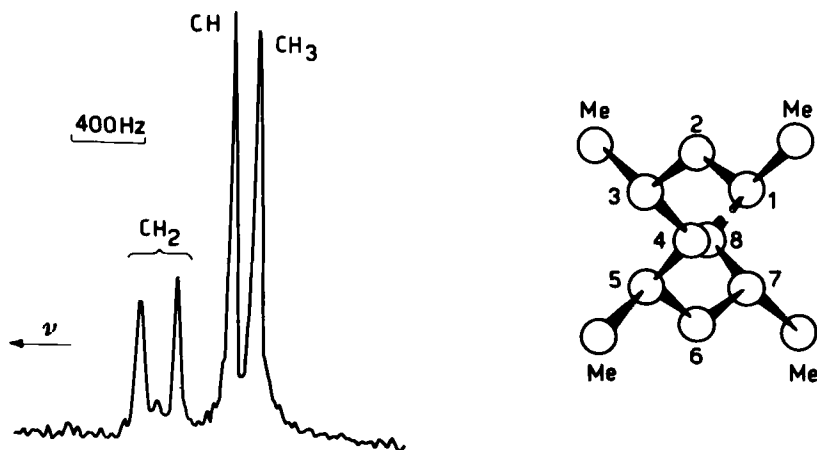


Figure 18. CP-MAS ^{13}C NMR spectrum of crystalline syndiotactic polypropylene in the helical conformation. From (243): Copyright Chem. Soc., London.

It is easy to foresee the future importance of this technique for an improved formulation of the structure–property relations of bulk polymers, especially for cross-linked polymers, where detailed structure is in fact difficult to arrive at.

Before concluding this Section I should like to outline briefly the importance of vibrational spectroscopy in conformational analysis of polymers. The renewed interest in this technique, which had been rather overshadowed by the spectacular development of NMR spectroscopy, derives from important instrumental improvements and new methodological and conceptual approaches (163, 244–246). The advent of the FT-IR interferometers has led to remarkable reductions in recording time and sample size. It has permitted the processing of the spectrum so as to improve sensitivity or resolution and to highlight the effect of small structural details like configurational and conformational defects, to separate the spectrum of a mixture into spectra of the single components (polymer/solvent, amorphous/crystalline phases), and so on. The great versatility of IR spectroscopy as an analytical method has been further enhanced in this way. At the same time, Raman spectroscopy has been greatly improved with the introduction of laser sources, both with fixed and tunable wavelengths (Raman resonant spectroscopy).

A better knowledge of force constants, the use of more detailed physical models, and the availability of large computers and of new methods of calculation has permitted the prediction, within close approximation, of the frequencies and, to a lesser degree, the intensities of absorptions of stereoregular polymers in ordered conformations (helix, zigzag, etc.). In this way data on molec-

ular dynamics, useful for the comprehension of various physical properties of polymers, have been obtained. As a matter of fact, elastic and inelastic neutron scattering, specific heat, elastic and acoustic properties of polymeric material greatly depend on the oscillations of the atoms. Modern spectroscopy makes use of theories and methods of solid state physics and its applications have been extended to morphological and rheological problems, apparently rather distant from its traditional field of application.

One of the principal advantages of vibrational spectroscopy, if examined from the point of view of conformational analysis, lies in the possibility of examining the same polymer under quite different conditions: in solution, in the amorphous or molten state, in the crystalline or paracrystalline state (247). Oriented films can also be studied through the use of linearly polarized light. These observations give insight into the conformational state of the polymer in each state and into the mechanism by which phase transitions take place. For example, the IR spectrum of isotactic crystalline polypropylene is dominated, in the 950–1000 cm^{-1} region, by two intense bands, one of which disappears almost completely after melting (248). The residual intensity of the band at 998 cm^{-1} , characteristic of a vibration parallel to the axis of the (3/1) helix, is considered to depend on the persistence in the melt of very short helical segments.

Absorption bands that disappear at the moment of melting or dissolution are associated with the order existing inside the solid polymer. Most of them arise from an intramolecular phase coupling of vibrations inside single macromolecules arranged in a regular conformation. These bands are properly indicated as regularity bands and not as crystallinity bands as they derive from the existence of a monodimensional (not tridimensional) order (249). A typical example is the 998- cm^{-1} absorption of isotactic polypropylene already discussed. True crystallinity bands occur when the weak reticular forces existing in a crystalline polymer induce a perturbation of the vibrations of the single chains and produce a splitting of the corresponding bands. A splitting of this kind is observed around 725 cm^{-1} in the IR spectra of crystalline polyethylene and also of crystalline *n*-alkanes.

The study of dynamics of a real polymer chain of finite length and containing some conformational defects represents a very difficult task. Due to the lack of symmetry and selection rules, the number of vibrational modes is enormous. In this case, instead of calculating the frequency of each mode, it is more convenient to determine the density of vibrational modes, that is, the number of frequencies that occur in a given spectral interval. The density diagram matches, apart from an intensity factor, the experimental spectrum. Conformational defects can produce "resonance frequencies" when the proper frequency of the defect is resonating with those of the perfect lattice (the ideal chain), or "quasi-localized frequencies" when the vibrational mode of the defect cannot be transmitted by the lattice. The number and distribution of the defects may be such

that nonnegligible dynamic perturbations and coupling between such defects may occur throughout the host lattice. The sensitivity of the vibrational spectrum to the presence of conformational defects can bring new light to the real structure of semicrystalline polymers and to the dynamics of phase changes at a microscopic level (250).

V. CHIRALITY IN POLYMERS

Interest in optically active polymers arose from analogy with macromolecules of biological origin. In addition, there was the hope to obtain new information to clarify the stereochemical features of synthetic polymers; this, in fact, did come about. Attempts to direct the course of polymerization using chiral reagents had been made already prior to the discovery of stereospecific polymerization. It was only after the 1950s, however, that the problem of polymer chirality was tackled in a rational way. The topic has been reviewed by several authors (251–257). In this section I shall try to illustrate three distinct aspects: the prediction of chirality in macromolecular systems, the problems regarding the synthesis of optically active polymers, and polymer behavior in solution.

If we ignore the rigid polymers described in the preceding section—several of which are effectively chiral and optically active (219–223)—all other linear polymers assume a random-coil conformation in solution. In this situation there is an apparent paradox (254): The probability of a macromolecule, even with a structure as simple as that of polyethylene, to exist in an achiral form is negligible. Equally negligible is the probability that two macromolecules with exactly enantiomeric conformations coexist in an accessible volume. It might be concluded that polyethylene has the properties of an optically active compound and, in solution, should rotate the plane of polarized light, contrary to experimental evidence. In fact, the shape of a single macromolecule evolves from one chiral conformation to another (also chiral), but after a very short time no correlation exists between successive conformations. The optical activity of each macromolecule should, therefore, be time-averaged and the average should be extended to all the macromolecules in a given sample. These considerations and the existence, within each macromolecule, of locally achiral segments, and of chiral segments with the same probability for both enantiomers, leads to the average rotation being effectively zero, with only random fluctuations towards positive and negative values very much below the sensitivity level of the known experimental methods. This description corresponds to that given by Mislow and Bickart (258) in a different context: They attribute the optical inactivity of analogous systems to their stochastic achirality.

A second concept—that of cryptochirality—also illustrated by Mislow and

Bickart (258) relates to magnitudes of optical activity well below the detection limits of the available instruments. It plays a role in the examination of polymer chirality and will be discussed later. Our attention will be focused on those polymers that display observable rotation and are, therefore, necessarily chiral. A clear separation among these classes of polymers—stochastically achiral, cryptochiral, and chiral—can be made with reference to a suitable model.

A. Prediction of Chirality in Flexible Macromolecular Systems

Mislow and Bickart (258) have recently discussed the properties, and specified the limitations and essential features, of models that can be used for the prediction of chirality of a molecular system. In the simplified and idealized representation of molecular structure, nonessential features are deliberately left out; the model summarizes some selected aspects of the system and completely disregards or even falsifies, others. The model must be adequate to the time scale in which the phenomenon is observed. In particular, in mobile conformational systems it should refer to a time-averaged structure. In other words, the model can have a higher symmetry than that observed under static conditions (e.g., by X-ray diffraction in the crystalline state or by NMR under slow exchange conditions) (259).

The use of zigzag or Fischer projections for flexible polymers is in accord with this premise. However, even when one chooses one of these representations (generally the Fischer projection) different models may be postulated according to whether or not the terminal groups are taken into consideration. In the development of macromolecular stereochemistry three types of models have been proposed: the infinite chain model (260), the finite chain with identical terminal groups (261), and the finite chain with nonidentical terminal groups (22). Point group symmetry is applied in the analysis of the latter two, whereas line group symmetry must be used for the former. As a consequence, one must consider, in addition to the usual rotation and reflection operations, translation along the chain axis, and its combinations with rotation (screw axis and screw operation) and reflection (mirror glide plane and glide reflection). To avoid the difficulties arising from the use of line symmetry, not well known to most stereochemists, the infinite chain model can conveniently be converted into a cyclic model (41): The planar representations of substituted cyclobutanes, cyclohexanes, and so on, are, as far as the present purpose is concerned, all equivalent to the Fischer projection of an infinite chain.

In an infinite Fischer projection, chirality is not consistent with the presence of the following elements of reflective symmetry (41, 46, 254): *d*, mirror plane containing the chain axis; *m*, an infinite number of mirror planes perpendicular to the chain axis; and/or *c*, mirror glide plane containing the chain axis. For

the two finite chain models, chirality requires the absence of σ_1 , the mirror plane containing the axis of the chain, and of the σ_2 , the mirror plane perpendicular to the axis of the chain at its midpoint.

If the first model (infinite chain) is adopted, isotactic vinyl polymers like polypropylene, **5**, are considered achiral due to the presence, in their Fischer projections, of an infinite number of m planes placed on all the carbon atoms of the chain. The tertiary carbon atoms are stereogenic but not chirotopic (i.e., pseudoasymmetric atoms) all having the same relative configuration: . . . r , r , r , r . . . or . . . s , s , s , s . . . (whether r or s is purely conventional). In the second model (finite chain with identical terminal groups) the molecule is achiral because of the presence of σ_2 which divides it into two mirror image parts. The tertiary carbon atoms, all different from each other because they are bonded to chain segments of different length, are asymmetric (with the exception of the one at the center which, if present, is pseudoasymmetric) and of opposite configuration in the two halves of the chain: $S_1, S_2, S_3, S_4 \dots (s) \dots R_4, R_3, R_2, R_1$.

In the third model (finite chain with different terminal groups) no reflection symmetry element exists in the Fischer projection. The individual macromolecules are, therefore, chiral and all the tertiary atoms are asymmetric and different. The stereochemical notation for a single chain, depending on the priority order of the end groups, can be $R_1, R_2, R_3 \dots R_{n-2}, R_{n-1}, R_n$ or $R_1, R_2, R_3 \dots S_{n-2}, S_{n-1}, S_n$.

The difference in the ligands of each tertiary atom is due mainly to the different length of chain segments to which it is bonded. If we consider that, in the absence of cooperative factors, optical activity is a short-range phenomenon, the contribution to the rotatory power of most parts of the chain is zero or near to zero. One can thus foresee that the optical activity of a single enantiomer is very small and falls into the domain of cryptochirality. Only oligomers of low molecular weight can present measurable optical activity.

Analogous but even more complex is the analysis of syndiotactic vinyl polymers. In the first model, **7**, individual macromolecules are achiral through the presence of the c and m planes; the sequence of tertiary atoms (stereogenic but not chirotopic) will be . . . $r, s, r, s, r, s \dots$

In the second model, two cases may be distinguished. If the chain possesses an odd number of tertiary atoms, the molecule is achiral through the presence of σ_2 , the sequence of the asymmetric atoms being $S_1, R_2, S_3, R_4 \dots s \dots S_4, R_3, S_2, R_1$. Its low molecular weight analog would be one of the meso stereoisomers of trihydroxyglutaric acid. If, instead, the chain possesses an even number of tertiary atoms, the molecule is chiral due to absence of any element of mirror symmetry (analogously to the chiral tartaric acid) but the individual enantiomers will have very low or negligible rotatory power. The configurational notation will be $S_1, R_2, S_3, R_4 \dots R_4, S_3, R_2, S_1$.

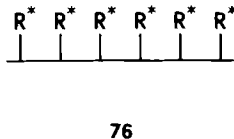
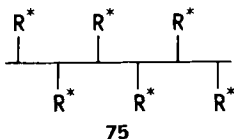
A polymer sample with even a limited dispersion of molecular weight consists of a mixture of molecules of the first and of the second type and is, therefore, cryptochiral (262).

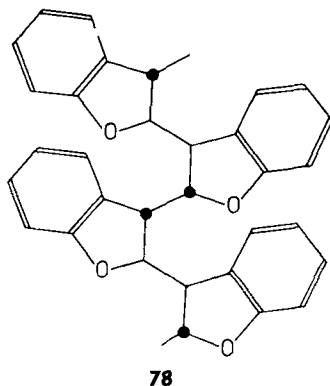
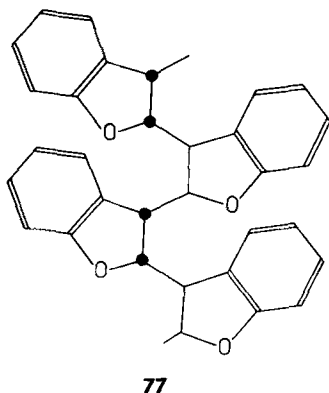
With the third model, also, the single chains are chiral but with negligible optical activity. Even in this case we are in the cryptochirality domain, except possibly with low molecular weight compounds.

It is evident that consideration of terminal groups brings the model nearer to the state of real polymers but reduces its predictive ability in regard to chirality. The set of chiral structures in accord with the infinite chain model is much more restricted and more clearly defined than that predicted using other models. Such a model represents the most severe test to be passed in the design of a chiral polymeric structure. The following analysis will, therefore, be carried out using the infinite chain model.

The elements of mirror symmetry d , m , and c can be removed in different ways, resulting in different classes of chiral polymers. Plane d containing the polymer chain is eliminated by the presence, in the main chain, of tertiary carbon atoms ($-\text{CHR}-$), or of quaternary atoms with different substituents ($-\text{CR}'\text{R}''-$), or with equal chiral substituents ($-\text{CR}^*\text{R}^*-$). Mirror glide plane c does not exist in isotactic structures, nor in syndiotactic ones in which the substituents are chiral and of the same configuration, **75** (33, 263). The perpendicular planes, m , are eliminated by the presence of chiral substituents of the same sign in syndiotactic, **75** (33, 263) or isotactic structures, **76** (263) or if the two directions of the chain are rendered nonreflective. This last condition can be realized in different ways; some of which follow (264):

1. By the presence of cyclic monomer units obtained, for example, from cyclic olefins (benzofuran, indene, etc.) (58, 254). The erythro- and threo-diisotactic structures (**26**, **27** or in a different representation **77**, **78**) are chiral. If B is equal to A (cyclobutene or analogous monomers) only the threo-diisotactic structure **27** is chiral.
2. By the presence of structural units of the type $-\text{X}-\text{CHR}-\text{Y}-$ in which X and Y are two different atoms or groups of atoms (265). Examples of X and Y are O, S, NH, CH_2 , $\text{CH}=\text{CH}$, CO, etc. The following isotactic polymers belong to this class: polyalkyloxiranes, -thiiranes, and -aziridines (repeating unit $-\text{O}-\text{CHR}-\text{CH}_2-$ (**36** and **37**), $-\text{S}-\text{CHR}-\text{CH}_2-$, and $-\text{NH}-\text{CHR}-\text{CH}_2-$), polyamino acids ($-\text{NH}-$

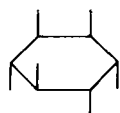




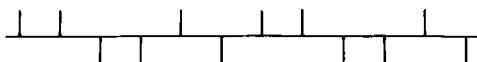
CHR—CO—), polyoxy acids (—O—CHR—CO—), poly-1-alkylbutadienes (—CH=CH—CHR—CH₂—). To the same class belong the polymers with two asymmetric atoms for every monomer unit, such as polysorbates (—CH=CH—CHA—CHB—, **32** and **33**) where both erythro- and threo-diisotactic forms are chiral, or polyhexadiene (—CH=CH—CHA—CHA—) and poly-2,3-epoxybutane (—O—CHA—CHA—), **39**, where only the threo-diisotactic structures are chiral, and the polymers of some bicyclic monomers such as those shown in **41** and **42**. Other examples are the polymers obtained by hydrogen transfer from substituted benzalacetone (**79**, Scheme 17) (266, 267).

3. By combining orientational isomerism ("forward" or "backward") with isotactic arrangement of —CHR— groups in the main chain, as already discussed for the case of polyallenes (Scheme 10) and polyketenes (Schemes 11, 12).
4. By the formation of complex tacticities. To identify the simplest of these structures the cyclic model reported earlier has been found quite useful (41). By analogy with *chiro*-inositol, **80**, it was predicted that a polymer constituted of a succession of six homosubstituted tertiary atoms of the type . . . , *R*, *S'*, *S''*, *S''*, *S'*, *R*, . . . , **81**, would be chiral. Until now this structure has neither been realized, nor have calculations been made to ascertain if it would be effectively optically active or simply cryptochiral.





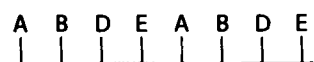
80



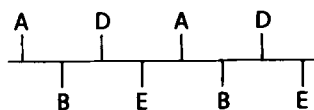
81

5. By the formation of copolymers. Alternate isotactic copolymers $\dots M_1M_2M_1M_2\dots$ of monomers $CHA=CHB$ with $CH_2=CH_2$, or of $CHA=CHA$ or $CHA=CHB$ with $CHD=CH_2$ or $CHD=CHE$ are chiral (38, 268, 269). Several examples are reported in 82–89 (Scheme 18). Chiral copolymers with more complex structure such as $\dots M_1M_1M_2M_1M_1M_2\dots$ may be obtained even from two vinyl monomers, as recently demonstrated by Wulff and Hohn (see 53) (93). The copolymers formed by monomer units, which (*vide supra*) themselves produce chiral homopolymers (270) are also chiral, unless accidental compensation occurs.

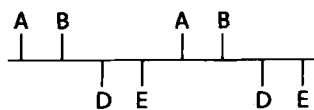
The treatment of irregular and atactic polymers, and, in general, real polymers (with statistical distribution of molecular weight and defects) is much more complex. With regard to atactic vinyl polymers it is not possible to recognize the presence of mirror symmetry, not even in the infinite chain model.



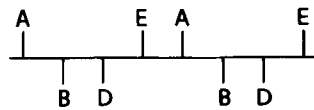
82



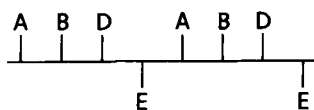
83



84



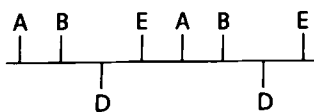
85



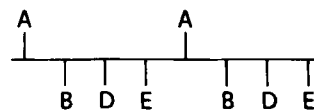
86



87



88



89

Scheme 18

However atactic vinyl polymers are generally considered to be at most crypto-chiral (271). Their optical inactivity may be ascribed to intra- or intermolecular factors. With regard to the latter aspect, Green and Garetz (272) recently carried out a statistical analysis and demonstrated that for a Bernoulli atactic polymer the probability of existence of two exactly enantiomeric molecules is negligible ($\approx 10^{-30}$ for a degree of polymerization of 100) and that its cryptochirality stems from an intermolecular compensation among diastereoisomers.

The difficulty in considering optically inactive mixtures of real macromolecules as racemic mixtures was discussed long ago (273). If this term is to be retained, it would be better to use an operational, and not a structural, definition. For example, an optically inactive mixture of constitutionally similar chiral macromolecules might be defined as racemic on the condition that the mixture is not separable into optically active fractions by the use of nonchiral methods. In accordance with this definition, an optically inactive mixture of dextrorotatory macromolecules of high molecular weight and of levorotatory macromolecules of low molecular weight is not racemic since it can be separated into fractions of opposite sign by solvent fractionation, by precipitation, or by chromatographic methods using achiral supports.

B. Synthesis of Optically Active Polymers from Chiral Monomers

The synthesis of optically active polymers was tackled with the purpose not only of clarifying the mechanism of polymerization and the conformational state of polymers in solution, but also to explore the potential of these products in many fields: as chiral catalysts, as stationary phases for chromatographic resolution of optical antipodes, for the preparation of liquid crystals, and so on.

Optically active polymers may be obtained by polymerization of optically active, racemic, or achiral monomers (255) (disregarding methods where chirality is introduced into the macromolecular compound after polymerization, e.g., by attachment of chiral substituents to preexisting reactive groups). Each class may be further subdivided according to the structure of the monomer and polymer.

The polymerization of enantiomerically pure monomers presents no relevant stereochemical problems when the asymmetric carbon atom is not involved in the reaction and no new centers of stereoisomerism are formed. This is the case, for example, in polycondensation of chiral diacids with diamines (274) and in ring-opening polymerization of substituted lactams (275) and *N*-carboxyanhydrides of α -amino acids (276). Interest here lies mainly in the properties of the polymer. Accidental racemization may sometimes occur but is not necessarily related to the mechanism of polymerization.

The polymerization of (+)-propylene oxide also belongs to this class since the opening of the three-member ring occurs mainly at the primary carbon

(O—CH₂ bond) (78, 277). More precisely, the formation of the crystalline polymer in the presence of FeCl₃ takes place according to such a mechanism, whereas the amorphous fraction of low or zero rotatory power produced at the same time contains a sizeable number of head-to-head, tail-to-tail sequences originating from reaction at the secondary carbon [O—CH(CH₃) bond] with inversion of configuration (278). From a single enantiomer, for example, (*S*), one obtains, by attack at the primary carbon, a noninverted unit with (*S*) configuration and, by attack at the secondary carbon, an inverted unit with (*R*) configuration (279).

This phenomenon of "chirality degradation" is carried to the extreme in the polymerization of (+)-*trans*-2,3-epoxybutane (81, 82). In the presence of *i*-Bu₃Al·0.5 H₂O as catalyst one obtains a highly crystalline but wholly inactive polymer: One of the two equivalent asymmetric atoms inverts its configuration during polymerization giving rise to a monomer unit with erythro or meso structure. The isotactic polymer, **40**, so formed is clearly achiral (280).

If the cyclic monomer does not have twofold symmetry, the inversion at a single carbon atom can produce optically active polymers, as in the case of the dioxo[3.2.1]bicyclooctane, **41** (85).

Different problems arise in the polymerization of chiral α -olefins and of other optically active vinyl, vinylidene, or related monomers: vinyl ethers, vinyl ketones, acrylates, methacrylates, aldehydes, and so on. Apart from a few isolated results, systematic research in this field was begun only around 1960, (252, 253, 256, 282–290) and carried out mainly by Pino and the Pisa group and by Goodman. These polymers possess stereogenic centers both in the main chain and in the substituents. All stereoisomeric forms, isotactic, **76**, syndiotactic, **75**, or atactic, of these polymers are chiral. In many cases their rotatory power increases (doubling and even tripling) as one passes from amorphous, more or less atactic, to crystalline isotactic polymers; the increase is more marked if the asymmetric atom of the substituent is in the α or β position with respect to the chain. Highly isotactic polymers often have a rotatory power far higher than that of the monomer or of low molecular weight model compounds. This fact is considered a clue to the presence, in solution, of strongly chiral conformations—helices—not compensated by their enantiomeric partners.

Polymerization of optically active isonitriles, **72**, also leads to the formation of helical polymers with a preferential screw sense (219–222). Various factors distinguish this system from the preceding ones: In the isonitrile case no new stereogenic atoms are formed during polymerization; the helices are rigid and there is no indication of conformational equilibrium in the system; the formation of a preferential screw sense is very probably a kinetically controlled process.

Further examples of polymerization of optically active monomers are concerned with 2,3-pentadiene (dimethylallene), which gives rise to a structure like **43**, already examined in Section II-C (87), with chiral acetylene compounds

In this context it is worth clarifying the usage of the terms stereospecific and stereoselective in polymer chemistry, usage, that is, in part, different from that commonly accepted in organic chemistry. Polymerization is said to be stereospecific when it leads to the formation of a tactic polymer, except for the case where the polymer merely retains the stereoisomerism present in the monomer. In its turn, a tactic polymer is defined as a regular polymer, the molecules of which can be described in terms of only one species of a configurational repeating unit in a single sequential arrangement (21).

For monomers like propylene oxide a highly stereoselective polymerization is also stereospecific [the monomer units in a chain being all (*R*) or all (*S*)] while for chirally substituted olefins a stereospecific polymerization would require both a high stereoselectivity and a high stereoregularity in the main chain. The term stereospecificity in polymer chemistry, especially in the older literature, often refers to the formation of new centers of stereoisomerism in the main chain: Following this use, a stereospecific vinyl polymerization is a polymerization involving an enantioface differentiation in achiral unsaturated monomers or a diastereoface differentiation in chiral unsaturated monomers (281). Stereoselective polymerization, in contrast, involves enantiomer differentiation in a mixture of chiral monomers. By way of an example, the process of converting propylene into isotactic polypropylene is a stereospecific polymerization. In contrast, a stereoselective polymerization is one in which a polymer molecule is formed from a mixture of stereoisomeric monomer molecules by incorporation, in each chain, of only one of the stereoisomeric species (302).

Processes (2) and (3) are both suitable for the preparation of optically active polymers, either directly or after fractionation. It must be remembered, however, that in practice all these processes are not clearly distinct. The boundary between processes (1) and (2), especially, is not obvious, being related to the amplitude of the statistical fluctuations. A statistical analysis of process (1) has shown that, for chains having a degree of polymerization equal to 1000, 5% of the macromolecules contain, on the average, an excess of 50 monomer units of a given sign (299, 303) (and another 5% a similar excess of monomer units of the opposite sign). A highly efficient fractionation in a chiral environment could, therefore, produce polymeric samples having measurable optical activity.

In stereoselective polymerization (case 2), microstructural analysis shows the presence of a rather long sequence of monomer units with the same configuration. The probability that single chains contain a high excess of units of the same sign is considerably greater than in the preceding case and chromatographic fractionation on chiral supports has often given positive results. The first experiments were made by Pino, Ciardelli, Lorenzi, and Natta on poly-4-methyl-1-hexene with an insoluble chiral polymer, poly-(*S*)-3-methyl-1-pentene (304, 305) as stationary phase: The first and last fractions have opposite rotatory power and their optical purity was estimated to be around 30%. Other examples concern

poly-3,7-dimethyl-1-octene (305), poly(*sec*-butyl vinyl ether) (306), and poly(propylene oxide) (307).

But the moderate enantiomeric purity usually observed was attributed both to the poor efficiency of the separation method and to the incomplete stereoselectivity of the polymerization process. In a few cases, however, stereoselectivity of 90–95% was found (308).

Stereoselective polymerization may proceed by ionic or coordination mechanisms. In many cases one admits that in the counterion or in the catalytic complex enantiomeric active centers exist, which give rise to predominantly (*R*) or (*S*) chains, respectively. Such centers may exist prior to polymerization or may be formed by reaction of a nonchiral precursor with the enantiomeric mixture of the monomers. Alternatively, one can think that the stereoselectivity depends mainly on the interaction between the entering monomer molecule (which is chiral) and the last unit in the chain (also chiral); according to this hypothesis, the enantiomeric excess inside each chain is generally low, because the occurrence of an accidental error brings about an inversion of the sense of stereoselection.

Stereoelective polymerization (type 3) requires the presence of a chiral catalyst with an excess of active centers of a given configuration or with a differential reactivity of the centers that catalyze polymerization of one or the other of the two enantiomers (299). With regard to racemic α -olefins, the best results were obtained with 3,7-dimethyloctene in the presence of $\text{TiCl}_4 + \text{Zn}[(S)\text{-2-methylbutyl}]_2$ as catalyst (309). The resulting polymer is dextrorotatory, $[\alpha]_D = +16.1$, and the residual monomer is levorotatory, $[\alpha]_D = -0.63$, (310). These values indicate a rather modest degree of stereoelectivity.

The behavior of chiral, racemic oxiranes and thiiranes in polymerization with an optically active catalyst is very interesting. The subject has been developed by the Japanese (Furukawa, Tsuruta, and Inoue) and French (Sigwalt, Spassky, and Sepulchre) schools (277, 298, 311–319). Both the polymer and the residual monomer are optically active. The polymer has the highest optical activity at the beginning of the reaction (the value depending on the degree of electivity of the process); then the rotatory power decreases progressively to a zero final value. In contrast, the optical activity of the residual monomer starts from zero and reaches, near the end of the reaction, a value close to that of the enantiomerically pure compound. In the case of methyloxirane and methylthiirane, this behavior is interpreted by an equation that links the enantiomeric purity $[\alpha]/[\alpha_0]$ of the residual monomer to the conversion by the “stereoelectivity ratio” [defined as the ratio between the disappearance rate of the two enantiomers ($r = k_R/k_S$)]. The ratio r depends on the nature of the catalyst, on the type of chiral cocatalyst and on the monomer. Good results are obtained using, as a catalyst, the reaction product between ZnEt_2 or CdEt_2 and a chiral glycol of the type $\text{R}-\text{CHOH}-\text{CH}_2\text{OH}$ (R is preferably *iso*-propyl or *tert*-butyl). Values of r as

high as 20 (corresponding, in practice, to an almost ideal stereoelective polymerization) have been obtained by using as chiral glycol optically pure (*S*)-2,2'-dihydroxy-1,1'-binaphthyl (319a). A similar phenomenon, but much more complex in its quantitative interpretation, was observed in the case of *tert*-butylthiirane.

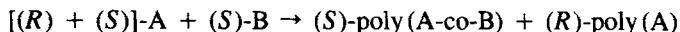
The poly(propylene oxide) obtained at low conversion has an enantiomeric purity of around 30%, is not homogeneous from the point of view of stereoregularity (or stereoselectivity), and can be separated into fractions of different tacticity and optical activity, the latter being greater for polymers of higher stereoregularity.

An intermediate case between the polymerization of enantiomerically pure and racemic monomers is the polymerization of a partially resolved mixture of enantiomers with variable optical purity. Two processes are distinguishable, depending on whether polymerization occurs in the presence of an achiral (or racemic) or of a chiral (optically active) catalyst.

With a conventional (achiral) Ziegler-Natta catalyst the relation between the optical activity of the polymer and the initial enantiomeric purity of the monomer was found to be linear for chiral α -olefins having the asymmetric carbon atom in the side chain in the γ position (306, 320). When the chiral center is nearer the main chain (in the α or β position) the optical activity of the polymer reaches an asymptotic value for a monomer enantiomeric purity of 70–80%. This is explained by admitting a certain degree of copolymerization between the two antipodes that does not disturb the helical conformation existing in the homopolymer, that conformation being largely responsible for the high rotation.

A somewhat different situation arises in the copolymerization of a racemic monomer with an optically active monomer of similar structure in the presence of a conventional stereospecific (or stereoselective) catalyst (299, 321). Examples concern the copolymerization of racemic 3,7-dimethyl-1-octene with (*S*)-3-methyl-1-pentene and of racemic *sec*-butyl vinyl ether with various optically active vinyl ethers. In all cases there was preferential copolymerization of one of the two enantiomers of the racemic monomer with the second monomer and simultaneous formation of an optically active homopolymer containing predominantly the noncopolymerized antipode, according to Scheme 20. The two products are easily separated, due to their different solubilities.

Stereoelective polymerization of enantiomerically unbalanced (i.e., partly resolved) mixtures of oxiranes and thiiranes has given surprising results (277, 318, 322). The stereoelectivity ratio, *r*, is greatly dependent on the enantio-



Scheme 20

meric purity of the initial monomer (i.e., that which comes into contact with the fresh initiator): In particular, with propylene sulfide r increases from 2.4 for a 50:50 (*R*)/(*S*) mixture to 7 for a 72.5:27.5 mixture, and to 8 for a 22.5:77.5 mixture. In other words r depends on the absolute value of the optical purity of the monomer, whereas the sign of the stereoselectivity depends on the configuration of the chiral glycol initiator only.

C. Asymmetric Polymerization

Until now I have discussed the methods of synthesis of optically active polymers from chiral monomers. As is well known in organic chemistry, it is also possible to produce chiral molecules with one preferred configuration by reaction of achiral molecules in the presence of some chiral influence. These reactions are known as asymmetric syntheses (36, 323–325); when an unsaturated compound is involved, the term enantioface-differentiating reaction is often used (281).

In the polymer field, reactions of this type are subject to several limitations related to the structure and symmetry of the resultant polymers. In effect, the stereospecific polymerization of propylene is in itself an enantioface-differentiating reaction, but the polymer lacks chirality. As already seen in Sect. V-A there are few intrinsically chiral structures (254) and even fewer that can be obtained from achiral monomers. With two exceptions, which will be dealt with at the end of this section, optically active polymers have been obtained only from 1- or 1,4-substituted butadienes, from unsaturated cyclic monomers, from substituted benzalacetone, or by copolymerization of mono- and disubstituted olefins. The corresponding polymer structures are shown as formulas 32 and 33, 53, 77–79 and 82–89. These processes are called asymmetric polymerizations (254, 257); the name enantiogenic polymerization has been recently proposed (301).

A salient difference between common asymmetric syntheses and asymmetric polymerizations lies in the multistep character of the polymerization processes. In organic chemistry an asymmetric reaction produces a single or only a few asymmetric carbon atoms with a preferential configuration. Also in catalytic processes (asymmetric hydrogenation, etc.) each reaction step produces a single molecule and is independent of the preceding reaction step. This is not, in general, the case for asymmetric polymerization where hundreds or thousands of asymmetric atoms are formed inside the same macromolecule and some correlation can exist between successive analogous events, such as the insertions of the single monomer units in the macromolecular chain.

A rationale of asymmetric polymerization was proposed for the first time by Frisch, Schuerch, and Szwarc in 1953 (38). These authors proposed two extreme mechanisms for the formation of optically active polymers. The first involves asymmetric initiation and stereoregular symmetric growth; in other words, a

process in which the asymmetric agent influences only the first step of the reaction and induces the formation of a *D* chain with a probability different from that of the *L* ($I_D \neq I_L$). After the first step, the conditional probability of the formation of a new monomer unit having the same sign as the preceding one is equal in the two enantiomeric cases ($p_{DD} = p_{LL}$).

In the second hypothesis there exists a mechanism of asymmetric growth in which, in each propagation step, the conditional probability of a sequence is different from that of its antipode ($p_{DD} \neq p_{LL}$). In this case an asymmetric catalyst (or broadly speaking, a chiral environment) is required whose action persists throughout the whole course of the polymerization.

Only with the second mechanism is it possible to obtain high molecular weight polymers of high rotatory power (which is, in fact, independent of the degree of polymerization), whereas, with the mechanism of asymmetric initiation, the optical activity falls off rapidly as the degree of polymerization increases—unless there is a very high degree of stereoregularity—due to the inability of the system to correct configurational errors that have come about during the polymerization.

Fueno, Shelden and Furukawa (326, 327) have extended the treatment of asymmetric growth by representing it by a first-order Markov chain governed by two independent probabilities p_{DL} and p_{LD} , i.e., the probability that after a *D* unit the chain continues with an *L* unit and vice versa. For sufficiently long chains the enantiomeric *D/L* ratio, and, therefore, the enantiomeric purity, is equal to the ratio of these probabilities ($D/L = p_{LD}/p_{DL}$) and is not related to their single values. For instance, a 60% enantiomeric purity, corresponding to an enantiomer ratio *D/L* of 4, can be attained with the following pairs of values p_{LD}/p_{DL} : 0.8/0.2; 0.4/0.1; 0.04/0.01, that is, with the processes of very different stereoregularity. The microtacticity of the chain can be expressed as follows: $D_5L_{1.25}D_5L_{1.25}$; $D_{10}L_{2.5}D_{10}L_{2.5}$, and $D_{100}L_{25}D_{100}L_{25}$, respectively, where the indices indicate the average length of the sequences. It is, therefore, possible to obtain polymers of moderate to fairly high optical purity even with processes of poor stereoregularity.

Asymmetric induction and stereoregularity can be treated, at least in part, as two distinct phenomena; however, it has been observed that the values of p_{LD} and p_{DL} can be divided into two parts: one dependent on chiral factors external to the chain (catalyst, environment, etc.) and the other dependent on the intramolecular chain induction. This latter is a factor of stereoregularity or cooperativity rather than of chirality (its value is identical for both the *DD* and *LL* successions) (328). Both factors can be expressed as differences of free energies of activation: In favorable cases, when they are of the same sign, asymmetric polymerization becomes easier (i.e., under the same conditions it gives a higher optical yield) than an analogous nonmacromolecular asymmetric synthesis.

Asymmetric polymerization has been achieved with all the principal methods

of polymer synthesis, that is, anionic, cationic, coordination, and radical processes. The first examples go back to 1960 (257) and the greater part of the research to the years immediately following. The subject has come to the fore again recently as several important new results have emerged, accompanied by a more complete interpretation of the older experiments.

Methyl sorbate and analogous monomers were polymerized in the presence of (*R*)-2-methylbutyllithium or of complexes between butyllithium and optically active Lewis bases (329, 330) (see formulas 32 and 33); the polymers show weak optical activity. The prevailing configuration of the $-\text{CH}(\text{CH}_3)-$ group was determined by the sign of rotation of the methylsuccinic acid obtained from the polymer after ozonization. The low optical purity ($\approx 6\%$) found is related to the presence of a remarkable stereochemical disorder (115, 116) and to the fact that the chiral agent is active, at least in the case of methylbutyllithium, only in the initiation reaction.

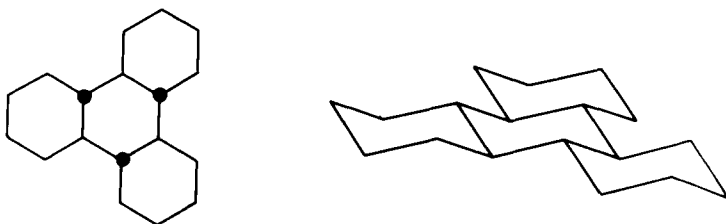
In contrast, the asymmetric polymerization of benzofuran in the presence of chiral counterions derived from the reaction of AlCl_3 or AlEtCl_2 with phenylalanine or other amino acids (61, 331), or from AlCl_3 , Et_3SnCl , and $(-)$ -menthyl-*O*- SnEt_3 (332) proceeds by a cationic mechanism. The optical activity of the polymer is very high $\{[\alpha]_D > 70^\circ$ on the usual polymer; or $\approx 90^\circ$ as an instantaneous value* or under particular experimental conditions (333)}. The fractionation of polybenzofuran according to molecular weight has led to the demonstration that polymerization follows a process of asymmetric growth under chiral catalyst control; that is, the specific rotation is largely independent of the degree of polymerization.

Of the possible chiral erythro- and threo-diisotactic forms (77 and 78), the threo appears more probable on a conformational basis (334). The polymer has a rigid skeleton and is generally amorphous but can be converted into a crystalline material by a nonconventional annealing process (335, 336).

An analogous structure was observed in the polymers derived from α - and β -naphthofuran in the presence of the AlCl_3 -phenylalanine complex (337); their rotations are $[\alpha]_D = 41$ and 145° , respectively. This latter value has, for a long time, been the highest specific rotation obtained by asymmetric polymerization. Unfortunately, in this and many other examples, it is not possible to correlate the values of optical activity with corresponding ones of optical purity. Difficulties exist, both on the experimental and on the theoretical level, in making such correlations, especially when the polymer microstructure is not exactly known.

Particular attention has been given to 1,3-pentadiene, the simplest hydrocarbon monomer capable of giving chiral polymers. Natta, Porri, and co-workers

*The instantaneous value of $[\alpha]$ in the course of a polymerization is expressed as $\Delta([\alpha] \cdot W)/\Delta W$ where $[\alpha]$ and W are the specific rotation and polymer yield at two different times during the polymerization; it is obtained from the slope of the plot of $([\alpha] \cdot W)$ vs. W .

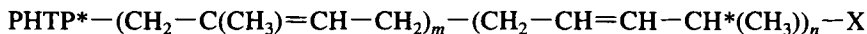


92

succeeded in obtaining optically active polymers with a 1,4-trans-isotactic structure in the presence of VCl_3 and tris-(*S*)-2-methylbutylaluminum ($[\alpha]_D \approx -1^\circ$) (338), and with a 1,4-cis isotactic structure in the presence of AlEt_3 and Ti (*O*-menthyl) $_4$ (339). This last polymer has a remarkable optical activity ($[\alpha]_D = -22.8^\circ$). The structure of these polymers corresponds to formula 32 ($\text{A} = \text{CH}_3$, $\text{B} = \text{H}$).

In 1967 the first radical asymmetric polymerization of pentadiene was achieved using the crystalline lattice of an inclusion compound as the chiral agent (340). The host was one of the enantiomers of perhydrotriphenylene (PHTP, 92), a high-symmetry chiral organic compound (341–343) capable of forming crystalline adducts with a large variety of organic compounds, including several macromolecules (344–347). When the crystals of a PHTP-monomer inclusion compound are subjected to γ radiation, a highly stereospecific polymerization occurs starting generally from a PHTP radical (345, 348–351). The enantiomeric purity, determined via methylsuccinic acid, is rather low ($\approx 7\%$). The process is nonetheless of interest because of the way the asymmetric induction is transmitted. Common radical polymerizations have, as a rule, led to a rather low degree of tacticity and are not able to control the growing chain end, as do ionic and coordination polymerizations.

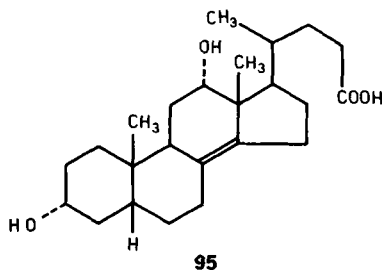
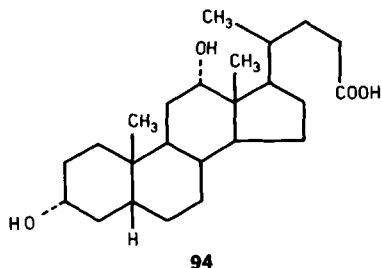
The trick used in asymmetric inclusion polymerization is to perform the reaction in a rigid and chiral environment. With more specific reference to chirality transmission, the choice between the two extreme hypotheses, influence of the starting radical (which is chiral because it comes from a PHTP molecule), or influence of the chirality of the channel (in which the monomers and the growing chain are included), was made in favor of the second by means of an experiment of block copolymerization. This reaction was conducted so as to interpose between the starting chiral radical and the chiral polypentadiene block a long nonchiral polymer block (formed of isoprene units) (352), 93. The isoprene-pentadiene block copolymer so obtained is still optically active and the



enantiomeric purity of the pentadiene block is equal to that observed in homopolymerization. Considering the length of the polyisoprene segment (200–500 monomer units equal to 1000–2500 Å) it seems reasonable to attribute the result to the interaction of the reacting system with the walls of the chiral channel. Given the hydrocarbon nature of all the compounds involved, the asymmetric induction stems only from the presence of weak and nonspecific van der Waals forces. The term “through space asymmetric induction” rather than the more common “through bond asymmetric induction” has been proposed for this reaction. From this point of view, interest in asymmetric inclusion and other solid state asymmetric polymerizations transcends the boundary of macromolecular stereochemistry, in as much as these techniques constitute an important step towards absolute asymmetric synthesis [defined as an asymmetric synthesis promoted only by a physical chiral force (281)].

Asymmetric inclusion polymerization was also studied with other hosts such as deoxycholic acid (DCA, **94**) and apocholic acid (ACA, **95**) using *cis*- or *trans*-pentadiene (353) or *cis*- and *trans*-2-methylpentadiene (354–356) as monomers. The resulting polymers are less regular than those obtained in PHTP but have a higher optical activity ($[\alpha]_D$ ranges from ca. 20° for polypentadiene to more than 300° for poly-2-methylpentadiene). Using ^{13}C NMR spectroscopy Audisio demonstrated that the succession of monomer units in polypentadiene follows a Bernoulli trial: This fact, together with the high molecular weight, the value of the enantiomeric purity, and the presence of a rather low degree of stereoregularity, is incompatible with a process of asymmetric initiation and symmetric growth (110). Therefore, this polymerization also occurs under the influence of channel chirality. Worth noting also is the very high rotatory power of poly-2-methylpentadiene obtained by Miyata and Takemoto in DCA and ACA (354–356). This polymer presents an interesting phenomenon to be discussed in the next section.

A further example of radical asymmetric polymerization is the copolymerization between maleic anhydride and styrene (357–359). The reaction takes place in an emulsion in the presence of lecithin and the asymmetric induction

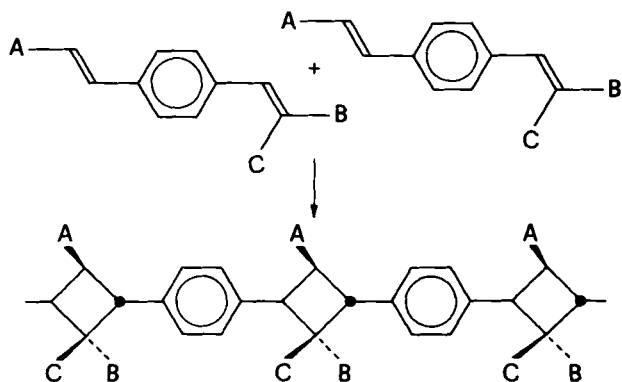


was attributed to the chiral nature of the micelles within which polymerization occurs.

Turning to solid state reactions I should like to mention the research of Lahav and Addadi on the photochemical oligomerization and polymerization of substituted benzene-1,4-diacrylate (Scheme 21) (360–363). Here the key to achieving an asymmetric synthesis lies in the preparation of chiral monomer crystals; this was possible by introducing a desymmetrizing group having no influence on the subsequent reaction. A careful study of the phase diagrams has led to the identification of a metastable phase in which crystals of opposite chirality contain equal amounts of the two molecular enantiomers. The photopolymerization of single metastable crystals has produced oligomers with significant values (up to 30%) of optical purity. As in the preceding case of polymerization of pentadiene in PHTP or DCA, one can speak here of an approach to absolute asymmetric synthesis.

Another result of great importance—the “conformational” asymmetric polymerization of triphenylmethyl methacrylate realized in Osaka (223, 364, 365)—has already been discussed in Sect. IV-C. The polymerization was carried out in the presence of the complex butyllithium-sparteine or butyllithium-6-benzylsparteine. The use of benzylsparteine as cocatalyst leads to a completely soluble low molecular weight polymer with optical activity $[\alpha]_D$ around 340° ; its structure was ascertained by conversion into (optically inactive) isotactic poly(methyl methacrylate). To the best of my knowledge this is the first example of an asymmetric synthesis in which the chirality of the product derives from hindered rotation around carbon-carbon single bonds.

The presence of helical conformations in nascent vinyl polymers has often been advanced as an explanation for some of the characteristics of stereoregular



Scheme 21

polymerization. Observation of the chiroptical properties of such polymers, when a chiral catalyst was used, is nevertheless impossible in most cases since the conformation of the solid polymer at the instant of its formation is not retained after phase transition (melting or dissolution), because of the generally low value of the inversion barrier of the sense of the helix.

The only exception to this statement (outside of the triphenylmethyl methacrylate case) in the literature up to now concerns the polychloral obtained in the presence of tetraethylammonium *O*-methyl- or *O*-acetylmandelate (366–368). The monomer was treated so as to give directly a polymeric film that is endowed with extremely high rotatory power ($[\alpha]_D$ exceeding -1800° , but preliminary data obtained with other initiators led the authors to suppose that values $> 3000^\circ$ could be attained).

D. Properties and Uses of Optically Active Polymers

The lack of CD spectral information in optically active polymers, such as poly- α -olefins with chiral pendant groups that do not absorb in the visible or UV regions precludes observation of the electronic transitions responsible for optical activity. The ORD curves of such polymers are plane and can be interpreted by a one-term Drude equation, with λ_0 lower than 180 nm. Under such conditions a systematic investigation of the value of the rotatory power at the sodium D line is very useful. The correlation between this value and the conformational state of the polymer was obtained for various cases by means of the Brewster method (288, 290, 369, 370). Although this approach is rough with respect to conformational analysis, several conclusions drawn from the study of poly- α -olefins are worth mentioning in that they offer a simple interpretation, at the level of a first approximation, for the phenomena observed. The particularly high value of the rotatory power, if compared to that of a low molecular weight model, is attributed to the limited number of accessible conformations and to the predominance in solution of conformations corresponding to a given helical sense of the main chain and endowed with high rotational strength. Helices of opposite sense, although less favored by the chirality of the side chain, are nevertheless possible. The conformational equilibrium being temperature dependent the rotatory power changes notably with temperature: $d[\alpha]_D/dt$ for poly- α -olefins is up to an order of magnitude greater than that of analogous low molecular weight substances. The synthesis of rigid aliphatic chiral hydrocarbons endowed with high rotatory power (371), and comparison of their optical activity in the solid state with that of chiral polymers that crystallize in homomorphic helices (372) confirm that the chiroptical behavior in solution of poly- α -olefins is related to conformational phenomena.

More elaborate models, from the point of view of conformational statistics, lead to analogous conclusions (373–375). Even admitting the possibility of in-

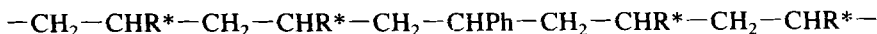
version of the screw sense of the single chain, the average length of the helical segments turned in one sense is thought to be different from that of the segments turned in the opposite way. In fact the two situations are not enantiomorphous due to the presence of the chiral substituents—all of the same configuration—and thus possess a different statistical weight. In this case also, a change in temperature modifies the conformational equilibrium and causes a variation in the rotatory power.

Copolymers between an achiral monomer and an enantiomer of a structurally similar monomer sometimes have optical activity higher than that derived by a simple additive rule (376). Thus, in the copolymer between 4-methylpentene and (*S*)-4-methylhexene the monomer units of the first type are forced to assume a conformation analogous to those of the second and contribute to the optical rotation of the polymer.

The ORD and CD curves of optically active polymers containing chromophoric groups show that the chromophores can be asymmetrically perturbed by the chirality of the substituents and of the main chain conformation. This is the case with poly(*sec*-butyl vinyl ketone) (377), which presents a Cotton effect at 292 nm, its intensity being greater in the prevalently isotactic polymer than in the atactic polymer.

More important, both from the synthetic and structural points of view, are copolymers between an optically active monomer lacking chromophores and an aromatic achiral monomer such as styrene, substituted styrenes, vinylnaphthalene, *N*-vinylcarbazole, and vinylchrysene (378, 379), which act as a chirality probe of the whole polymer structure (96). In the CD spectra, strong dichroic bands corresponding to the absorptions of the aromatic systems are observed. Dichroism increases with the degree of isotacticity and with the content of optically active monomer up to an asymptotic value and depends, for the same chromophoric group, on the nature of the chiral monomer. The origin of the dichroic bands derives from the local chiral perturbation and from the exciton coupling between chromophores of different monomer units present in the same helical chain. Experimental and theoretical studies regarding hydrocarbon systems (α -olefins and vinyl aromatic hydrocarbons) have been reported in the literature (380, 381).

More recently, such studies have been extended to nonhydrocarbon chiral comonomers, for example, menthyl acrylate and menthyl methacrylate (379, 382). Of notable interest, especially for microsequence investigation, are fluorescence studies combined with CD spectra carried out on copolymers containing the carbazole fragment (382). It is interesting to note that the induction of



chirality in the chromophore occurs also in atactic copolymers obtained by radical polymerization. In this case helices in the true sense do not exist; however, the local conformations are chiral and noncompensated.

The influence of the solvent on chiroptical properties of synthetic polymers is dramatically illustrated in the case of poly(propylene oxide). Price and Osgan had already shown, in their first article, that this polymer presents optical activity of opposite sign when dissolved in CHCl_3 or in benzene (78). The hypothesis of a conformational transition similar to the helix-coil transition of polypeptides was rejected because the optical activity varies linearly with the content of the two components in the mixture of solvents. Chiellini observed that the ORD curves in several solvents show a maximum around 235 nm, which should not be attributed to a Cotton effect and which was interpreted by a two-term Drude equation. He emphasized the influence of solvation on the position of the conformational equilibrium (383). In turn, Furukawa, as the result of an investigation in 35 different solvents, focused on the polarizability change of methyl and methylene groups in the polymer due to the formation of a contact complex with aromatic solvents (384).

The effect of temperature on the optical activity of poly- α -olefins has already been discussed: Although higher than that observed in analogous low molecular weight compounds, the variation of the rotatory power is only 2–5% for each 10 K. Much more important is the phenomenon observed by Miyata and Takemoto on 1,4-*trans*-poly-2-methylpentadiene obtained by inclusion polymerization in deoxycholic acid and apocholic acid (354–356). The presence of some steric disorder confers a certain solubility in common solvents on this polymer, in contrast to the insolubility of highly isotactic samples (385, 386). The optical activity at the D line measured in CCl_4 at 20°C, amounts to 90° for the polymer obtained from the *trans* monomer and to 320° for that obtained from the *cis* monomer. However the rotatory power decreases rapidly when the temperature increases and disappears almost completely around 60°C. In the same way the viscosity of CCl_4 solutions tends to diminish. Both return to the original values on cooling, after a long time interval. These results were interpreted by the authors in terms of a reversible conformational change of the polymeric chains in solution. However, this interpretation seems insufficient to explain the entire experimental evidence (387). The value of the rotatory power in CCl_4 at room temperature is not constant but is dependent on the thermal history of the sample after dissolution. It was also observed that the "solution" was slightly cloudy. Experimental results obtained by different techniques (polarimetry, turbidimetry, light scattering, capillary and rotation viscosimetry), suggested that the phenomenon is not of a purely molecular origin but should be attributed to the presence of some type of multimolecular aggregate.

Among the possible uses of optically active polymers, the preparation of stationary chiral phases for chromatographic resolution of enantiomers is the

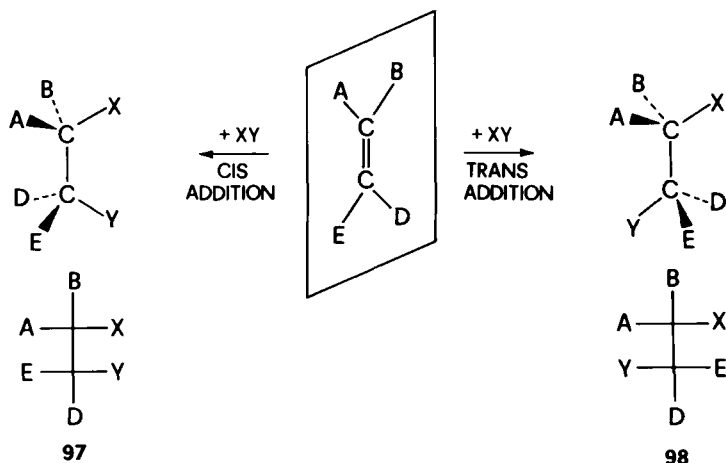
one that has matured sufficiently for practical application to present-day needs. The first positive result was obtained by Pino, Ciardelli, Lorenzi, and Natta a long time ago with poly-(*S*)-3-methylpentene as a chiral support: An optically inactive solution of the polymer obtained from racemic 4-methylhexene with a stereoselective catalyst was thus separated into fractions of opposite rotation (304). The separation with respect to the prevailing configuration of the substituents is accompanied by a separation with respect to molecular weight and stereoregularity (273). Van Beijnen, Nolte, and Drenth similarly resolved poly-*tert*-butyliminomethylene using glass beads coated with poly-*sec*-butyliminomethylene obtained from (*S*)-(+)-*sec*-butyl isocyanide (221). The fractions of higher rotatory power were successively separated on Sephadex according to their molecular weight, obtaining $[\alpha]_{578} = +56^\circ$, a value corresponding to that of the presumably pure enantiomer. Fractionation appears to be based on a strict helix-helix interaction between the support and substrate and is specific for this class of substances. In effect attempts to resolve other organic substances such as hexahelicene have given only negligible results ($<0.1\%$).

In contrast, the use, in chromatography, of poly(trityl methacrylate) appears much more promising. Both the insoluble polymer and macroporous silica gel coated with a soluble polymer have been used. The latter system gives better results, especially with regard to elution time. The columns have proved quite efficient in resolution of a great variety of chiral organic compounds (365, 388). Other examples of useful chiral polymer supports are the substituted polyacrylamides (389). Earlier used adsorbents obtained by reacting optically active amines with polyacryloyl chloride have been superseded by new chiral phases prepared by direct polymerization of optically active acrylamides.

VI. STEREOCHEMICAL CONTROL DURING POLYMERIZATION

The first stereochemical analysis of the polymerization mechanism of unsaturated monomers was proposed by Arcus 30 years ago (58, 269). The diastereomeric relationships within a single chain may be connected to monomer configuration by two factors: the type of addition to the double bond (*cis* or *trans*) and the way in which successive monomer molecules approach the growing chain. For a $\text{CHA}=\text{CHB}$ olefin the relationship between the structure of the monomer and that of the adding monomeric unit is illustrated in Scheme 22 (31), where *cis* or *trans* addition indicates that the new bonds are formed in the same half-space or in the two opposite half-spaces, provided there is no rotation around the central C—C single bond.

The way of presentation or of approach was originally defined with respect to the arrangement of two adjacent monomers. In more general terms the presentation was later defined with respect to one of the two enantiotopic faces (Re



Scheme 22

or Si) of the unsaturated monomer (50). The derivation of stereoregular configurations resulted from considering a constant addition mode in all the stages (always cis or always trans) and two possible ways of presentation, called constant or alternate presentation, according to whether addition occurs always on the same enantioface (Re or Si) or alternately on one and the other face: constant presentation affords isotactic polymers, alternate presentation syndiotactic ones.

This scheme was widely used for the interpretation of the polymerization of various monomers, but was questioned on the basis that the polymer structure is only vaguely related to the occurrence of true cis or trans addition (390). The three-dimensional structure of a given monomeric unit can be defined only when such a unit (e.g., the n -th one) is bonded on both sides to other monomeric units (i.e., after sequence $n - 1$, n , $n + 1$ has been formed) and depends at least on two distinct reactions: Addition of the n -th unit to the chain-end containing the $(n - 1)$ th unit, and that of the $(n + 1)$ th to the n -th unit. The stereochemical relationship between monomer and corresponding monomeric unit is the global result of all the stages of the addition process and cannot be ascribed merely to a single aspect of the reaction mechanism, as, for instance, the reaction between the monomer and the growing-chain-catalyst system (391). Determination of the addition stereochemistry in the sense here discussed represents a criterion according to which various mechanisms can be accepted or rejected. This test is of great significance for highly regular polymerization but is much less relevant in processes with weak stereochemical control.

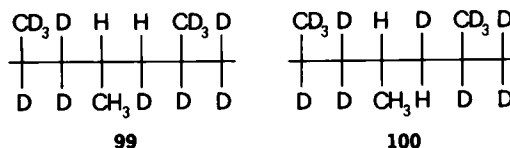
The addition mechanism was studied using both vinyl monomers specifically labeled with deuterium atoms on the methylene group and disubstituted $\text{CHA}=\text{CHB}$ olefins. The polymerization of the two stereoisomers, cis and trans,

of propylene-1- d_1 with Ziegler-Natta catalysts led specifically to the two distinct diisotactic polymers (see Sect. II-B and formulas 14-17) (57), thus indicating that addition occurs with a constant mechanism. The erythro-threo configuration of the two polymers was assigned by comparison of their IR spectra (392) with those calculated for the two structures (393, 394). The results indicate that cis addition occurs in the isotactic polymerization of propylene.

The same type of addition—as shown by X-ray analysis—occurs in the cationic polymerization of alkenyl ethers $R-CH=CH-OR'$ and of β -chlorovinyl ethers (395). However, NMR analysis showed the presence of some configurational disorder (396). The stereochemistry of acrylate polymerization, determined by the use of deuterated monomers, was found to be strongly dependent on the reaction environment and, in particular, on the solvation of the growing-chain-catalyst system at both the α and β carbon atoms (390, 397-399). Non-solvated contact ion pairs such as those existing in the presence of lithium catalysts in toluene at low temperature, are responsible for the formation of three isotactic sequences from cis monomers and, therefore, involve a trans addition; in contrast, solvent separated ion pairs (fluorenyllithium in THF) give rise to a predominantly syndiotactic polymer. Finally, in mixed ether-hydrocarbon solvents where there are probably peripherally solvated ion pairs, a predominantly isotactic polymer with nonconstant stereochemistry in the β position is obtained. It seems evident from this complexity of situations that the microtacticity of anionic poly(methyl methacrylate) cannot be interpreted by a simple Bernoulli distribution, as has already been discussed in Sect. III-A.

Turning to propylene, cis addition was found also for syndiotactic polymers (400, 401). This result deserves additional comment. It is known that only one disyndiotactic polymer is obtained from a $CHA=CHB$ olefin (see Sect. II-B) but this is no longer true when one considers the syndiotactic copolymers between two differently labeled monomers. The syndiotactic copolymer between perdeuteropropylene and propylene-1- d_1 can have either of the two structures **99** or **100**. Here the monomer unit deriving from the second monomer (present in small quantity) can be clearly identified as to its stereochemistry.

The NMR proton spectra of the syndiotactic copolymers obtained from perdeuteropropylene with the 1- d_1 -cis or the 1- d_1 -trans monomer present a doublet around 1 δ attributed to the methylene proton of the r dyad coupled to the methine proton. In the two polymers the vicinal coupling constants are different, 4.8 Hz

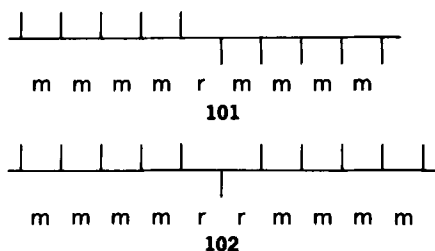


for the polymer from the trans monomer and 8.3 Hz for the cis monomer. Through the joint use of conformational analysis and the Karplus equation, Zambelli showed that these findings agree only with a cis addition (401). With analogous techniques he confirmed the occurrence of cis addition in the isotactic polymers as well. The constancy of the stereochemistry of addition in the Ziegler-Natta polymerization of propylene makes mechanistic studies easier, the degree of stereoregularity being dependent only on the selection power of the growing-chain-catalyst complex towards the enantiotopic faces of the monomer.

The Arcus approach can be extended to the analysis of the polymerization of 1,4-disubstituted butadienes. The main differences concern the presence of a further element of stereoisomerism, the cis or trans configuration of the double bond in the chain, and the fact that the chemical monomer unit ($-\text{CHA}-\text{CH}=\text{CH}-\text{CHB}-$) does not coincide with the stereochemically significant chain segment (corresponding to $=\text{CH}-\text{CHB}-\text{CHA}-\text{CH}=-$).

The relation between polymer microstructure and polymerization mechanism was discussed in Sect. II-D according to copolymerization theory. However, additional consideration is necessary in order to avoid both oversimplifications in the theoretical approach and unnecessary complications in the statistical treatment. The growing chain-end in a vinyl polymerization is chiral and is, therefore, sensitive to diastereomeric interactions (402). If no other sources of chirality are present, one may assume that, inside a given chain, the probability of a certain succession, let us say 00 , is equal to that of its antipode, 11 , provided the sequence influencing the latter reaction is exactly enantiomeric to the former. In such a case the monomer unit distribution follows a symmetric Bernoulli or Markov scheme and is regulated by the same parameters for the distribution of m and r sequences ($p_{00} = p_{11} = p_m$ for a Bernoulli process, $p_{000} = p_{111} = p_{mm}$ for first-order Markov chains, and so on—see Table 4, columns 2 and 3, respectively). This consideration is valid for almost all radical polymerization and for certain ionic and coordination polymerizations, particularly when they lead to the formation of syndiotactic polymers. But if the reaction is influenced by a chiral catalyst (even if racemic) p_{00} is not necessarily equal to p_{11} inside a single chain (and sometimes not even throughout the entire system). The fraction of m or r dyads, and that of longer sequences, must be calculated as the sum of the successions 00 and 11 , 01 and 10 , and so on (111) (see Table 4, column 4).

To illustrate this point it is particularly instructive to examine the configurational defects existing in isotactic polypropylene. The steric control during polymerization can in principle be attributed to two different factors: the influence of the chirality of the last entered unit (this case falls within the discussion of symmetric chains reported previously) or that of the catalytic site. The chirality of the latter may be preexisting or may arise at the moment of polymer-



ization but, in any case, is independent of that of the chain (403). The two different hypotheses entail a different response of the reactive system to accidental perturbation such as configurational inversion, as shown in formulas 101 and 102. In the first case, once an error has occurred, no memory exists of the preceding situation and the chain continues with the inverted configuration (. . . *11110000* . . .): After a succession of *m* dyads an isolated *r* dyad is found and then again *m* dyads (. . . *mmmrmmm* . . .), 101. In the second case, the chiral catalyst imposes a return to the preceding configuration, (. . . *11110111* . . .) with the formation of an *rr* defect (. . . *mmmrmmm* . . .), 102. This point was clarified by an analysis of the ^{13}C NMR spectrum of polypropylene at the pentad level. In a highly isotactic sample one can observe, in addition to the main isotactic signal (. . . *mmmm* . . .), three weak peaks in an intensity ratio 2:2:1 attributable, respectively, to the pentads *mmmr* (*11110*), *mmrr* (*11101*), and *mrrm* (*11011*) (141, 405, 406). The opposite hypothesis should give rise to only two signals of equal intensity *mmmr* (*11110*) and *mmrm* (*11100*); however, the latter was not detected in the spectrum. One may conclude, with a high degree of confidence, that the stereochemical control in the iso-specific polymerization of propylene in the presence of heterogeneous catalysts is determined by the chirality of the catalytic center.

The same conclusion is reached by considering the response of the system when an ethylene molecule is inserted instead of propylene. The effect of the chain end containing an ethylene unit [$-\text{CH}(\text{CH}_3)-\text{CH}_2-\text{CH}_2-\text{CH}_2-$ catalyst] on the stereochemistry of a new propylene unit should be much weaker than that existing in homopolymerization [$-\text{CH}(\text{CH}_3)-\text{CH}_2-$ catalyst], since it corresponds to a 1,5- and not to a 1,3-asymmetric induction. The new propylene unit should have *0* or *1* configuration with almost the same probability. In contrast, stereochemical control tied to the catalytic center should impose the same configuration on the propylene unit before and after the introduction of the error. This is precisely what does happen with common iso-specific catalysts (407).

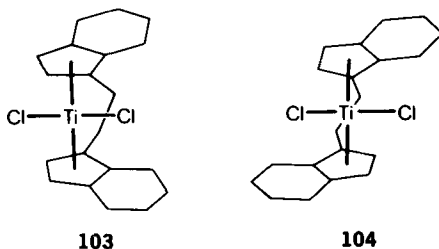
The probabilistic aspect of error propagation in isotactic polypropylene was treated both as a second-order Markov chain (in terms of *m* and *r* dyads) (408) and, in terms of a model of enantiomorphic catalyst sites, as asymmetric Ber-

noulli chains, in terms of *0* and *1* units. The latter treatment is much preferable since it requires a single probabilistic parameter instead of four, offers a simpler and more rational interpretation of the polymerization mechanism, and shows better agreement with experimental data.

For syndiotactic polypropylene the symmetric Bernoulli trial, expressed in *m* and *r* dyads, is quite adequate for the representation of experimental data, and agrees with the stereochemical control being exerted by the growing chain end (145, 409). In its turn, atactic polypropylene is considered as a mixture of the products of two superposed processes, of the type discussed for isotactic and syndiotactic polymers, and is described by a simplified two-state model (145).

The hypothesis of stereochemical control linked to catalyst chirality was recently confirmed by Ewen (410) who used a soluble chiral catalyst of known configuration. Ethylenebis(1-indenyl)titanium dichloride exists in two diastereoisomeric forms with C_s (meso, **103**) and C_2 (**104**) symmetry, both active as catalysts in the presence of methylalumoxanes and trimethylaluminum. Polymerization was carried out with a mixture of the two isomers in a 44/56 ratio. The polymer consists of two fractions, their formation being ascribed to the two catalysts: a pentane-soluble fraction, which is atactic and derives from the meso catalyst, and an insoluble crystalline fraction, obtained from the racemic catalyst, which is isotactic and contains a defect distribution analogous to that observed in conventional polypropylenes obtained with heterogeneous catalysts. The failure of the meso catalyst in controlling the polymer stereochemistry was attributed to its mirror symmetry; in its turn, the racemic compound is able to exert an asymmetric induction on the growing chains due to its intrinsic chirality.

Propylene polymerization at low temperature with an achiral soluble catalyst provided a further interesting result (410). The ^{13}C NMR spectrum of the polymer prepared in the presence of dicyclopentadienyldiphenyl titanium shows three peaks in the methyl region, corresponding to the pentads *mmmm*, *mmmr*, and *mmrm*, the last two having the same intensity. This finding corresponds to structure **101** and hence to steric control exerted by the chain end and agrees with a symmetric Bernoulli distribution of configurational defects. It is noteworthy that this kind of mechanism was observed only in the absence of any chiral compound other than the growing chain end.



Analysis of the poly(methyl methacrylate) sequences obtained by anionic polymerization was undertaken at the tetrad level in terms of two different schemes (10): one, a second-order Markov distribution (with four independent conditional probabilities, p_{mmr} , p_{mrr} , p_{rmr} , and p_{rrr}) (44), the other, a two-state mechanism proposed by Coleman and Fox (122). In this latter scheme one supposes that the chain end may exist in two (or more) different states, depending on the different solvation of the ion pair, each state exerting a specific stereochemical control. A dynamic equilibrium exists between the different states so that the growing chain shows the effects of one or the other mechanism in successive segments. The deviation of the experimental data from the distribution calculated using either model is, however, very small, below experimental error, and, therefore, it is not possible to make a choice between the two models on the basis of statistical criteria only.

VII. CONCLUSIONS

In the preceding Sect. I have tried to illustrate the problems and developments of polymer stereochemistry from both the historical and logical points of view. A clear connection exists between synthetic and structural aspects: For the solution of problems yet unsolved an interdisciplinary approach is required involving not only polymer chemistry but also spectroscopy, crystallography, statistical thermodynamics, solid state physics, and so on.

In the course of time a shift in interest has occurred from highly stereoregular to more disordered polymers, as a result of the development of new experimental techniques and the increasing maturity of scientific knowledge. Once the fundamental aspects were clarified it was easier to frame the structural problem of macromolecular compounds in a general scheme and to examine single cases with the help of statistical methods. Analysis of microtacticity represents today, together with the knowledge of molecular weight distribution, a current standard of polymer characterization, a kind of molecular fingerprint largely used in the evaluation of industrial products.

Nowadays attention is turned also to the supermolecular level, that is, to the morphologic aspects, to the nature of interfaces, to the formation of new phases, or of particular aggregates (liquid crystals, gels, etc.). Interest has also been directed to the study of chain mobility for its influence on frictional properties of polymers. In recent years there have been many successful approaches to a microscopic theory (in contrast to a phenomenological approach) of the physico-mechanical behavior of macromolecular materials.

At the synthetic level, stereochemical problems are far from being exhausted. A common research target today is that of the so-called tailor-made polymers, that is, polymers suited to specific uses: electronic (semi- and superconductors),

biomedical (both as drugs and as biocompatible materials for prostheses), as catalysts for selective chemical reactions, and for asymmetric syntheses (synzymes). The ability to predict the right structure needed for a given property and to realize its synthesis is much increased compared to the past but, even today, is still largely tied to the skill and imagination of the chemist himself.

With regard to fundamental principles I have shown the relation as well as the differences between the stereochemical treatment of low molecular weight and that of macromolecular compounds. If some confusion has resulted in the past, it is due to the improper use of concepts and of methods outside their proper field. Macromolecular stereochemistry can be subjected to physico-mathematical approaches based on concepts of system and structure and on topological principles. Interesting developments in this regard were recently published by Danusso and co-workers (411–413).

To conclude this review I must pay a tribute to the work and figure of Giulio Natta who pioneered macromolecular stereochemistry and was an active protagonist in the field for many years. The most important aspects of his discoveries and the present significance of the research derived therefrom have been illustrated by his students and by scientists from all over the world (16, 18). As may be seen from the present article, many of the fundamental discoveries were derived from the work of his research group at the Milan Polytechnic. A large part of the later development, also, is the fruit of a cultural tradition that has influenced the whole Italian school of polymer chemistry.

I personally had the good fortune to participate in the research on polymer stereochemistry from the beginning, and to witness its full development. I consider this article to be an homage to the memory of Giulio Natta and an account of his scientific heritage.

ADDENDUM, MAY 1986

Numerous articles relevant to polymer stereochemistry have appeared since this chapter was completed, most of them dealing with conformational analysis, spectroscopy, and chirality. In this addendum I shall discuss only a few items pertaining to the optical activity of rigid polymers. This matter has recently received a lot of attention and merits a more detailed discussion than was presented earlier.

As already reported in Sects. IV-C and V, there are a few examples of chiral polymers not containing classical asymmetric carbon atoms or other elements of localized chirality (substituted biphenyls, etc.). In such cases chirality is related to the presence of rigid helical conformations and optical activity derives from an excess of chain segments turned in one or the other sense. We may distinguish polymers in which conformational rigidity (and hence the possibility

to observe optical activity) is confined to the solid state from those that exhibit such behavior even in solution. Polychloral has already been cited as an example of the former type (366–368). High optical activity was attained by Vogl by dispersing an asymmetric catalyst in the monomer above the so-called ceiling temperature, that is, the temperature above which polymerization does not occur for thermodynamic reasons (414). The monomer-initiator mixture was placed between glass plates and polymerization started by cooling the assembly in cold water. The rotary power of the polymeric films obtained by this technique is very high (up to 5000°). According to the authors this value cannot be explained merely in terms of birefringence phenomena (this contribution is estimated between 3 and 20% of the experimental value). The polymer structure was determined by X-ray analysis: Polychloral, which is insoluble and does not melt, is said to be isotactic (415, 416) and to possess a helical conformation with four monomer units per turn.

Optical activity was observed in the solid state even in a sample of native isotactic polypropylene. Kaminsky was able to achieve this result by using a soluble catalytic system analogous to that already reported by Ewen (410). Substitution of zirconium for titanium in the reaction with the bisindenyl derivative affords only a chiral complex analogous to **104** and not the meso compound **103** (417, 418). The complex was resolved and used, in the presence of aluminum compounds, for the polymerization of propylene. The native polymer thus obtained in the solid state contains only (or prevailing) helices of a given sign, due to the control exerted by the optically active catalyst. The rotatory power of the solid polymer (measured in suspension or in the form of a thin film) ranges from -65 to -250° . Of course, optical activity disappears upon melting or dissolving the sample.

The conformation of semirigid polymers in solution has been studied for chiral and achiral polyisocyanates (419). The "persistence length (155)," a quantity related to the rigidity of the macromolecular chain, was found to be higher in polyisocyanates obtained from optically active monomers. This fact is attributed to the different energies of the two diastereoisomeric helices (right handed and left handed, but always containing the side-chain substituent of the same configuration), which make the conformational inversion more difficult than in the case of achiral or racemic monomers.

A method for obtaining optically active polyiminomethylenes from achiral monomers was recently devised by Nolte, Drenth and co-workers (420). It consists in the copolymerization of an achiral monomer (e.g., phenyl isocyanide) with an optically active isocyanide endowed with a low tendency to polymerize. The chiral monomer is incorporated in one of the two helices and, due to its low reactivity, stops or slows down its growth. The other helix is unaffected by this phenomenon and continues to grow, permitting the almost complete conversion of the achiral monomer into an optically active polymer.

Optically active oligomers of trityl methacrylate (see 73) have been studied by Wulff (421): They were converted into optically active oligomers of methyl methacrylate. The same transesterification reaction performed on the optically active poly(trityl methacrylate) with higher molecular weight affords inactive poly(methyl methacrylate). This result fits perfectly the scheme discussed in Sect. V-A: Isotactic polymers with different end groups are cryptochiral and hence optically inactive if they are of high molecular weight, but short-chain oligomers can show measurable optical activity.

Highly optically active oligo(methyl methacrylate) with an average polymerization degree between 5 and 15 has been obtained by direct polymerization in the presence of potassium *t*-butoxide or butyllithium complexed with chiral crown ethers, according to Cram and Sogah (422): This product unexpectedly shows a slow mutarotation; its rotatory power decreases time with and rotation approaches zero over a period of hours. The same behavior was observed with oligo(*tert*-butyl methacrylate), but not with oligo(benzyl methacrylate), whose rotation remains constant over similar time spans. The high initial rotation was attributed to the helicity of the products induced by the catalyst chirality, the small residual activity being due to the chirality of the short chains with different terminal groups in a random coil conformation or in a compensated mixture of opposite helices. The higher conformational stability of the benzyl oligomer with respect to the *tert*-butyl derivative, which is demanded by this interpretation, was considered rather unusual even by the authors themselves. In view of potential interest in the study of the rates of conformational transitions, these results need to be more critically considered; additional experimental data would help in a better evaluation of this work.

ACKNOWLEDGMENTS

I wish to thank all the people who have participated in the research described in this article and who have made important contributions to the development of polymer stereochemistry; many of their names are found in the bibliography. I particularly thank my Italian colleagues for having put their bibliographic files at my disposal. The technical assistance of Mr. M. Lovati, University of Milan, in recording the NMR spectra is gratefully acknowledged. This study has been partly supported by Consiglio Nazionale delle Ricerche (CNR), Rome, and by the Italian Ministry of Education, Rome, Italy.

REFERENCES

1. The historical and cultural background of the discoveries of Ziegler and Natta and the development of their research in the following 10 years has been described in the Nobel Lectures of the protagonists (2, 3).

2. Ziegler, K. (a) *Angew. Chem.* **1964**, *76*, 545; (b) Nobel Lectures, Chemistry, 1963–1970, Elsevier, New York, 1972, p. 6.
3. Natta, G. *Chim. Ind. (Milan)* **1964**, *46*, 397; *Science* **1965**, *147*, 261; ref 2(b), p. 27.
4. According to IUPAC recommendations (5) the term *molecular weight* is synonymous with *relative molecular mass* and will be used throughout this article.
5. IUPAC Macromolecular Division, Macromolecular Nomenclature Commission *Makromol. Chem.* **1984**, *185*, unnumbered pages at the end of the first issue.
6. Goodman, M. *Top. Stereochem.* **1967**, *2*, 73.
7. "The Stereochemistry of Macromolecules"; Ketley, A. D. Ed.; Dekker: New York, **1968**.
8. "Encyclopedia of Polymer Science and Technology"; Mark, H.F.; Gaylord, N. G.; Bikales, N. M. Eds.; Interscience: New York, **1964–1972**.
9. "Chimie Macromoléculaire," Champetier, G., Ed.; Hermann: Paris, **1970**.
10. Bovey, F. A. "High Resolution NMR of Macromolecules"; Academic: New York, **1972**.
11. Randall, J. C. "Polymer Sequence Determination"; Academic: New York, **1977**.
12. Elias, H. G. "Macromolecules"; Plenum: New York, **1977**.
13. "Macromolecules"; Bovey, F. A.; Winslow F. H., Eds.; Academic: New York, **1979**.
14. "Optically Active Polymers"; Sélégny, E., Ed.; Reidel: Dordrecht, **1979**.
15. "Preparation and Properties of Stereoregular Polymers"; Lenz, R. W.; Ciardelli, F., Eds.; Reidel: Dordrecht, **1979**.
16. "Structural Order in Polymers"; Ciardelli, F.; Giusti, P., Eds.; Pergamon Press: Oxford, **1981**.
17. Bovey, F. A. "Chain Structure and Conformation of Macromolecules"; Academic: New York, **1982**.
18. "Giulio Natta: Present Significance of His Scientific Contribution"; Carrà, S.; Parisi, F.; Pasquon, I.; Pino, P., Eds.; Editrice di Chimica: Milan, **1982**.
19. "Macromolecole: Scienza e Tecnologia"; Ciardelli, F.; Farina, M.; Giusti, P.; Cesca, S., Eds.; Pacini: Pisa, **1983**.
20. Huggins, M. L.; Natta, G.; Desreux, V.; Mark, H. J. *Polym. Sci.* **1962**, *56*, 153; *Pure Appl. Chem.* **1966**, *12*, 643.
21. IUPAC Macromolecular Division, Macromolecular Nomenclature Commission *Pure Appl. Chem.* **1981**, *53*, 733.
22. Natta, G. *Atti Accad. Naz. Lincei, Mem. Classe Sci. Fis. Mat. Nat., Sez. II^a* **1955**, *4*, 61.
23. Natta, G.; Corradini, P. *Atti Accad. Naz. Lincei, Mem. Classe Sci. Fis. Mat. Nat., Sez. II^a* **1955**, *4*, 73.
24. Natta, G.; Pino, P.; Corradini, P.; Danusso, F.; Mantica, E.; Mazzanti, G.; Moraglio, G. *J. Am. Chem. Soc.* **1955**, *77*, 1708.
25. Natta, G.; Corradini, P. *Rend. Accad. Naz. Lincei* **1955**, *19*, 229; *J. Polym. Sci.* **1956**, *20*, 251.
26. This treatment can be extended without modification to polymers obtained from vinylidene monomers with different substituents ($\text{CH}_2=\text{CR}_1\text{R}_2$) and from aldehydes (RCHO) in which the oxygen atom replaces the methylene group.
27. In his early papers Natta referred to the state of the art of that time along the lines discussed by Flory (28). Until the early 1950s, the lack of crystallinity in vinyl polymers was attributed to the configurational disorder present in such compounds, considered as copolymers of *d* and *l* structural units. These units were defined with reference to a macromolecule having the chain in a zigzag planar disposition, the substituents of one type being above the plane

and those of the other, below. Flory discussed the structure of the only crystalline vinyl polymer known at that time: the poly(vinyl isobutyl ether) obtained by Schildknecht (29). In contrast to the latter's opinion that the crystallinity was attributable to the tendency of the monomer units to alternate regularly between *d* and *l* configurations, Flory advanced the opposite hypothesis, namely, that sequences of like configuration might be present. On the basis of crystallographic and spectroscopic evidence Natta affirmed that in the new propylene polymer all the asymmetric atoms, at least for long sections of the chain, have the same steric configuration (22). Due to the difficulty of inserting this fact into existing stereochemical theory he proposed the term isotactic and gave an illustration of the structure corresponding to formula 4. In the same article he discussed the chirality of an isotactic chain of finite length and different terminal groups: Recognizing the presence, in principle, of two enantiomeric chains, he predicted the existence of the phenomenon of internal compensation due to the almost complete superposability of a chain with its mirror image, the only exceptions being the end groups. According to Natta, the concepts of isotacticity could be extended also to condensation polymers obtained from chiral monomers of a single configuration, such as poly-L- α -amino acids, thus forming a bridge with stereochemical and structural problems of natural biopolymers.

28. Flory, P. J. "Principles of Polymer Chemistry"; Cornell University Press: Ithaca, 1953.
29. Schildknecht, C. E.; Gross, S. T.; Davidson, H. R.; Lambert, J. M.; Zoss, A. O. *Ind. Eng. Chem.* **1948**, *40*, 2104.
30. Natta, G.; Danusso, F. *Chim. Ind. (Milan)* **1958**, *40*, 743; *J. Polym. Sci.* **1959**, *34*, 3.
31. Natta, G.; Farina, M.; Peraldo, M. *Chim. Ind. (Milan)* **1960**, *42*, 255; *Makromol. Chem.* **1960**, *38*, 13; *J. Polym. Sci.* **1960**, *43*, 289.
32. Natta, G.; Corradini, P. *Nuovo Cimento Suppl.* **1960**, *15*, 9.
33. In reality it is questionable if such polymers can be considered syndiotactic: see rule 8 in ref. 21.
34. Natta, G.; Pino, P.; Mazzanti, G. *Chim. Ind. (Milan)* **1955**, *37*, 927.
35. Natta, G.; Pino, P.; Mazzanti, G. *Gazz. Chim. Ital.* **1957**, *87*, 528.
36. Eliel, E. L. "Stereochemistry of Carbon Compounds"; McGraw-Hill: New York, 1962.
37. Luisi, P. L.; Ciardelli, F. In "Reactivity, Mechanism and Structure in Polymer Chemistry" Jenkins, A. D.; Ledwith, A., Eds.; Wiley: New York, 1974, p. 471.
38. Frisch, H. L.; Schuerch, C.; Szwarc, M. *J. Polym. Sci.* **1953**, *11*, 559.
39. Morawetz, H. "Macromolecules in Solution"; Interscience: New York, 1965, 1st ed.; **1975**, 2nd ed.
40. Flory, P. in ref. 16, p. 3.
41. Farina, M.; Peraldo, M.; Natta, G. *Angew. Chem.* **1965**, *77*, 149; *Int. Ed. Engl.* **1965**, *4*, 107.
42. Mislow, K.; Siegel, J. *J. Am. Chem. Soc.* **1984**, *106*, 3319.
43. Further discussion and comparison of the various models will be made in the section dealing with polymer chirality.
44. Frisch, H. L.; Mallows, C. L.; Bovey, F. A. *J. Chem. Phys.* **1966**, *45*, 1565.
45. Price, F. P. *J. Chem. Phys.* **1962**, *36*, 209.
46. Farina, M. In ref. 19, p. 41.
47. Corradini, P. In ref. 7, Vol. 3, p. 1.
48. In his 1966 Welch Lecture (49), Corradini credits the original idea of this classification to S. Lifson. Unfortunately, the text of the published lecture contains no bibliographic reference.

49. Corradini, P. *Proc. Robert A. Welch Found. Conf. Chem. Res.* **1966**, 91.
50. Hanson, K. R. *J. Am. Chem. Soc.* **1966**, 88, 2731.
51. Hirschmann, H.; Hanson, K. R. *J. Org. Chem.* **1971**, 36, 3293.
52. Hirschmann, H.; Hanson, K. R. *Top. Stereochem.* **1983**, 14, 183.
53. Mislow, K.; Raban, M. *Top. Stereochem.* **1967**, 1, 1.
54. Bovey, F. A.; Tiers, G.V.D. *J. Polym. Sci.* **1960**, 44, 173.
55. Bovey, F. A.; Tiers, G.V.D. *Fortschr. Hochpolym. Forsch.* **1963**, 3, 139.
56. Natta, G. *Angew. Chem.* **1956**, 68, 393; *Chim. Ind. (Milan)* **1956**, 38, 751.
57. Natta, G.; Farina, M.; Peraldo, M. *Rend. Accad. Naz. Lincei* **1958**, 25, 424.
58. Arcus, C. L. *J. Chem. Soc.* **1955**, 2801.
59. Dauben, W. G.; Pitzer, K. S. In "Steric Effects in Organic Chemistry"; Newman, M. S., Ed.; Wiley: New York, 1956, p. 10.
60. Cais, R. E. *Macromolecules* **1980**, 13, 806.
61. Natta, G.; Farina, M.; Peraldo, M.; Bressan, G. *Chim. Ind. (Milan)* **1961**, 43, 161; *Makromol. Chem.* **1961**, 43, 68.
62. Natta, G.; Porri, L.; Corradini, P.; Morero, D. *Rend. Accad. Naz. Lincei* **1956**, 20, 560.
63. An extensive examination of this material, including historical aspects, was published by Natta and Porri (64).
64. Natta, G.; Porri, L. "Elastomers by Coordinate Anionic Mechanism A. Diene Elastomers," In "The Polymer Chemistry of Synthetic Elastomers;" Vol. 2; Kennedy, J. P.; Törnquist, E. G., Eds.; Wiley: New York, **1969**; p. 597.
65. Natta, G.; Corradini, P. *Angew. Chem.* **1956**, 68, 615.
66. Natta, G.; Corradini, P.; Porri, L. *Rend. Accad. Naz. Lincei* **1956**, 20, 728.
67. Natta, G.; Porri, L.; Corradini, P.; Morero, D. *Chim. Ind. (Milan)* **1958**, 40, 362.
68. Natta, G.; Corradini, P. *Nuovo Cimento Suppl.* **1960**, 15, 111.
69. Meyer, K. H.; Mark, H. *Berichte* **1928**, 61, 1939.
70. Meyer, K. H.; Mark, H. "Der Aufbau der Hochpolymeren organischen Naturstoffe"; Akademische Verlagsgesellschaft: Leipzig, **1930**, p. 205.
71. Meyer, K. H. "Natural and Synthetic High Polymers"; Interscience: New York, **1950**, p. 186.
72. Natta, G.; Porri, L.; Corradini, P.; Zanini, G.; Ciampelli, F. *Rend. Accad. Naz. Lincei* **1960**, 29, 257; *J. Polym. Sci.* **1961**, 51, 463.
73. Natta, G.; Porri, L.; Stoppa, G.; Allegra, G.; Ciampelli, F. *J. Polym. Sci., Part B* **1963**, 1, 67.
74. Farina, M. *Chim. Ind. (Milan)* **1964**, 46, 761.
75. Tsunetsugu, T.; Fueno, T.; Furukawa, J. *Makromol. Chem.* **1968**, 112, 220.
76. Natta, G.; Farina, M.; Corradini, P.; Peraldo, M.; Donati, M.; Ganis, P. *Chim. Ind. (Milan)* **1960**, 42, 1361.
77. Lorenzi, G. P.; Tomasic, L. *J. Am. Chem. Soc.* **1977**, 99, 8322.
78. Price, C. C.; Osgan, M. *J. Am. Chem. Soc.* **1956**, 78, 4787.
79. Natta, G.; Corradini, P.; Dall'Asta, G. *Rend. Accad. Naz. Lincei* **1956**, 20, 408.
80. Riande, E.; de la Campa, J. G.; Guzman, J.; De Abajo, J. *Macromolecules*, **1984**, 17, 1431.
81. Vanderberg, E. J. *J. Am. Chem. Soc.* **1961**, 83, 3538.
82. Vandenberg, E. J. *J. Polym. Sci. Part B* **1964**, 2, 1085.

83. Kops, J. *J. Polym. Sci. Part A* **1972**, *10*, 1275.
84. Kops, J. In ref. 15, p. 225.
85. Komada, H.; Okada, M.; Sumitomo, H. *Macromolecules* **1979**, *12*, 5.
86. Hashimoto, K.; Sumitomo, H. *Macromolecules* **1980**, *13*, 786.
87. Porri, L.; Rossi, R.; Ingrosso, G. *Tetrahedron Lett.* **1971**, 1083.
88. Natta, G.; Mazzanti, G.; Pregaglia, G. F.; Binaghi, M.; Peraldo, M. *J. Am. Chem. Soc.* **1960**, *82*, 4742.
89. Natta, G.; Mazzanti, G.; Pregaglia, G. F.; Binaghi, M.; Cambini, M. *Makromol. Chem.* **1962**, *51*, 148.
90. Pregaglia, G. F.; Binaghi, M. In ref. 8, Vol. 8, p. 45.
91. Farina, M.; Di Silvestro, G. unpublished results.
92. Farina, M.; Di Silvestro, G. *Tetrahedron Lett.* **1975**, 183.
93. Wulff, G.; Hohn, J. *Macromolecules* **1982**, *15*, 1255.
94. Casiraghi, G.; Cornia, M.; Ricci, G.; Casnati, G.; Andreotti, G. D.; Zetta, L. *Macromolecules* **1984**, *17*, 19.
95. Casiraghi, G.; Cornia, M.; Sartori, G.; Casnati, G.; Bocchi, V. *Makromol. Chem.* **1982**, *183*, 2611.
96. Inoue, H.; Helbig, M.; Vogl, O. *Macromolecules* **1977**, *10*, 1331.
97. Arichi, S.; Pedram, M. Y.; Cowie, J. M. C. *Eur. Polym. J.* **1979**, *15*, 107, 113.
98. Möller, M.; Ritter, W.; Cantow, H. *J. Polym. Bull.* **1981**, *4*, 609.
99. Farina, M.; Di Silvestro, G.; Sozzani, P. *Macromolecules* **1982**, *15*, 1451.
100. Farina, M.; Di Silvestro, G.; Sozzani, P.; Savaré, B. *Macromolecules* **1985**, *18*, 923.
101. Di Silvestro, G.; Sozzani, P.; Savaré, B.; Farina, M. *Macromolecules* **1985**, *18*, 928.
102. We use a convention different from Bovey's (10, 13, 54) and in line with the preceding treatment. The differences between the two representations concern mainly vicinal atoms and are quite marginal within the framework of vinyl polymers.
103. Price, F. P. In "Markov Chains and Monte Carlo Calculations in Polymer Science"; Lowry, G. C., Ed.; Dekker: New York, **1970**, p. 187.
104. The impossibility of distinguishing the two methylene hydrogens in a syndiotactic polymer is another way of saying that only one disyndiotactic structure for polymers of disubstituted $\text{CHA}=\text{CHB}$ olefins exists.
105. Stehling, F. C.; Knox, J. R. *Macromolecules* **1975**, *8*, 595.
106. Suter, U. W.; Neuenschwander, P. *Macromolecules* **1981**, *14*, 528.
107. Chujo, R.; Kamei, M.; Nishioka, A. *Polym. J.* **1972**, *3*, 289.
108. The stereosequence nomenclature used in those articles is different from that recommended by IUPAC (21) and used in this article. The three main points of difference concern the use of letters *m* and *r* (or *M* and *R*) to define the position of substituents that are not chemically equivalent, the use of the zigzag projection to define the steric relationships among adjacent substituents, and the use of the terms dyad, triad, and so on, to define successions of two, three, and so on, nonequivalent centers of stereoisomerism. The first problem can be overcome by the use of other letters, for example, *e* and *t* (or *E* and *T*) for erythro and threo (396); for the second it suffices to exchange the letters, as becomes clear if a Fischer projection is employed instead of a zigzag one (see the preceding discussion regarding diisotactic polymers 14–17). As regards the third point, a source of ambiguity derives from the fact that the terms dyad, triad, and so on, are generally used with reference to successive monomer units

and to sequences of chemically equivalent centers. This is particularly critical in the comparison of deuterated and nondeuterated vinyl polymers; in view of this, a different nomenclature is desirable.

109. Zetta, L.; Gatti, G.; Audisio, G. *Macromolecules* **1978**, *11*, 763.
110. Audisio, G.; Silvani, A.; Zetta, L. *Macromolecules* **1984**, *17*, 29.
111. Shelden, R. A.; Fueno, T.; Tsunetsugu, T.; Furukawa, J. *J. Polym. Sci., Polym. Lett.* **1965**, *3*, 23.
112. Spassky, N.; Leborgne, A.; Hull, W. E. *Macromolecules* **1983**, *16*, 608.
113. Sépulchre, M.; Spassky, N.; Van Ooteghem, D.; Goethals, E. J. *J. Polym. Sci., Polym. Chem. Ed.* **1974**, *12*, 1683.
114. In consideration of their original meaning, meso and racemic, the IUPAC rules (21) prohibit the use of symbols *m* and *r* for polymers in which the chain segment connecting two homologous centers is not symmetric with respect to the direction of observation. However, the use of a simple terminology to indicate the diastereomeric relations of homologous stereogenic centers is highly desirable. Spassky's proposal could be a departure point, in part also because it employs a terminology—*isotactic* and *syndiotactic*—perhaps too quickly eliminated or limited in the context of microstructural analysis. An alternative proposal would be to continue to use the letters *m* and *r* without any reference to their origin. A useful mnemonic rule might be that of correlating *m* to *maintenance* and *r* to *reversal* of configuration. I thank P. Sozzani for this suggestion.
115. Farina, M.; Grassi, M.; Di Silvestro, G. *Eur. Polym. J.* **1985**, *21*, 71.
116. Grassi, M.; Di Silvestro, G.; Farina, M. Preprints of the 6th AIM Meeting, Pisa, Italy, **1983**, p. 109.
117. Woodbrey, J. C. in ref. 7, Vol. 3, p. 61.
118. "NMR and Macromolecules"; Randall, J. C. Ed.; ACS Symposium Series 247, **1984**.
119. Flory, P. J. *Macromolecules* **1970**, *3*, 613.
120. Tincher, W. C. *J. Polym. Sci.* **1962**, *62*, S 148; *Makromol. Chem.* **1965**, *85*, 20.
121. Schaefer, J.; Natush, D. F. S. *Macromolecules* **1972**, *5*, 416.
122. Coleman, B. D.; Fox, T. G. *J. Chem. Phys.* **1963**, *38*, 1065.
123. Peat, I. R.; Reynolds, W. F. *Tetrahedron Letters* **1972**, 1359.
124. Bovey, F. A.; Schilling, F. C.; Kwei, T. K.; Frisch, H. L. *Macromolecules* **1977**, *10*, 559.
125. Satoh, S.; Chujo, R.; Ozeki, T.; Nagai, E. *J. Polym. Sci.* **1962**, *62*, 101.
126. Stehling, S. J. *J. Polym. Sci., Part A* **1964**, *2*, 1815.
127. Woodbrey, J. C. *J. Polym. Sci., Part B* **1964**, *2*, 315.
128. Natta, G.; Lombardi, E.; Segre, A. L.; Zambelli, A.; Marinangeli, A. *Chim. Ind. (Milan)* **1965**, *47*, 378.
129. Gatti, G. In ref. 19, p. 118.
130. Segre, A. L. *Macromolecules* **1968**, *1*, 93.
131. Zambelli, A.; Segre, A. L.; Farina, M.; Natta, G. *Makromol. Chem.* **1967**, *110*, 1.
132. Zambelli, A.; Segre, A. L. *J. Polym. Sci., Polym. Lett.* **1968**, *6*, 473.
133. Heatley, F.; Zambelli, A. *Macromolecules* **1969**, *2*, 618.
134. Flory, P. J.; Baldeschiwiler, J. D. *J. Am. Chem. Soc.* **1966**, *88*, 2873.
135. Flory, P. J.; Fujiwara, Y. *Macromolecules* **1969**, *2*, 327.
136. Flory, P. J. *J. Polym. Sci., Polym. Phys. Ed.* **1973**, *11*, 621.

137. Ferguson, R. C. *Trans. N.Y. Acad. Sci.* **1967**, *29*, 495.
138. Zambelli, A.; Zetta, L.; Sacchi, C.; Wolfgruber, C. *Macromolecules* **1972**, *5*, 440.
139. Johnson, L. F.; Heatley, F.; Bovey, F. A. *Macromolecules* **1970**, *3*, 175.
140. Crain Jr, W. O.; Zambelli, A.; Roberts, J. D. *Macromolecules* **1971**, *4*, 330.
141. Zambelli, A.; Dorman, D. E.; Brewster, A. I. R.; Bovey, F. A. *Macromolecules* **1973**, *6*, 925.
142. Randall, J. C. *J. Polym. Sci., Polym. Phys. Ed.* **1974**, *12*, 703; **1976**, *14*, 2083.
143. Zambelli, A.; Locatelli, P.; Bajo, G.; Bovey, F. A. *Macromolecules* **1975**, *8*, 687.
144. Ferro, D. R.; Zambelli, A.; Provasoli, A.; Locatelli, P.; Rigamonti, E. *Macromolecules* **1980**, *13*, 179.
145. Zambelli, A.; Locatelli, P.; Provasoli, A.; Ferro, D. R. *Macromolecules* **1980**, *13*, 267.
146. Zambelli, A.; Gatti, G. *Macromolecules* **1978**, *11*, 485.
147. Schilling, F. C.; Tonelli, A. E. *Macromolecules* **1980**, *13*, 270.
148. Ovenall, D. W. *Macromolecules* **1984**, *17*, 1458.
149. Aue, W. P.; Bartholdi, E.; Ernst, R. R. *J. Chem. Phys.* **1976**, *64*, 2229.
150. Freeman, R.; Morris, G. A. *Bull. Magn. Reson.* **1979**, *1*, 5.
151. Wüthrich, K. *Makromol. Chem. Suppl.* **1981**, *5*, 234.
152. Bruch, M. D.; Bovey, F. A. *Macromolecules* **1984**, *17*, 978.
153. Bruch, M. D.; Bovey, F. A.; Cais, R. E. *Macromolecules* **1984**, *17*, 2547.
- 153a. Schilling, F. C.; Bovey, F. A.; Bruch, M. D.; Kozłowski, S. A. *Macromolecules* **1985**, *18*, 1418.
- 153b. Kusanagi, H.; Tadokoro, H.; Chatani, Y. *Macromolecules* **1976**, *9*, 531.
154. Flory (155) and other American writers use the opposite convention making $\theta = 0^\circ$ for the trans or anti conformation. As a result the numerical values of the torsion angles reported here are often different from those reported in the original literature. Differences are found in the formulas involving trigonometrical functions and in the appearance of energy maps. Specific conventions are used for vinyl polymers.
155. Flory, P. J. "Statistical Mechanics of Chain Molecules"; Wiley-Interscience: New York, **1969**.
156. Allegra, G.; Immirzi, A. *Makromol. Chem.* **1969**, *124*, 70.
157. Abe, A.; Jernigan, R. L.; Flory, P. J. *J. Am. Chem. Soc.* **1966**, *88*, 631.
158. Owing to the lack of symmetry, a preexponential factor of two must be introduced into the statistical weight calculations for the G^+T , TG^- , G^+G^{*-} and $G^{*+}G^-$ conformations of *n*-pentane. Alternatively one may consider the presence of 7 (TT , TG^+ , TG^- , G^+T , G^-T , G^+G^+ , and G^-G^-) or 11 conformers (G^+G^{*-} , G^-G^{*+} , $G^{*+}G^-$, and $G^{*-}G^+$ besides the preceding) all with preexponentials equal to one.
159. Bunn, C. W. *Trans. Faraday Soc.* **1939**, *35*, 482.
160. Bunn, C. W. *Proc. R. Soc. (London)* **1942**, *A 180*, 40, 67, 82.
161. Bunn, C. W. *J. Chem. Soc.* **1947**, 297.
162. Wunderlich, B. "Macromolecular Physics"; Academic: New York, **1973**.
163. Tadokoro, H. "Structure of Crystalline Polymers"; Wiley-Interscience: New York, **1979**.
164. Klug, A.; Crick, F. H. C.; Wyckoff, H. W. *Acta Crystallogr.* **1958**, *11*, 199.
165. Corradini, P. *Rend. Accad. Naz. Lincei* **1960**, *28*, 1.
166. Natta, G.; Corradini, P.; Bassi, I. W. *Gazz. Chim. Ital.* **1959**, *89*, 784.

167. Pauling, L.; Corey, R. B.; Branson, H. R. *Proc. Natl. Acad. Sci. U.S.* **1951**, *37*, 205.
168. Natta, G.; Corradini, P.; Ganis, P. *Rend. Accad. Naz. Lincei* **1962**, *33*, 200.
169. Natta, G.; Pasquon, I.; Corradini, P.; Peraldo, M.; Pegoraro, M.; Zambelli, A. *Rend. Accad. Naz. Lincei* **1960**, *28*, 539.
170. Natta, G.; Peraldo, M.; Allegra, G. *Makromol. Chem.* **1964**, *75*, 215.
171. Shimanouchi, T.; Mizushima, S. *J. Chem. Phys.* **1955**, *23*, 707.
172. Hughes, R. E.; Lauer, J. L. *J. Chem. Phys.* **1959**, *30*, 1165.
173. Ganis, P.; Temussi, P. A. *Makromol. Chem.* **1965**, *89*, 1.
174. Brückner, S. In ref. 19, p. 100.
175. Liquori, A. M. "Proceedings of the 4th Summer School on Chemistry, Varenna, 1959"; *Rend. Accad. Naz. Lincei, Chim. Inorg.*, **1961**, 311.
176. De Santis, P.; Giglio, E.; Liquori, A. M.; Ripamonti, A. *Nuovo Cimento* **1962**, *26*, 616.
177. Natta, G.; Corradini, P.; Ganis, P. *Makromol. Chem.* **1960**, *39*, 238.
178. Corradini, P.; Allegra, G. *Rend. Accad. Naz. Lincei* **1961**, *30*, 516.
179. Allegra, G.; Ganis, P.; Corradini, P. *Makromol. Chem.* **1963**, *61*, 225.
180. Corradini, P.; Petraccone, V.; Pirozzi, B. *Eur. Polym. J.*, **1976**, *12*, 831.
181. Allegra, G.; Benedetti, E.; Pedone, C. *Macromolecules* **1970**, *3*, 727.
182. Tanaka, T.; Chatani, Y.; Tadokoro, H. *J. Polym. Sci., Polym. Phys. Ed.* **1974**, *12*, 515.
183. Stroupe, J. D.; Hughes, R. E. *J. Am. Chem. Soc.* **1958**, *80*, 2341.
184. Liquori, A. M.; Anzuino, G.; Coiro, V. M.; D'Alagni, M.; De Santis, P.; Savino, M. *Nature (London)* **1965**, *206*, 358.
185. Atkins, E. D. T.; Isaac, D. H.; Keller, A.; Miyasaka, K. *J. Polym. Sci., Phys. Ed.* **1977**, *15*, 211.
186. Corradini, P.; Guerra, G.; Petraccone, V.; Pirozzi, B. *Eur. Polym. J.* **1980**, *16*, 1089.
187. It must be noted that, in many publications, the determination of the shape and general dimensions of the molecule is considered a *configurational* and not a *conformational* problem. Expressions like "configurational statistics of chain molecules" are frequently used. Flory employed the term "configuration" in the sense widely used in scientific language before the introduction of stereochemical nomenclature. In statistical mechanics, for example, configuration denotes each state of a system distinguishable from other states. In particular, Flory reserves the term conformation for arrangements of atoms in small molecules and in small segments of long chains, and also in referring to the regular forms of macromolecules as they occur in the crystalline state. For formless arrangements of the macromolecule, which are collectively designated as the random coil, the term configuration is said to be preferred. According to Flory, confusion with the specific meaning of configuration used in stereochemistry can be avoided by use of an appropriate prefix, for example, stereochemical configuration (155). In this article, dedicated mainly to stereochemists, I have not adopted the Flory nomenclature but have retained the term configuration in its stereochemical significance: It is concerned with the specification of single stereoisomers independently of the specific shape assumed by the molecule and of its physical state. I recognize that the usage of "configuration" within a statistical mechanics description of polymers is quite appropriate, and the possibility of confusion is, in fact, quite remote.
188. Volkenstein, H. V. "Configurational Statistics of Polymeric Chains"; Timasheff, S. N.; Timasheff, M. J. transl.; Wiley-Interscience: New York, **1963**.
189. Birshtein, T. M.; Ptitsyn, O. B. "Conformations of Macromolecules"; Timasheff, S. N.; Timasheff, M. J. transl.; Wiley-Interscience: New York, **1966**.

190. Flory, P. J. *Macromolecules* **1974**, *7*, 381.
191. Allegra, G. In ref. 19, p. 54.
192. Birshtein, T. M.; Ptitsyn, O. B. *Vysokomol. Soedin.* **1960**, *2*, 628.
193. Corradini, P.; Ganis, P.; Oliverio, P. *Rend. Accad. Naz. Lincei* **1962**, *33*, 320.
194. Flory, P. J.; Mark, J. E.; Abe, A. *J. Am. Chem. Soc.* **1966**, *88*, 639.
195. Allegra, G. *Makromol. Chem.* **1968**, *117*, 24.
196. Allegra, G.; Brückner, S. *Macromolecules* **1977**, *10*, 106.
197. Heatley, F.; Salovey, R.; Bovey, F. A. *Macromolecules* **1969**, *2*, 619.
198. Value calculated by G. Allegra on the basis of formulas reported in ref. 179: $C_{\infty} = 7.3$ at 180°C; experimental value estimated by Nakajima and Sayjio (199) at the same temperature: 4.8.
199. Nakajima, A.; Sayjio, A. *J. Polym. Sci., Part A* **1968**, *6*, 735.
200. Boyd, R. H.; Breitling, S. M. *Macromolecules* **1972**, *5*, 279.
201. Allegra, G.; Calligaris, M.; Randaccio, L.; Moraglio, G. *Macromolecules* **1973**, *6*, 397.
202. Suter, U. W.; Flory, P. J. *Macromolecules* **1975**, *8*, 765.
203. Brückner, S. *Macromolecules* **1981**, *14*, 449.
204. Suter, U. W.; Pucci, S.; Pino, P. *J. Am. Chem. Soc.* **1975**, *97*, 1018.
205. Suter, U. W. *Macromolecules* **1981**, *14*, 523.
206. Grant, D. M.; Paul, E. G. *J. Am. Chem. Soc.* **1964**, *86*, 2984.
207. Grant, D. M.; Cheney, B. V. *J. Am. Chem. Soc.* **1967**, *89*, 5315, 5319.
208. Bovey, F. A. In "Proceedings of the International Symposium on Macromolecules, Rio de Janeiro, 1974," E. B. Mano Ed.; Elsevier: Amsterdam, **1975**, p. 169.
209. Provasoli, A.; Ferro, D. R. *Macromolecules* **1977**, *10*, 874.
210. Tonelli, A. E. *Macromolecules* **1978**, *11*, 565.
211. Carman, C. J. *Macromolecules* **1973**, *6*, 725.
212. Tonelli, A. E.; Schilling, F. C. *Acc. Chem. Res.* **1981**, *14*, 233.
213. Morgan, P. W. *Macromolecules* **1977**, *10*, 1381.
214. Shashoua, V. E. *J. Am. Chem. Soc.* **1959**, *81*, 3156.
215. Natta, G.; Di Pietro, J.; Cambini, M. *Makromol. Chem.* **1962**, *56*, 200.
216. Overberger, C. G.; Moore, J. A. In ref. 8, Vol. 7, p. 743.
217. (a) Bur, A. J.; Fetters, L. J. *Chem. Rev.* **1976**, *76*, 727. (b) Aharoni, S. M. *Macromolecules* **1979**, *12*, 94.
218. (a) Millich, F. *Chem. Rev.* **1972**, *72*, 101. (b) Millich, F.; Baker, G. K. *Macromolecules* **1969**, *2*, 122.
219. Nolte, R. J. M.; Van Beijnen, A. J. M.; Drenth, W. *J. Am. Chem. Soc.* **1974**, *96*, 5932.
220. Drenth, W.; Nolte, R. J. M. *Acc. Chem. Res.* **1979**, *12*, 30.
221. Van Beijnen, A. J. M.; Nolte, R. J. M.; Drenth, W. *Rec. Trav. Chim. Pays-Bas* **1980**, *99*, 121.
222. Van Beijnen, A. J. M.; Nolte, R. J. M.; Naaktgeboren, A. J.; Zwikker, J. W.; Drenth, W.; Hezemans, A. M. F. *Macromolecules* **1983**, *16*, 1679.
223. Okamoto, Y.; Suzuki, K.; Ohta, K.; Hatada, K.; Yuki, H. *J. Am. Chem. Soc.* **1979**, *101*, 4763.
224. Keller, A. In ref. 16, p. 135.

- 224a. Corradini, P.; Petraccone, V.; Allegra, G. *Macromolecules*, **1971**, *4*, 770.
225. "Organization of Macromolecules in the Condensed Phase", Proceedings of the Faraday Discussion held at Cambridge, U.K. 1979; *Disc. Faraday Soc.* **1979**, 68.
226. The main applications of neutron scattering in the study of the physical properties of polymers are (227): (1) small angle elastic scattering used to study chain conformation and thermodynamic interactions in bulk polymers and in solutions; (2) quasielastic neutron scattering that uses the Doppler broadening of the energy profile of the incident neutrons to study main chain motion of polymer chains in the melt and in solutions; (3) inelastic neutron scattering, used to obtain molecular spectra of polymers free from the restrictions of optical selection rules.
227. Allen, G. *Makromol. Chem. Suppl.* **1979**, *3*, 335.
228. Flory, P. J.; Yoon, D. Y. *Nature (London)* **1978**, *272*, 226.
229. Yoon, D. Y.; Flory, P. J. *Polym. Bull.* **1981**, *4*, 695.
230. Flory, P. J.; Yoon, D. Y.; Dill, K. A. *Macromolecules* **1984**, *17*, 862.
231. Yoon, D. Y.; Flory, P. J. *Macromolecules* **1984**, *17*, 868.
232. Gawrisch, W.; Brereton, M. G.; Fischer, E. W. *Polym. Bull.* **1981**, *4*, 689.
233. Guenet, J. M.; Picot, C. *Macromolecules* **1983**, *16*, 205.
234. Sadler, D. M. *Polymer* **1983**, *24*, 1401.
235. Spells, S. J.; Sadler, D. M. *Polymer* **1984**, *25*, 739.
236. Spells, S. J.; Keller, A.; Sadler, D. M. *Polymer* **1984**, *25*, 749.
237. Kirste, R. G.; Fruse, W. A.; Schelten, J. *Makromol. Chem.* **1973**, *162*, 299.
238. An alternative point of view is proposed by other authors (239).
239. Pechold, W. *Makromol. Chem. Suppl.* **1984**, *6*, 163.
240. Schaefer, J.; Stejskal, E. O.; Buchdahl, R. *Macromolecules* **1977**, *10*, 384.
241. Jelinski, L. W. In ref. 17, p. 223.
242. Yannoni, C. S. *Acc. Chem. Res.* **1982**, *15*, 201.
243. Bunn, A.; Cudby, M. E. A.; Harris, R. K.; Packer, K. J.; Say, B. J. *J. Chem. Soc., Chem. Commun.* **1981**, 15.
244. Krimm, S. *Fortschr. Hochpolym. Forsch.* **1960**, *2*, 51; *Pure Appl. Chem.* **1968**, *16*, 369.
245. Miyazawa, T. In ref. 7, Vol. 3, p. 147.
246. Painter, P. C.; Coleman, M. M.; Koenig, J. L. "The Theory of Vibrational Spectroscopy and its Applications to Polymeric Materials"; Wiley: New York, **1982**.
247. A macromolecule containing N atoms ($N \approx 10^4$) in an unspecified conformation presents, in principle, $3N - 6$ vibration modes all potentially observable in the spectrum. In reality many of these modes have coincident or almost coincident frequencies. The number of vibrations is, however, very high and the spectrum presents rather diffuse bands due to the partial superimposition of noncoincident vibrations. An ideal polymer of infinite length and with regular conformation possesses translational symmetry that greatly reduces the number of permitted modes. This number is tied to the number of atoms present in the structural unit and to the selection rules related to the molecular symmetry. For example, crystalline isotactic polypropylene has a ternary helical symmetry [$s(3/1)$], which allows the existence of 25 A-vibrations whose dipole changes parallel to the axis and 26 pairs of E-vibrations, perpendicular to the axis (245).
248. Zerbi, G.; Gussoni, M.; Ciampelli, F. *Spectrochim. Acta* **1967**, *23A*, 301.
249. Zerbi, G.; Ciampelli, F.; Zamboni, V. *J. Polym. Sci., Part C* **1964**, *7*, 141.

250. Zerbi, G. In "Polymer Characterization"; Craver, C. D., Ed.; "Advances in Chemistry" No. 203, Am. Chem. Soc., Washington, D.C., 1983, p. 487.
251. Schulz, R. C.; Kaiser, E. *Adv. Polym. Sci.* **1965**, *4*, 236.
252. Pino, P. *Adv. Polym. Sci.* **1965**, *4*, 393.
253. Goodman, M.; Abe, A.; Fan, Y. L. *Makromol. Rev.* **1966**, *1*, 1.
254. Farina, M.; Bressan, G. In ref. 7, Vol. 3, p. 181.
255. Selegny, E.; Merle-Aubry, L. In ref. 14, p. 15.
256. Ciardelli, F.; Chiellini, E.; Carlini, C. In ref. 14, p. 83.
257. Farina, M. In ref. 18, p. 173.
258. Mislow, K.; Bickart, P. *Israel J. Chem.* **1976/1977**, *15*, 1.
259. As an example chosen in the macromolecular field the ^{13}C NMR spectrum of syndiotactic polypropylene might be mentioned: In solution (averaged random coil conformation, molecular model corresponding to 7) it presents three signals; in the crystal state, where a chiral rigid conformation exists [(2/1)2 helix], it shows four signals (Figure 17).
260. This model was introduced by Frisch, Schuerch, and Szwarc (38) who discussed the chirality of vinyl polymers assuming that effects due to the chain length and the nature of the terminal groups were negligible. Arcus (58) spoke of nonterminal chain segments. The infinite chain model was explicitly used by Natta, Danusso, Corradini, Farina, and others (30-32).
261. Natta, Pino, and Mazzanti cited this model in 1957 (35). It represents a simplification of the one with different terminal groups used by Natta in his first paper on isotactic polymers.
262. It should be observed that the concept of cryptochirality according to Mislow and Bickart concerns the properties of a real sample while here it seems to be intrinsic to the model.
263. In an earlier discussion (254) polymers in which the chirality depends only on the presence of chiral side groups were said to be nonintrinsically chiral, in contrast with intrinsically chiral polymers where the chirality is independent of the internal structure of the substituent.
264. Substituted carbon atoms in the polymers described in the next paragraphs are often indicated as true or classic asymmetric carbon atoms. In this way one can distinguish between carbon atoms whose four substituents are constitutionally different in the proximity of the atom under consideration, from the tertiary atoms of vinyl isotactic polymers. For these, only the different length of the two chain segments and/or the structure of the end groups make all the ligands different from each other.
265. This possibility was indicated for the first time by Frisch, Schuerch, and Szwarc (38) in their discussion of copolymer chirality.
266. Aliev, A. D.; Khanmamedov, T. K.; Krentsel, B. A. *Vysokomol. Soedin., Ser. B* **1969**, *11*, 329.
267. Khanmamedov, T. K.; Aliev, A. D.; Krentsel, B. A. *Izv. Akad. Nauk SSSR, Ser. Khim.* **1970**, *9*, 2040.
268. Arcus, C. L. *J. Chem. Soc.* **1957**, 1189.
269. Arcus, C. L. In "Progress in Stereochemistry," Vol. 3; De La Mare, P. B. D.; Klyne, W. Eds.; Butterworths: London, **1962**, p. 264.
270. Schmitt, G. J.; Schuerch, C. *J. Polym. Sci.* **1961**, *49*, 287.
271. In the literature a few claims have been made concerning the optical activity of high molecular weight vinyl or vinylidene polymers, generally poly(methyl methacrylate). Although the authors of these claims consider their data to be reliable, their results are in contrast with a large body of other experimental evidence. The point might be reconsidered in the light of a more detailed knowledge of the stability of helical conformations in solution (see Addendum and ref. 422).

272. Green, M. M.; Garetz, B. A. *Tetrahedron Lett.* **1984**, 25, 2831.
273. Pino, P.; Montagnoli, G.; Ciardelli, F.; Benedetti, E. *Makromol. Chem.* **1966**, 93, 158.
274. Overberger, C. G.; Takekoshi, T. *Macromolecules* **1968**, 1, 7.
275. Overberger, C. G.; Jabloner, H. *J. Polym. Sci.* **1961**, 55, 32.
276. Fasman, G. D.; Tooney, N.; Shalitin, Y. In ref. 8, Vol. 2, p. 837.
277. Sigwalt, P. *Makromol. Chem. Suppl.* **1979**, 3, 69.
278. Price, C. C.; Spector, R. *J. Am. Chem. Soc.* **1965**, 87, 2069.
279. The formation of inverted units can be greatly reduced if an alkaline catalyst is used (277, 278).
280. The opposite case is also worthy of consideration. *cis*-2,3-Epoxybutane is a meso compound but the two halves of the molecule, and particularly the two O—CH(CH₃) bonds, are not equivalent but enantiotopic. Ring opening polymerization occurring selectively on one of the bonds converts the (*R*, *S*) monomer into a succession of monomer units —(*R*, *R*)—(*R*, *R*)— and so on, or —(*S*, *S*)—(*S*, *S*)— and so on. A chiral initiator can effect an enantiotopic differentiation (281) and thus give rise to an optically active polymer with an excess of (*R*, *R*) or (*S*, *S*) units (81, 82).
281. Izumi, Y.; Tai, A. "Stereodifferentiating Reactions"; Kodansha: Tokyo, **1977**.
282. Pino, P.; Lorenzi, G. P.; Lardicci, L. *Chim. Ind. (Milan)* **1960**, 42, 712.
283. Pino, P.; Lorenzi, G. P. *J. Am. Chem. Soc.* **1960**, 82, 4745.
284. Bailey, W. J.; Yates, E. T. *J. Org. Chem.* **1960**, 25, 1800.
285. Nozakura, S.; Takeuchi, S.; Yuki, H.; Murahashi, S. *Bull. Chem. Soc. Japan* **1961**, 34, 1673.
286. Goodman, M.; Abe, A. *J. Polym. Sci.* **1962**, 59, S 37.
287. Abe, A.; Goodman, M. *J. Polym. Sci., Part A* **1963**, 1, 2193.
288. Pino, P.; Ciardelli, F.; Lorenzi, G. P.; Montagnoli, G. *Makromol. Chem.* **1963**, 61, 207.
289. Goodman, M.; Clark, K. J.; Stake, M. A.; Abe, A. *Makromol. Chem.* **1964**, 72, 131.
290. Pino, P.; Ciardelli, F.; Zandomenighi, M. *Ann. Rev. Phys. Chem.* **1970**, 21, 561.
291. Ciardelli, F.; Benedetti, E.; Pieroni, O. *Makromol. Chem.* **1967**, 103, 1.
292. Ciardelli, F.; Lanzillo, S.; Pieroni, O. *Macromolecules* **1974**, 7, 174.
293. Goodman, M.; Chen, S. *Macromolecules* **1970**, 3, 398; **1971**, 4, 625.
294. Benedetti, E.; Ciardelli, F.; Pieroni, O.; Rossi, R. *Chim. Ind. (Milan)* **1968**, 50, 50.
295. Janovich, Z.; Fles, D. *J. Polym. Sci. Part A1*, **1971**, 9, 1103.
296. Porri, L.; Pini, D. *Chim. Ind. (Milan)* **1973**, 55, 196.
297. Loening, K. L.; Cross, L. C.; Corradini, P.; Fox, R. B.; Smets, G. J.; Suhr, C.; Tsuruta, T. *IUPAC Information Bulletin* **1971**, No. 13.
298. Tsuruta, T. *J. Polym. Sci., Part D* **1972**, 6, 179.
299. Pino, P.; Oschwald, A.; Ciardelli, F.; Carlini, C.; Chiellini, E. In "Coordination Polymerization: A Memorial to Karl Ziegler"; Chien, J. C. W. Ed.; Academic: New York, **1975**, p. 25.
300. Ciardelli, F.; Carlini, C.; Montagnoli, G.; Lardicci, L.; Pino, P. *Chim. Ind. (Milan)* **1968**, 50, 860.
301. Sigwalt, P., personal communication.
302. From a kinetic point of view processes (1) and (2) are characterized by equal macroscopic reaction rates for both enantiomers ($v_R = v_S$), while for (3) $v_R \neq v_S$ (in the extreme case, one of the two rates is zero). At the microscopic level, for a stereoselective polymerization

(2) promoted by a racemic catalytic system, $k_{RR} + k'_{SR} \neq k'_{SS} + k_{RS}$ where the prime relates to a chain growing at a given site and the subscript RS indicates the reaction of a growing chain end containing an R end unit with an S monomer, and so on. For symmetry reasons, a second chain placed in an enantiomeric situation should have $k''_{RR} + k''_{SR} = k'_{SS} + k'_{RS}$. Also considered as stereoselective are those polymerizations which proceed in the absence of any chiral influence (except the chain and the monomer) where $k_{RR}/k_{RS} = k_{SS}/k_{SR}$, provided the ratio is markedly greater than one. In nonselective processes, on the other hand, the value of this ratio is close to one.

303. Luisi, P. L.; Montagnoli, G.; Zandomenighi, M. *Gazz. Chim. Ital.* **1967**, *97*, 222.
304. Pino, P.; Ciardelli, F.; Lorenzi, G. P.; Natta, G. *J. Am. Chem. Soc.* **1962**, *84*, 1487.
305. Pino, P.; Montagnoli, G.; Ciardelli, F.; Benedetti, E. *Makromol. Chem.* **1966**, *93*, 158.
306. Chiellini, E.; Montagnoli, G.; Pino, P. *J. Polym. Sci., Part B* **1969**, *7*, 121.
307. Marchetti, M.; Chiellini, E.; Sépulchre, M.; Spassky, N. *Makromol. Chem.* **1979**, *180*, 1305.
308. Montagnoli, G.; Pini, D.; Lucherini, A.; Ciardelli, F.; Pino, P. *Macromolecules* **1969**, *2*, 684.
309. Pino, P.; Ciardelli, F.; Lorenzi, G. P. *J. Am. Chem. Soc.* **1963**, *85*, 3888.
310. Pino, P.; Ciardelli, F.; Lorenzi, G. P. *Makromol. Chem.* **1964**, *70*, 182.
311. Inoue, S.; Tsuruta, T.; Furukawa, J. *Makromol. Chem.* **1962**, *53*, 215.
312. Tsuruta, T.; Inoue, S.; Yoshida, N.; Furukawa, J. *Makromol. Chem.* **1962**, *55*, 230.
313. Furukawa, J.; Akutsu, S.; Saegusa, T. *Makromol. Chem.* **1965**, *81*, 100.
314. Tsuruta, T. in ref. 7, Vol. 2, p. 117.
315. Furukawa, J.; Kawabata, N.; Kato, A. *J. Polym. Sci., Part B* **1967**, *5*, 1073.
316. Spassky, N.; Sigwalt, P. *C. R. Acad. Sci., Ser. C* **1967**, *265*, 624.
317. Sépulchre, M.; Spassky, N.; Sigwalt, P. *Macromolecules* **1972**, *5*, 92.
318. Spassky, N. in ref. 14, 111.
319. Tsuruta, T. *Makromol. Chem. Suppl.* **1981**, *5*, 230.
- 319a. Sépulchre, M.; Spassky, N. *Makromol. Chem. Rapid Commun.* **1981**, *2*, 261.
320. Pino, P.; Ciardelli, F.; Montagnoli, G.; Pieroni, O. *J. Polym. Sci., Part B* **1967**, *5*, 307.
321. Ciardelli, F.; Carlini, C.; Montagnoli, G. *Macromolecules* **1969**, *2*, 296.
322. Sépulchre, M.; Spassky, N.; Sigwalt, P. *Israel J. Chem.* **1976/1977**, *15*, 33.
323. Markwald, W. *Berichte* **1904**, *37*, 1368.
324. Pracejus, H. *Fortschr. Chem. Forsch.* **1967**, *8*, 493.
325. Morrison, J. D.; Mosher, H. S. "Asymmetric Organic Reactions"; Prentice-Hall: New York, 1971.
326. Fueno, T.; Furukawa, J. *J. Polym. Sci., Part A* **1964**, *2*, 3681.
327. Fueno, T.; Shelden, R. A.; Furukawa, J. *J. Polym. Sci., Part A* **1965**, *3*, 1279.
328. Farina, M. *Makromol. Chem.* **1969**, *122*, 327.
329. Natta, G.; Farina, M.; Donati, M.; Peraldo, M. *Chim. Ind. (Milan)* **1960**, *40*, 1363.
330. Natta, G.; Farina, M.; Donati, M. *Makromol. Chem.* **1961**, *43*, 251.
331. Farina, M.; Bressan, G. *Makromol. Chem.* **1963**, *61*, 79.
332. Takeda, Y.; Hayakawa, Y.; Fueno, T.; Furukawa, J. *Makromol. Chem.* **1965**, *83*, 234.
333. Farina, M.; Natta, G.; Bressan, G. *J. Polym. Sci., Part C* **1963**, *4*, 141.
334. Di Silvestro, G.; Grassi, M.; Farina, M. Preprints of the IUPAC International Symposium on Macromolecules, Firenze, Italy, **1980**; Vol. 2, p. 166.

335. Bressan, G.; Broggi, R. *Chim. Ind. (Milan)* **1968**, *50*, 1326.
336. Bressan, G. *Chim. Ind. (Milan)* **1969**, *51*, 705.
337. Bressan, G.; Farina, M.; Natta, G. *Makromol. Chem.* **1966**, *93*, 283.
338. Natta, G.; Porri, L.; Carbonaro, A.; Lugli, G. *Chim. Ind. (Milan)* **1961**, *43*, 529.
339. Natta, G.; Porri, L.; Valente, S. *Makromol. Chem.* **1963**, *67*, 225.
340. Farina, M.; Audisio, G.; Natta, G. *J. Am. Chem. Soc.* **1967**, *89*, 5071.
341. Farina, M. *Tetrahedron Lett.* **1963**, 2097.
342. Farina, M.; Audisio, G. *Tetrahedron Lett.* **1967**, 1285.
343. Farina, M.; Audisio, G. *Tetrahedron* **1970**, *26*, 1827, 1839.
344. Farina, M.; Allegra, G.; Natta, G. *J. Am. Chem. Soc.* **1964**, *68*, 516.
345. Farina, M.; Natta, G.; Allegra, G.; Löffelholz, M. *J. Polym. Sci., Part C* **1967**, *16*, 2517.
346. Allegra, G.; Farina, M.; Immirzi, A.; Colombo, A.; Rossi, U.; Broggi, R.; Natta, G. *J. Chem. Soc., Part B* **1967**, 1020.
347. Farina, M. "Inclusion Compounds of Perhydrotriphenylene." In "Inclusion Compounds," Vol. 2; Atwood, J. L.; Davies, J. E. D.; MacNicol, D. D., Eds.; Academic: London, **1984**, p. 69.
348. Farina, M.; Pedretti, U.; Gramegna, M. T.; Audisio, G. *Macromolecules* **1970**, *3*, 475.
349. Farina, M. In "Proceedings of the International Symposium on Macromolecules, Rio de Janeiro, 1974"; E. B. Mano, Ed.; Elsevier: Amsterdam **1975**, p. 21.
350. Farina, M. *Makromol. Chem. Suppl.* **1981**, *4*, 21.
351. Farina, M. "Inclusion Polymerization." In "Inclusion Compounds," Vol. 3; Atwood, J. L.; Davies, J. E. D.; MacNicol, D. D., Eds.; Academic London, **1984**, p. 297.
352. Farina, M.; Di Silvestro, G.; Sozzani, P. *Makromol. Chem., Rapid Commun.* **1981**, *2*, 51.
353. Audisio, G.; Silvani, A. *J. Chem. Soc. Chem. Commun.* **1976**, 481.
354. Miyata, M.; Takemoto, K. *Polym. J.* **1977**, *9*, 111.
355. Miyata, M.; Kitahara, Y.; Takemoto, K. *Polym. Bull.* **1980**, *2*, 671.
356. Miyata, M.; Kitahara, Y.; Takemoto, K. *Polym. J.* **1981**, *13*, 111.
357. Doiuchi, T.; Minoura, Y. *Macromolecules* **1977**, *10*, 260.
358. Doiuchi, T.; Kubouchi, K.; Minoura, Y. *Macromolecules* **1977**, *10*, 1208.
359. Minoura, Y. In ref. 14, p. 159.
360. Addadi, L.; Cohen, M. D.; Lahav, M. *J. Chem. Soc., Chem. Commun.* **1975**, 471.
361. Addadi, L.; Gati, E.; Lahav, M.; Leiserowitz, L. *Israel J. Chem.* **1976-1977**, *15*, 116.
362. Addadi, L.; Lahav, M. *J. Am. Chem. Soc.* **1978**, *100*, 2838; **1979**, *101*, 2152.
363. Addadi, L.; Cohen, M. D.; Lahav, M. in ref. 14, p. 183.
364. Okamoto, Y.; Suzuki, K.; Yuki, H. *J. Polym. Sci., Polym. Chem. Ed.* **1980**, *18*, 3043.
365. Okamoto, Y.; Honda, S.; Okamoto, I.; Yuki, H.; Murata, S.; Noyori, R.; Takaya, H. *J. Am. Chem. Soc.* **1981**, *103*, 6971.
366. Corley, L. S.; Vogl, O. *Polym. Bull.* **1980**, *3*, 211.
367. Hatada, K.; Shimizu, S.; Yuki, H.; Harris, W. J.; Vogl, O. *Polym. Bull.* **1981**, *4*, 179.
368. Harris, W. J.; Vogl, O. Preprints of the 28th IUPAC Macromolecules Symposium Amherst, MA, **1982**, p. 169.
369. Brewster, J. H. *J. Am. Chem. Soc.* **1959**, *81*, 5475.
370. Brewster, J. H. *Top. Stereochem.* **1967**, *2*, 1.
371. Pucci, S.; Aglietto, M.; Luisi, P. L.; Pino, P. *J. Am. Chem. Soc.* **1967**, *89*, 2787.

372. Pino, P.; Lorenzi, G. P.; Bonsignori, O. *Chim. Ind. (Milan)* **1966**, *48*, 760.
373. Birshtein, T. M.; Luisi, P. L. *Vysokomol. Soedin.* **1964**, *6*, 1238.
374. Allegra, G.; Corradini, P.; Ganis, P. *Makromol. Chem.* **1966**, *90*, 60.
375. Abe, A. *J. Am. Chem. Soc.* **1968**, *90*, 2205.
376. Carlini, C.; Ciardelli, F.; Pino, P. *Makromol. Chem.* **1968**, *119*, 244.
377. Pieroni, O.; Ciardelli, F.; Botteghi, C.; Lardicci, L.; Salvadori, P.; Pino, P. *J. Polym. Sci., Part C* **1969**, *22*, 993.
378. Pino, P.; Carlini, C.; Chiellini, E.; Ciardelli, F.; Salvadori, P. *J. Am. Chem. Soc.* **1968**, *90*, 5025.
379. Ciardelli, F.; Chiellini, E.; Carlini, C.; Aglietto, M. *Pure Appl. Chem.* **1980**, *52*, 1857.
380. Ciardelli, F.; Salvadori, P.; Carlini, C.; Chiellini, E. *J. Am. Chem. Soc.* **1972**, *94*, 6536.
381. Hug, W.; Ciardelli, F.; Tinoco, I. *J. Am. Chem. Soc.* **1974**, *96*, 3407.
382. Ciardelli, F.; Aglietto, M.; Carlini, C.; Chiellini, E.; Solaro, R. *Pure Appl. Chem.* **1982**, *54*, 521.
383. Chiellini, E.; Salvadori, P.; Osgan, M.; Pino, P. *J. Polym. Sci., Part A* **1970**, *8*, 1589.
384. Furukawa, J. In ref. 14, p. 317.
385. Farina, M.; Audisio, G.; Gramegna, M. T. *Macromolecules* **1972**, *5*, 617.
386. Sozzani, P.; Di Silvestro, G.; Grassi, M.; Farina, M. *Macromolecules* **1984**, *17*, 2532.
387. Sozzani, P.; Di Silvestro, G.; Farina, M. "Preprints of the 30th IUPAC International Symposium on Macromolecules, The Hague," Netherlands, **1985**, p. 263.
388. Okamoto, Y.; Yashima, E.; Hatada, K.; Mislou, K. *J. Org. Chem.* **1984**, *49*, 557.
389. Blaschke, G. *Angew. Chem., Intern. Ed. Engl.* **1980**, *19*, 13.
390. Fowells, W.; Schuerch, C.; Bovey, F. A.; Hood, F. P. *J. Am. Chem. Soc.* **1967**, *89*, 1396.
391. Natta, G.; Peraldo, M.; Farina, M.; Bressan, G. *Makromol. Chem.* **1962**, *55*, 139.
392. Peraldo, M.; Farina, M. *Chim. Ind. (Milan)* **1960**, *42*, 1349.
393. Miyazawa, T.; Ideguchi, T. *J. Polym. Sci., Part B* **1963**, *1*, 389.
394. Tadokoro, H.; Ukita, M.; Kobayashi, M.; Murahashi, S. *J. Polym. Sci., Part B* **1963**, *1*, 405.
395. Natta, G.; Farina, M.; Peraldo, M.; Corradini, P.; Bressan, G.; Ganis, P. *Rend. Accad. Naz. Lincei* **1960**, *28*, 442.
396. Higashimura, T.; Hoshino, M.; Hirokawa, Y.; Matsuzaki, K.; Uryu, T. *J. Polym. Sci., Polym. Chem. Ed.* **1977**, *15*, 2691.
397. Fox, T. G.; Garrett, B. S.; Goode, W. E.; Gratch, S.; Kincaid, J. F.; Spell, A.; Stroupe, J. D. *J. Am. Chem. Soc.* **1958**, *80*, 1768.
398. Schuerch, C.; Fowells, W.; Yamada, A.; Bovey, F. A.; Hood, F. P.; Anderson, E. W. *J. Am. Chem. Soc.* **1964**, *86*, 4481.
399. Yoshino, T.; Komiyama, J.; Shinomiya, M. *J. Am. Chem. Soc.* **1964**, *86*, 4482.
400. Zambelli, A. *J. Chem. Soc., Chem. Commun.* **1967**, 1252.
401. Zambelli, A.; Giongo, M. G.; Natta, G. *Makromol. Chem.* **1968**, *112*, 183.
402. This assertion does not contradict that stated in Sec. V-A regarding the nonchirality of stereoregular vinyl polymers of infinite length. When dealing with mechanisms of polymerization, the structure of the chain end cannot be ignored. The model to use is, therefore, that of a finite chain with different end groups.
403. In the layer lattice of α , γ , or δ TiCl_3 , each Ti atom is bonded to three other Ti atoms through six bridged Cl atoms (404). The local symmetry of the Ti atoms is D_3 so that each titanium

is chiral and surrounded by three atoms of opposite configuration. The symmetry of the active centers on the crystal edges is lower because of the presence of other ligands.

404. Allegra, G. *Makromol. Chem.* **1971**, *145*, 235.
405. Wolfgruber, C.; Zannoni, G.; Rigamonti, E.; Zambelli, A. *Makromol. Chem.* **1975**, *176*, 2765.
406. This conclusion appears inverted with respect to the original communication owing to an assignment error of the *mr*-centered pentads existing at that time (141). The present interpretation agrees with more recent attributions (105, 143, 405).
407. Zambelli, A.; Tosi, C. *Adv. Polym. Sci.* **1974**, *15*, 31.
408. Zambelli, A. In "NMR Basic Principles and Progress," Vol. 4; Springer-Verlag: Berlin **1971**, p. 101.
409. Zambelli, A. in ref. 18, p. 147.
410. Ewen, J. A. *J. Am. Chem. Soc.* **1984**, *106*, 6355.
411. Danusso, F.; Tieghi, G.; Riccò, T. *Polymer* **1979**, *20*, 805.
412. Danusso, F.; Tieghi, G.; Protto, P. *Gazz. Chim. Ital.* **1980**, *110*, 407.
413. Danusso, F. *Eur. Polym. J.* **1983**, *19*, 867.
414. Vogl, O.; Corley, L. S.; Harris, W. J.; Jaycox, G. D.; Zhang, J. *Makromol. Chem. Suppl.* **1985**, *13*, 1.
415. Vogl, O.; Miller, H. C.; Sharkey, W. H. *Macromolecules* **1972**, *5*, 658.
416. Novak, A.; Whalley, E. *Trans. Faraday Soc.* **1959**, *55*, 1490.
417. Kaminsky, W. Communication presented at the International Symposium on Future Aspects of Olefin Polymerization, Tokyo, **1985**.
418. Kaminsky, W. In "History of Polyolefins," Seymour, R. B.; Cheng, T. Eds.; Reidel: Dordrecht, **1986**, p. 257.
419. Green, M. M., personal communication.
420. Kamer, P. J.; Cleij, M. C.; Harada, T.; Nolte, R. J. M.; Drenth, W. In "Preprints of the 30th IUPAC International Symposium on Macromolecules, The Hague," **1985**, p. 40.
421. Wulff, G. *Nachr. Chem. Tech. Lab.* **1985**, *33*, 956.
422. Cram, D. J.; Sogah, D. Y. *J. Am. Chem. Soc.* **1985**, *107*, 8301.

Stereochemical Aspects of Vibrational Optical Activity

TERESA B. FREEDMAN AND LAURENCE A. NAFIE

*Department of Chemistry
Syracuse University
Syracuse, New York*

Abbreviations	114
I. Introduction	114
A. Preliminary Remarks	114
B. Definitions	115
C. Motivation	116
D. Scope	118
II. Experimental Methods	119
A. Vibrational Circular Dichroism (VCD) Measurement	119
B. Raman Optical Activity (ROA) Measurement	120
C. Experimental Parameters	120
III. Theoretical Models	122
A. Intensity Expressions	123
1. Vibrational Circular Dichroism	123
2. Raman Optical Activity	124
3. Intensity Models	125
B. Coupled Oscillator Models	126
C. Generalized Models for VCD	128
1. Fixed Partial Charge Model	129
2. Charge Flow Models	129
3. Vibrational Ring Current Model	130
4. Localized Molecular Orbital Model	130
5. Other Molecular Orbital Models	131
D. Generalized Models for ROA	132
IV. Stereochemical Applications	132
A. Applications of the Degenerate Coupled Oscillator Model	133
1. Dimethyl Tartrate	133
2. Steroids	137
B. Simple Chiral Molecules	138
1. Deuterated Phenylethanes	139
2. CH ₃ C*H Molecules	140
C. Chiral Ring Molecules	144
1. Small Ring Molecules	144
2. The CH ₂ CH ₂ C*H Chiral Fragment	148

3. Low-Frequency Skeletal Motions	153
4. Other Ring Molecules	158
D. Amino Acids and Peptides	160
1. Amino Acids	161
2. Simple Peptides	176
3. Polypeptides	177
4. Urethane Amino Acid Derivatives	178
E. Transition Metal Complexes	182
1. <i>Bis</i> Cu(II) Amino Acid Complexes	182
2. <i>Tris</i> (ethylenediamine) Co(III) Complexes	184
3. Co(III) Alanine Complexes	188
F. Carbohydrates	193
G. Chiral Allenes and Azides	197
V. CONCLUSIONS	199
Addendum	201
Acknowledgments	201
References	202

ABBREVIATIONS

APT	Atomic polar tensor
CF	Charge flow
FPC	Fixed partial charge
FTIR	Fourier transform infrared
LMO	Localized molecular orbital
NMO	Nonlocalized molecular orbital
ROA	Raman optical activity
VCD	Vibrational circular dichroism
VOA	Vibrational optical activity

I. INTRODUCTION

A. Preliminary Remarks

During the early stages in the development of stereochemical concepts near the beginning of this century, chemists had to rely on rather indirect methods to deduce basic stereochemical information, such as the absolute configuration of a chirality center at carbon. In most cases, arguments were based on the chemical transformation of a molecule of interest to a molecule of known stereochemistry. Although optical rotation was a valuable tool in this process, absolute stereochemistry could not be deduced directly by spectroscopic techniques. The fine details of stereochemistry such as preferred conformational states and their rel-

ative populations were beyond the capability of the methodology of that day to ascertain.

In the intervening years a rapidly advancing sophistication in spectroscopic instrumentation has made possible the direct study of stereochemical detail in molecules. Such techniques as scanning circular dichroism, high-field nuclear magnetic resonance (NMR), laser Raman scattering, and Fourier transform infrared absorption have been primarily responsible for the advances in spectroscopic stereochemical methodology. Parallel developments in theoretical calculations of molecular properties using molecular orbital techniques have provided an independent basis for evaluating the conclusions reached by experimental methods. This has been accomplished by predicting the most stable conformational states in molecules as well as providing the means to understand the results of spectroscopic measurements through the calculation of intensities and the simulation of observed spectra.

Perhaps the most fascinating aspect of molecular stereochemistry is the property known as chirality, the noncongruence of an object with its mirror image. The only spectroscopic techniques capable of directly probing molecular chirality are those that take advantage of the mirror relationship between the left and right circularly polarized states of electromagnetic radiation. A chiral molecule can interact in a differential manner with left versus right circularly polarized radiation, thus generating diastereomeric interactions. The field of spectroscopy that is concerned with the measurement of this differential interaction relates to what is known as *optical activity*. The most familiar manifestations of optical activity are optical rotation, or optical rotatory dispersion when measured as a function of wavelength, and circular dichroism (1). In recent years a number of new manifestations of optical activity have been developed that have extended the ways in which stereochemical information can be gathered (2). The subject of this chapter concerns one such development, the measurement of optical activity in vibrational transitions.

B. Definitions

Over the past decade two forms of vibrational optical activity have become established. One is called vibrational circular dichroism (VCD), the extension of electronic circular dichroism into the infrared vibrational region of the spectrum. The first measurements of VCD were reported by George Holzwarth and co-workers at the University of Chicago in 1973 for crystals (3) and 1974 for neat liquids (4). In VCD one measures the small difference in the absorption of a sample for left versus right circularly polarized incident infrared radiation. The early stages of the development of VCD have been reviewed from several perspectives (5-8).

The other form of optical activity in vibrational transitions is known as Raman optical activity (ROA). Here, also, one measures an intensity difference for left compared to right circularly polarized incident radiation; however, optical activity in light scattering has no direct analog in electronic spectroscopy. ROA was first measured by Laurence Barron, A. D. Buckingham, and M. P. Bogaard in 1973 (9) and several reviews of the subject have since appeared (10-14).

Both VCD and ROA have been extensively developed along both experimental and theoretical lines (15). In the process, two sensitive new approaches to the direct investigation of molecular stereochemistry have become available. While other forms of vibrational optical activity (VOA) may yet be developed, the present two appear to be the most fundamental and the easiest to measure. In addition, they represent complementary rather than redundant approaches to the same stereochemical structural information.

C. Motivation

The primary motivation for the development and application of vibrational optical activity lies in the enhanced stereochemical sensitivity that it provides in relation to its two parent spectroscopies, electronic optical activity and ordinary vibrational spectroscopy. Over the past 25 years, optical rotatory dispersion and more recently electronic circular dichroism have provided useful stereochemical information regarding the structure of chiral molecules and polymers in solution; however, the detail provided by these spectra has been limited by the broad and diffuse nature of the spectral bands and the difficulty of accurately modeling the spectra theoretically.

By contrast, VCD and ROA intensities arise from the set of $3N-6$ normal vibrational modes in a molecule. These modes provide the basis for a rich set of transitions that for the most part are well resolved, that take place in the electronic ground state, and that can be described in terms of nuclear displacements and the correlated motion of electronic charge density. While the same is true for ordinary infrared absorption and Raman scattering, these measurements lack the stereosensitivity to absolute configuration and conformational state found in VCD and ROA. This enhanced sensitivity can be seen most easily by noting that enantiomers have mirror image VOA spectra but identical ordinary vibrational spectra. Thus, VCD and ROA intensities arise completely from the absolute, three-dimensional orientation of groups in space without any bulk, nonstereosensitive component.

The information content of VCD spectra is both structural and dynamic. The structural dependence arises from the exact equilibrium conformations of the molecule in both a nuclear and an electronic sense. The dynamic dependence is present in the vibrational dynamics of the molecule in each vibrational tran-

sition investigated. Thus, VOA intensities depend on the equilibrium structure and the way in which this structure changes with the vibrational motion.

The comprehensive manner by which VOA intensities relate to the details of molecular stereochemistry can be appreciated by recognizing that the set of $3N-6$ vibrational degrees of freedom is defined in the *same* space that specifies the parameters of molecular conformation. No other form of molecular spectroscopy is so closely related to molecular stereochemistry. It is literally true that VOA spectra arise from stereospecific vibrational oscillations of a chiral molecule. A challenge facing VOA spectroscopy at the present is how to fully extract this structural and conformational information from the spectra.

The question naturally arises as to whether vibrational spectroscopy, enhanced with vibrational optical activity, can in principle completely specify the stereochemical parameters of a molecule. The answer appears to be yes provided that not more than a few molecular conformations are present in significant amount in the sample to be studied. For a single conformation, $3N-6$ internal coordinates are required to specify the conformation. Provided that the vibrational force field and the quantum mechanical description of the electronic contributions to the vibrational intensities are available, one could consider the $3N-6$ VCD or ROA intensities as a complete, stereospecific set of parameters that would be consistent with only one set of $3N-6$ internal coordinates. Additional conformational states would add further complexity and would require a spectral decomposition of the observed VOA spectra. Of course, this picture is oversimplified with respect to the present state of the art. Accurate vibrational force fields for chiral molecules have only been partially developed; questions still remain regarding the quantum mechanical description of the electronic motion, and a complete set of $3N-6$ VOA intensities is not yet accessible, at least for VCD. Nevertheless, the long-range potential for the extraction of highly detailed stereochemical information about molecules in random phases, for example, liquids, solutions, gases, matrices, glasses, disoriented films, and so on, is very high.

In spite of this potential, no single spectroscopic technique can be expected to provide the answers to all stereochemical problems. Rather, a particular stereochemical problem is best approached by a variety of complementary techniques. At present the most powerful tool for stereochemical analysis is NMR. In contrast to VCD and ROA, the spectral content of NMR is generally devoid of chirality information. Nevertheless, NMR provides sensitive molecular markers that are influenced by the electronic shielding of surrounding electronic charge density, as well as the distances to neighboring nuclear centers. A great deal of information is thus available on structure and conformation in molecules that complements data of a more chemical bonding nature available from ordinary vibrational spectroscopy and VOA.

An intriguing aspect of VOA spectra in general and VCD spectra in particular is the relationship of the observed intensities to properties of molecules that lie beyond the Born–Oppenheimer approximation. The basic problem is that VCD intensities depend on the magnetic as well as the electric dipole transition moment; however, the electronic contribution to the magnetic dipole transition moment vanishes within the Born–Oppenheimer approximation (16–18). In other words, VCD intensities depend in part upon non-Born–Oppenheimer effects in molecules. In particular, they depend on the generation of electronic current density in molecules in response to the momenta of the vibrational nuclear motion (17, 18). As a result, the full understanding of the origin of VCD in molecules will provide a deeper understanding of the dynamic relationship between electronic and nuclear momenta, an understanding that is absent at the level of the Born–Oppenheimer approximation. This momentum relationship may ultimately prove to be fundamental to understanding the detailed circumstances under which molecules come together and react.

D. Scope

The goal of this chapter is to review the field of vibrational optical activity from the perspective of stereochemical applications. As mentioned previously, VCD and ROA have been reviewed separately as well as jointly (5–15). The earlier reviews were more comprehensive in their approach; however, with the growing sophistication of VOA, more specialized reviews are becoming appropriate, as well as necessary from the standpoint of length. Recently, one of the authors presented a review that focused on experimental and theoretical advances in VOA with but little space devoted to chemical applications (15). The present chapter provides the opportunity to consider in depth the stereochemical aspects of VOA in terms of specific applications. By extension, the long-term potential for VOA to contribute to molecular stereochemistry will also be considered. Experimental and theoretical background will be introduced only as necessary for appreciation of the fundamental stereochemical significance of the topic to be discussed. As a final point, the closely related field of magnetic vibrational optical activity, as measured by Barron in the resonance Raman effect and by Keiderling in infrared absorption, will not be discussed, primarily for reasons of space. Although these magnetic spectroscopies are still in an early stage of development, their presentation would require extensive additional background information and would tend to detract from the primary objective of elucidating the stereochemical potential of natural vibrational optical activity. In addition, the fact that only nonchiral molecules or chromophores have been investigated by magnetic VOA to date is further justification for omitting this otherwise interesting work.

II. EXPERIMENTAL METHODS

The measurement of vibrational optical activity requires the optimization of signal quality, since the experimental intensities are between three and six orders of magnitude smaller than the parent IR absorption or Raman scattering intensities. To date all successful measurements have employed the principles of modulation spectroscopy so as to overcome short-term instabilities and noise and thereby to measure VOA intensities accurately. In this approach, the polarization of the incident radiation is modulated between left and right circular states and the difference intensity, averaged over many modulation cycles, is retained. In spite of this common basis, there are major differences in measurement technique and instrumentation between VCD and ROA; consequently, the basic experimental methodology of these two techniques will be described separately.

A. Vibrational Circular Dichroism (VCD) Measurement

Instrumentation in VCD has passed through several generations. The first generation, still in use, is restricted to the frequency region above $\sim 2000\text{ cm}^{-1}$ and, therefore, involves the measurement, primarily, of hydrogen stretching vibrations (19, 20). In this instrument the frequency is limited by the long wavelength cutoff of an InSb detector. The instrument is designed around a dispersive grating spectrometer with a glower or tungsten-halogen lamp as a source and an IR photoelastic modulator oscillating in the kilohertz frequency range to effect the modulation between left and right circular polarization states. The sample is placed immediately after the modulator and the resulting beam focused at the detector.

A second generation of development has involved extension of spectral coverage through the mid-infrared region to $\sim 950\text{ cm}^{-1}$. This was achieved by use of an improved source, xenon arc (21) or carbon rod (22), and a detector having longer wavelength sensitivity. Improvements in the photoelastic modulator which improved modulation and throughput efficiencies were also forthcoming from a commercial manufacturer (Hinds-International).

The most recent advance in VCD instrumentation has been its adaptation to Fourier transform infrared (FTIR) measurement (23–25). The details of this technique involve a new method of FTIR measurement termed double-modulation FTIR spectroscopy. Thus spectra of very high quality and resolution have been obtained using a standard VCD modulator and detector, a glower source, and a commercially available FTIR spectrometer system. In fact an entire FTIR–VCD spectrometer can be assembled from a few commercially available components. It is found that the major advantages of resolution, throughput, and

absolute frequency calibration that characterize ordinary FTIR measurements compared to dispersive measurements are also available with the double-modulation technique applied to VCD measurement. To date FT-VCD measurements have spanned the frequency range from 3400 to 600 cm^{-1} (23–26).

B. Raman Optical Activity (ROA) Measurement

The measurement of ROA intensities has involved two generations of instrumentation. The basic technique involves the use of an electrooptic modulator to switch the polarization of the incident laser radiation between left and right circular polarization states in a square-wave fashion (since it was demonstrated at an early stage that sine wave modulation could lead to serious polarization artifacts in ROA measurement). The first ROA instruments were constructed about scanning grating monochromators. In an ROA experiment the scattered light is collected by a lens, focused at the entrance slit of the monochromator, and the emerging light measured by a photomultiplier detector. The detector counts for each of the two incident circular polarization states are stored separately; they are subtracted for ROA and added for obtaining the ordinary Raman intensity. Measurement times for a complete ROA spectrum spanning $\sim 1600 \text{ cm}^{-1}$ typically are a day or more.

A few years after the discovery of ROA, measurements were successfully completed that employed a multichannel detection system (27, 28). In this way, large regions of an ROA spectrum can be measured simultaneously, thus overcoming a major drawback of the experiment. Other improvements were introduced, such as a dual-arm light collection system to reduce polarization artifacts (29). As in ordinary Raman spectroscopy, there are two independent polarization measurements that can be performed in ROA experiments. The easier and more common measurement corresponds to depolarized Raman scattering in which the scattered light is passed through an analyzing polarizer placed parallel to the scattering plane defined by the incident and scattered light beams. If the analyzer is rotated to an orientation perpendicular to the scattering plane, polarization artifacts become larger. The results of only a few such measurements have been published (28). Because of the problem of interfering polarization artifacts, successful ROA measurements require very careful optical alignment and balancing. At this stage in the development of experimental methodology, it appears that ROA is somewhat more specialized and less experimentally accessible than FTIR-VCD measurements.

C. Experimental Parameters

The result of a direct instrumental measurement of VCD yields a spectrum of ΔA versus wavelength, λ , or wave number $\bar{\nu}$, where ΔA equals A_L minus A_R .

The quantities A_L and A_R are the decadic absorbances for left and right circularly polarized radiation, respectively. The ordinary IR absorption is given by the average of A_L and A_R , namely,

$$A = \frac{1}{2}(A_L + A_R) \quad [1]$$

and

$$A = -\log_{10} (I/I_0) \quad [2]$$

where I and I_0 are the average transmissions with and without the sample. If the Beer-Lambert law is valid, the effects of path length and solution concentration can be removed to yield the molar absorptivity, ϵ , given by

$$\epsilon = \frac{A}{Cl} \quad [3]$$

where C is the concentration in moles per liter and ℓ is the path length in centimeters. Correspondingly, VCD spectra are often presented in terms of $\Delta\epsilon$, equal to ϵ_L minus ϵ_R .

Another quantity of interest in VCD spectroscopy is the anisotropy ratio, g , given by

$$g = \frac{\Delta\epsilon}{\epsilon} = \frac{\Delta A}{A} \quad [4]$$

Strictly speaking, the values of ϵ , $\Delta\epsilon$, A , and ΔA need to be obtained by integration over the spectral band; however, since, for a fundamental transition, the VCD and its parent absorption band have the same shape, the anisotropy ratio can be obtained, in the absence of interfering bands due to other transitions, by taking the ratios of intensities at corresponding spectral positions, such as peak locations. The anisotropy ratio is also of interest for theoretical reasons since it is a dimensionless quantity that can be compared to the results of calculations (*vide infra*).

The corresponding quantities may be defined for ROA measurements based on the scattering intensities ΔI and I given by

$$\Delta I = I_L - I_R \quad [5]$$

$$I = I_L + I_R \quad [6]$$

where I_L and I_R are Raman counts for left and right circularly polarized incident

radiation, respectively. A dimensionless quantity termed the chirality number can be defined to be

$$q = \frac{2\Delta I}{I} = \frac{\Delta d\sigma}{d\sigma} = \frac{d\sigma_L - d\sigma_R}{\frac{1}{2}(d\sigma_L + d\sigma_R)} \quad [7]$$

where $d\sigma_L$ and $d\sigma_R$ are the differential cross sections of a single molecule for left and right circularly polarized incident radiation. A factor of $\frac{1}{2}$ is included in the denominator of eq. [7] because I in eq. [6] is the sum of I_L and I_R rather than the average (as employed for absorption in eq. [7]). If samples are used that are not enantiomerically pure, the measurements of ΔA and ΔI must be corrected to obtain proper molecular values for $\Delta\epsilon$ and $\Delta d\sigma$.

Although the sign convention for circular dichroism and VCD is well established, the situation for ROA is not uniform. In this article we employ the left minus right convention; however, the opposite convention has been widely employed. The problem of the sign convention has recently been discussed from the perspectives of both conventions (30, 31).

III. THEORETICAL MODELS

The wealth of structural information provided by vibrational spectroscopy is largely due to the fact that vibrational motion (bond stretching, angle deformation, torsion, etc.) of many functional groups or bond types occurs at characteristic frequencies, which depend in a known manner on the chemical environment of that group. For example, carbon-hydrogen stretching occurs near 3000 cm^{-1} ; an intense IR band near 1720 cm^{-1} is indicative of a C=O stretch, and methylene scissors motion is observed near 1450 cm^{-1} . In these cases the vibrational normal mode of the molecule is fairly localized. In large molecules, many vibrational modes involve mixtures of different types of vibrational internal coordinates and are delocalized; however, the frequency of this type of mode can vary over a wide range and dispersed vibrational motion is not generally of diagnostic use in making structural correlations. In a symmetrical molecule, the vibrational motions are restricted to specific symmetry types that cannot mix with other symmetry species, for example, the symmetric and antisymmetric OH stretching modes in water.

The stereospecificity of vibrational optical activity, on the other hand, arises from the fact that the vibrations take place in a chiral framework and VOA intensities depend in large part on the extent and phasing of coupling or mixing of vibrational motion in different parts of the molecule. In addition, many local symmetry restrictions are lifted in chiral molecules, for example, the local de-

generacy in the antisymmetric methyl CH stretching mode is removed, giving rise to two bands.

VOA spectra are generally interpreted in terms of two types of effects, which give rise to characteristic spectral patterns. First, many spectra consist of bisignate (+ -) or (- +) VOA couplets, or a group of bands of alternating sign in a given region, which are conservative, that is, the integrated VOA intensity of all the bands in a given region is approximately zero. This type of feature can be explained in terms of the coupled motion of chirally disposed oscillators (32), and can provide direct stereochemical information. The second type of pattern observed is monosignate VOA intensity, which introduces bias into the spectra, that is, net positive or negative integrated intensity for a spectral region. This effect is attributed in large part to electronic motion that is generated by the nuclear vibration but does not perfectly follow the nuclear trajectories. Monosignate VCD features can be correlated with the presence of closed rings and intramolecular hydrogen bonding (*vide infra*).

In this section we describe some of the theoretical models that have been applied to the interpretation of VOA spectra, with an aim toward understanding the link between the spectral features and the molecular stereochemistry. The application of the models is included in the discussion of individual molecules in Sect. IV.

A. Intensity Expressions

1. Vibrational Circular Dichroism

The intensity of a vibrational transition $1 \leftarrow 0$ for the fundamental of normal mode Q_a is proportional to the *dipole strength*, D_{10} , defined as

$$D_{10}^a = |(\mu^a)_{10}|^2 \quad [8]$$

where $(\mu^a)_{10}$, the electric dipole transition moment, is related to $(\partial\mu/\partial Q_a)_0$, the change in the molecular dipole moment due to the vibrational motion. We denote the frequency of the vibration as ω_a .

Vibrational circular dichroism arises from the interference of the electric dipole transition moment $(\mu^a)_{01}$ and the magnetic dipole transition moment $(m^a)_{10}$ and is proportional to the *rotational strength*, R_{10} , where

$$R_{10}^a = \text{Im} (\mu^a)_{01} \cdot (m^a)_{10} \quad [9]$$

In this expression Im refers to the imaginary part of the scalar product, since $(m^a)_{10}$ is a pure imaginary quantity. The rotational strength is positive or neg-

ative depending on the angle between the vectors $(\mu^a)_{01}$ and $(\mathbf{m}^a)_{10}$; R_{10} is zero when these are orthogonal, or when $\mu = 0$ or $\mathbf{m} = 0$.

In terms of transition matrix elements of the electric and magnetic dipole moment operators, the transition dipole moments are

$$(\mu^a)_{10} = \left\langle 1_a \left| \sum_i e_i \mathbf{r}_i \right| 0 \right\rangle \quad [10]$$

$$(\mathbf{m}^a)_{10} = \left\langle 1_a \left| \sum_i \frac{e_i}{2m_i c} \mathbf{r}_i \times \mathbf{p}_i \right| 0 \right\rangle \quad [11]$$

for all the particles in the molecule with mass m_i , charge e_i , position \mathbf{r}_i , linear momentum \mathbf{p}_i , and angular momentum $\mathbf{r}_i \times \mathbf{p}_i$.

The dipole and rotational strengths are related to the experimentally observed intensities by

$$g = \frac{\Delta\epsilon}{\epsilon} = \frac{4R}{D} \quad [12]$$

The stereochemical sensitivity of VCD may be viewed as arising from the simultaneous interaction of linear oscillation of charge and the electric field of the IR radiation, and circular oscillation of charge and the magnetic field of the radiation.

2. Raman Optical Activity

The expressions for ROA intensity are quite complex (10–14). For the purposes of this chapter, we need only consider that ROA intensity for the fundamental of normal mode Q_a arises from products such as

$$\frac{\hbar}{2\omega_a} \left(\frac{\partial \alpha_{\alpha\beta}}{\partial Q_a} \right)_0^* \left(\frac{\partial G'_{\alpha\beta}}{\partial Q_a} \right)_0 \quad [13]$$

and

$$\frac{\hbar}{2\omega_a} \left(\frac{\partial \alpha_{\alpha\beta}}{\partial Q_a} \right)_0^* \left(\frac{\partial A_{\gamma\delta\beta}}{\partial Q_a} \right)_0 \quad [14]$$

where $\alpha_{\alpha\beta}$ is the α, β element of the polarizability tensor, $G'_{\alpha\beta}$ is an element of the magnetic dipole optical activity tensor, and $A_{\gamma\delta\beta}$ is an element of the electric quadrupole optical activity tensor, defined as

$$\alpha_{\alpha\beta} = \frac{2}{\hbar} \sum_{e \neq g} \frac{\omega_{eg}}{(\omega_{eg}^2 - \omega^2)} \operatorname{Re} [\langle g | \mu_\alpha | e \rangle \langle e | \mu_\beta | g \rangle] \quad [15]$$

$$G'_{\alpha\beta} = -\frac{2}{\hbar} \sum_{e \neq g} \frac{\omega}{(\omega_{eg}^2 - \omega^2)} \operatorname{Im} (\langle g | \mu_\alpha | e \rangle \langle e | m_\beta | g \rangle) \quad [16]$$

$$A_{\alpha\beta\gamma} = \frac{2}{\hbar} \sum_{e \neq g} \frac{\omega_{eg}}{(\omega_{eg}^2 - \omega^2)} \operatorname{Re} (\langle g | \mu_\alpha | e \rangle \langle e | \Theta_{\beta\gamma} | g \rangle) \quad [17]$$

for ground state g , excited state e , and angular frequency ω . In addition to the electric and magnetic dipole transition moments defined as in eqs. [10] and [11], the ROA expressions require the transition moments of the electric quadrupole moment operator,

$$\Theta_{\alpha\beta} = \frac{1}{2} \sum_i e_i (3r_{i\alpha}r_{i\beta} - r_i^2\delta_{\alpha\beta}) \quad [18]$$

Optical activity in light scattering thus arises from interference between the molecular polarizability and optical activity tensors.

3. Intensity Models

Although progress is being made in calculating VCD using molecular orbital theory with the exact quantum mechanical operators, much of the information of stereochemical importance derived from VOA spectra is based on interpretations using simplified intensity models. These models employ approximate forms for the magnetic dipole transition moment that can be calculated within the Born–Oppenheimer approximation. The general approach is to consider the contributions from local subunits that can be atoms, local dipoles, bonds, polarizability units, localized molecular orbitals, and so on. The position of a particle, i , within a subunit, a , can be expressed as $\mathbf{R}_a + \mathbf{r}_{ia}$ where \mathbf{R}_a locates an origin in the subunit and \mathbf{r}_{ia} measures position within the subunit. For the magnetic dipole transition moment this decomposition gives rise to two types of contributions from the subunit. The first contribution is equal to $(-i\omega/2c)\mathbf{R}_a \times \boldsymbol{\mu}_a$ where $\boldsymbol{\mu}_a$ is the electric dipole transition moment contribution from the subunit (32), and the second is an intrinsic subunit contribution \mathbf{m}_a . In ROA, one considers both intrinsic magnetic optical activity tensor or quadrupole optical activity tensor contributions from the subunit and terms that depend on the location of the subunit times the polarizability tensor contribution of the subunit (10–14). In both ROA and VCD the intrinsic contributions are the most difficult to calculate and are often ignored.

Specific models are described more fully in the next section.

B. Coupled Oscillator Models

The simplest mechanism for generating either VCD or ROA intensity is the coupled oscillator (32–34). We consider a vibrational perturbation (potential energy coupling, kinetic energy coupling, dipolar coupling, etc.), which mixes the motion of local oscillators a and b, with ground-state oscillator wave functions ψ_a^0 and ψ_b^0 , and first excited state wave functions ψ_a^1 and ψ_b^1 . The coupling generates the two mixed excited states

$$\psi_+ = c_1 \psi_a^1 \psi_b^0 + c_2 \psi_a^0 \psi_b^1 \quad \text{in phase combination} \quad [19]$$

$$\psi_- = c_2 \psi_a^1 \psi_b^0 - c_1 \psi_a^0 \psi_b^1 \quad \text{out of phase combination} \quad [20]$$

for positive c_1 and c_2 .

Denoting the electric and magnetic dipole transition moments of oscillators a and b as μ_a , \mathbf{m}_a and μ_b , \mathbf{m}_b , respectively, the rotational strength of the coupled oscillator is given by (34)

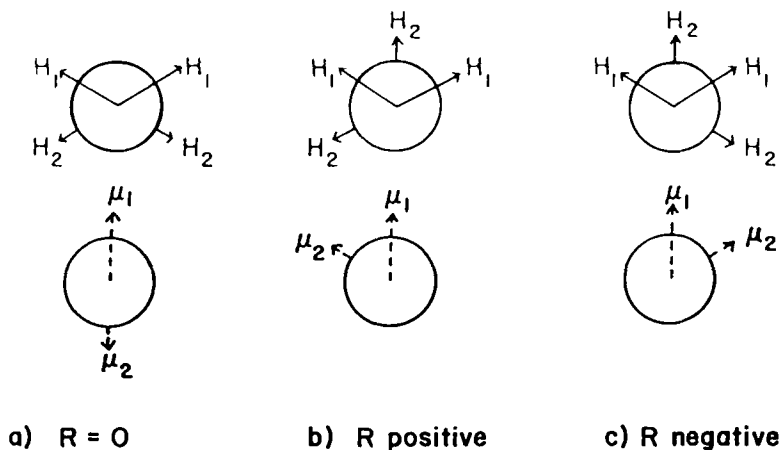
$$R^\pm = \frac{1}{2} \text{Im} (\mu_a \cdot \mathbf{m}_a + \mu_b \cdot \mathbf{m}_b) \\ \pm \frac{1}{2} \left[\text{Im} (\mu_a \cdot \mathbf{m}_b + \mu_b \cdot \mathbf{m}_a) - \frac{\omega}{2c} \mathbf{R}_{ab} \cdot \mu_a \times \mu_b \right] \quad [21]$$

for two degenerate oscillators with unperturbed frequency ω and separation vector \mathbf{R}_{ab} . For this case, $c_1 = c_2 = 1/\sqrt{2}$ (eqs. [19] and [20]), R^+ and the upper(+) sign for the terms in brackets on the right-hand side of the equation refer to the in-phase combination, and R^- and the lower(−) sign to the out of phase combination.

The first term in eq. [21] is the contribution of the intrinsic rotational strengths if oscillators a and/or b are themselves chiral. The second term is the coupled oscillator contribution due to the intrinsic moments and the third term is the coupled oscillator contribution due to the geometric arrangement of the two electric dipole oscillators. The latter two contributions give rise to a conservative bisignate couplet in the observed spectrum, if the coupled modes are sufficiently separated in frequency such that the positive and negative contributions do not cancel.

As an example, we consider the CH stretching motion of adjacent methylene groups, $-\text{CH}_2\text{CH}_2-$. The individual CH_2 units are achiral ($\mathbf{m}_a = \mathbf{m}_b = 0$) and only the final term in eq. [21] is important. We show here the Newman

projections of the in-phase combination of the symmetric methylene stretching modes for three possible orientations, and the corresponding relative direction and phase of the electric dipole transition moments.



In the *trans* conformation (a), the CH_2CH_2 moiety is achiral, μ_1 and μ_2 are colinear and no VCD can be generated, that is, the rotational strength is zero. In the two *gauche* conformations (b) and (c), the CH_2CH_2 units have opposite chirality, and generate coupled oscillator VCD intensity of opposite sign.

For two achiral, nondegenerate oscillators, $|c_1| \neq |c_2|$ in eqs. [19] and [20], and the rotational strength is given by (33)

$$R^\pm \cong \mp \frac{\omega_{av}}{2c} \lambda [\mathbf{R}_{ab} \cdot \boldsymbol{\mu}_a \times \boldsymbol{\mu}_b] \quad [22]$$

where ω_{av} is the average frequency of the two oscillators and λ is the mixing parameter

$$\lambda = \frac{\langle \psi_a^1 \psi_b^0 | V_{ab} | \psi_a^0 \psi_b^1 \rangle}{E_a - E_b} \quad (23)$$

In this case the coupling still generates a bisignate VCD couplet, but the magnitude of the intensity and the degree of mixing depends on the energy separation of the uncoupled modes, $E_a - E_b$.

Stereochemical information can clearly be derived from the analysis of VCD couplets using the coupled oscillator model. While the magnitude of μ_a and μ_b

can be obtained from the absorption spectra, two independent pieces of information are necessary. First, a vibrational assignment is required that defines the energy ordering of the in- and out-of-phase combinations. For oscillators with large local dipole strengths, such as O—H or C=O stretches, a simple dipole interaction potential may be adequate to define the mixing. In most cases, the interaction potential V_{ab} is poorly specified and a more complete normal coordinate analysis may be required. Second, for unlike oscillators, such as the coupling of C=C and C=O motion, the direction of the local electric dipole transition moment for a given phase of the vibrational motion of the local group must be determined, which may require molecular orbital calculations.

In ROA, the analogous model, derived by Barron (11), is termed the two group model. The coupling of oscillators on the two groups generates a bisignate ROA couplet through terms involving local polarizability tensor and local optical activity tensor elements, with a form analogous to eq. [21].

Another source of VOA intensity, which can be expressed in an analytical form similar to that of the local coupled oscillator model is the chiral mixing of inherently achiral vibrations (11). The symmetry requirements for a normal mode Q_a to exhibit nonzero VOA are that the corresponding components μ_o and m_o for VCD, or $\alpha_{\alpha\beta}$ and $G'_{\alpha\beta}$ for ROA, have the symmetry of the normal mode Q_a . This cannot happen in an achiral molecule. However, introducing chirality by adding a substituent to an achiral molecule provides a source of vibrational perturbation that can allow mixing of vibrations of different symmetry in the parent achiral molecule. This source of VOA can also generate bisignate couplets. VOA in vibrations that are degenerate under local symmetry can arise via this mechanism.

C. Generalized Models for VCD

A number of theoretical models of VOA can be considered as generalizations of the coupled oscillator concept to more than two oscillators. For VCD, these models have the form

$$R_{10}^a = \frac{\hbar}{4c} \sum_i \left[\left(\frac{\partial \mu_i}{\partial Q_a} \right)_0 \right] \cdot \left[\sum_i \mathbf{R}_{i,0} \times \left(\frac{\partial \mu_i}{\partial Q_a} \right)_0 \right] \quad [24]$$

where $(\partial \mu_i / \partial Q)_0$ is the contribution from a local unit i (at equilibrium position $\mathbf{R}_{i,0}$ relative to the molecular origin) to the total electric dipole moment derivative of the molecule $\sum_i (\partial \mu_i / \partial Q)_0 = (\partial \mu / \partial Q)_0$. R_{10} , eq. [24], can be rearranged to

$$R_{10}^a = \frac{\hbar}{4c} \sum_i \sum_{j < i} (\mathbf{R}_{i,0} - \mathbf{R}_{j,0}) \cdot \left(\frac{\partial \boldsymbol{\mu}_i}{\partial Q_a} \right)_0 \times \left(\frac{\partial \boldsymbol{\mu}_j}{\partial Q_a} \right)_0 \quad [25]$$

which is in the form of a sum over all the pairs of local "coupled" oscillators. Contributions of intrinsic group magnetic dipole transition moments are ignored in these models.

The generalized models of this type for VCD include the fixed partial charge model (35), the charge flow or bond current models (36, 37), the molecular orbital charge flow model (38), the localized molecular orbital model (39–41), and the atomic polar tensor model (42). Contributions to the magnetic moment due to charge flow around closed rings are included in the vibrational ring current model (43). These models will be described in more detail later. In addition, a bond-dipole theory has been proposed (12) and compared to the charge flow model (44). Contributions to the VCD from localized vibrations due to induced moments in adjacent highly polarizable groups has also been considered in the dynamic polarization model (45) and in the "induced dipole" mechanism (46).

1. Fixed Partial Charge Model

The fixed partial charge (FPC) model (35) assumes that the electrons follow the nuclear motion perfectly and serve merely to screen the nuclear charge. The dipole moment derivative contribution from each nucleus is $\xi_n(\partial \mathbf{R}_n / \partial Q_a)_0$ where ξ_n is the partial charge and $(\partial \mathbf{R}_n / \partial Q_a)$ is the trajectory of nucleus n in normal mode Q_a .

$$R_{10}^a(\text{FPC}) = \frac{\hbar}{4c} \left[\sum_n \xi_n \left(\frac{\partial \mathbf{R}_n}{\partial Q_a} \right)_0 \right] \cdot \left[\sum_n \mathbf{R}_{n,0} \times \xi_n \left(\frac{\partial \mathbf{R}_n}{\partial Q_a} \right)_0 \right] \quad [26]$$

This model has proven adequate for the description of VCD in the CH stretching region of a number of molecules.

2. Charge Flow Models

The charge flow (CF) models (36, 37) relax the restriction of perfect nuclear following, and allow the screened nuclear charge to change during the vibrational motion. The *charge flux* $(\partial \xi_n / \partial Q_a)_0$ is assumed to arise from currents, (I_{nl}) , along all the bonds connecting atom n to atoms l ,

$$(\partial \xi_n / \partial Q_a)_0 = - \sum_l (\partial I_{nl} / \partial P_a)_0 \quad [27]$$

where P_a is the time derivative of Q_a .

In these models, the local dipole moment derivative contribution becomes

$$\left(\frac{\partial \mu_n}{\partial Q_a}\right)_0 = \xi_{n,0} \left(\frac{\partial \mathbf{R}_n}{\partial Q_a}\right)_0 - \frac{1}{2} \sum_t (\mathbf{R}_{n,0} - \mathbf{R}_{t,0}) \left(\frac{\partial I_{nt}}{\partial P_a}\right)_0 \quad [28]$$

The charge flow description in ref. (37) is expressed in terms of bond charges and bond moments, but is equivalent to the expression in eq. [28] for atomic contributions (36, 38).

3. *Vibrational Ring Current Model*

Vibrationally generated electronic charge flow around a closed molecular ring can occur at constant electron density, that is, without altering the charge flux, eq. [27], and therefore without contributing to the electric dipole transition moment. The vibrational ring current contribution to the magnetic dipole transition moment (43) is proportional to

$$\frac{1}{c} \left(\frac{\partial I_{\text{ring}}}{\partial P_a}\right)_0 \sum_{n \rightarrow t} \frac{1}{2} \mathbf{R}_n \times \mathbf{R}_t \quad [29]$$

where $(\partial I_{\text{ring}}/P_a)_0$ is the change in current around the ring due to the nuclear motion in normal mode Q_a , and the summation is taken over consecutive pairs of nuclei all around the ring. For a planar ring, eq. [29] reduces to

$$\frac{1}{c} \left(\frac{\partial I_{\text{ring}}}{\partial P_a}\right)_0 \mathbf{S} \quad [30]$$

where \mathbf{S} is a vector whose magnitude is the area of the ring and direction is given by the right-hand rule for positive current flow in a closed loop. The sense of positive vibrational ring current can be determined by empirical rules that will be described in Sects. IV and V. The vibrational ring current contributions are considered in addition to the VCD intensity described by the charge flow models.

4. *Localized Molecular Orbital Model*

The localized molecular orbital model (LMO) (39–41) treats the electrons and nuclei separately. The nuclear contribution is identical to eq. [26] with $\xi_n = Z_n e$, the nuclear charge screened by the inner shell electrons that are assumed to follow the nuclei. The local units for the contribution from the valence elec-

trons are localized molecular orbitals at equilibrium centroid position $\mathbf{r}_{k0,0}$. The centroid displacement during vibrational motion is $(\partial \mathbf{r}_{k0,0} / \partial Q_a)_0$

$$R_{10}^a(\text{LMO}) = \frac{\hbar}{4c} \left\{ \sum_n Z_n e \left(\frac{\partial \mathbf{R}_n}{\partial Q_a} \right)_0 - \sum_k e \left(\frac{\partial \mathbf{r}_{k0,0}}{\partial Q_a} \right)_0 \right\} \\ \cdot \left\{ \sum_n (\mathbf{R}_{n,0} \times Z_n e \left(\frac{\partial \mathbf{R}_n}{\partial Q_a} \right)_0) - \sum_k \mathbf{r}_{k0,0} \times e \left(\frac{\partial \mathbf{r}_{k0,0}}{\partial Q_a} \right)_0 \right\} \quad [31]$$

5. Other Molecular Orbital Models

Several other molecular orbital models have been applied to the analysis of VCD spectra, primarily using CNDO wave functions. The nonlocalized molecular orbital model (NMO) is the MO analog of the charge flow models, based on atomic contributions to the dipole moment derivative (38). Currents are restricted to lie along bonds. An additional electronic term is introduced in the MO model that corresponds to *s-p* rehybridization effects during vibrational motion.

An approximate form of the NMO model, the atomic polar tensor (APT) model, has also proved effective (42). Rather than considering local contributions, this model considers contributions from the derivative of the total molecular dipole moment with respect to Cartesian displacement of a given nucleus, $(\partial \boldsymbol{\mu} / \partial \mathbf{R}_n)_0$. The latter are the elements of the atomic polar tensor for atom *n*.

$$R_{10}^a(\text{APT}) = \frac{\hbar}{4c} \left\{ \sum_n \left(\frac{\partial \boldsymbol{\mu}}{\partial \mathbf{R}_n} \right)_0 \cdot \left(\frac{\partial \mathbf{R}_n}{\partial Q_a} \right)_0 \right\} \\ \cdot \left\{ \sum_n (\mathbf{R}_{n,0} \times \left(\frac{\partial \boldsymbol{\mu}}{\partial \mathbf{R}_n} \right)_0) \cdot \left(\frac{\partial \mathbf{R}_n}{\partial Q_a} \right)_0 \right\} \quad [32]$$

This model has the advantage that the atomic polar tensor elements can be determined at the equilibrium geometry from a single molecular orbital calculation. Coupled with a set of trajectories $(\partial \mathbf{R}_n / \partial Q)_0$ obtained from a normal coordinate analysis, the IR and VCD intensities of all the normal modes of a molecule can be obtained in one calculation. In contrast, the other MO models require a separate MO calculation for each normal mode, since the $(\partial \boldsymbol{\mu}_i / \partial Q)_0$ contributions for each unit are determined by finite displacement of the molecule along each normal coordinate. Both the APT and FPC models are useful in readily assessing how changes in geometry or refinements in the vibrational force field affect the frequencies and intensities of all the vibrational modes of a molecule.

D. Generalized Models for ROA

Theoretical models for Raman optical activity have been proposed that can also be considered as a generalization of the coupled oscillator form to a large number of local units. These models include the general two group model (11), the atom dipole model (47), the bond polarizability theory (12), the localized MO (48), and equivalent orbital polarizability (49) models and the Raman atomic polar tensor model (43). Details of these theories will not be presented here. The application of the theoretical models of ROA has been somewhat limited, largely due to the unavailability of reliable force fields and assignments in the low frequency and fingerprint regions in which most ROA data have been obtained.

IV. STEREOCHEMICAL APPLICATIONS

In this section we shall describe the results of VOA studies from the perspective of their stereochemical significance. The stereochemical applications of ROA through 1983 have recently been reviewed by Barron (14) and we consider here only a recent application from our laboratory, as well as some stereochemical correlations with existing ROA data that were uncovered as a result of this work. In some cases for VCD, the results of a study have an immediate stereochemical impact on the molecules under investigation. In other cases, the VCD is analyzed for a molecule possessing a known, well-defined stereochemical structure with the aim of understanding the observed VCD and laying a foundation for future applications.

As discussed earlier, VCD depends on both the electric and magnetic dipole moment derivatives in a molecule. The simpler descriptions of VCD focus only on local electric dipole moment derivatives that have an overall chiral disposition. More advanced descriptions of VCD allow for induced electronic currents or charge flows in molecules, which give rise to additional magnetic dipole moment intensity. Such additional contributions are likely whenever delocalizable electron density is present in a molecule.

In the subsections that follow we shall occasionally offer an explanation, in terms of stereochemistry, of additional VCD intensity originating in vibrationally generated electronic ring currents in order to understand the observed spectra better. These interpretations are a qualitative, rather than quantitative, application of the vibrational ring current model summarized in Sect. III-C-3. In some cases the observed spectra were published at a time when the importance of current effects was not recognized. In offering these interpretations, we are seeking a more complete understanding of existing VCD spectra and a more unified view of how such current related VCD effects arise in molecules.

In anticipation of such discussions, the following general points will be pre-

sented as a conceptual basis. Since the sign of the rotational strength depends on the relative orientations of the electric and magnetic dipole transition moments ($R = \text{Im } \mu \cdot m$), the directions of the vectors μ and m must be determined for the normal mode in question. When an aliphatic CH bond is stretched, the positive end of the electric dipole moment derivative is directed from H to C. This has been established through MO calculations at both the semiempirical and *ab initio* level. The elongation of an NH or OH bond results in a positive moment in the direction N \rightarrow H or O \rightarrow H, respectively, opposite to the result of a CH bond stretch. Elongation of a C=O bond results in a positive O \rightarrow C moment. Bond contraction reverses the directions of these moments.

The direction of the magnetic dipole transition moment due to vibrationally generated currents is derived from the following considerations: (a) When a CH or NH bond is elongated, electron density, to some degree, is drawn out of the rest of the molecule in the direction of the hydrogen; CH or NH contraction injects electron density into the rest of the molecule. (b) In a hydrogen-bonded ring, a bond stretch that decreases the length of the hydrogen bond causes electron density to flow into the hydrogen-bonded region from the more electron rich of the hydrogen-bonded atoms. (c) The magnetic dipole transition moment is expressed in terms of positive current flow, which is opposite in direction to the flow of electrons. (d) The direction of the magnetic dipole moment derivative is determined by applying the right-hand rule to positive current flow in an arc or ring, that is, when the fingers of the right hand are directed around the arc or ring in the direction of positive current, the thumb points in the direction of the magnetic moment. The preferred sense of positive vibrationally generated current flow in a ring will be discussed for individual examples in the next sections.

A. Applications of the Degenerate Coupled Oscillator Model

Studies of molecules containing pairs of OH or C=O oscillators have provided the most direct application of the degenerate coupled oscillator model of VCD to determine molecular conformation in solution.

1. Dimethyl Tartrate

One of the first applications of VCD to stereochemical analysis was a study of the solution conformation of (2*S*,3*S*)-dimethyl tartrate, (1-3), in CCl₄ (50, 51). This molecule can assume three rotameric forms about the central C—C bond, and intramolecular hydrogen bonding resulting in the formation of a pair of either five- or six-membered rings is possible. The VCD spectra in dilute solution (Figure 1) exhibit a bisignate couplet in the OH stretching region ($\sim 3500 \text{ cm}^{-1}$), a monosignate band in the CH-stretching region, a bisignate couplet in

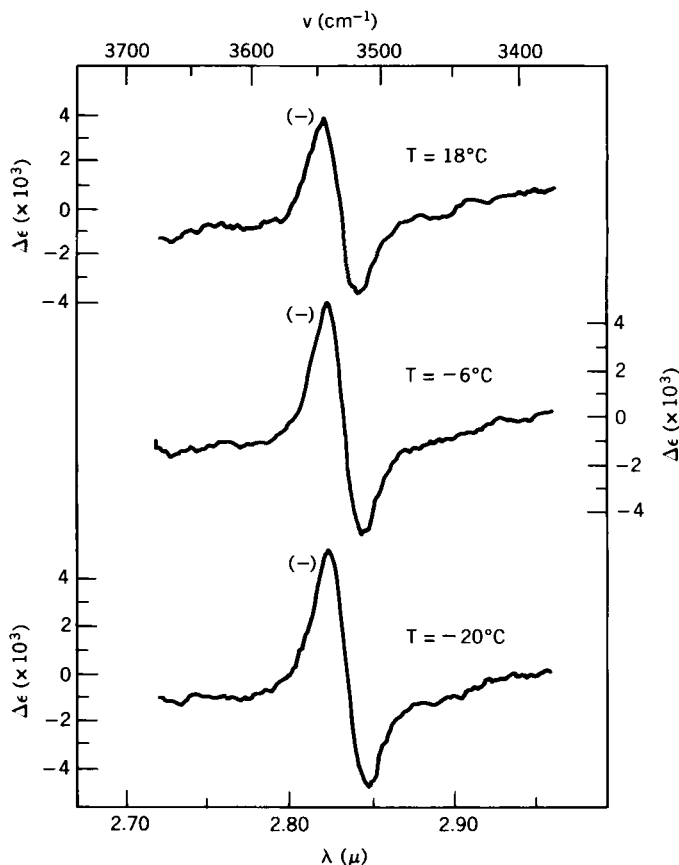
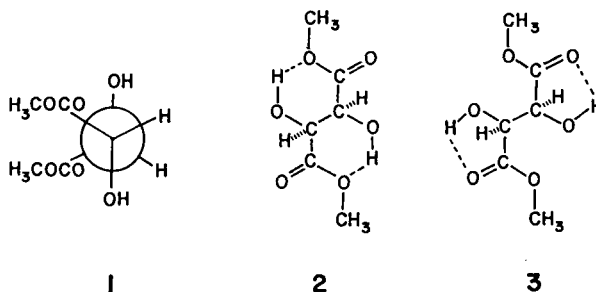


Figure 1. VCD in the OH-stretching region of $(-)-(2S,3S)$ -dimethyl tartrate, 0.01 M in CCl_4 , at three temperatures. Sample path length 0.48 cm, time constant 10 s, resolution 16 cm^{-1} . (Reproduced with permission from ref. 51. Copyright 1980 American Chemical Society.)

the $\text{C}=\text{O}$ stretching region ($\sim 1750\text{ cm}^{-1}$), and a pair of couplets in the $1000\text{--}1400\text{-cm}^{-1}$ region. Although it had been suggested that the OH couplet could arise from two different species (e.g., the five- and six-membered hydrogen-bonded ring forms **2** and **3**) in roughly equal concentration (52), Su and Keiderling (51) demonstrated that the OH stretching VCD of dimethyl tartrate maintains a fairly conservative bisignate line shape over the temperature range 18 to -20°C , and that for dimethyl malate, which has one OH group and can form only a single six-membered or five-membered hydrogen-bonded ring, only a very weak monosignate OH stretching VCD feature is observed. These observations support their conclusion that only one molecular species is responsible



for the VCD couplets. Furthermore, in a sample with 50% OH, 50% OD groups, the bisignate VCD pattern is reduced in intensity by a factor of four in both the OH and OD stretching regions, compared to the $-d_0$ or $-d_2$ molecules, as expected if half the sample, which has mixed OH/OD groups, and hence no coupled oscillator, has no (or very weak) VCD signal. Thus the dimethyl tartrate OH and C=O VCD couplets are most likely due to a degenerate coupled oscillator mechanism.

The ^{13}C satellite splitting in the ^1H NMR of the vicinal CH groups is consistent only with conformers with gauche CH bonds (51). Analysis of the VCD spectrum places further restrictions on the possible conformation. Su and Keiderling used the degenerate coupled oscillator model, eq. [21], assuming no intrinsic magnetic moment contributions and using the dipolar interaction potential,

$$V_{ab} = \frac{1}{|\mathbf{R}_{ab}|^3} \left[(\boldsymbol{\mu}_a \cdot \boldsymbol{\mu}_b) - \frac{3(\mathbf{R}_{ab} \cdot \boldsymbol{\mu}_a)(\mathbf{R}_{ab} \cdot \boldsymbol{\mu}_b)}{|\mathbf{R}_{ab}|^2} \right] \quad [33]$$

to determine the sense and magnitude of the splitting

$$\nu^\pm = \nu_0 \pm V_{ab} \quad [34]$$

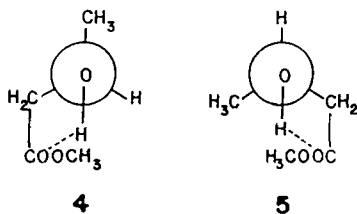
Eight possible geometries with gauche CH groups and hydrogen bonding to either the carbonyl or methoxy oxygens were considered.

The sign patterns of the calculated rotational strengths for both the OH and C=O couplets were in agreement with experiment only for the rotamer with trans OH groups, 1 and the two possible intramolecular hydrogen-bonding patterns, shown in 2 and 3.

Further considerations provide evidence in support of the five-membered ring. The rotational strengths ($\text{esu}^2 \text{cm}^2$) measured for the OH stretch of (*S*)-methyl mandelate (-2×10^{-43}) (52), (*S*)-methyl lactate (-1.1×10^{-43}) (53), and (2*S*)-dimethyl malate (-1.9×10^{-43}) (51) are comparable in both sign

and magnitude. All represent the intrinsic rotational strength for a single intramolecularly hydrogen-bonded OH group in these molecules (which is considerably smaller than the OH coupled oscillator contribution in dimethyl tartrate, $\pm 1.8 \times 10^{-42}$ esu² cm²). Although dimethyl malate can form either a five- or a six-membered ring, the similarity in the OH stretching VCD to that in the other two esters for which only five-membered rings are possible, suggests that the five-membered ring is also preferred in dimethyl malate. A recent interesting study of methyl 3-hydroxybutyrate (53) suggests two (or more) possible six-membered hydrogen-bonded ring conformations, for example, **4** and **5**, which would explain the observed bisignate OH stretching VCD in that molecule. However, the much narrower bandwidth in dimethyl tartrate is not consistent with a similar mixture of six-membered rings in the latter. The absorption spectrum of dimethyl tartrate (**50**) is in fact quite similar to that of methyl lactate (**53**). The weak high frequency feature in methyl lactate (3615 cm^{-1}) has been assigned to an OH having an intramolecular hydrogen bond to the methoxy oxygen atom (**54**), while the lower frequency intense band (3555 cm^{-1}) is due to the OH hydrogen bonded to the carbonyl oxygen. In dimethyl tartrate, no VCD corresponding to the weak high frequency band at $\sim 3590\text{ cm}^{-1}$ is observed; the strong VCD couplet is centered above the intense 3540-cm^{-1} mode, which is thus most likely due to $\text{O}-\text{H} \cdots \text{O}=\text{C}$, that is, structure **3** and not **2**.

Finally, the CH stretching VCD in dimethyl tartrate (**7**), tartaric acid (**34**), and lactic acid (**55**) all show a single monosignate feature that is positive in sign for the (*S*) configuration about the asymmetric carbon atoms and is associated with stretching of the methine CH. From our analysis of the L-amino acids and L-lactic acid VCD spectra (*vide infra*), we proposed a mechanism for intrinsic methine stretching VCD for a C*H bond adjacent to a ring closed by hydrogen bonding or transition metal coordination. In this model, discussed more fully in Sect. IV-D, a positive VCD can arise from positive charge flow (current) around the ring flowing away from the methine carbon along the C=O (or C—O) bond and toward the methine carbon along the OH bond, induced by contraction of the methine C*H bond. Due to the similarities in structure and similarities in magnitude of the *g* value (anisotropy ratio) of the VCD, an analogous mecha-



nism is likely for the methine C*H stretching VCD in tartaric acid and dimethyl tartrate. In (2*S*,3*S*)-dimethyl tartrate, the corresponding sense of vibrationally induced charge flow around the six-membered rings would result in small negative methine VCD (μ and m directed in opposing directions) for the in-phase methine stretching mode and cancellation of currents (no intrinsic VCD) for the out-of-phase mode. Only the five-membered hydrogen bonded ring conformation, also present in lactic acid, would give rise to the observed positive methine VCD feature.

This analysis of the VCD in the OH, CH, and C=O stretching regions as well as the ^1H NMR spectrum supports structure 3 for the dimethyl tartrate solution conformation. The assignment of couplet components to the in- and out-of-phase coupled oscillator motions is crucial to the analysis. For vibrations with very large dipole strengths, such as OH and C=O stretching modes, the dipolar coupling mechanism gives a contribution to the splitting on the order of $2\text{--}5\text{ cm}^{-1}$ and resulting coupled oscillator rotational strengths that agree fairly well with experiment. Assuming that additional sources of coupling do not reverse the relative phases in the coupled modes, only a single structure is consistent with the spectral data.

2. Steroids

A second application of the degenerate coupled oscillator model is the interpretation of the VCD of dicarbonyl-containing steroids by Narayanan and Keiderling (56). These molecules consist of a rigid framework with the two carbonyl substituents at a variety of positions. The VCD in the C=O stretching region for five of the six steroids studied consists of a bisignate couplet (Figure 2). In applying the coupled oscillator model, the separation and relative orientation of the carbonyl groups was determined using the Warshel-Lifson energy minimization technique based on a decalin framework, and the magnitude of the electric dipole transition moment was obtained from the absorption spectra. The calculated separation of dipoles (assumed to lie along the C=O bonds), measured between the centers of mass of the carbonyls, ranged from 4.57 to 6.89 Å, with the dihedral angle between the carbonyls assuming values between 16 and 350°. The calculated splitting between the coupled modes, based on dipolar interaction, ranged from 1.5 to 4.8 cm^{-1} , with the in-phase component at high frequency. The simulated VCD spectra, using the R^\pm values calculated using the degenerate coupled oscillator model and the observed absorption linewidths, agree with the experimental VCD in sign, shape, and magnitude (within a factor of two) for four of the six steroids in the study. In one case, the sense, but not the magnitude of the couplet was reproduced, and in the final compound the observed VCD is monosignate. In the latter two examples, the separation of the dipoles are the largest and the calculated splitting the smallest of the compounds

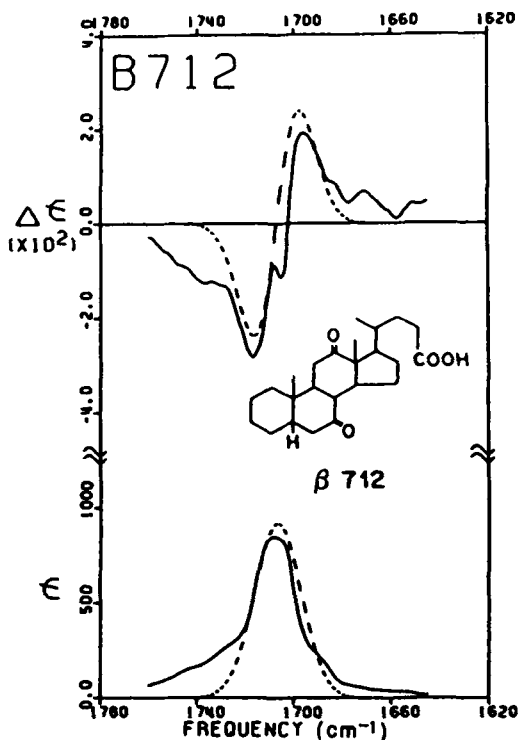


Figure 2. VCD and absorption spectra in the C=O stretching region of steroid $\beta 712$, 0.026 M in CHCl_3 . Sample path length 0.05 cm, resolution 11 cm^{-1} , time constant 10 s. Theoretical absorption and VCD spectra (---) were calculated using the degenerate coupled oscillator model. (Reproduced with permission from ref. 56. Copyright 1983 American Chemical Society.)

studied. Possibly a second source of VCD intensity, such as an intrinsic VCD for the C=O oscillation, while dominated by the dipolar coupling at shorter distances, becomes observable when the dipoles are more remote. The authors rule out effects from the ester or acid groups, and introducing deviations in dipolar orientation preserved the sense and approximate calculated magnitudes in most cases. This application of the degenerate coupled oscillator model again depends on having symmetrical (achiral) oscillators with very large dipole strengths.

B. Simple Chiral Molecules

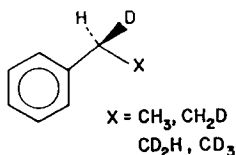
Several studies have focused on small molecules having a single asymmetric carbon, with a goal toward testing theoretical models and making structural

correlations that can be extended to more complex systems. The VCD investigations of deuterated phenylethanes, α -phenylethane derivatives, and alcohols are discussed here. Studies of simple amino acids and α -hydroxy acids are included in Sect. IV-D.

1. Deuterated Phenylethanes

Havel (46) reports the CH and CD stretching VCD of the deuterium substituted optically active phenylethanes, (*S*)-(+)-1-phenylethane-1-*d*₁, -1,2-*d*₂, -1,2,2-*d*₃, and -1,2,2,2-*d*₄ shown in 6.

Complete assignments and normal coordinate analysis were obtained, based on IR and Raman spectra, including an analysis of Fermi resonance interactions in the CH and CD stretching regions. Both fixed partial charge (FPC) and charge flow calculations of the VCD spectra were carried out, using atomic charges and charge flow parameters for CH bonds transferred from studies on methane. For the $-\text{CH}_2\text{D}$ and $-\text{CD}_2\text{H}$ species, the three staggered conformations were included. Both an orthogonal and a cis conformation for the phenyl ring were considered, the plane of the phenyl group being perpendicular or parallel to the $\text{C}^*-\text{C}(\text{Me})$ bond, respectively. Introducing charge flow produced considerably better overall agreement with experiment in the signs for the VCD bands, assuming either cis or orthogonal phenyl conformations, as compared to using the FPC model. In both types of calculation, however, the magnitudes of the calculated rotational strengths were an order of magnitude or more too low, particularly for an isolated C^*H or C^*D vibration. A significant improvement in the magnitudes of the calculated VCD was realized by taking into account the polarizability of the phenyl groups. Vibration of the aliphatic CH (or CD) bonds induces an oscillating electric dipole moment in the phenyl ring that affects the electric and magnetic dipole transition moment. This induced dipole contribution had the largest effect on the methine C^*H and C^*D intensities with a factor of 2 increase in calculated dipole strength and a factor of 10 in rotational strength and smaller contributions to the intensities of methyl group vibrations. These calculations gave good agreement with experiment both in sign and magnitude



for the isolated methine modes in the preferred orthogonal phenyl conformation, and suggest that unsaturated, polarizable groups play an important role in generating VCD intensity. The experimental g values for the isolated methine motions are $\sim 3\text{--}5 \times 10^{-5}$.

2. $\text{CH}_3\text{C}^*\text{H}$ Molecules

The VCD spectra of molecules of the form $\text{CH}_3\text{C}^*\text{HR}_1\text{R}_2$ have been investigated in the CH stretching region (20, 57–59) and the $1600\text{--}900\text{-cm}^{-1}$ mid-infrared region (59, 60). The ROA of this type of molecule has also been recorded (11–14). In particular, α -deuterated ethanol and α -phenylethane derivatives have been studied.

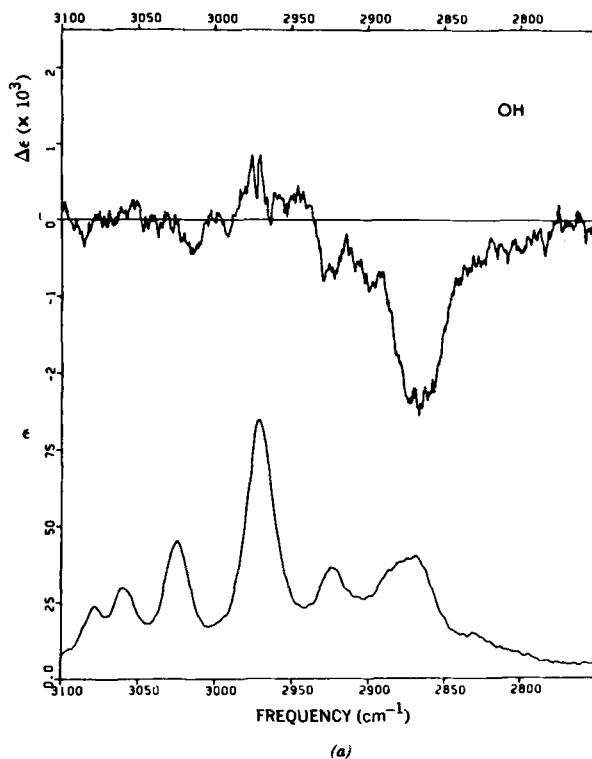


Figure 3. VCD and absorption spectra in the CH stretching region (a) α -phenylethanol, 0.074 M in CCl_4 , path length 0.10 cm, (b) (+)- α -phenylethyl isocyanate, 0.087 M in CCl_4 , sample path length 0.15 cm. The time constant was 10 s, and the resolution was 6 cm^{-1} . (Reproduced with the permission of North Holland Publishing Co., from ref. 59.)

Pultz (58) has analyzed the VCD spectra of molecules with a nonplanar HC*OH moiety, including (*R*)-CH₃C*HDOH and -OD (58), α -phenylethanol (20, 58, 59), and 2,2,2-trifluoro-1-phenylethanol (16, 20). The CH stretching VCD of these molecules [e.g., Figure 3(a)] is characterized by a broad feature corresponding to the C*H stretch and is strongly biased. Pultz carried out rotational strength calculations using the charge flow model for CH₃C*HDOH and for the HC*OH fragment. Their results indicate that the normal mode can be described as a mixture of C*H stretch with a small amount of C*OH bending, which depends on the HC*OH torsional angle. In this model, the electric dipole transition moment is primarily due to charge flow in the C*H bond and lies along that bond, whereas the charge flow in the OH bond induced by the COH angle deformation makes the dominant contribution to the magnetic dipole transition moment.

By considering the variation with torsion angle of both the mixing coefficient and the component of the charge flow magnetic moment perpendicular to the

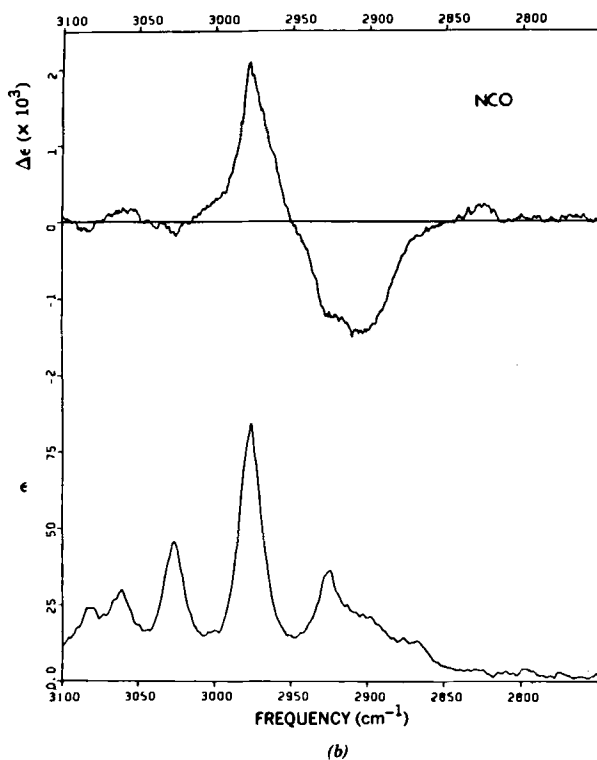
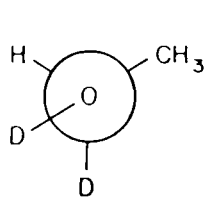
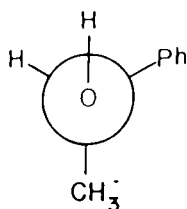


Figure 3. (Continued)



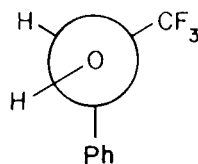
positive (C*H)
negative (C*D)

7



negative (C*H)

8



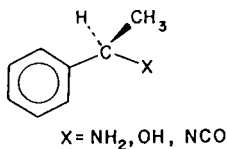
positive (C*H)

9

HC*O plane, the rotational strength as a function of HCOH dihedral angle can be determined for the charge flow model. Similar calculations using the localized MO model showed that recoil of the C* causes the oxygen lone pairs to rotate, generating the magnetic moment for this model.

Shown in 7-9 are the most probable conformations for several chiral alcohols, in the (*R*) configuration, along with the experimental sign for the C*H (or C*D) rotational strength (dilute CCl₄ solution). The charge flow calculation predicts the correct sign for each molecule in the orientation shown.

A second group of molecules studied are substituted α -phenylethane derivatives of the general formula 10 [(*R*) configuration]. The CH stretching VCD of these three species (59) (Figure 3) is characterized by positive VCD in the antisymmetric methyl (CH₃^a) stretching region (~ 2975 cm⁻¹), strong broad negative VCD in the methine stretching region, centered at 2850 cm⁻¹ (NH₂), 2900 cm⁻¹ (NCO) and 2890 cm⁻¹ (OH), and weaker negative VCD corresponding to the ~ 2920 , ~ 2870 -cm⁻¹ Fermi resonance diad involving the symmetric methyl mode (CH₃^s). The phenyl group modes show only weak VCD in the CH stretching region (3100-3000 cm⁻¹). In addition (*S*)-(+)-2,2,2-trifluoro-1-phenylethanol (dilute solution) (20) exhibits a single broad negative C*H stretching VCD at 2908 cm⁻¹ and in (+)-*N,N*-dimethyl(1-phenyl-



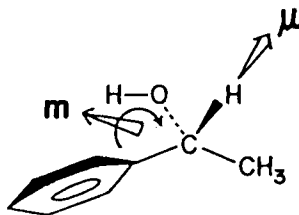
10

ethyl)amine (20), (*R*)-(+)-1-phenylethanethiol, and (*R*)-(+)-1-chloro-1-phenylethane (57), the distinctive negative methine feature is absent.

The CH stretching VCD spectra of these phenylethane derivatives have been interpreted using the vibrationally generated electronic ring current mechanism (57). In particular, the large intrinsic negative VCD intensity observed for the C*H stretch in the —OH, —NH₂, and —NCO derivatives and in dilute solutions of (*S*)-(-)-2,2,2-trifluoro-1-phenylethanol correlates with the presence of a ring adjacent to the C*H that is closed by hydrogen bonding between the —OH or —NH₂ groups and the phenyl group, or by $\pi \dots \pi$ interaction between the phenyl and —NCO groups. As shown in **11** for C*H contraction in (*R*)-1-phenylethanol, the electric dipole transition moment μ lies along C*H, with the positive end directed to the hydrogen, and has a component out of the page. For the sterically preferred conformation in which the C*H bond lies in the plane of the phenyl ring, positive charge flow, generated by the C*H contraction, around the ring $\text{COH} \dots \text{C(Ph)}$ in the direction shown in **11**, produces the magnetic dipole transition moment m , which is directed away from μ . The scalar product of μ and m is therefore negative, in agreement with the observed negative rotational strength for the C*H stretching vibration. Elongation of C*H reverses the direction of both μ and m . This sense of ring current, directed from the heteroatom to C* for C*H contraction, gives rise to the correct sign for the C*H stretching VCD in all the cases considered thus far in which the methine lies adjacent to an intramolecular ring. For the α -phenylethane derivatives, the anisotropy ratio is largest for the alcohol, consistent with a larger ring current due to a stronger hydrogen bond (eqs. [29] and [30]).

In the case of a chloro, thio, or dimethylamino substituent, the hydrogen-bonded ring does not form, and the VCD due to C*H stretching is weak or absent (20, 57). The characteristic methyl stretching VCD features observed for the α -phenylethane derivatives have also been interpreted in terms of currents generated about rings due to methyl-phenyl π interaction (57).

The mid-infrared VCD of some members of this series has also been investigated (59, 60) with an aim, in part, to identify features diagnostic of conformation. In the methyl deformation region (1450 cm⁻¹), all members of the



(*R*) - **11**

series (+)-C₆H₅CHXCH₃, X = NH₂, OH, NCO exhibit a single monosignate (−) VCD that has the same shape as the absorption band. Su and Keiderling (59) assign this characteristic feature to an interaction of methyl deformation and phenyl modes based on the following observations: (1) a perturbed degenerate oscillator mechanism for the antisymmetric methyl deformation would generate a bisignate couplet, which is not observed; (2) in (+)-*p*-bromophenylethylamine the absorption frequency of the phenyl mode and, along with it, most of the negative VCD shifts to 1405 cm^{−1}; (3) if the methyl antisymmetric deformations are not present at 1450 cm^{−1}, as in (*S*)-(+)-methyl mandelate, the remaining phenyl VCD at 1450 cm^{−1} appears with much lower intensity. A similar assignment has been made from ROA studies (12, 61).

Polavarapu et al. (60) have obtained FTIR-VCD (1625–600 cm^{−1}) for neat samples of the three substituted α-phenylethanes, **10**, X = NH₂, OH, NCO. In (+)-α-phenylethylamine, seven VCD bands are observed, all with positive sign. Features near 1370 and 1200 cm^{−1} were identified as possibly useful probes for the configuration of similar analogs.

The mid-infrared region is considerably more difficult to interpret than the CH stretching region. This fact again points to the fact that chromophores responsible for VCD are delocalized over the chiral frame.

C. Chiral Ring Molecules

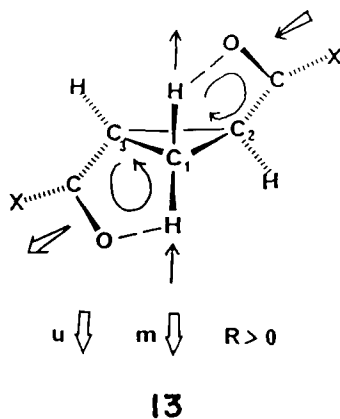
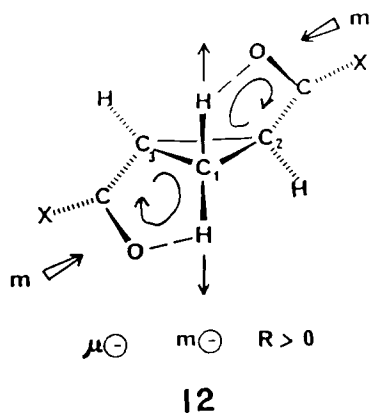
The early investigations of VCD revealed generally intense and distinctive VCD spectra for chiral ring molecules (20). Because VCD displays both positive and negative intensities and because it is highly sensitive to three-dimensional structure, molecules that can exist in a large number of different conformational states usually exhibit VCD spectra that are complex. Band intensities are often diminished by the overlap of opposing VCD contributions. Since conformational freedom is restricted in a ring, a large number of current VCD studies involve chiral ring molecules. Their conformational simplicity allows easier measurement and theoretical interpretation. In fact, a great deal of fundamental knowledge about VCD has been gained through the study of such molecules.

1. Small Ring Molecules

Several VCD studies have been reported to date on three- and four-membered chiral ring molecules. The first of these by Heintz and Keiderling (62) focused on trans disubstituted cyclopropanes. These molecules have a rigid ring and a twofold axis of symmetry; the substituents included carbomethoxy, carboxy, chlorocarbonyl, and cyano groups. The purpose of this study was to elucidate the basic VCD features of a series of structurally related molecules and to

compare the measured spectra to theoretical predictions using the fixed partial charge model. Aside from the substituent, these molecules possess no conformational freedom and vibrations associated with the ring itself are free of such complications. It was found that the VCD patterns for the ester could be generally predicted by FPC calculations in the CH stretching region; however, both the effects of change in substituent and the VCD in the mid-infrared could not be described by this model. The failure of the FPC model in the mid-infrared VCD region is general for all VCD spectra recorded to date. For both the acid chloride and dimethyl ester species, the C=O stretches give rise to a bisignate VCD feature (negative to lower frequency) that arises due to the coupled oscillator mechanism. Either a *cis-cis* or *trans-trans* arrangement of the two C=O oscillators relative to the cyclopropane ring was found to be consistent with the observed sense of the VCD couplet.

As mentioned earlier, FPC calculations carried out in the hydrogen stretching region are very nearly conservative. The simplest VCD spectra for the substituted cyclopropanes involve only two CH oscillators at the apex of the cyclopropane ring; the two corner methine CH groups were deuterated and the substituent was either deuterated methyl or involved no CH bonds. As an example, the VCD spectrum in the CH region of (+)-dimethyl *trans*-1,2-cyclopropanedicarboxylate- d_8 (with C_1-d , C_2-d , and methyl- d_3) is shown in Figure 4. Clearly, the CH stretching region is monosignate and strongly biased to positive VCD intensity. In accordance with a growing body of examples to be enumerated in this chapter, we suggest that this positive bias originates in vibrationally generated electronic current in intramolecular rings. As shown in **12** and **13**, the antisymmetric and symmetric methylene stretching modes can be seen to give rise to the positive VCD features near 3110 and 3020 cm^{-1} , respectively, in the following fashion.



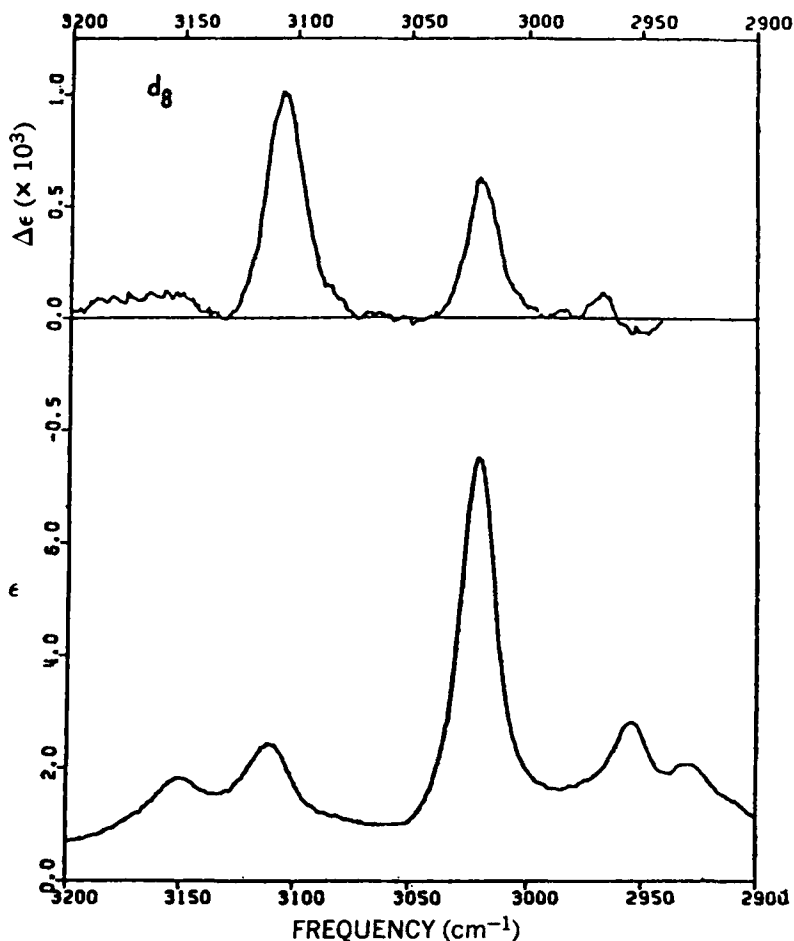


Figure 4. VCD and absorption spectra in the CH stretching region of (+)-dimethyl-*trans*-1,2-cyclopropanedicarboxylate-*d*₈, 0.050 *M* in CCl₄. Sample path length 0.35 cm, time constant 10 s. (Reproduced with permission from ref. 62. Copyright 1981 American Chemical Society.)

With the carbomethoxy groups oriented such that their planes bisect the cyclopropane ring and the carbonyl bonds are both *cis* to the ring (in agreement with conformational studies on the monoester), each methylene CH bond is involved in an intramolecular hydrogen-bonded ring with the carbonyl group *cis* to that bond. As the CH bond elongates, the hydrogen-bond distance is decreased and the hydrogen bond is strengthened by the flow of electrons from the electron rich oxygen. Since a closed pathway for electron flow is present, positive current will, therefore, flow around the ring in the direction C—H → O=C during CH

elongation and in the direction $C=O \rightarrow H-C$ during CH contraction. These ring currents give rise to the magnetic dipole transition moments \mathbf{m} with direction shown in 12 and 13. In 12, the symmetric stretch, the electric dipole transition moment μ is directed into the page. Since the resultant magnetic moment \mathbf{m} also is directed into the page, the rotational strength $\mu \cdot \mathbf{m}$ is positive, in agreement with the observed VCD at 3020 cm^{-1} . For the antisymmetric stretch, 13, μ lies in the plane of the page pointing down, and the resultant \mathbf{m} due to the two ring currents also points down, giving positive VCD, as observed at 3110 cm^{-1} . For this mode, the two ring currents generate bond currents $C_2 \rightarrow C_1$ and $C_1 \rightarrow C_3$, which can in turn give rise to a current around the cyclopropane ring, generating additional magnetic moment directed downward in 13. This additional ring current, which is not possible in the symmetric stretch, may account for the 10-fold increase in anisotropy ratio ($g = \Delta\epsilon/\epsilon$) for the antisymmetric as compared to the symmetric stretch. Further evidence in support of the vibrational ring current mechanism for the apex methylene stretching VCD is seen in *trans*-1,2-cyclopropanedicarbonitrile. Here the hydrogen-bonded rings containing the methylene CH bonds cannot form, and, in fact, virtually no CH stretching VCD is observed for the dinitrile with deuterated *trans* methine hydrogen atoms.

Polavarapu and Michalska (63) have reported mid-infrared VCD in (*S*)-(-)-epoxypropane both in the vapor phase and as a neat liquid. This paper reports the first comparison of gas phase and liquid phase VCD as well as the first report of VCD from degenerate methyl rocking modes. The stereochemical significance lies in the identification of VCD marker bands for the molecular geometry since the molecule is completely rigid from the standpoint of vibrational spectroscopy. Due to its extreme simplicity as a chiral molecule, epoxypropane (propylene oxide) is very important from a theoretical perspective.

Another molecule of theoretical importance to VCD is *trans*-1,2-dideuteriocyclobutane. The molecule exists in two equienergetic conformational states in which the deuterium atoms are either both in the axial or equatorial positions. Interconversion takes place through a change in the puckering of the four-membered ring. Because this molecule is a saturated hydrocarbon, there are no regions of readily delocalizable electronic structure. Not surprisingly, the VCD in the CH and CD stretching regions as reported by Annamalai et al. (64) are nearly conservative, and the FPC model is able to describe the VCD intensity as well as the LMO model. In this molecule vibrationally induced charge flow is minimal and coupled CH moments describe the hydrogen stretching spectra very well.

In these examples we see that small, chiral, ring molecules can serve as simple prototypes of mechanisms for VCD intensity and for detailed comparison to theoretical calculations. The apex CH_2 vibrations in dimethyl- d_6 *trans*-cyclopropanedicarboxylate-1,2- d_2 generate VCD almost entirely from vibrationally

generated ring currents since the nuclear vibrating chromophore (nuclear motion) is essentially achiral. In contrast, *trans*-1,2-dideuteriocyclobutane generates VCD from a chiral arrangement of CH (or CD) oscillators that behave as if the electron density perfectly (rigidly) follows the nuclear motion. In the examples that follow, these two mechanisms recur repeatedly as fundamental components of VCD spectra.

2. The Chiral $\text{CH}_2\text{CH}_2\text{C}^*\text{H}$ Fragment

A large number of studies (20, 65–72) have focused on the CH-stretching VCD of six-membered ring molecules containing a $\text{CH}_2\text{CH}_2\text{C}^*\text{H}$ fragment.

Laux et al. (70, 71) have viewed this fragment as an inherently dissymmetric chromophore that generates a characteristic VCD pattern that is fairly independent of the chemical environment of the chromophore. As depicted in the two possible chair conformations in **14** and **15**, the $\text{CH}_2\text{CH}_2\text{C}^*\text{H}$ fragment in the ring is itself chiral, and vibrations within the chromophore are both electric dipole and magnetic dipole allowed. The VCD pattern due to the fragment is determined by the absolute geometry of the chromophore, and in cases where an equilibrium between chair forms is established, the VCD spectra permit the conformer in excess to be identified.

In Table 1, VCD data for 15 ring compounds are summarized (70). These ring molecules, which include amines, alcohols, ketones, and other species, all exhibit a $(+ - +)$ or $(- + -)$ VCD pattern in the $2890\text{--}2960\text{-cm}^{-1}$ region when the $\text{CH}_2\text{CH}_2\text{C}^*\text{H}$ fragment is present. Although vibration of additional ring hydrogens and ring constituents contribute to the VCD in this region, deuteration studies (72) demonstrate that this characteristic VCD pattern is due to the $\text{CH}_2\text{CH}_2\text{C}^*\text{H}$ fragment. Based on correlations with known structures and theoretical calculations, Laux et al. (70) assign the $(+ - +)$ pattern to the absolute conformation of the fragment in **14** and the opposite $(- + -)$ pattern to the conformation in **15**. Although the $\text{CH}_2\text{CH}_2\text{C}^*\text{H}$ fragments in **14** and **15** are not truly enantiomeric due to the axial vs. equatorial position of the methine, the VCD features (*vide infra*) are largely determined by vibrations of the $-\text{CH}_2\text{CH}_2-$ moieties, which are mirror images in **14** and **15**. For all the

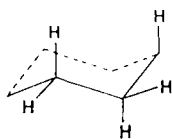
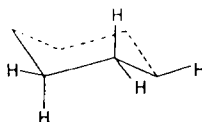
**14****15**

Table 1
Observed Frequencies and Sign Patterns for the Characteristic VCD Bands of the $\text{CH}_3-\text{CH}_2-\text{C}^*\text{H}$ Fragments in Molecules of Known Absolute Configuration^a

Molecule	Observed Band Maxima, $\pm 3 \text{ cm}^{-1}$	Observed Sign Pattern	Predicted Sign Pattern
(R)-(+)-3-Methylcyclohexanone	2948, 2929, 2912	+ - +	+ - +
(R)-(+)-3-Methylcyclohexanone-2,2,6,6-d ₄	2951, 2930, 2915	+ - +	+ - +
(R)-(+)-3- <i>tert</i> -Butylcyclohexanone	2953, 2934, 2913	+ - +	+ - +
(R)-(+)-3- <i>tert</i> -Butylcyclohexanone-2,2,6,6-d ₄	2953, 2934, 2915	+ - +	+ - +
(-)-Menthone	2948, 2928, 2909	+ - +	+ - +
(+)-Isomenthone	2954, 2935, 2906	- + -	- + -
(+)-Limonene	2939, 2915, 2893	+ - +	+ - +
(+)- <i>p</i> -Menth-1-ene	2942, 2925, 2895	+ - +	+ - +
(+)- <i>p</i> -Menth-1-en-9-ol	2960, 2923, 2893	+ - +	+ - +
(-)- β -Pinene	2956, 2939, 2922	- + -	- + -
(-)- α -Pinene	Pattern absent	Pattern absent	
(-)- <i>cis</i> -Myrtanylamine	2970, 2944, 2923	+ - +	+ - +
(+)-Pulegone	2949, 2927, 2903	+ - +	+ - +
(-)-Menthol	2945, 2928, 2911	+ - +	+ - +
(-)-Perillyl alcohol	2941, 2921, 2892	- + -	- + -

^aReprinted with permission from ref. 70. Copyright 1982 American Chemical Society.

molecules included in Table 1, the observed sign pattern is that which is predicted for the most probable chair conformation.

As an example of spectra of molecules containing the $\text{CH}_2\text{CH}_2\text{C}^*\text{H}$ chiral fragment, the spectra of (–)-menthone and (+)-isomenthone are shown in Figure 5. (–)-Menthone has two bulky substituents and the favored chair conformation is **16**, which corresponds to **14** with both substituents in equatorial positions. The observed (+ – +) VCD pattern is that predicted for this fragment geometry. For isomenthone both chair conformations **18** and **19** are populated since, in each, one alkyl substituent is axial and one equatorial. However, the

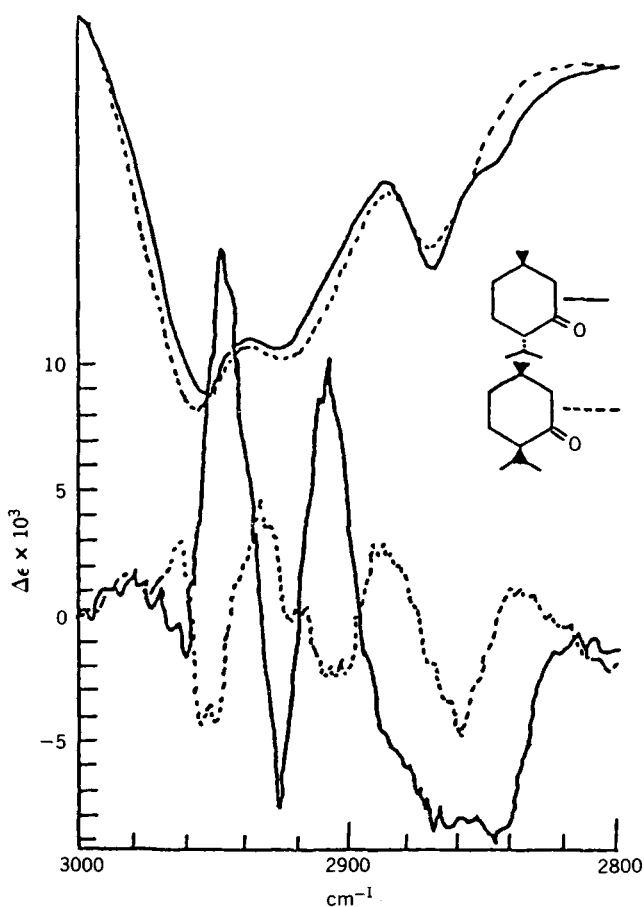
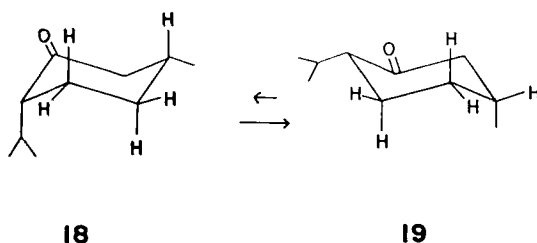
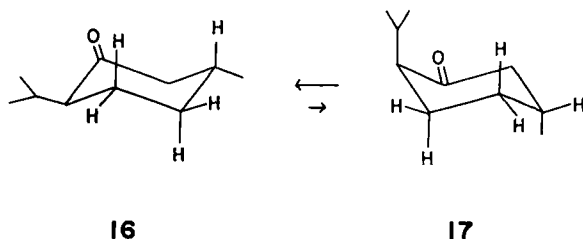
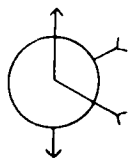


Figure 5. VCD (lower traces) and transmission spectra (upper trace) in the CH stretching region of (–)-menthone (—), 0.059 M in CCl_4 , and (+)-isomenthone (---), 0.062 M in CCl_4 . (Reproduced with permission from ref.70. Copyright 1982 American Chemical Society.)

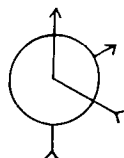


conformation with the more bulky equatorial substituent should be favored, giving a net excess of conformer **19**. The VCD of isomenthone (Figure 5) is weaker than that of menthone and exhibits a $(- + -)$ VCD pattern that corresponds to the excess of **19**.

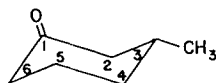
The vibrational assignments for the characteristic VCD features of the chiral fragment have been the subject of considerable investigation. Laux (71) considered the isolated dissymmetric chromophore using nondegenerate coupled oscillator theory, allowing coupling among the two asymmetric methylene stretching modes and the methine stretch, and determined the sign of the coupling constants that would give rise to the observed spectra. The highest frequency mode (positive VCD for **14**) corresponds to the phase of combination of the two antisymmetric methylene CH stretching modes in which the two axial CH bonds stretch while the equatorial bonds contract (**20a**). The central (negative for **14**) peak arises from the other phase of these motions in which one axial CH bond stretches while the other contracts (**20b**).



20a positive VCD



20b negative VCD

**21**

Laux (71) assigns the lowest frequency mode to the methine stretch weakly coupled to the antisymmetric stretch of the adjacent methylene. In addition to the coupled oscillator considerations, normal coordinate and FPC model VCD calculations have also been carried out both for the fragment and for some ring molecules (65, 67–69, 71).

More extensive studies in our laboratory on (+)-(3*R*)-methylcyclohexanone, **21**, the prototype ring molecule containing the CH₂CH₂CH fragment, have led to a better understanding of the VCD spectra (72). We have compared IR and VCD spectra for 3-methylcyclohexanone and five specifically deuterated isotopomers (2,6-*d*₄, 3-*d*₁, 4-*d*₂, 5-*d*₂, and methyl-*d*₃) to determine more precise assignments. Using nuclear trajectories obtained from a normal coordinate analysis, the IR absorption and VCD intensities for the 12 CH stretching modes were calculated using the FPC, APT, and LMO models. These studies confirm that the two highest frequency characteristic VCD modes assigned to the fragment are indeed primarily due to coupled motion of the antisymmetric CH₂ stretches on C-4 and C-5, phased as shown in **20a** and **20b**. In terms of a coupled oscillator description, these two modes in 3-methylcyclohexanone arise from nearly degenerate local CH₂ vibrations that mix primarily due to kinetic energy effects.

The third characteristic feature assigned to the fragment, the positive band at ~2910 cm⁻¹, however, is not primarily due to C*H motion as previously suggested. The deuteration studies identify the mode at 2910 cm⁻¹ as a Fermi resonance mixture of the C(4)H₂ symmetric stretch with the overtone of the CH₂ scissors mode on that carbon. The positive VCD intensity arises from the fact that the unperturbed C(4)H₂ symmetric stretch (~2882 cm⁻¹) and the C*H stretch (~2880 cm⁻¹) mix via kinetic energy coupling, giving rise to a non-degenerate coupled oscillator. The combination that is ca. 80% C(4)H₂ symmetric stretch and ca. 20% C*H stretch (positive VCD) moves to 2910 cm⁻¹ due to the Fermi resonance interaction, and appears in these ring molecules as the lower frequency positive feature in the (+ - +) VCD pattern. The other combination, primarily C*H stretch, contributes negative VCD near 2880 cm⁻¹ [see Figure 5 for (-)-menthone], which is obscured by other overlapping vibrations in some of the ring molecules. In conformation **15**, mixing of the C(3)H and C(4)H₂ motions cannot give rise to a VCD couplet, due to parallel μ_a and

μ_b . In molecules with conformation **15**, the third VCD feature near 2900 cm^{-1} can result from coupling of the $\text{C}(4)\text{H}_2$ and $\text{C}(5)\text{H}_2$ symmetric stretching modes or $\text{C}(5)\text{H}_2$ and $\text{C}^*(6)\text{H}$ modes in some species.

Laux (71) cautions that in some molecules containing chiral $\text{CH}_2\text{CH}_2\text{C}^*\text{H}$, the characteristic $(+ - +)$ or $(- + -)$ pattern is partially obscured or distorted by perturbing effects from some ring substituents. The mixed antisymmetric methylene stretches that give rise to the high frequency $(+ -)$ or $(- +)$ couplet are perhaps not so subject to these perturbations and may still serve as a stereochemical probe even when, for example, the Fermi resonance, which shifts the third feature to higher frequency, is absent.

The presence of an "inherently dissymmetric chromophore" in a molecule clearly provides a key to obtaining stereochemical information from both electronic CD and, as demonstrated by the $\text{CH}_2\text{CH}_2\text{C}^*\text{H}$ fragment, from VCD spectra. As with any spectroscopic structural probe, the characteristic spectral features of the chromophore must not significantly mix with nor be overlapped by other vibrations in the molecule.

The CH stretching VCD in these six-membered ring molecules is fairly conservative, and the spectra are adequately explained by VCD mechanisms in which electronic motion perfectly follows nuclear motion ("nuclear following mechanisms").

3. Low-Frequency Skeletal Motions

In addition to the characteristic CH stretching VCD, a number of molecules that are structurally similar to 3-methylcyclohexanone exhibit characteristic ROA features in the skeletal region below 700 cm^{-1} , Figure 6 (11). In particular, a bisignate couplet near 500 cm^{-1} is observed in six-membered ring compounds with a carbonyl substituent [(+)-pulegone (73), (+)-camphor (74), (+)-3-bromocamphor (74), (+)-nopinone (75)]; and a broad low frequency couplet is observed in ketones with a 3-methyl substituent (75). The ROA of 3-methylcyclohexanone exhibits a third characteristic couplet near 400 cm^{-1} . In all cases the sense of the observed couplets correlates with the absolute configuration of the most stable chair conformation.

Several calculational and descriptive models of ROA have been applied to the interpretation of the 3-methylcyclohexanone low-frequency ROA spectrum (11, 75-77). The main difficulty in understanding the source of ROA couplets in general has been the lack of a complete, accurate description of the normal modes that give rise to specific ROA features. A study carried out recently in our laboratory (77) used the Raman spectra of specifically deuterated isotopomers of 3-methylcyclohexanone and the APT model of ROA (43) as a basis for generating a more accurate force field for the skeletal modes. From the com-

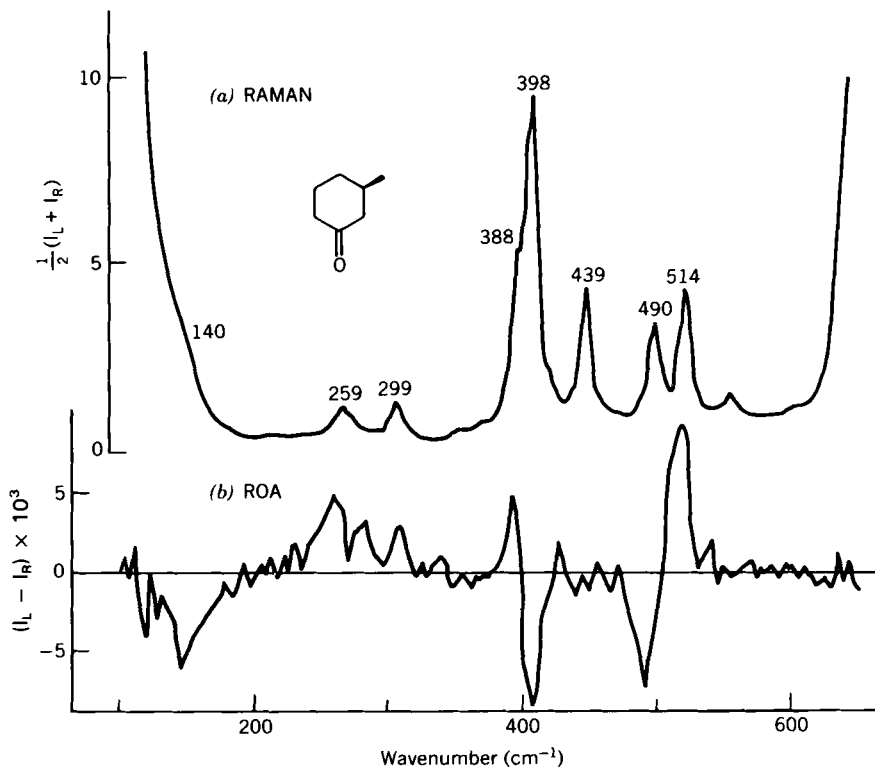


Figure 6. ROA and Raman spectrum of (+)-(3*R*)-methylcyclohexanone in the skeletal region, as a neat liquid. The ROA spectrum has been redrawn on a linear ordinate scale from the data in ref. 11. (Reproduced with permission from ref. 77. Copyright 1984 American Chemical Society.)

parison of stereoprojections of the molecule at equilibrium and displaced along a calculated normal coordinate, we have been able to decompose each skeletal mode into contributions from motions of the C₆ ring skeleton and from oscillations of the carbonyl or methyl group in or out of an equatorial ring plane. As an example, the stereoprojections of the modes that generate the 514, 490-cm⁻¹ and 398, 388-cm⁻¹ ROA couplets are shown in Figure 7. Below each stereoprojection is the schematic pattern for the primary nuclear motion involved in the vibration and the linear combination of achiral deformation modes that generates this pattern. In the diagram, the integer adjacent to each atom gives the relative sense and magnitude for the deformation of the valency angle centered at that atom, a positive integer denoting an increase in angle.

The symmetry species notation given for each contribution refers to sym-

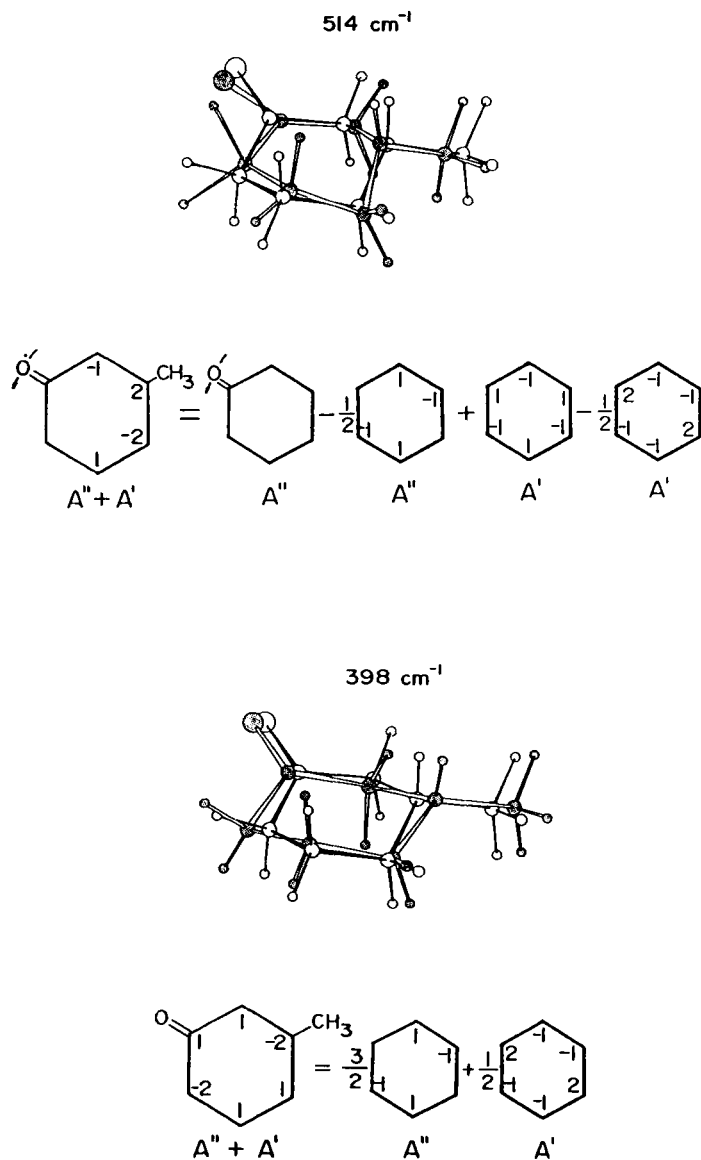
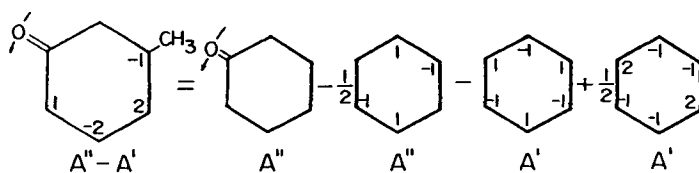
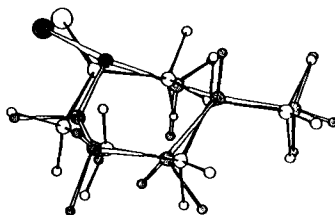


Figure 7. Stereoprojections of the 514, 490, 398, and 388- cm^{-1} normal modes of showing the equilibrium (white circles and black bonds) and vibrationally displaced molecules (shaded circles and white bonds). Beneath each mode is a schematic representation of the predominant pattern of motion and the linear combination of achiral cyclohexanone motions that generate the vibration. (Reproduced with permission from ref. 77. Copyright 1984 American Chemical Society.)

490 cm^{-1}



388 cm^{-1}

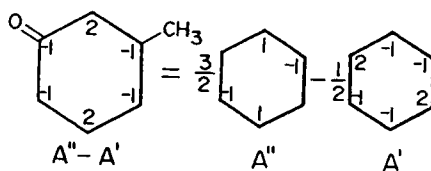
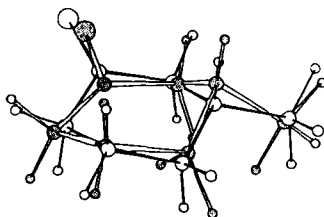


Figure 7. (Continued)

metric (A') or antisymmetric (A'') motion relative to the symmetry plane for cyclohexanone. From the diagram we see that each couplet can be described as an in- and out-of-phase combination of skeletal motions of cyclohexanone of A' and A'' symmetries. Thus, in this case the mechanism for generating the ROA couplets can be described in terms a chiral mixing of inherently achiral vibrations (11, 77): The addition of the methyl group to the achiral cyclohexanone ring to form chiral 3-methylcyclohexanone provides a source of chiral vibrational perturbation that permits mixing of skeletal modes of cyclohexanone that have similar energies but different symmetries.

The broad low frequency ROA couplet in 3-methylcyclohexanone can be similarly described as an in- and out-of-phase mixture of torsional ring motions. The remaining skeletal modes cannot be described in terms of a perturbed pair and, in fact, no significant ROA intensity is observed for these modes. We have also calculated the ROA intensities for (+)-(3*R*)-methylcyclohexanone using the Raman atomic polar tensor model and have obtained good agreement in sign and magnitude for all 10 skeletal vibrations below 600 cm^{-1} .

The descriptive interpretation for the 3-methylcyclohexanone skeletal modes in this region can be applied to the ROA spectra of similar molecules. For example, the modes in 3-methylcyclohexanone near 500 cm^{-1} involve both in plane $\text{C}=\text{O}$ deformation and ring deformation. Thus a couplet in this region is observed in similar molecules with a carbonyl group and a saturated C_6 ring, for example, in (+)-pulegone, (+)-camphor, (+)-3-bromocamphor, and (+)-nopinone. However, no such couplet is seen in molecules for which the skeletal motions at 500 cm^{-1} are greatly altered, such as those in which a vinylidene or hydroxyl group has been substituted for the carbonyl (76), or in which a double bond has been inserted in the ring (76), or again in which a large number of ring substituents has been added.

It is likely that the coupling of vibrations due to chiral perturbation is a major source for the generation of ROA couplets in the region below 1500 cm^{-1} , in which vibrations are generally spread out over the nuclear frame. Other descriptive mechanisms have been proposed, such as the splitting of degenerate modes or the coupling of vibrations of identical, chirally disposed groups (11–14), but these have not been as yet definitively applied to specific ROA features.

Due to the difficulties in interpretation and the sensitivity of vibrations in the fingerprint and skeletal regions to structural alterations, the application of ROA to stereochemical problems remains limited. However, the recent advances in experimental techniques and theoretical descriptions are promoting increased research activity in ROA. Especially in aqueous solution, where VCD signals are obscured by the solvent and in low frequency regions, in which VCD spectra are not yet available, Raman optical activity remains a promising tool for stereochemical investigations.

4. Other Ring Molecules

We mention here several VCD studies of chiral ring molecules that fall outside of the categories discussed previously. The first is an early study by Keiderling and Stephens (78) of (+)-(5*S*)-1,6-spiro[4,4]nonadiene, shown in Figure 8. Four conformations of the molecule were considered, which are distinguished by the direction of pucker of each of the two five-membered diene rings as shown in the figure. Consistent force field calculations predict that these conformations are within 0.1 kcal of one another. FPC-VCD calculations were carried out for each conformation and the results were averaged. The calculated VCD was close to the observed VCD in the aliphatic CH stretching region but not in the olefinic region. Lack of quantitative agreement was attributed to the approximate nature of the force field and the VCD (FPC) model. In hindsight, it is clear that some description of charge flow is necessary to better interpret the VCD spectra. With such a description, it should be possible to determine the population and contributions of the four conformers to the experimental result. Temperature studies would further aid such an analysis.

Another interesting molecule is (+)-(*R*)-2,2'-diamino-1,1'-binaphthyl, **22**, a twisted binaphthyl having C_2 symmetry, for which Barnett *et al.* have presented VCD data in the NH stretching region (79). The observed spectra are monosignate, positive for both the ν_a and ν_s stretching modes of the two NH_2 groups. Clearly the degenerate coupled oscillator mechanism is not dominant and an interpretation is presented based on the interaction of the amine NH dipole moments on one naphthyl group with the other naphthyl ring. The interaction is one of dipole-induced dipole through the anisotropic polarizability of the

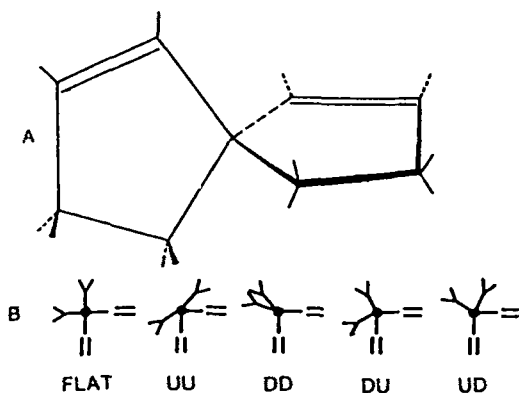
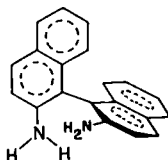


Figure 8. (+)-(5*S*)-1,6-spiro[4,4]nonadiene configuration (A) and schematic representation of the puckering of the various conformations (B). (Reproduced with permission from ref. 78. Copyright 1979 American Chemical Society.)



22

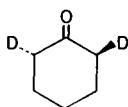
opposing naphthyl ring. The induced dipole moment is then chirally disposed in relation to the inducing NH_2 dipole moment. This mechanism, referred to as the dynamic polarization model (45), is shown to explain most of the observed VCD intensity in the symmetric NH_2 stretching mode, $\nu_{\text{NH}_2}^s$. The anisotropy ratio for this VCD band is ca. 10^{-4} . Since an $\text{NH} \cdots \pi$ type hydrogen bond is possible in this molecule, a description based on vibrationally induced charge flow (currents) may also be fruitful, similar to that proposed for α -phenylethylamine, Sect. IV-B-2.

Two six-membered ring molecules, $(-)$ -*trans*-(2*S*,6*S*)-cyclohexanone- d_2 **23**, and $(+)$ -(2*R*)-cyclohexanone- d_1 **24**, have been studied in the CH and CD stretching regions by Polavarapu et al. (80). These molecules are chiral only due to isotropic substitution.

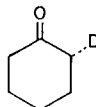
The CH stretching VCD for $(-)$ -cyclohexanone-2,6- d_2 , **23**, consists of a number of bands of alternating sign, with an overall positive bias. FPC calculations are in qualitative agreement with part of the VCD in this region.

The CD bond stretching VCD spectrum of **24** consists of three negative features between 2150 and 2250 cm^{-1} that can be attributed to the lone CD stretching mode for the two chair conformations, one with an axial CD bond and the other with an equatorial CD bond, with additional intensity arising from a Fermi enhanced overtone or combination mode. The FPC model predicts VCD intensities in this region three orders of magnitude below the experimental values.

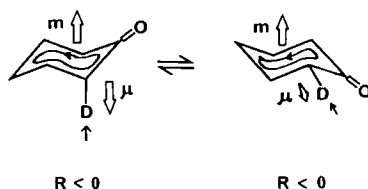
The negative CD bond stretching VCD can be explained by the ring current mechanism. As shown in **25** for contraction of the CD bond, electrons are injected into the cyclohexanone ring with preferred electron flow away from the bond with the more tightly held electron density, in this case the $\text{C}_\alpha\text{--C(O)}$ bond. Positive current flow around the ring gives rise to the magnetic moment,



23



24



25

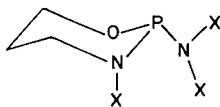
m, directed upward in **25**. For both axial and equatorial CD bonds, the scalar product of **μ** and **m** is negative, corresponding to negative VCD as observed.

For (–)-cyclohexanone-2,6-*d*₂ **23**, the two chair conformations are equivalent, with the axial and equatorial CD bonds chirally oriented. The CD stretching VCD, positive at $\sim 2200\text{ cm}^{-1}$ and negative between $2130\text{--}2170\text{ cm}^{-1}$, is consistent with that predicted for coupled motion of the two CD bonds. In this case, the splitting between the modes is due to different CD bond force constants for the axial and equatorial positions.

More recently, Su et al. (81) have measured the VCD in the mid-infrared region for a series of four chiral cyclophosphamides, **26**, where X is either chlorine or hydrogen. They observe an absorption band that occurs between 1205 and 1225 cm^{-1} in the four molecules having strong negative VCD in all cases. They refer to this band as a “VCD marker band” because it appears to correlate better with the absolute configuration of these molecules than does the optical rotation at the sodium D line in the visible region of the spectrum.

D. Amino Acids and Peptides

Studies of amino acids and peptides have been a major component of VCD research. From a biophysical standpoint, VCD provides a unique source of solution phase structural and conformational information. In addition, the previously discussed molecules have been the focus of numerous theoretical investigations. The major role of electronic currents in generating biased VCD was first recognized in interpreting amino acid VCD spectra. The polypeptide spectra have provided a test for theoretical descriptions of VCD in α -helical polymers.



26

1. Amino Acids

The VCD of amino acids and transition metal complexes of amino acids has been the subject of ongoing investigation in our laboratory (82–90), from which has emerged new information on solution geometries and on the ring current mechanism for generating intense monosignate VCD intensity.

The VCD in the CH stretching region of L-amino acids at neutral pH is characterized by a strong positive bias that is associated with the methine $C_\alpha H$ stretch near 2970 cm^{-1} , and additional features associated with the amino acid side chain. Tables 2 and 3 (89) are a compilation of the VCD and absorption maxima, the VCD bias (net integrated intensity over the CH-stretching region) and information on solubility and rotameric distribution of the amino acids and amino acid transition metal complexes in D_2O solution without pD adjustment. Other naturally occurring amino acids (tyrosine, tryptophan, glutamic acid, and aspartic acid) have very low solubilities at neutral pD, and their VCD spectra could not be obtained. L-Lactic acid is included due to its spectral similarities to alanine. The rotameric distributions about the β carbon have been determined using NMR. The CH stretching VCD of the Cu(II) or Co(III) complexes of several amino acids have also been investigated. In the complexes, the methine stretching frequency shifts $15\text{--}20\text{ cm}^{-1}$ to lower frequency and the VCD bias increases by up to a factor of four. Typical spectra are shown in Figures 9 to 11.

L-Alanine, the simplest chiral amino acid, has been the subject of the most extensive study and serves as the prototype for the other amino acids. A complete vibrational assignment has been obtained (85, 86) based on solution phase IR and Raman spectra and solid phase Raman spectra for alanine- d_0 , alanine- $C_\alpha d_1$, alanine- $C_\beta d_3$, and alanine- $C_\alpha d_1\text{-}C_\beta d_3$. In the CH stretching region, the antisymmetric methyl stretches are assigned at 3006 and 2989 cm^{-1} , the methine stretch at 2970 cm^{-1} , and the Fermi resonance diad involving the symmetric methyl stretch and the overtone of the antisymmetric methyl deformation at 2950 and 2893 cm^{-1} . The calculated frequency for the unperturbed symmetric methyl stretch is 2930 cm^{-1} .

The CH stretching VCD spectra (86) in D_2O (Figure 12) exhibit (1) a strong positive monosignate VCD feature ($g = 2.5 \times 10^{-4}$, 2970 cm^{-1}) for L-alanine- $C_\beta d_3\text{-}N d_3$, due to the single $C_\alpha H$ oscillator; (2) a weak, fairly conservative (+ − −) VCD spectrum for L-alanine- $C_\alpha d_1\text{-}N d_3$, due to methyl group vibrations only; and (3) for L-alanine- $N d_3$, a strong positive $C_\alpha H$ VCD modulated by the methyl group features.

A number of theoretical models have been used to calculate the alanine CH stretching VCD intensities, as summarized in Table 4. Although all four models reproduce the (+ − + −) sign pattern from high to low frequency in the VCD of L-alanine- $N d_3$, only the LMO and NMO models predict the large positive

Table 2
VCD and IR Absorption Maxima, VCD Bias, Solubility and C_α-C_β Rotameric Conformational Distribution for the Amino Acids and Lactic Acid^a

L-Amino Acid	$\Delta\epsilon_{\max} \times 10^4, \bar{\nu}$ (10 ³ cm ² mol ⁻¹ , cm ⁻¹)	VCD ^b Bias \times 10 ⁴ (10 ³ cm mol ⁻¹)	$\epsilon_{\max}, \bar{\nu}_{\max}$ (10 ³ cm ² mol ⁻¹ , cm ⁻¹)	Solubility (H ₂ O, 25°C, g/kg)	I (I')	II (II')	III ^c (III')
Glycine-C _α d ₁	-2, 3020 ± 2	-85	5, 3020 ± 2	250	—	—	—
Alanine-C _β d ₃	+5, 2970	+200	2, 3020	167	—	—	—
Alanine	+11, 2970	+285	14, 2995	167	—	—	—
Lactic acid	+5.2, 2920	+380	9, 2995	very sol.	—	—	—
Serine	+3, 2970	+120	15, 2960	422	28	10	62
Cysteine	+9, 2975	+360	8, 2955	100	45	17	38
Cysteine · DCI	+1, 3000	+60	10, 2950	—	—	—	—
Asparagine	+6, 2970	+300	8, 2955	28	50	12	38
Glutamine	+6, 2970	+325	16, 2945	26	—	—	—
Phenylalanine	+5, 2970	+90	12, 2940	28	52	20	28
Histidine	+5, 2985	+275	8, 2935	42	48	23	29

Valine	+7, 2975	+175	70, 2980	58	(59)	(24)	(17)
Leucine	+16, 2965	+200	100, 2970	22	67	21	12
Isoleucine	+15, 2970	+105	100, 2980	34.5	(50)	(12)	(50)
Threonine	+12, 2975	+50	32, 2985	v. sol.	(72)	(21)	(7)
<i>Allo</i> -threonine	+5, 2970	+250	31, 2990	v. sol.	(77)	(15)	(8)
Pencillamine	+9, 2960	+120	38, 2990	100	—	—	—
Methionine	+6, 2980	+300	23, 2930	56	51	40	9
Lysine · DCl	+5, 2980	+325	37, 2950	737	—	—	—
Arginine · DCl	+5, 2970	+275	25, 2950	856	C _γ exo, ^k	C _γ endo	—
Proline	+7, 2990	+455	18, 3000	1620	C _γ exo ^l	—	—
4-Hydroxy- proline	+9, 2990	+320	14, 2950	361	C _γ exo ^l	—	—
<i>Allo</i> -4-hydroxy- proline	+7.5, 2970	+340	15, 2955	—	C _γ exo ^l	—	—

^aReprinted with permission from ref. 89. Copyright 1985 American Chemical Society.

^bNet integrated VCD area $\int \Delta \epsilon d\tilde{\nu}$.

^cRotameric distribution, in percent, for structures I, II, III (see text for definition). Numbers in parentheses refer to structures I'; II'; III'; which are obtained from I, II, III by substituting R₂ for H_β trans to H_α, CO₂⁻ and ND₃⁺, respectively.

Table 3
VCD and IR Absorption Maxima and VCD Bias for the Cu(II) Complexes and Co(III) Complex of Amino Acids^a

Complex	$\Delta\epsilon_{\max} \times 10^4, \bar{\nu}_{\max}$ ($10^3 \text{ cm}^2 \text{ mol}^{-1}; \text{cm}^{-1}$)	$\Delta\epsilon$ Bias (10^3 cm mol^{-1})	$\Delta\epsilon_{\max}, \bar{\nu}_{\max}$ ($10^3 \text{ cm}^2 \text{ mol}^{-1}; \text{cm}^{-1}$)	Solvent
<i>bis</i> [L-alaninato]Cu(II)	+35, 2950	+1400	32, 2985	D ₂ O
(Δ) α' - <i>tris</i> [L-alaninato]Co(III)	+25, 2955	+1625	33, 2950	D ₂ O
<i>bis</i> [L-serinato]Cu(II)	+15, 2950	+900	35, 2960	D ₂ O
<i>bis</i> [L-valinato]Cu(II)	+25, 2970	+1625	170, 2975	D ₂ O
<i>bis</i> [L-threoninato]Cu(II)	+30, 2980	+1200	75, 2980	D ₂ O
<i>bis</i> [L-prolinato]Cu(II)	+30, 2950	+1650	75, 2990	D ₂ O

^aReprinted with permission from ref. 89. Copyright 1985 American Chemical Society.

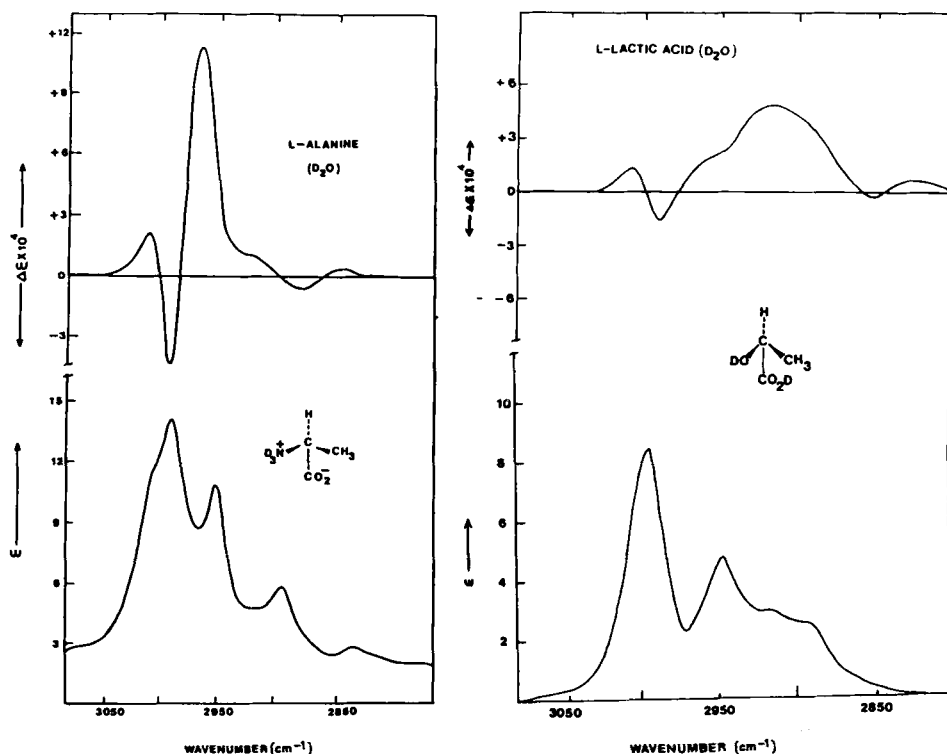


Figure 9. VCD and absorption spectra in the CH stretching region of (a) L-alanine, 1.7 M in D₂O, path length 200 μm and (b) L-lactic acid, 2.1 M in D₂O, path length 300 μm. (Reproduced with permission from ref. 89. Copyright 1985 American Chemical Society.)

VCD in L-alanine-*C*_β-*d*₃-*N*-*d*₃ and the positive bias in L-alanine-*N*-*d*₃. These two models allow for electronic motion (LMO centroid displacement or charge flow along bonds) in parts of the molecule distant from the primary nuclear motion. The observed and calculated spectra using the LMO model are compared in Figure 13 and an example of the calculated nuclear and LMO centroid displacements are presented in Figure 14 for the methine stretching mode.

The observation that all the L-amino acids, the L-amino acid transition metal complexes, and the α-L-hydroxy acids in neutral solution exhibit a positive maximum for the C_αH stretching VCD and a positive VCD bias over the entire CH stretching region forms the empirical basis for the methine C_αH stretching chirality rule (88). The proposed mechanism for this chirality rule is based on a chromophore consisting of a molecular fragment having the L configuration

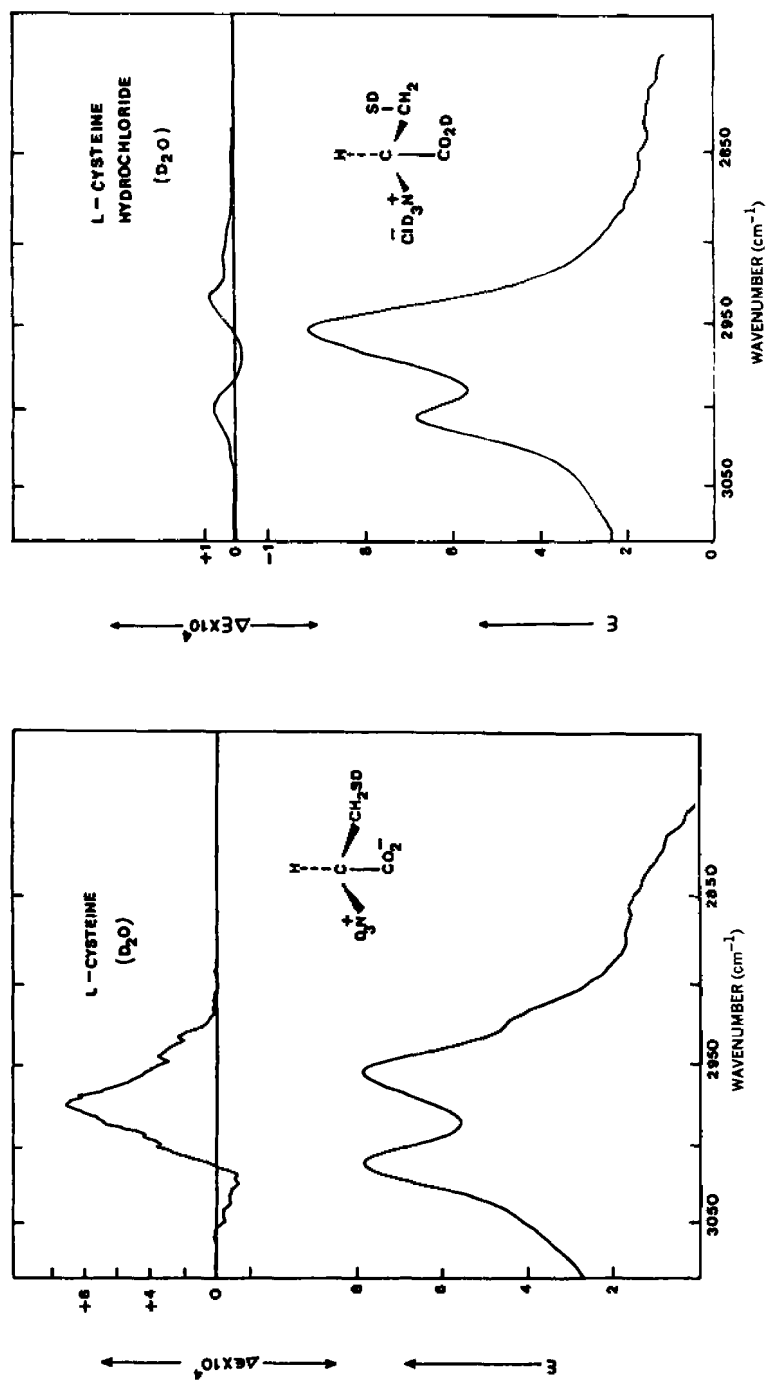


Figure 10. VCD and absorption spectra in the CH stretching region of (a) L-cysteine 0.83 M in D₂O, path length 200 μ M, and (b) L-cysteine hydrochloride, 0.8 M in D₂O, path length 200 μ M. (Reproduced with permission from ref. 89. Copyright 1985 American Chemical Society.)

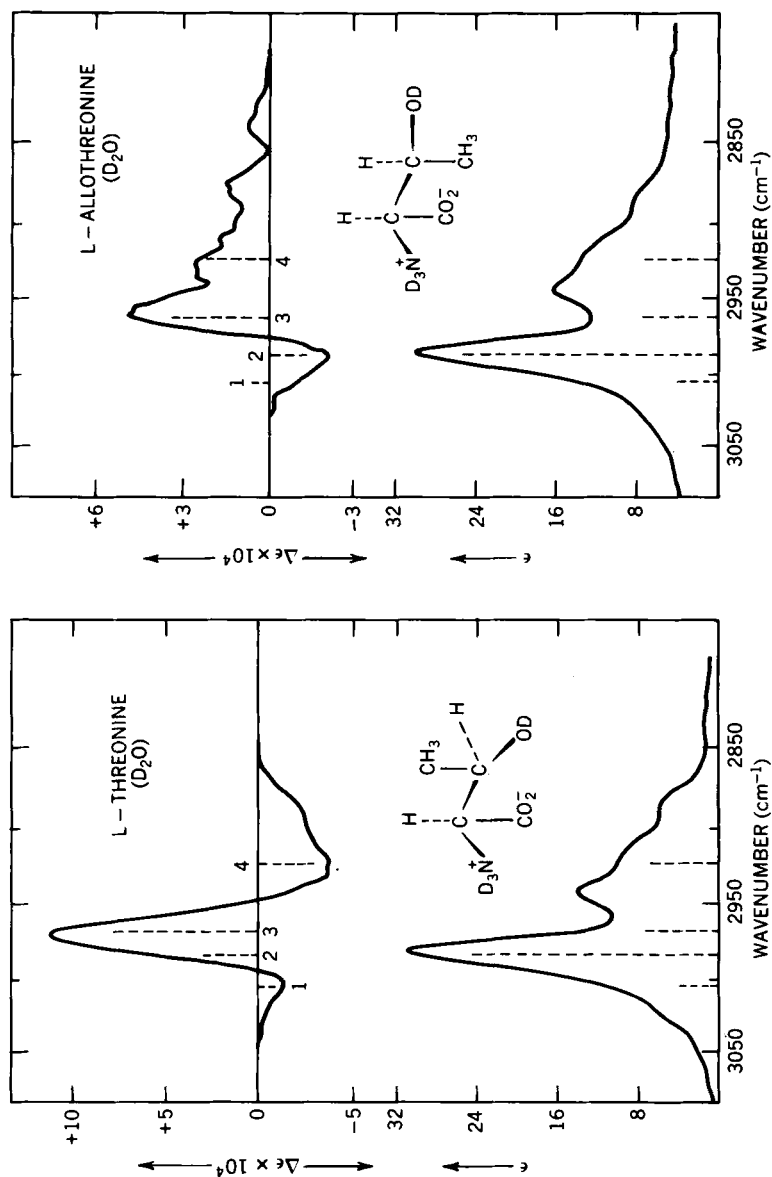


Figure 11. VCD and absorption spectra in the CH stretching regions of (a) L-threonine, 0.63 M in D_2O , path length 200 μM , and (b) L-allothreonine, 1.8 M in D_2O , path length 200 μM .

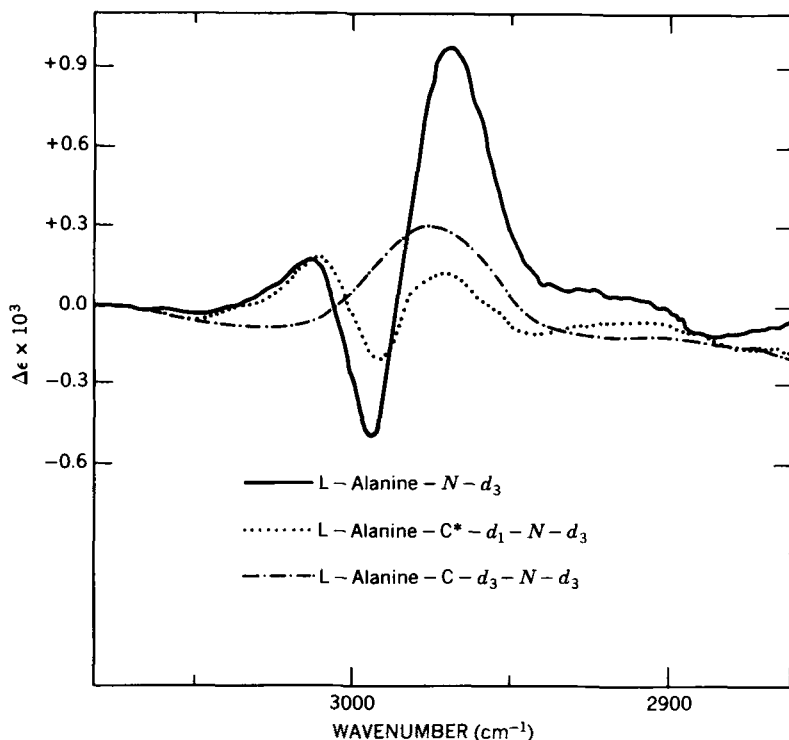
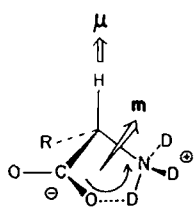


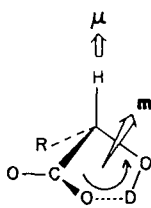
Figure 12. Comparison of the VCD spectra of L-alanine- $N-d_3$ (—), L-alanine- $\alpha-d_1$ - $N-d_3$ (·····), and L-alanine- $\beta-d_3$ - $N-d_3$ (- · - ·) in D_2O . (Reproduced with permission from ref. 86. Copyright 1982 American Chemical Society.)

with a methine bond adjacent to an intramolecular ring closed by hydrogen bonding ($CO_2 \cdots D_3^+N$ or $HOCO \cdots HO$) or transition metal coordination ($O-M-N$), 27–29.

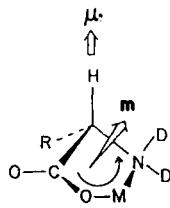
The methine stretching vibration is proposed to induce an oscillating current in the ring. Depicted in 27–29 for the methine contraction, which results in an



27



28



29

Table 4
Rotational and Dipole Strength Calculations for the CH-Stretching Vibrations of L-alanine Using the Localized Molecular Orbital, Nonlocalized Molecular Orbital, Atomic Polar Tensor, and Fixed Partial Charge Models^a

Frequency (calc), cm ⁻¹	LMO		NMO		APT		FPC		Experiment		Descrip- tion
	D ^b	R ^c	R	D	R	D	R	D	R		
L-alanine-N-d ₃											
3009	2.21	1.77	0.018	2.22	1.40	1.42	0.545	0.57	0.54	CH ₃ ^{asym}	
2993	5.13	-9.06	-7.53	5.16	-9.23	1.34	-1.71	0.58	-2.43	CH ₃ ^{asym}	
2970	4.80	18.6	15.0	4.74	12.2	0.45	1.59	0.45	5.58	C*H	
2930	2.87	-7.35	-6.50	2.82	-5.58	0.41	-0.365	0.30	-1.15	CH ₃ ^{sym}	
L-alanine-C*-d ₁ -N-d ₃											
3007	1.45	0.944	-0.250	1.44	0.980	1.25	-0.065	0.53	0.70	CH ₃ ^{asym}	
2993	4.72	-0.372	0.550	4.70	-0.812	1.22	0.073	0.67	-0.53	CH ₃ ^{asym}	
2932	3.25	-1.23	-0.490	3.12	0.139	0.43	0.0016	0.52	-0.39	CH ₃ ^{sym}	
L-alanine-C-d ₃ -N-d ₃											
2970	5.74	4.58	1.11	5.80	-1.57	0.73	0.0345	0.37	2.11	C*H	

^aSee refs. 38, 42, 86, and 87. Reprinted with permission from ref. 38. Copyright 1984 American Chemical Society.

^bDipole strength (esu² cm²) × 10³⁹.

^cRotational strength (esu² cm²) × 10⁴⁴.

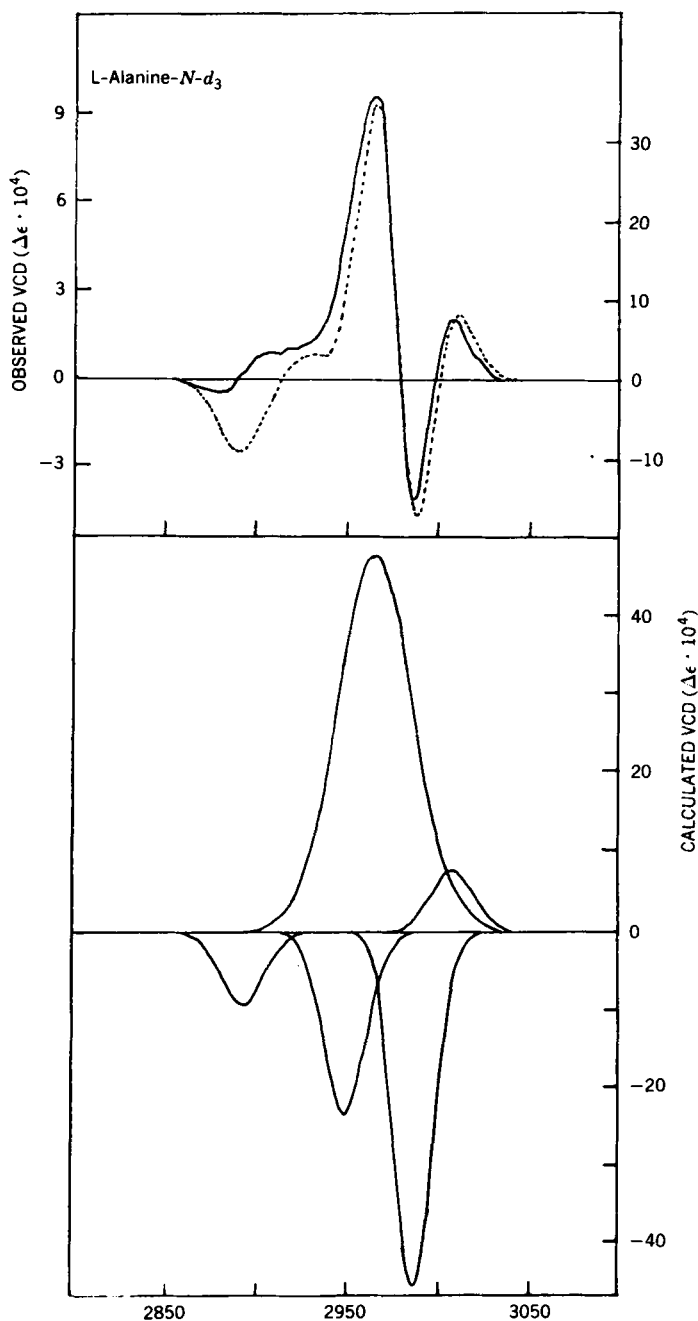


Figure 13. Comparison of the CH stretching VCD spectrum of L-alanine- $N\text{-}d_3$ in D_2O (—) and the individual VCD bands (lower) and net VCD spectrum (----) calculated using the localized molecular orbital model. Different ordinate scales are used for the experimental and theoretical spectra. (Reproduced with permission from ref. 87. Copyright 1982 American Chemical Society.)

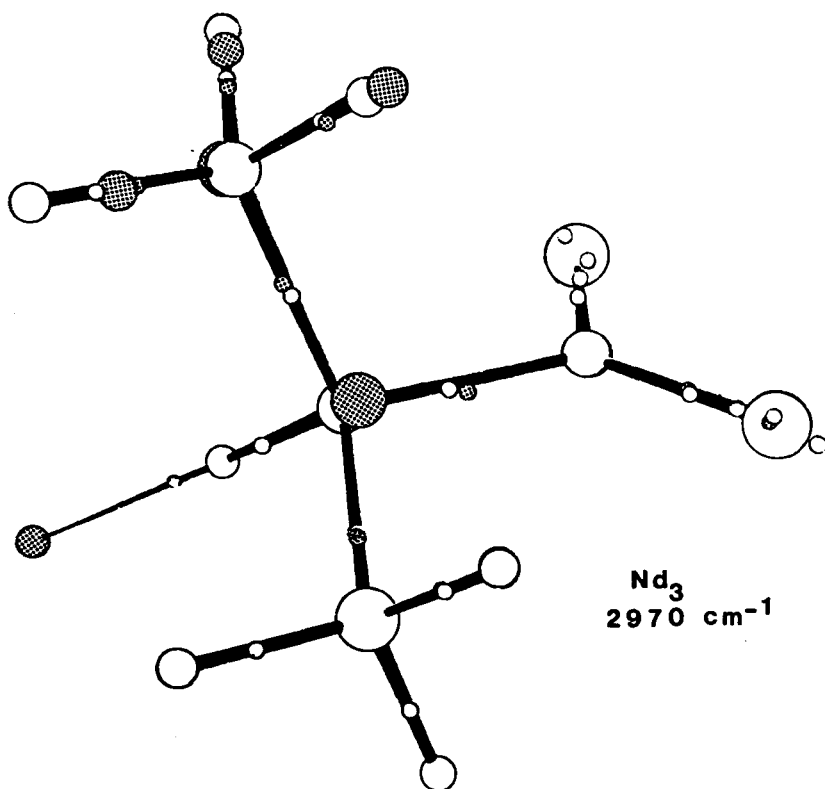


Figure 14. Stereoprojections of the methine stretching vibrations in L-alanine- N - d_3 and L-alanine- β - d_3 - N - d_3 , showing the equilibrium positions of the nuclei (large white circles) and LMO centroids (small white circles) and their exaggerated displacements (dotted circles). (Reproduced with permission from ref. 87. Copyright 1982 American Chemical Society.)

electric dipole transition moment μ as shown, the sense of positive charge circulation indicated (from the heteroatom to C_α) will result in a magnetic dipole transition moment contribution whose scalar product with μ is positive. This type of mechanism is not adequately described by the present position dependent calculational VCD models, particularly if vibrationally induced charge flow around the ring occurs that does not affect the electron density at the nuclei and hence does not contribute to μ . Although spectroscopic evidence for such a hydrogen-bonded ring has not previously been presented for amino acids, bands in the IR spectra in the OH stretching region of α -hydroxy acids are assigned to intramolecular five-membered ring conformers as in **28** (54, 91). In the transition metal complexes, where the carboxyl group is rigidly held in a conformation similar to the proposed hydrogen-bonded configuration, the VCD is quite similar in pattern, but with enhanced bias. The latter effect may be attributed

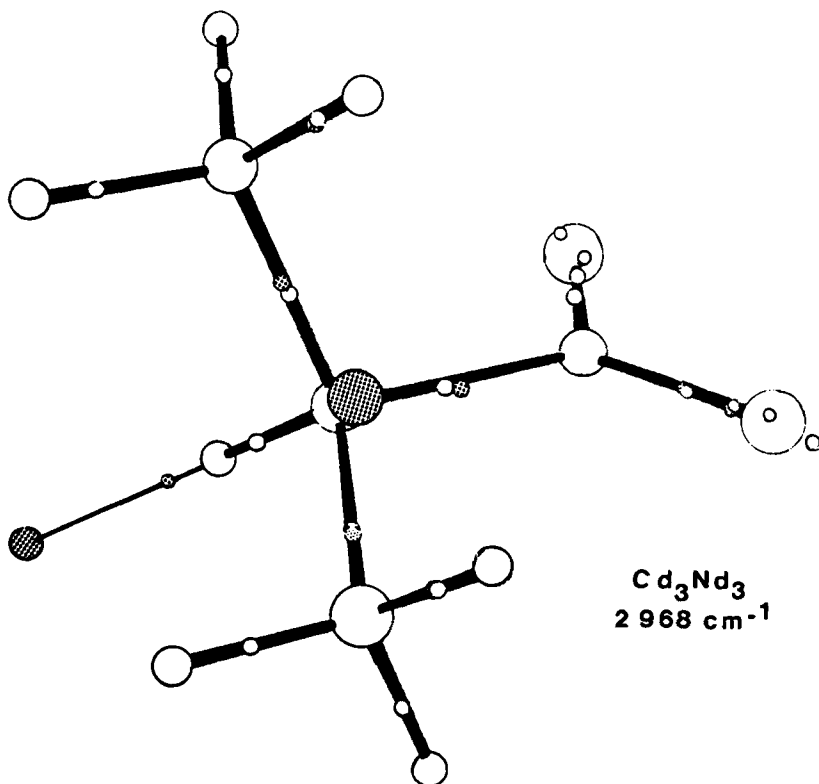


Figure 14. (Continued)

to the rigidity of the complexes and the participation of the electronic structure of the metal. Furthermore, evidence from NMR shows that the most prevalent rotameric forms about the $\text{C}_\alpha\text{--C}_\beta$ bond are those that avoid positioning a bulky substituent trans to the ND_3^+ . In the proposed hydrogen-bonded conformation, the carboxylate oxygen that is not involved in the hydrogen bonding would sterically interfere with bulky substituents trans to the ND_3^+ .

Finally, the loss of VCD bias in L-cysteine \cdot DCl (in D_2O) (Figure 10) and L-alanine- $N\text{-d}_3 \cdot$ DCl (Figure 15) is consistent with the disruption of the intramolecular hydrogen bonding and charge flows at low pD.

In addition to the VCD from the methine C_αH stretching vibration, which alone gives rise to a strong positive bias in the CH stretching region, the CH stretching VCD of amino acids contains contributions from two other sources. Minor features can be attributed to combination bands of the very intense antisymmetric carboxylate stretch at $\sim 1610\text{ cm}^{-1}$ with the symmetric carboxylate

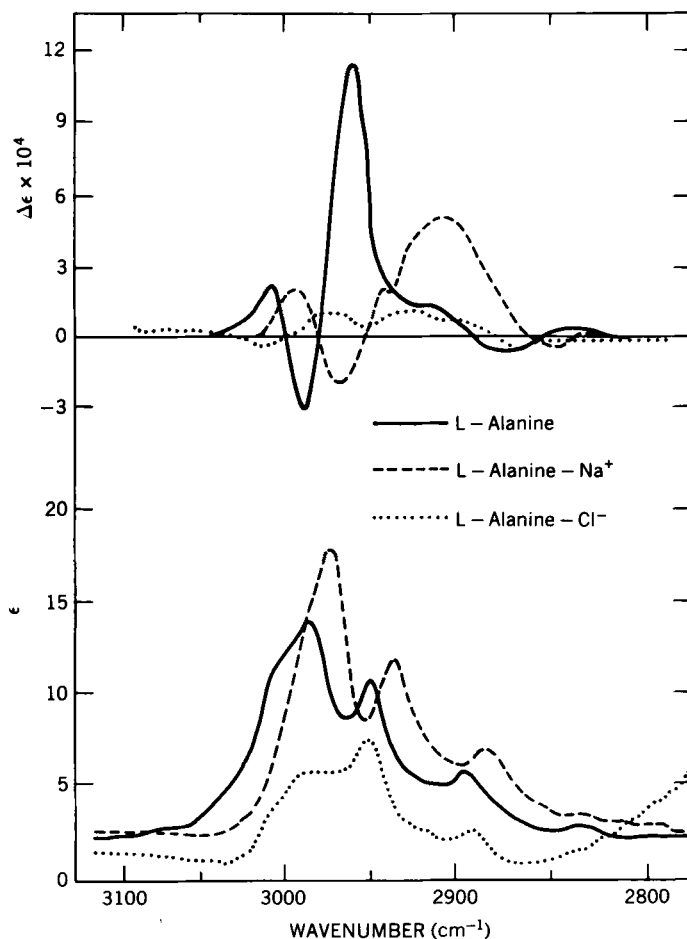
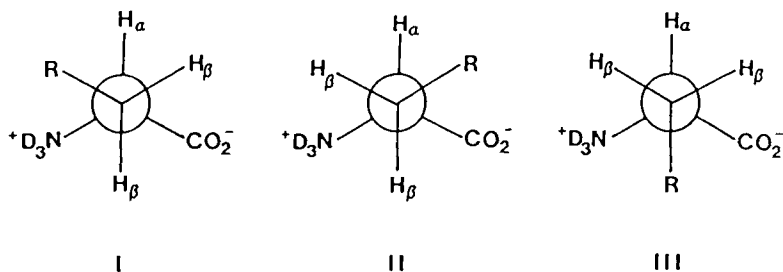


Figure 15. VCD and absorbance spectra in the CH stretching region of deuterated L-alanine ($\text{CH}_3\text{CHND}_3^+\text{CO}_2^-$) (—), 1.4 M, L-alanine \cdot NaOD ($\text{CH}_3\text{CHND}_2\text{CO}_2^-$) (---), 1.4 M, and L-alanine \cdot DCl ($\text{CH}_3\text{CHND}_3^+\text{COOD}$) (\cdots), 1.4 M (93):

stretch and the two C_αH bending modes that lie at lower frequency. The more intense secondary features arise from mixing among the C_αH and side-chain aliphatic CH stretching motions. If the side chain is itself not involved in hydrogen bonding, the additional spectral features can be adequately described by a perfect nuclear following contribution from the coupled vibrational motions. For example, the FPC model, which considers oscillating nuclear charges screened by electrons that follow the nuclear motion exactly, can be used to predict the VCD pattern. A normal coordinate analysis is necessary to obtain

the description of the normal modes, that is, the contributions, including relative phases, of the four CH oscillators in each mode. For the CHCH_3 moiety, a conservative $(+ - + -)$ pattern, from high to low frequency, is predicted for the two antisymmetric methyl stretches, the methine stretch, and the symmetric methyl stretch in alanine. The observed L-alanine- $N\text{-}d_3$ spectrum can then be interpreted as a superposition of this pattern and the positive methine C_αH contribution due to the ring current mechanism. In L-lactic acid, the same $(+ - + -)$ pattern is predicted, with the C_αH stretch now occurring as the lowest frequency mode. Again, the observed spectrum is consistent with a superposition of the two contributions, with the symmetric methyl stretch positive and the methine VCD intensity diminished somewhat as compared with alanine due in part to the negative perfect following contribution. Contributions to the methyl stretching VCD due to vibrational ring currents have also been proposed (57).

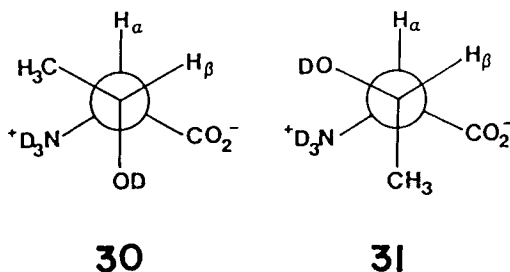
In the more complex amino acids, the rotameric distribution, **I**, **II**, and **III**, about the β carbon must be considered. Since in conformer **III** the $\text{C}_\alpha\text{HC}_\beta\text{H}_2$ fragment is achiral, little perfect following contribution is expected. In rotamers **I** and **II**, the $\text{C}_\alpha\text{HC}_\beta\text{H}_2$ fragments have opposite chirality, and give rise to perfect following patterns of opposite sign. From Table 2, conformer **I** is, in general, preferred over conformer **II**. For the antisymmetric methylene, methine, and symmetric methylene stretches in conformer **I**, FPC calculations predict a $(+ - +)$ VCD pattern. This pattern is in fact observed in L-cysteine.DCl, for which the proposed ring current is altered. Adding a positive ring current enhanced methine feature to the $(+ - +)$ FPC pattern gives rise to the L-cysteine and L-serine VCD spectra at neutral pH. The remaining amino acids with side chains of the form $-\text{CH}_2\text{R}$ with no γ hydrogens [L-asparagine, L-phenylalanine, L-histidine (90)] have VCD spectra similar to those of L-serine and L-cysteine, that is, a broad positive methine with positive features attributable to the methylene fundamentals. The amino acids with side-chain $-\text{CH}_2\text{CH}_2\text{R}$, L-methionine, L-glutamine, L-lysine.DCl, and L-arginine.DCl (in the latter two, the DCl is associated with the side-chain amino group) (90) also have positive VCD



with positive secondary features, indicative of trans methylene groups along the chain, or equal population of any gauche CH_2 chain conformations.

The VCD spectra (90) of amino acids with $-\text{CHRR}'$, $-\text{CR}_2\text{R}'$, $-\text{CH}_2\text{CHR}_2$, or proline side chains are more complex and more difficult to interpret completely. L-Threonine and L-allothreonine present an interesting case in which intramolecular hydrogen bonding involving the side chain is probable. The absorption spectra in the CH stretching region for L-threonine and L-allothreonine (Figure 11) are practically identical, whereas the VCD spectra are quite distinct. The NMR data indicate over 70% population of the rotamer for which ND_3^+ and the β proton are trans. In these conformations, **30** for threonine and **31** for allothreonine, intramolecular $\text{N}-\text{D} \cdots \text{O}-\text{C}_\beta$ hydrogen bonding is favorable in both molecules, in addition to the $\text{CO}_2^- \cdots \text{D}_3\text{N}^+$ ring. The L-threonine and L-allothreonine VCD spectra can be understood in terms of positive current around the $\text{C}_\alpha-\text{N}-\text{D} \cdots \text{O}-\text{C}_\beta$ ring in the direction $\text{O} \rightarrow \text{C}_\beta$, induced by contraction of the C_βH bond. Such an oscillating current will give rise to negative C_βH VCD in threonine and positive C_βH VCD in allothreonine [band 4 in Figure 11(a) and (b)] in addition to positive C_αH VCD in both molecules (band 3) from the $\text{C}_\alpha\text{CO}_2^- \cdots \text{DN}^+$ ring. The antisymmetric methyl stretching modes are responsible for the $(-+)$ or $(+-)$ features labeled 1 and 2 in Figure 11. The β carbon in threonine has the opposite chirality to L-lactic acid, replacing the carboxyl in lactic acid with $-\text{CHCO}_2\text{ND}_3^+$ in the threonines. The $-\text{C}_\beta\text{HCH}_3$ VCD in threonine is of opposite sign and opposite bias to that in lactic acid (Figure 9), whereas in L-allothreonine, the β carbon has a configuration corresponding to L-lactic acid and the $\text{C}_\beta\text{HCH}_3$ VCDs in these two compounds have the same sense. Although in the threonines separate amino hydrogens are involved in the two rings, in the most prevalent rotamer(III) of serine, the carboxylate and hydroxyl group can interact with the same $\text{N}-\text{H}$, which may explain the small C_αH VCD and small VCD bias in serine.

Studies of amino acid VCD outside the CH-stretching region has been limited. For L-alanine, the VCD in the $1600\text{--}1200\text{-cm}^{-1}$ region is characterized by a bisignate couplet at $1337\text{ cm}^{-1}(-)$ and $1291\text{ cm}^{-1}(+)$ corresponding to the two perpendicular methine bending modes (92, 93).



2. Simple Peptides

The CH stretching VCD of simple alanyl peptides has also been investigated. The VCD spectra L-alanyl-L-alanine- $N-d_3$ and L-alanyl-L-alanyl-L-alanine- $N-d_3$ (83) are similar to that of alanine, with a large broad positive methine contribution. In the di- and tripeptides, the VCD maximum shifts to 2950 cm^{-1} , with a shoulder at 2970 cm^{-1} . A negative feature corresponding to the antisymmetric methyl stretch occurs at 3000 cm^{-1} .

The VCD spectra of glycyl-L-alanine and L-alanylglycine (83, 93) (Figure 16) are in striking contrast to one another. The strong positive methine VCD

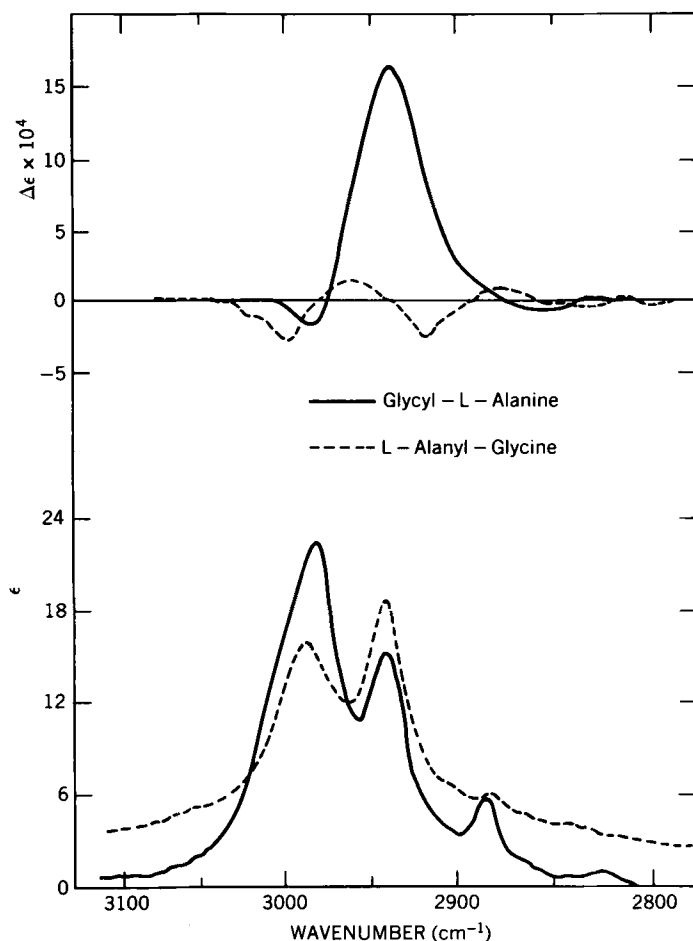
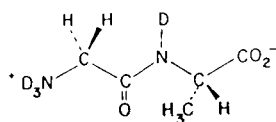
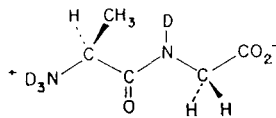


Figure 16. VCD and absorbance spectra in D_2O of glycyl-L-alanine (—) 1.7 M, and L-alanylglycine (---) 1.7 M (93).



32



33

and bias is still observed in glycyl-L-alanine, **32**, but in L-alanylglycine, **33**, the VCD is weak and nearly conservative. It is of interest to compare the spectra of these two peptides with those of L-alanine at high and low pD, in Figure 15.

In both glycyl-L-alanine and the sodium salt of alanine (high pD), the methine stretch shifts to lower frequency, ~ 2925 and 2900 cm^{-1} , respectively, with the positive bias maintained. Similarly, in both L-alanylglycine and L-alanine $\cdot \text{DCI}$ (low pD) the weak VCD patterns are similar and the bias nearly eliminated. Apparently the proposed ring current mechanism is still operative at the C-terminal residue at high pD where the carboxylate maintains a negative charge, but at low pD and at the N-terminal position, where a protonated carboxylate or the similar peptide linkage are present, the vibrationally induced ring current is absent. Possible explanations for this include increased hydrogen bonding to the solvent at the expense of intramolecular hydrogen bonding or an alteration in the nature of the $\text{N}-\text{H} \cdots \text{O}-\text{C}$ hydrogen bond and of the coupling of methine motion with ring current due to the alterations in electronic structure.

3. Polypeptides

Vibrational circular dichroism in polypeptides has been measured both in the near-infrared region for hydrogen stretching fundamentals and in the mid-infrared region associated with hydrogen bending and carbonyl stretching vibrations. The first such VCD measurements were carried out by Singh and Keiderling (94) for α -helical poly(γ -benzyl-L-glutamate) in chloroform solution. They observed sigmoidal couplets in the amide A band (NH stretch) and the amide I band (CO stretch), and monosignate contributions in the CH stretching region (positive) and the amide II region (negative). The couplets have the opposite sense for the amide A (+, -) and the amide I (-, +) regions. The results for the amide I region were found to agree with theoretical calculations carried out earlier by Schellman (95) and Snir et al. (96). In a subsequent experimental study, Lal and Nafie (97) reported the VCD in the amide A and amide I regions for a variety of α -helical polypeptides. It was found that the sense of the VCD couplets in these two regions is diagnostic of the sense of the α -helical conformation and not of the absolute configuration of the constituent amino acid residues. This conclusion was deduced from the opposite nature of the VCD couplets for polypeptides formed from L-amino acids that adopt the

usual right-handed α -helical conformation compared with those that form left-handed α -helices.

In more recent work, Sen and Keiderling (98) have investigated the amide II region with the same set of polypeptides as employed by Lal and Nafie. The sign of the amide II band is opposite for left- and right-handed α -helices having L-amino acid constituents. In addition, the amide II VCD peak appears at higher frequencies for the left-handed α -helices, thus showing a structural sensitivity for left- versus right-handed helices. VCD spectra of deuterated polypeptides were also measured that showed a new negative, low-frequency VCD band in the amide I region for a right-handed α helix. The new, triad VCD pattern from higher to lower frequency in this case was $(-, +, -)$.

Recent work in our laboratory has involved a remeasurement of the amide I region of poly(γ -benzyl-L-glutamate) in CHCl_3 solution using an FTIR spectrometer (99). FTIR-VCD measurements can be performed at higher resolution while retaining signal quality. The result of this remeasurement is given in Figure 17 where the resolution was 4 cm^{-1} (compared to $\sim 10\text{ cm}^{-1}$ for the earlier dispersive VCD measurements). The absorption features at 1735, 1650, and $1550\text{ (}1520\text{)}\text{ cm}^{-1}$ correspond to the glutamate carbonyl stretch band, the amide I band, and the amide II perpendicular (parallel) band, respectively. No VCD is present in the glutamate stretch; two small negative VCD features are seen in the amide II region; and three VCD features $(- + -)$ appear under higher resolution in the amide I band.

While the presence of three VCD band components was not predicted earlier (95, 96), the amide I band for an infinite helix in IR absorption (and VCD) is composed of three components: A mode polarized parallel to the helix axis and two degenerate modes polarized perpendicular to that axis. Observation of three VCD bands means that the degeneracy in the perpendicular bands has been lifted. In fact, we have been able to show (99) using a resolution enhancement technique called Fourier self-deconvolution (100) that the new low-frequency negative band is actually the polarized component and that the two large VCD features originate from the split perpendicular bands rather than from the splitting of the parallel and perpendicular modes as was originally predicted by theory (95, 96). The stereochemical consequences of observing such a large VCD effect have to do with the conformational behavior of the α helix in solution compared to that of a perfect, infinite helix. There is now agreement between the VCD sign patterns of the deuterated and nondeuterated amide I vibrations. In the deuterated amide, the polarized VCD component moves to lower frequency and becomes observable at $\sim 10\text{ cm}^{-1}$ resolution (98).

4. Urethane Amino Acid Derivatives

Another class of molecules has been found recently to exhibit strong VCD in the carbonyl stretching region. In Figure 18 we present such spectra for two

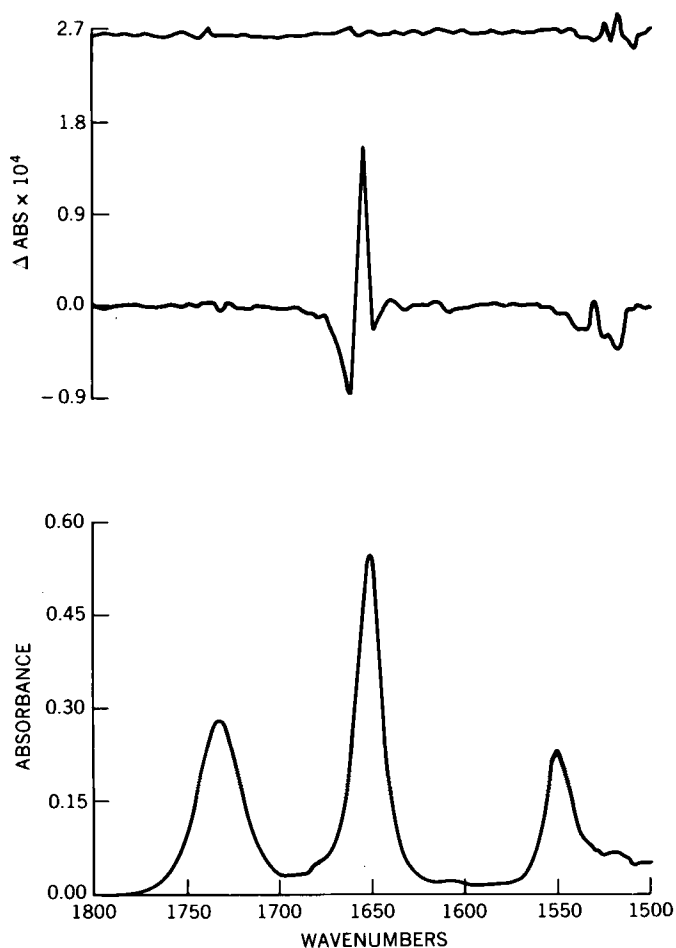


Figure 17. FTIR absorbance (lower), VCD (middle) and VCD noise estimate (upper) for the 1800–1500- cm^{-1} region of poly- γ -benzyl-L-glutamate, 2 mg/ml in CHCl_3 , path length 0.5 mm, resolution 4 cm^{-1} . (Reproduced by permission of Wiley, from ref. 99.)

alanyl urethane molecules, *N*-CBZ-L-alanine and *N*-*t*-Boc-L-alanine as solutions in CDCl_3 (101). From other studies it has been proposed that these molecules predominantly adopt an intramolecularly hydrogen-bonded conformation designated C_7 , as shown in **34a**, where the angles ϕ and ψ (the Ramachandran angles for peptides) are -80° and $+80^\circ$, respectively. The observed $\text{C}=\text{O}$ stretching VCD spectra are bisignate (+, -) couplets.

The absorption spectra in the carbonyl stretching region of the urethane derivatives have been assigned to the free acid $\text{C}=\text{O}$ stretch and strongly hydrogen

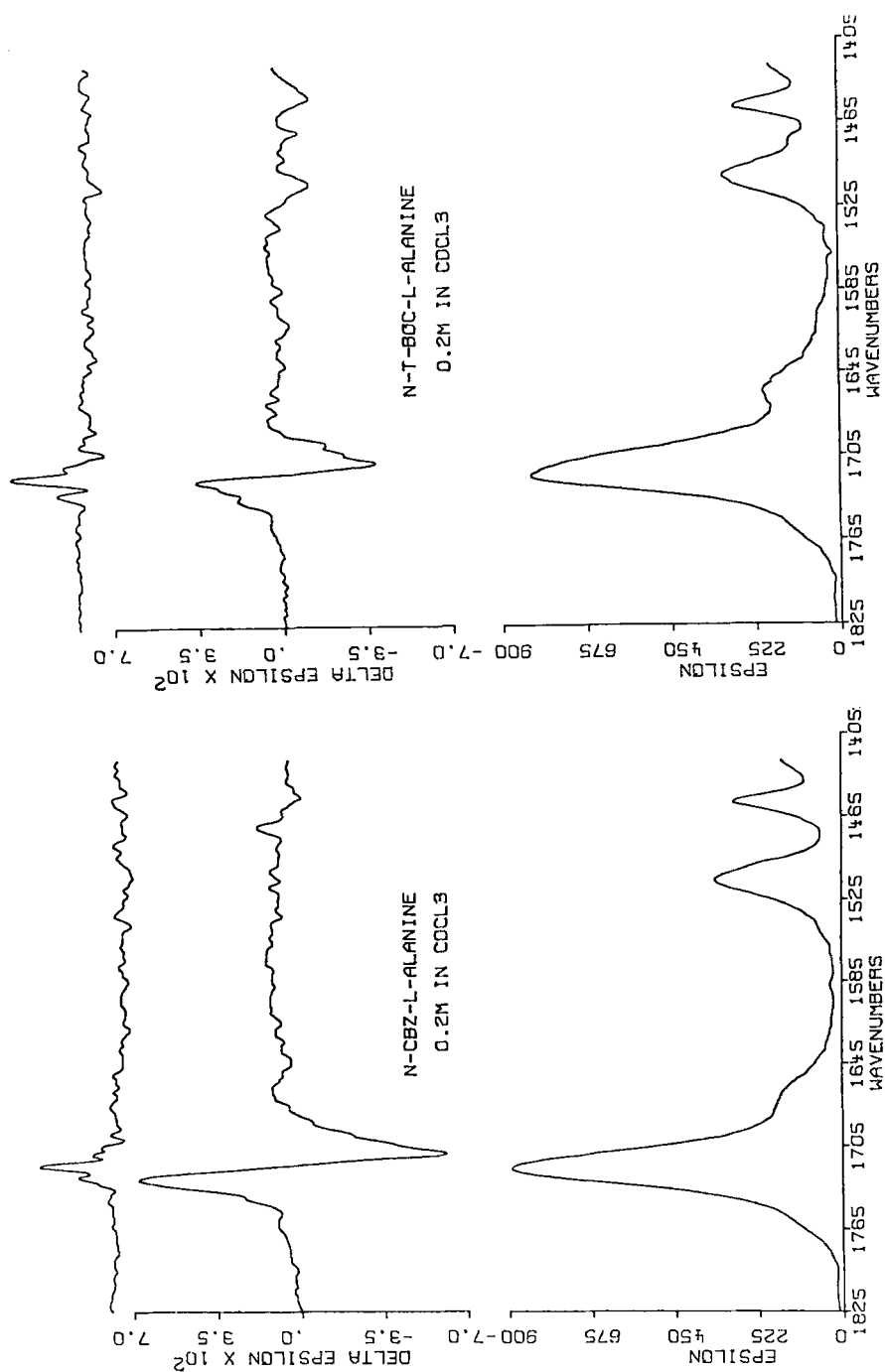
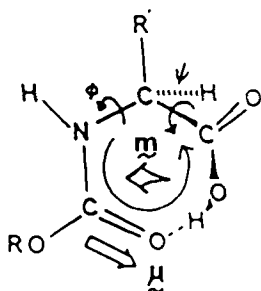
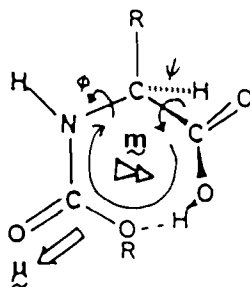


Figure 18. FTIR absorbance (lower), VCD (middle), and VCD noise level (upper) for the 1800–1400- cm^{-1} region of (a) N-Cbz-L-alanine, 0.2 M in CDCl_3 , and (b) N-T-BOC-L-alanine, 0.2 M in CDCl_3 (101).



34a



34b

bonded urethane C=O stretch giving rise to the high and low frequency shoulders, respectively, that do not exhibit appreciable VCD, and to an intermolecularly hydrogen-bonded acid C=O stretch of the dimer ($\sim 1725\text{ cm}^{-1}$) and the free and intramolecularly hydrogen-bonded urethane C=O stretches ($\sim 1715\text{ cm}^{-1}$), which give rise to the main absorption band and to the VCD couplet. These nearly degenerate carbonyl and urethane modes can couple to one another.

Intensity calculations based on the coupled oscillator model, eqs. [21] and [22] (Sect. III-B) and the dipolar interaction potential, eqs. [32] and [33] (Sect. IV-A-1), have been applied to several possible intramolecularly hydrogen-bonded forms of *N*-*t*-BOC-L-alanine in both the trans (**34a**) and cis (**34b**) conformations, including (ϕ, ψ) angles that permit hydrogen bonding to the nitrogen, to the urethane carbon π orbital, to the urethane oxygen lone pair, **34a**, or to the alkyl oxygen lone pair, **34b**. Only for the cis conformation, **34b**, do the calculations predict a VCD couplet with the same sense as observed experimentally (negative lobe to lower frequency).

As the concentration in CDCl_3 is reduced, or when the solvent is changed to DMSO, the positive lobe of the VCD couplet decreases relative to the negative lobe, and the VCD spectra in the C=O stretching region become distinctly negatively biased. Similar effects are observed for the corresponding proline derivatives. Upon dilution, the absorption intensity at $\sim 1725\text{ cm}^{-1}$, due to intermolecularly hydrogen-bonded acid C=O stretch, decreases, whereas the relative intensity of the free acid C=O stretch at 1760 cm^{-1} increases. This shift in C=O (acid) frequency greatly reduces the interaction between the urethane and acid carbonyl groups, decreasing the intensity of the VCD couplet.

The negative VCD observed in dilute solution at the urethane C=O stretching frequency, and the negative bias observed at higher concentrations is due to an intrinsic contribution from the urethane carbonyl stretch. In either the cis or trans conformation, the urethane C=O stretch can generate current around an

intramolecularly hydrogen-bonded ring. Negative ring current enhanced VCD is predicted for the sense of current shown in **34a** or **34b** (92, 101).

E. Transition Metal Complexes

A number of measurements of VCD in transition metal complexes have been carried out in our laboratory at Syracuse. The principal motivation for these studies has been to investigate the effect of transition metal complexation on the VCD of ligand molecules, to determine the degree to which vibrational coupling between ligands occurs, and to look for additional examples of electronic charge flow as a mechanism for VCD intensity enhancement. In some respects our studies are the vibrational analogs of the classical studies of electronic optical activity in these molecules (102) that have proven invaluable in elucidating the sensitivity of optical activity to the configuration and conformations of molecules.

1. *Bis Cu(II) Amino Acid Complexes*

One of our primary interests in the study of the amino acids is the measurement of the VCD in their bidentate transition metal complexes. A number of *bis* Cu(II) amino acid complexes have been investigated in the CH stretching region as solutions in D₂O (90). As mentioned earlier and listed in Table 2, these VCD spectra exhibit increased positive bias compared to those of the corresponding free amino acids. We have also measured the VCD spectra of some *bis* Cu(II) amino acid complexes as solutions in DMSO-*d*₆ (103). Using this solvent, it is possible to measure spectra in both the CH and NH stretching regions, whereas in D₂O the deuterium exchanged ND stretching modes are obscured by solvent bands. In Figure 19 we present the spectra of the *bis* Cu(II) complexes of threonine and proline in DMSO-*d*₆. The absorption and VCD spectra in the CH stretching region closely match the corresponding spectra obtained in D₂O. The strong positive VCD bias associated with the methine C_αH stretching mode is clearly evident in these spectra. The VCD spectra in the NH stretching region are strikingly different in these two complexes. The difference stems from the fact that an additional chiral center is present in the proline complex at the nitrogen atom that has the stereochemistry as shown in Figure 19. Because the NH VCD is not conservative, that is, its bias is strongly negative, one can argue that VCD stems largely from electronic currents induced by the NH stretching motion. Coupling with the CH modes can be effectively ruled out due to the similarity of the VCD in the CH stretching region in DMSO-*d*₆ compared to the spectra in D₂O in which the amine is deuterated and coupling between CH and amino modes is removed.

An explanation of the NH stretching VCD in this complex can be formulated in analogy to the ring current mechanism for VCD bias in the C_αH stretching

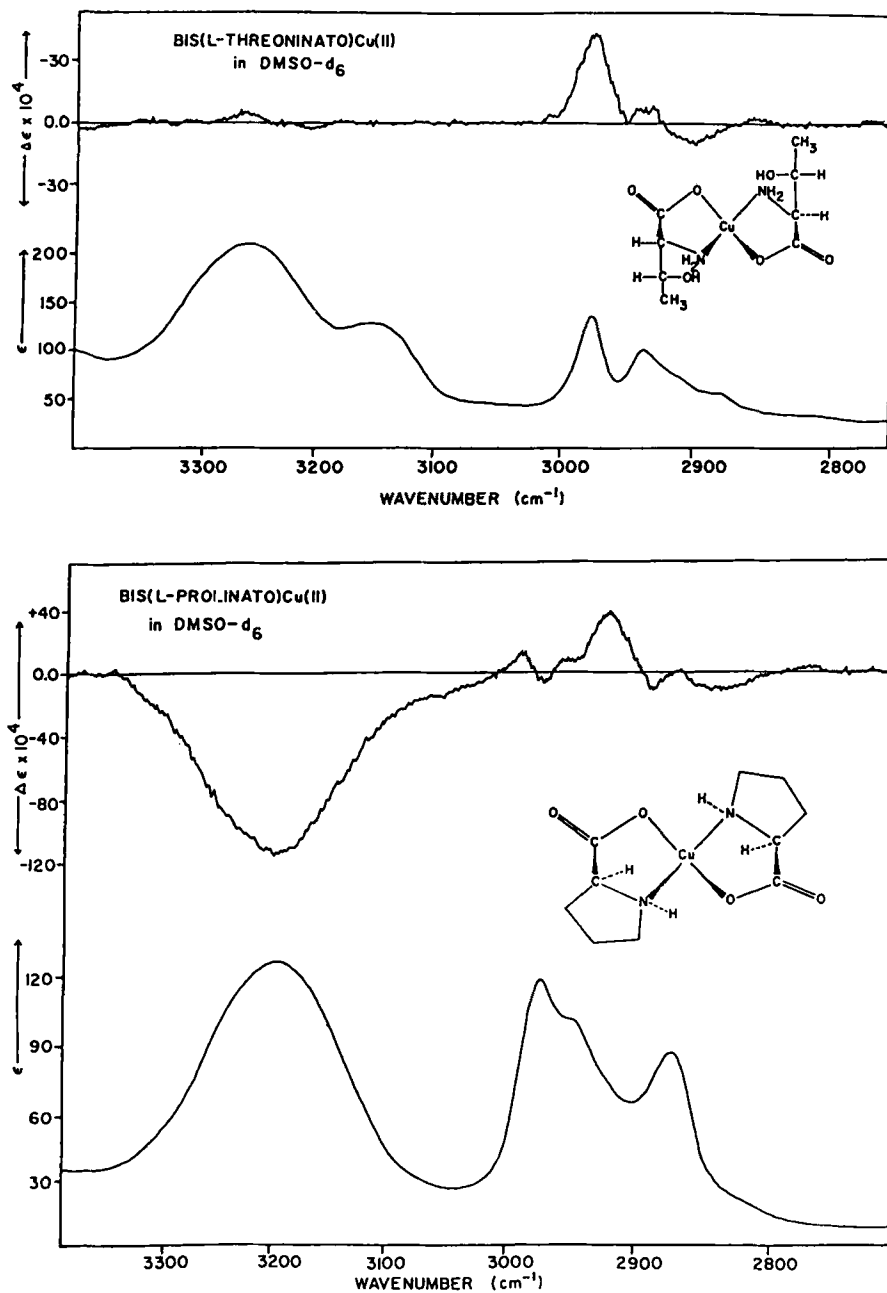
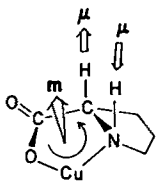


Figure 19. VCD and absorption spectra in the CH and NH stretching regions of (a) *bis*(L-threoninato)Cu(II) in DMSO- d_6 and (b) *bis*(L-prolinato)Cu(II), in DMSO- d_6 (103).

**35**

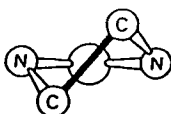
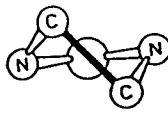
mode of these molecules. In the diagram for structure **35** we show the direction of the dipole moments for the contraction of the $C_\alpha H$ and NH bonds in this complex as well as the sense of positive current flow and the direction of the magnetic dipole moment due to ring current generated by the $C_\alpha H$ contraction, cf., diagram **29**. If the contraction of the NH bond generates a current in the ring containing $Cu(II)$ that is in the same sense as for the $C_\alpha H$ bond contraction then a *negative* VCD bias will be observed since the direction of μ is opposite for NH compared to $C_\alpha H$ for the same sense of vibrational displacement (contraction or elongation).

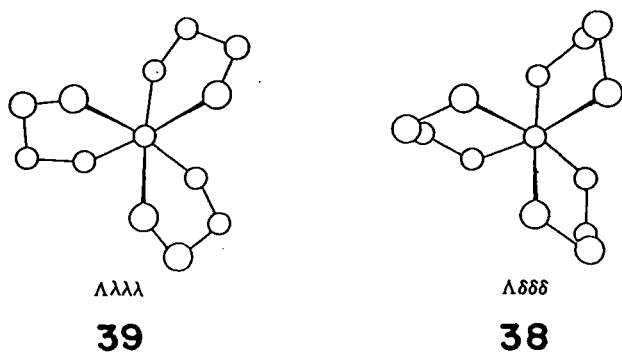
2. *Tris(ethylenediamine) Co(III) Complexes*

An investigation of the NH stretching VCD in $Co(III)$ *tris*(ethylenediamine) complexes, $Co(en)_3^{3+}$, has shown interesting conformational effects that can be attributed to hydrogen bonding to halide ions (104).

In a metal complex (102), five-membered chelate rings formed by 1,2-diamines exist in two puckered conformations, the enantiomeric λ and δ forms **36** and **37**. For an achiral ligand in a bis or tris complex, steric interactions between rings are present, and the two conformations are no longer equivalent energetically.

For a *tris*(ethylenediamine) complex, in the Λ configurations (left-handed propeller), the $\Lambda(\delta\delta\delta)$ *lel*-configuration **38** is most favored, and the $\Lambda(\lambda\lambda\lambda)$ *ob*-configuration **39**, the least favored energetically. However, the intermediate $\lambda\delta\delta$ and $\delta\lambda\lambda$ forms are statistically favored over the extreme forms. Recent

 λ **36** δ **37**



studies indicate that $\Lambda(\delta\delta\lambda)$ is the most stable in the absence of hydrogen bonding (105).

The VCD in the NH stretching ($3300\text{--}3000\text{ cm}^{-1}$) and CH-stretching ($3000\text{--}2850\text{ cm}^{-1}$) regions of $(+)\text{-Co(en)}_3^{3+}$ in $\text{DMSO-}d_6$ are shown in Figure 20 for the chloride, bromide, and iodide salts. In the iodide absorption spectrum, fea-

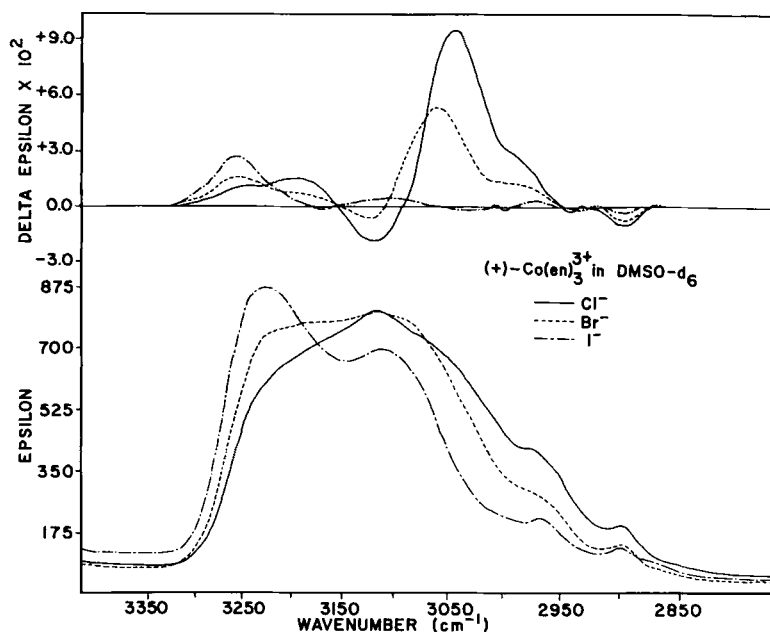


Figure 20. VCD and absorbance spectra in the NH and CH stretching regions of *tris*(ethylenediamine)cobalt(III) in $\text{DMSO-}d_6$, as chloride salt (—), 0.061 M; bromide salt (---), 0.063 M; iodide salt (- · - · -), 0.067 M. Path length is 100 μM . (Reproduced with permission from ref. 104. Copyright 1986 American Chemical Society.)

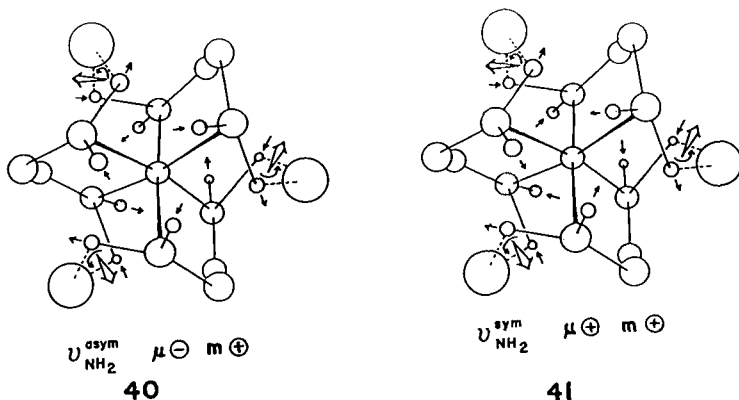
tures corresponding to the antisymmetric NH_2 (3225 cm^{-1}), symmetric NH_2 (3112 cm^{-1}), antisymmetric CH_2 (2965 cm^{-1}), and symmetric CH_2 (2900 cm^{-1}) stretching modes are observed, which correspond to weak VCD features. In the chloride and bromide salts, the NH absorption spectra broaden, with a loss of resolution and a general shift to lower frequency. A concurrent increase in VCD intensity and shift in frequency are noted. The bromide and chloride spectra are indicative of interaction with the anion and a mixture of $\text{NH} \cdots \text{Cl}^-$ or $\text{NH} \cdots \text{Br}$ hydrogen bonded and free species, as well as a mixture of ring conformations.

In Figure 21 two extreme cases are presented, Co(en)_3^{3+} in the presence of I^- or a large excess of Cl^- . With the large iodide anion, hydrogen-bonding interactions are weak and the spectra represent the "free" cation. The low intensity of the NH stretching VCD for the iodide salt indicates only a small excess of one (probably λ) of the enantiomeric ring conformations over the other.

With an excess of the smaller chloride ion, hydrogen-bonding interactions are maximized. The absorption spectra are sharper, and four features corresponding to the NH_2 and CH_2 modes are again resolved (3125 , 3041 , 2965 , 2890 cm^{-1}) indicative of a species with all NH_2 groups hydrogen bonded in an equivalent manner. The changes in the VCD spectrum are even more dramatic. A large increase in intensity is noted in both the antisymmetric NH_2 stretching region (negative) and the symmetric stretching region (positive).

Chloride ions have been determined by other studies to occupy the bridging sites between neighboring ligands shown in **40** and **41** in DMSO solution (106). This type of hydrogen bonding has been postulated to stabilize the $\Lambda(\delta\delta\delta)$ configuration in the Cl^- and Br^- crystals, but is absent in the I^- crystal (105).

The $\Lambda(\delta\delta\delta)$ complex has D_3 symmetry. Each ring (C_2 symmetry) contributes two antisymmetric NH_2 stretching modes, of A and B local (ring) symmetry, and two symmetric NH_2 stretching modes, of A and B symmetry. In the com-



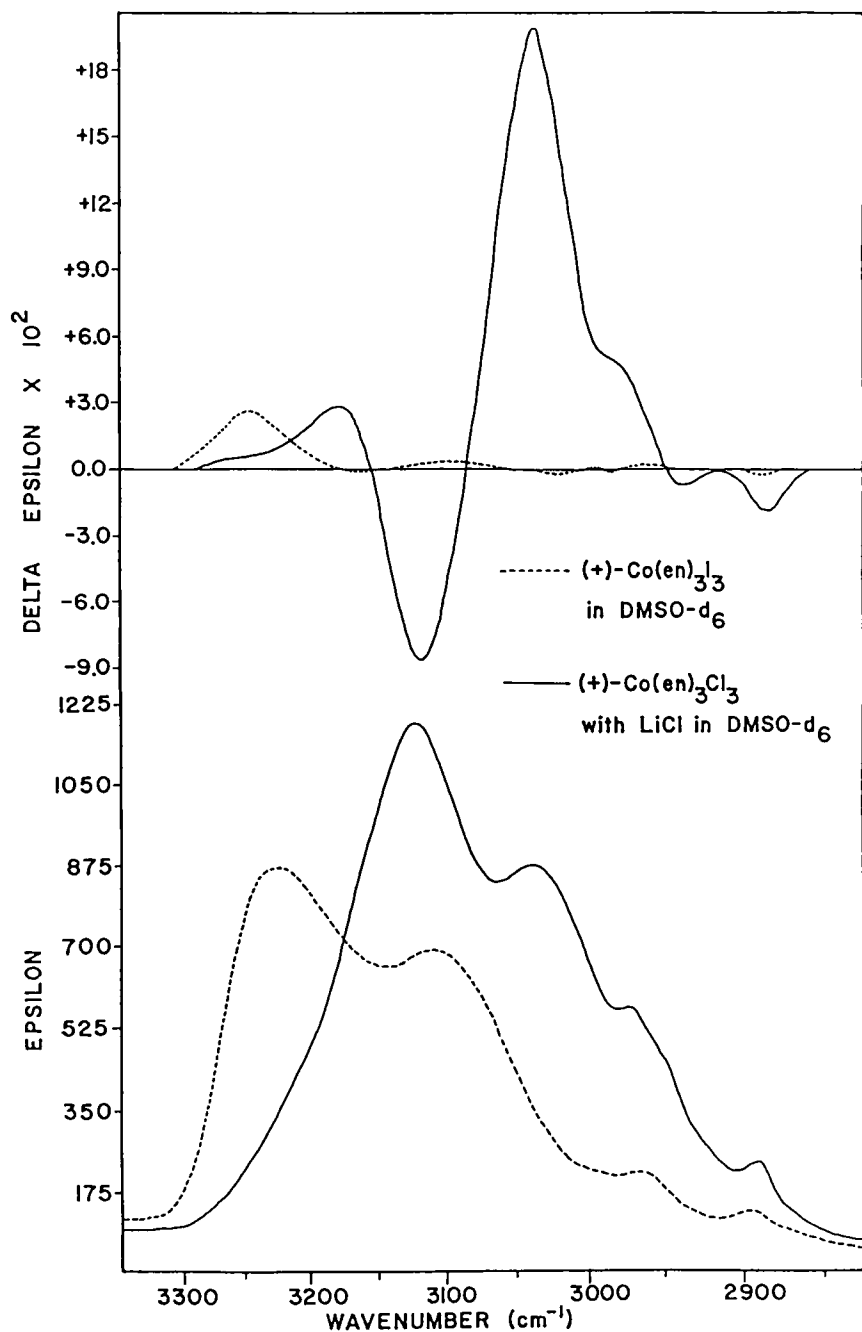


Figure 21. VCD and absorbance spectra in the NH and CH stretching regions of *tris*(ethylenediamine)cobalt(III) in DMSO-d_6 as the iodide salt (---), 0.067 *M*, and as the chloride salt (—), 0.06 *M* with 0.6 *M* LiCl. Path length is 100 μm . (Reproduced with permission from ref. 104. Copyright 1986 American Chemical Society.)

plex, the three corresponding A or B ring modes are phased to give vibrations of A_1 or A_2 and E symmetry. Contributions to the VCD spectrum of the complex due to exciton coupling among the local NH_2 oscillators on different rings are predicted to generate bisignate couplets in each region. Since the observed spectra are strongly biased in both the symmetric and antisymmetric stretching region, the exciton contributions are either weak or largely cancel due to a very small energy difference between the two components of the couplets. A mechanism involving vibrationally induced currents through the bridging chloride can explain the large monosignate VCD features in the symmetric and antisymmetric NH stretching regions. For example, the two A_2 vibrations of the complex generated by the B ring modes are shown in **40** (antisymmetric NH_2 stretch), and **41** (symmetric NH_2 stretch). In both cases, the motions of the hydrogen-bonded NH groups induce an $N-H \cdots Cl \cdots H-N$ current as shown, since elongation of one NH bond strengthens the $H \cdots Cl$ hydrogen bond and leads to flow of electrons from the Cl^- into the hydrogen-bonded region, while the contracting $N-H$ weakens the second $H \cdots Cl$ bond. The net magnetic dipole transition moment for the three $H \cdots Cl \cdots H$ bridges is positive, out of the page in both **40** and **41**. The electric dipole transition moment is directed into the page in **40**, producing negative VCD, and out of the page in **41** giving positive VCD, in agreement with the observed spectra.

The $Co(en)_3^{3+}$ VCD spectra also exhibit interesting anion dependency in the CH stretching and mid-infrared $1600-1100\text{-cm}^{-1}$ regions. Corresponding features are also observed for the chromium complex.

3. *Co(III) Alanine Complexes*

L-Alanine forms four diastereomeric *tris*-L-alaninato cobalt(III) complexes, in which the ligands are arranged as either a left-handed, Λ , or right-handed, Δ , propeller with the three nitrogens occupying either facial or meridional octahedral coordination sites. The absorption and VCD spectra in the $3400-2800\text{ cm}^{-1}$ have been recorded in our laboratory for all four isomers in D_2O/D_2SO_4 (55, 90) and D_2O/DCl solution (107). Proton exchange on the nitrogens is minimized at low pH, allowing the NH stretching modes to be observed.

The absorption spectra of the two meridional or two facial complexes are quite similar. The VCD spectra of corresponding Λ and Δ configurations are not exact mirror images, since L-alanine is a chiral ligand. As an example, the VCD of the facial (Λ)- β -*tris*[L-alaninato]Co(III) and (Δ)- β' -*tris*[L-alaninato]-Co(III) complexes in D_2O/D_2SO_4 are shown in Figure 22. The configurational effect due to the opposite handedness of the propellers is reflected in the approximate $\Lambda(-+)$ and $\Delta(+ -)$ patterns for the antisymmetric and symmetric NH_2 stretching regions (~ 3250 and 3100 cm^{-1}). The deviation of the two VCD spectra from exact mirror symmetry is termed the "vicinal" effect, which arises

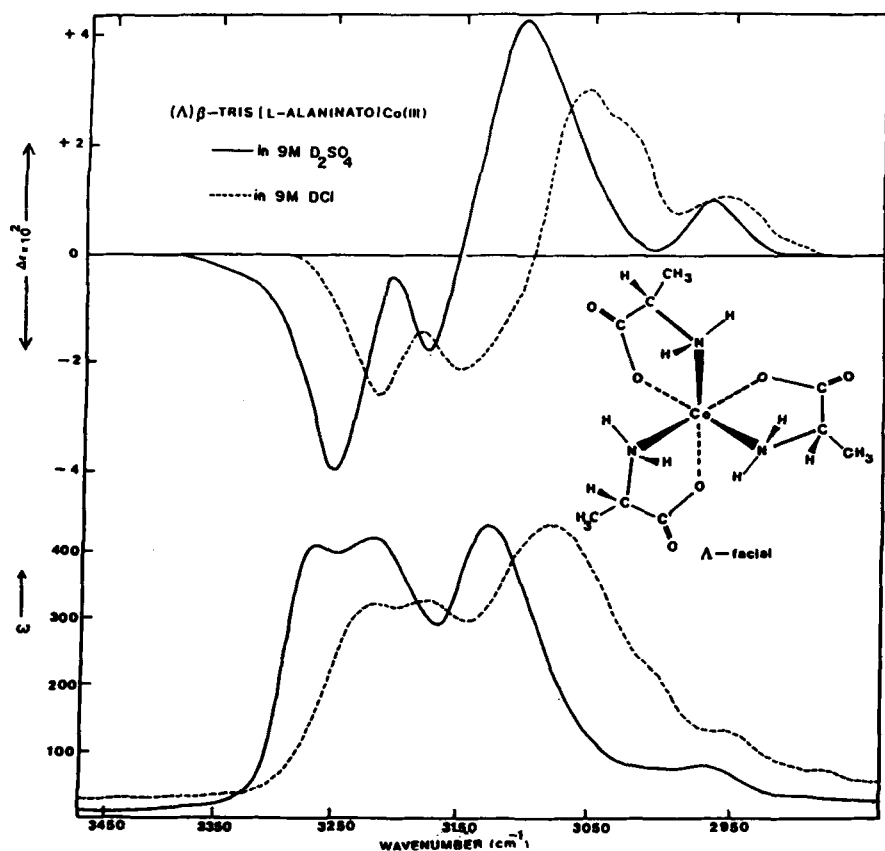


Figure 22. VCD and absorbance spectra in 9 M D_2SO_4 (—) and 6 M DCl (---) in the NH stretching region of (a) $(\Delta)\beta$ -tris(L-alaninato)Co(III), 0.17 M, 50- μM path length and (b) $(\Delta)\beta'$ -tris(L-alaninato)Co(III), 0.39 M, 50- μM path length (90, 107).

from the presence of an asymmetric center on each ligand. For example, the methyl group is axial in the Δ configuration and equatorial in the Λ configuration.

In D_2O/DCl solution, hydrogen bonding between $N-H \cdots Cl^-$ is possible, and both the absorption and VCD spectra shift to lower frequency, with some alteration in relative magnitudes.

The spectra of these alanine complexes have not been analyzed in detail. The large configurational effect in the facial complexes may be indicative of coupling among the NH vibrations on different ligands, which can occur both through radiative coupling of the strong NH dipoles or through potential or kinetic energy coupling mediated by the Co—N bonds. Alternatively, hydrogen bonding be-

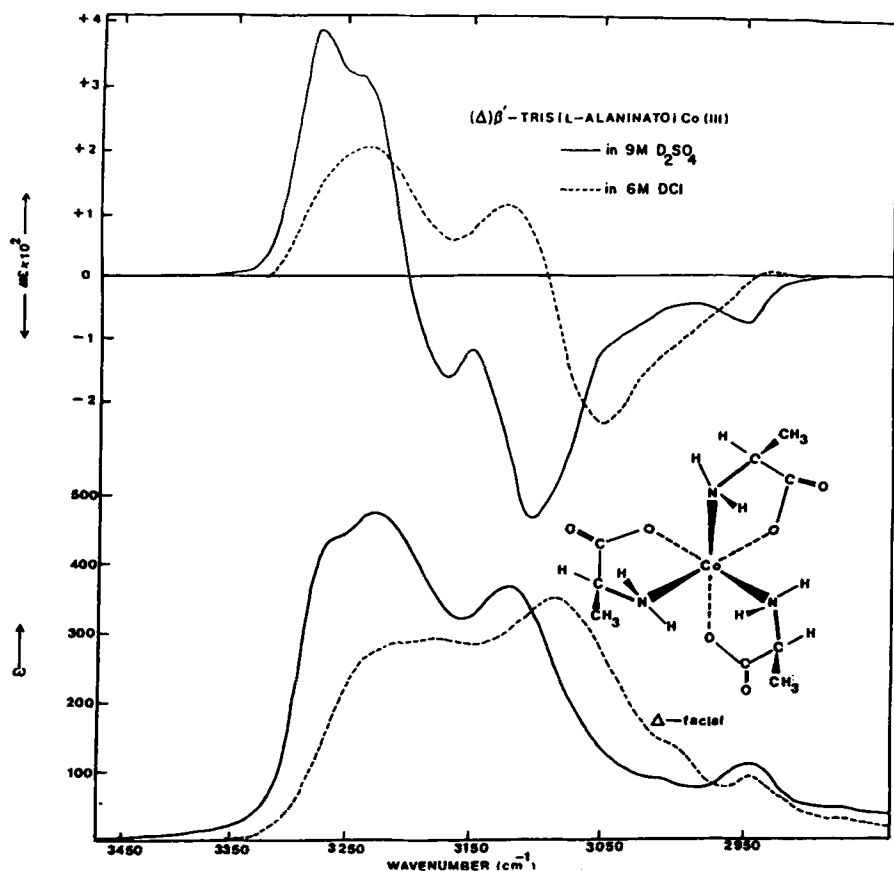


Figure 22. (Continued)

tween different ligands may provide pathways for vibrationally generated ring currents.

In an effort to isolate the contribution to the VCD spectrum of one alaninato ligand in a Co(III) complex, we synthesized and resolved (108) the two complexes, Δ - and Λ -[(L-alaninato)bis(acetylacetonato)]Co(III). The structures of these isomers would be enantiomeric except for the presence of the L-alaninato ligand in both complexes. The hydrogen stretching (NH and CH) absorption and VCD spectra of these two complexes as DMSO-*d*₆ solutions are presented in Figure 23. In the CH stretching region, the VCD spectra are virtually the same, consisting primarily of the positively biased VCD contribution of the lone C_αH stretch in alanine, a common component of the two complexes. The NH stretching region consists of two absorption bands, the antisymmetric alaninato NH₂ stretching mode at $\sim 3230\text{ cm}^{-1}$ and the corresponding symmetric NH₂

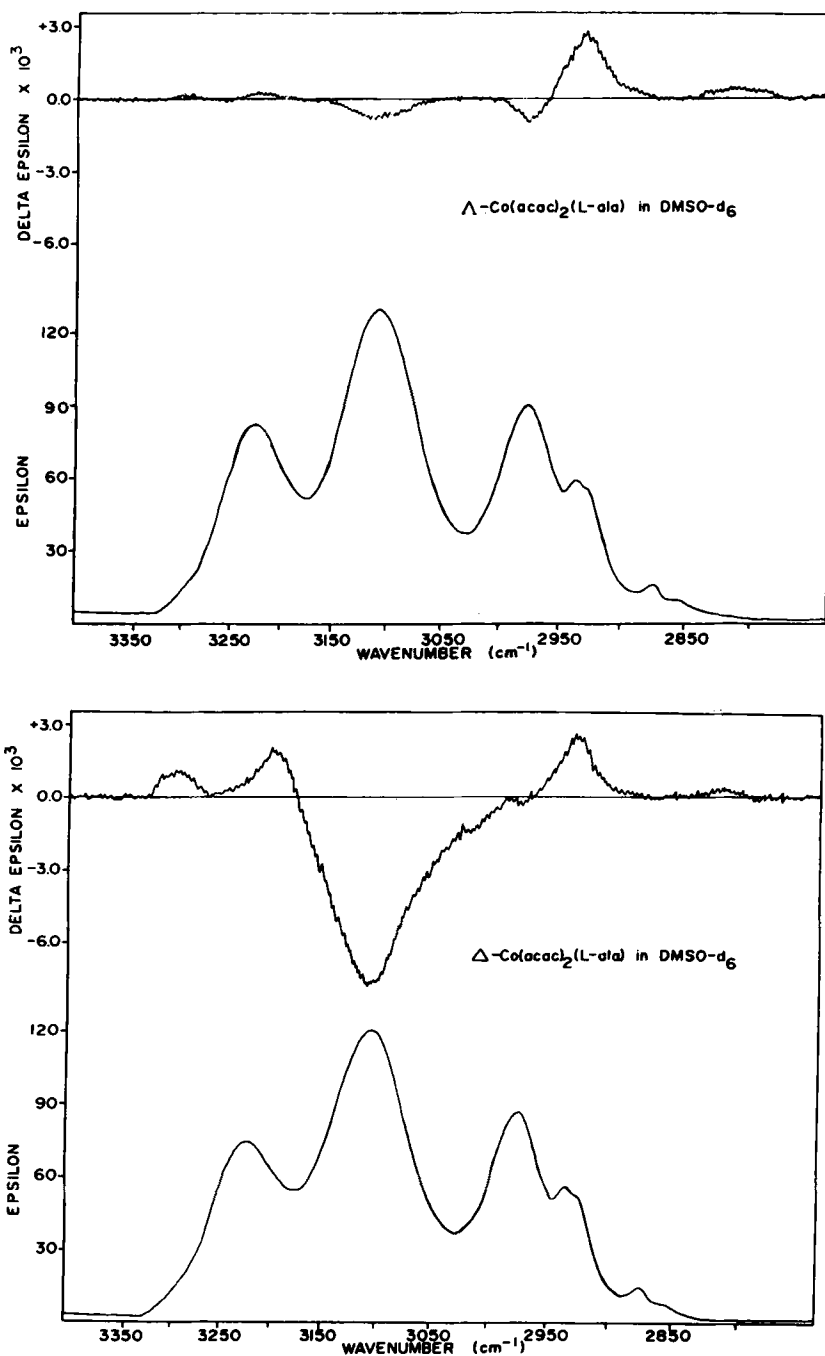
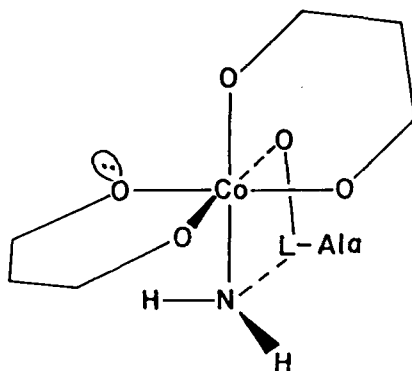
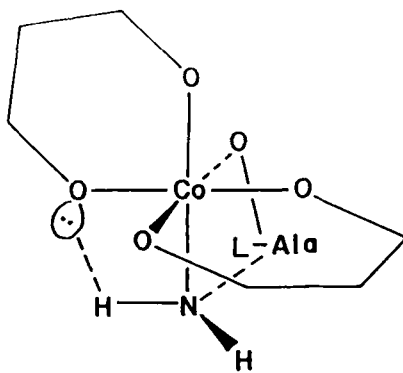


Figure 23. VCD and absorbance spectra in the CH and NH stretching regions of DMSO-*d*₆ solutions of (a) Λ -(L-alaninato)bis(acetylacetonato)Co(III) and (b) Δ -(L-alaninato)bis(acetylacetonato)Co(III) (Reproduced with permission from ref. 108. Copyright 1985 American Chemical Society.)

band at $\sim 3100\text{ cm}^{-1}$. The VCD spectra in this region have the same relative shape (+, +, -) for the two complexes; however, the VCD of the Δ complex is stronger by nearly an order of magnitude. Apparently additional VCD intensity is being generated due to a mechanism that does not alter the VCD pattern. In addition, the differing configurational environment for L-alaninato in the two complexes is not a factor.

The spectra in this figure represent one of the strongest cases for the ring current mechanism of VCD intensity enhancement. In this case, currents increase the magnetic dipole transition moment without altering the relative arrangement of electric dipole transition moments and the relative intensity pattern is preserved. In the structures **42** and **43**, we show that in the Δ complex, **42**,

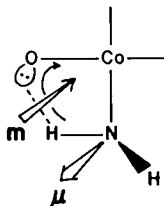


an intramolecular hydrogen bond can form between one of the alanine amine hydrogens and an oxygen (lone pair) on one of the acac (acetylacetonate) ligands. The relevant NH bonds on alanine and oxygen lone pairs on the acac ligands are shown. It is known from X-ray crystal studies (109) that the L-alaninato ligand puckers in a manner that leads one NH bond to lie in the plane of the upper acac ring in both complexes and the other NH bond to point away from this plane. The in-plane NH bond closely approaches the oxygen lone pair in the Δ complex but not in the Λ complex since the sp^2 lone pair does not point toward the NH hydrogen in the latter. The out-of-plane NH hydrogen has no close approach to an oxygen lone pair. In the symmetric NH_2 stretch of the Δ complex, one can have the electric and magnetic moments in **44** for the NH elongations and positive current flow, which explains the large negative VCD at $\sim 3100\text{ cm}^{-1}$. The sense of current in **44** is determined by the flow of electron density from oxygen to the amine hydrogen as it approaches, thus strengthening the hydrogen bond as the $O \cdots H$ bond distance decreases.

As a final point for this complex we show in Figure 24 the mid-infrared VCD for both of these complexes. Here we can see coupled acac modes arising from the coupled oscillator mechanism at ~ 1520 and 1390 cm^{-1} , the in-plane anti-symmetric C—C and symmetric C—O stretching modes, respectively. The opposite nature of these VCD couplets reflects the mirror image relationship of the two acac ligands in these two complexes. Below 1390-cm^{-1} alanine CH bending modes begin to contribute eliminating the mirror symmetry between the two spectra.

F. Carbohydrates

Three published papers (110–112) and the chapter of a Ph.D. thesis (46) have reported VCD results in carbohydrates. The significance of these studies derives from the important biological roles that carbohydrates play in living systems. All three contributions are concerned with either sugars or their derivatives. From a structural point of view these molecules are quite interesting due to the presence of several adjacent stereogenic centers and the availability of different



44

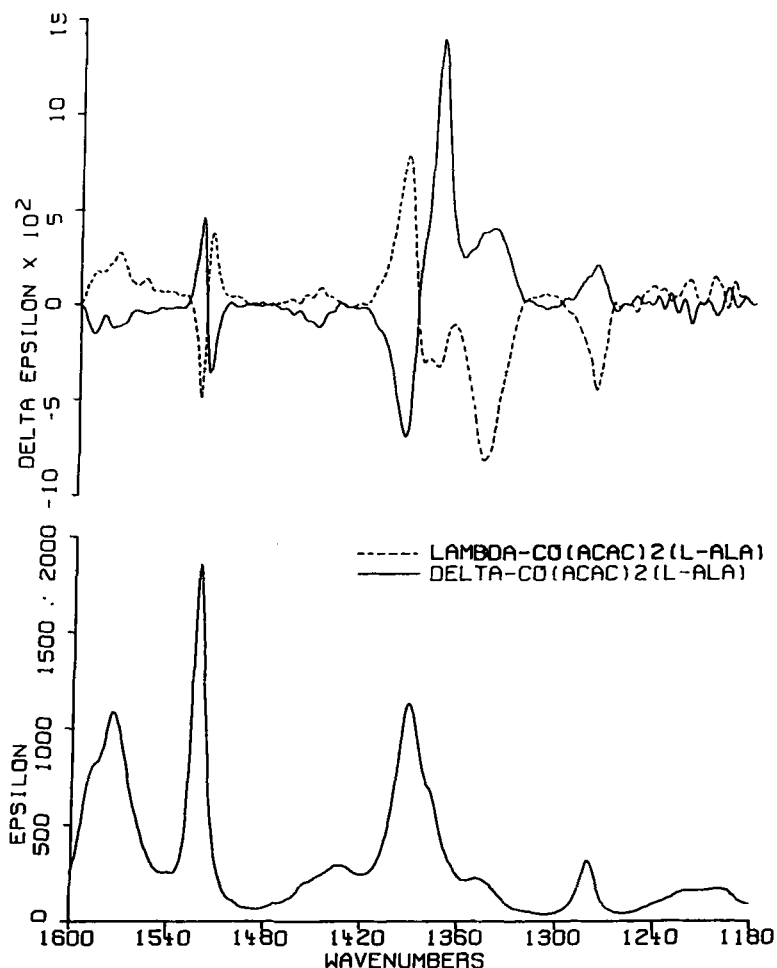


Figure 24. FTIR VCD and absorbance spectra in the 1600–1180- cm^{-1} region of DMSO- d_6 solutions of Λ -(L-alaninato)*bis*(acetylacetonato)Co(III) (---) and Δ -(L-alaninato)*bis*(acetylacetonato)Co(III) (—). (Reproduced with permission from ref. 108. Copyright 1985 American Chemical Society.)

sugars for which these centers are individually inverted. Thus, the interaction of adjacent centers can be studied directly.

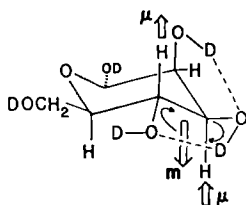
The first published paper devoted to the VCD of sugars compared the CH stretching spectra of α - and β -methyl-D-glucoside in D_2O (110). It was found that inversion at the anomeric center produced a nearly mirror image VCD spectrum from which it was concluded that most of the CH stretching VCD

features could be attributed to the O—CH₃ group. This was confirmed by measuring the VCD of the corresponding O—CD₃ species and finding little if any measurable VCD intensity.

A more recent study has reported VCD in the mid-infrared region for a variety of sugars dissolved in DMSO-*d*₆ (111). A VCD marker band near 1150 cm⁻¹ has been found that correlates with the absolute configuration of the C—OH framework of the sugar ring. Apparently the C—O and C—C stretching modes couple sufficiently to probe the overall chirality of the sugar frame. This chirality rule appears promising as a means of probing the absolute stereochemistry of sugars and should eventually prove to be more sensitive and reliable than measurements using electronic optical activity.

A third source of reported results on VCD in sugars is contained in the Ph.D. thesis of H. A. Havel from the University of Minnesota (46). This extensive study considers VCD in the CH stretching region for a wide variety of sugars and their peracetates. The VCD of eight aldohexoses are initially presented and analyzed. The spectra exhibit either no VCD intensity or strong, broad monosignate bands. These molecules assume the ⁴C₁ chair conformation in which the hydroxymethyl group is in the more favorable equatorial position. An empirical correlation is found, termed the "CH-bond helix" rule in which the chiral orientations of C(2)H, C(3)H, and C(4)H bonds are correlated with the presence (or absence) of pertinent VCD bands (and their signs). A corollary to this rule is that molecules that possess a pseudoplane of symmetry through the C(3) carbon and ring oxygen (excluding the differences at the C(1) and C(5) positions) show little if any VCD. The coupled oscillator model is applied to the CH bonds at the C(2), C(3), and C(4) positions; however, the model fails to account for the completely monosignate nature of the VCD in those molecules showing nonzero VCD. Nevertheless a correlation is also found between the VCD and the mode arising from the coupling of the three CH groups having the relative phase and amplitude, $6^{-1/2}(\Delta r_2 - 2\Delta r_3 + \Delta r_4)$, for the C(2)H, C(3)H, and C(4)H bonds. This correlation correctly predicts which sugars will exhibit zero VCD and the sign of those that exhibit nonzero VCD. No complete explanation is given as to why this correlation exists. The other two coupled oscillator modes, $3^{-1/2}(\Delta r_2 + \Delta r_3 + \Delta r_4)$ and $2^{-1/2}(\Delta r_2 - \Delta r_4)$, do not show a correlation.

We have recently determined (112) that both the sign and the approximate magnitude of the monosignate VCD bands in the CH stretching region of the sugars can be explained in terms of vibrationally induced currents in intramolecularly hydrogen-bonded rings in the sugars. The predictions of the ring current mechanism, which are similar to those for the methine C_αH stretch in the amino acids and lactic acid discussed previously, focuses on the orientation of the OD hydrogen-bonded rings relative to the attached CH oscillators. For example, a large broad negative VCD band is observed for D-mannose in D₂O.

**45**

In the C1 conformation, this molecule is depicted as in **45**, where hydrogen bonds between the hydroxyl groups associated with C(2) and C(3) as well as C(3) and C(4) are shown. If the two CH groups attached to a hydrogen-bonded ring are oscillating out of phase, they will both induce a current of the same sense in that ring. The coupled mode, $6^{-1/2}(\Delta r_2 - 2\Delta r_3 + \Delta r_4)$ satisfies this criterion for both rings in **45**. The positive current, magnetic dipole moment, and electric dipole moment for contraction of C(4)H and elongation of C(3)H are shown to give strong negative VCD contributions at C(3) and C(4). Again we have followed the rule that current oscillations will be dominant in a C—X bond where X is oxygen or nitrogen, over the oscillations in a C—C bond, in order to determine the sense of current. A similar analysis for out-of-phase CH stretching motion associated with the ring involving the center C(3) and C(2) leads to a weak positive VCD contribution from C(3) and a strong negative one at C(2). The strength of the contribution depends on the orientation of the plane of the ring relative to the CH oscillator. The contribution is strong when the ring and CH moieties are perpendicular; it is weak when these moieties are parallel. Overall a very strong negative contribution is predicted for mannose, as observed.

We have found in general that when two equatorial hydroxyl groups are adjacent as for C(3) and C(4) in D-mannose, two strong monosignate VCD contributions of the same sign arise for the out-of-phase CH stretching motion. For the in-phase vibration the ring currents will cancel and no VCD is predicted. For adjacent equatorial and axial hydroxyl groups, a strong VCD effect and a weak effect of the opposite sign are found. Finally, for adjacent axial hydroxyl groups, no hydrogen bond can be formed and no VCD current contribution results. For some sugars that possess a strong preference for the α or β configuration at the anomeric carbon [C(1)], the possibility of a ring involving C(1) and C(2) needs to be considered.

A final topic that has been considered (46) concerns the VCD in the CH stretching region of the peracetates of sugars. Here, no hydroxyl hydrogen bonds can form. No VCD arises from the methyl on the acetate groups as demonstrated by deuteration. Most of the spectra have both positive and negative VCD con-

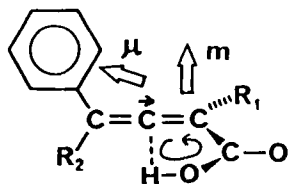
tributions, although a systematic bias to negative VCD for the D-sugar peracetates was observed. Coupled oscillator theory was applied to all five of the CH groups in the sugar and agreement with experiment was found if steric distortions forced the six-membered ring to leave a perfect chair conformation. The distortion, for instance, allows pairs of adjacent axial CH oscillators to become conformationally chiral. No explanation has been provided for the bias in the observed spectra although some form of intramolecular association may be involved.

G. Chiral Allenes and Azides

VCD has been observed for the antisymmetric stretching mode of the linear $C=C=C$ (allene) or $N=N=N^-$ (azide) group in a chiral environment. These motions occur in the $1900\text{--}2100\text{-cm}^{-1}$ region, and are not significantly coupled with the vibrations of other nuclei in the molecule.

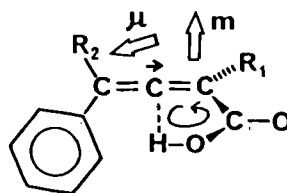
The VCD spectra of a series of chiral allenes have been recorded at the University of Minnesota using a dispersive VCD instrument (113). The spectrum of one of these compounds has been verified by FTIR-VCD (23). The molecules have a phenyl and a carboxyl substituent on opposite ends of the allene, and alkyl or hydrogen substituents in the remaining two positions. All the corresponding (*S*)-(+) enantiomers, **46**, exhibit a single positive VCD feature and the (*R*)-(-) enantiomers, **47**, a negative VCD feature, at 1945 cm^{-1} , with an anisotropy ratio of ca. 4×10^{-5} .

The allene VCD spectra can be interpreted in terms of the ring current mechanism (114). As shown in **46** and **47**, for a conformation that maintains a planar orientation due to conjugation with the allene, for both the phenyl and carboxyl groups relative to the adjacent portion of the allene group, an intramolecular hydrogen bond is possible between the carboxyl hydrogen and a π orbital of the central allene carbon atom. The antisymmetric $C=C=C$ stretch can be de-



$R > 0$

46



$R < 0$

47

scribed as a linear displacement of the central carbon toward one end of the group accompanied by smaller displacements of the end carbon atoms in the opposite direction. During motion of the central carbon nucleus away from the phenyl group, it is reasonable for electrons to be drawn out of the conjugated phenyl group and through the allene in the direction of the central carbon motion; this flow of negative charge results in an electric dipole transition moment μ directed slightly away from the linear $C=C=C$ direction toward the phenyl group as depicted in **46** and **47**. Concurrently, negative charge flows into the conjugated carboxyl group, and due to the hydrogen bond, a ring current is generated in the $\overline{C=C-C-O-H}$ ring that results in a magnetic dipole transition moment m perpendicular to this ring as shown. Due to the contribution to μ from the phenyl group, the two moments are not orthogonal, and nonzero VCD is predicted, positive for the (*S*)-(+) enantiomers, **46**, and negative for the (*R*)-(-) enantiomers, in agreement with experiment.

The geometry and electronic structure of the azide ion, N_3^- , is quite similar to that of allene. The rotational strength observed for the antisymmetric stretching vibration of the azide (2025 cm^{-1}) in azidomethemoglobin A (Figure 25), measured by Marcott, et al., is $-3 \times 10^{-40}\text{ esu}^2\text{ cm}^2$, with an anisotropy ratio 0.02 (115). These values are two orders of magnitude or more greater than normally observed for VCD.

The large rotational strength for the azide stretch in azidomethemoglobin A can be understood in terms of vibrationally generated ring currents. As shown in diagram **48**, the azide ion, coordinated to the iron atom of the heme, is situated between pyrroles 2 and 3 and makes an angle of 21° with the heme

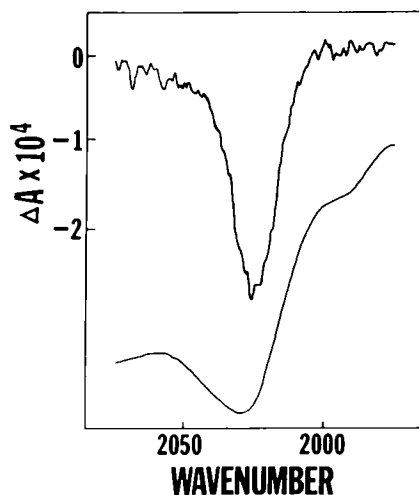
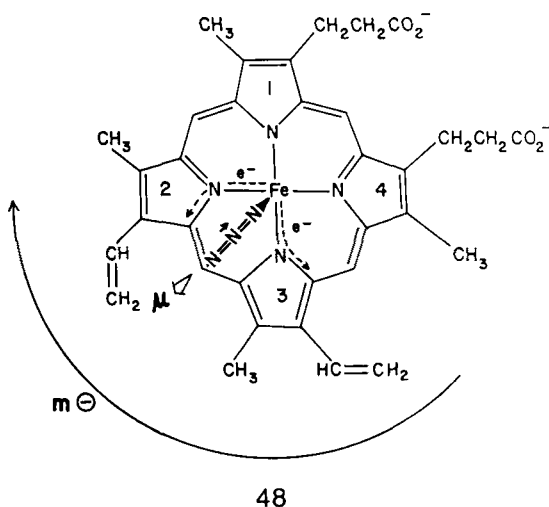


Figure 25. VCD and IR transmission spectra of azidomethemoglobin A, 4.77 mM (in tetramer) in pH 6.0 phosphate buffer. Sample path length 0.058 mm, resolution 10 cm^{-1} , time constant 3 s. (Reproduced with the permission of Reidel from ref. 115a.)



plane. Due to the chirality of **48**, the azide ion finds itself in a chiral environment. Vibrational motion of the central azide nitrogen toward the iron corresponds to an electric dipole transition moment, μ , directed along N—N—N away from the heme. According to the ring current mechanism, the motion of this nitrogen injects electrons, via the iron atom, into the heme. With a preferred flow of electrons toward the vinyl groups, counterclockwise electron flow around the heme is initiated. The magnetic moment, m , due to clockwise positive ring current, is directed into the plane of **48** and results in negative $\mu \cdot m$, as observed. The large region of delocalizable electron density and low-lying electronic states appear to be responsible for the extremely large rotational strength (cf., eq. [30]).

V. CONCLUSIONS

It is clear from the preceding material that stereochemical applications of VCD are developing rapidly. This has been made possible by a growing body of VCD spectra from which the salient features relating to stereochemical details in molecules have been extracted. Progress in the area of ROA is somewhat more modest, in part due to the greater complexity of the relationship between the theoretical description of ROA intensities and molecular stereochemistry (14).

Through many examples, it has been demonstrated that VCD arises essentially from two rather distinct mechanisms. The first is the coupling of achiral oscillators that are chirally disposed in their spatial relationship to one another. The mechanism is embodied in its purest form in the simple coupled oscillator

model and the FPC model. The latter model is merely a nondegenerate coupled oscillator model where the vibrational force field and kinetic energy matrix provide the coupling between the local achiral oscillators. VCD from this mechanism is always conservative over the range of coupling.

The second major mechanism of VCD is the production of vibrationally generated electronic current density by the vibrational motion of a local oscillator. Usually, such currents are induced in molecular rings, or fragments of rings, and the local oscillator may either be attached to the ring or contained in it. The resulting VCD per oscillator is biased and monosignate.

Based on an analysis of the occurrences of the ring current mechanism in VCD, the following general points can be made. First, the mechanism requires the formation of an intramolecular ring having a region of delocalizable electron density near the inducing local oscillator. Usually, the closed ring involves some form of intramolecular hydrogen bonding (σ or π) or transition metal complexation. Second, two simple rules can be stated for determining the sense of current flow in a ring depending upon whether the driving oscillator is attached to the ring or is in it.

Rule 1: When an oscillator attached to a ring contracts, electrons are inserted into the ring such that positive current flows preferentially toward the inducing oscillator along the bonded region having less tightly held electron density. Elongation of the oscillator withdraws electrons from the ring, generating the opposite sense of positive current.

Rule 2: When an oscillator involved in the hydrogen-bonding interaction elongates, the hydrogen-bond length decreases, strengthening the bond and generating electron flow from the more electron rich of the hydrogen-bonding atoms into the hydrogen-bonded region. For $X-H \cdots Y$, positive current flows from the hydrogen-bonded region toward Y, the electron rich substituent, during $X-H$ elongation, and away from Y during $X-H$ contraction.

These rules are consistent with the examples found to date of VCD derived from electronic current associated with intramolecular rings.

The stereochemical significance of VCD can now be appreciated both in a structural sense through the geometrical sensitivity of VCD to chirally displaced local moments in molecules and in a combined structural-dynamic sense through its dependence on local electric dipole moments and induced magnetic dipole moments that arise from electronic currents moving in a stereospecific way in intramolecularly bonded ringlike structures. The sense of current is based on the relative ability of electron density in bonds to follow the electron density oscillations in a driving local oscillator. In this mechanism VCD is uniquely sensitive to *intra*- as opposed to *intermolecular* hydrogen bonding. VCD is thus an excellent probe of molecular self-association. Intermolecular associations are

suppressed because the associating molecules are, in general, not vibrationally coupled. The sensitivity to currents means that VCD is sensitive to the mobility (induced by nuclear momenta) of electron density, not just to its distribution.

As noted earlier, the dynamic sensitivity of VCD carries it beyond the Born-Oppenheimer approximation (17, 18). Even though non-Born-Oppenheimer calculations have recently been initiated (116-119), the use of molecular orbital methods to describe these vibrationally induced currents is lagging behind the measurement and interpretation of VCD based on such currents. Nevertheless, the empirical basis that is now emerging for understanding VCD intensities based on chirally oriented oscillators and induced currents makes possible the immediate application of this methodology to stereochemical problems of widespread interest.

ADDENDUM, MAY 1986

A number of recent VCD investigations have been reported by several laboratories. Keiderling and co-workers have extended their earlier work on polypeptide films (120) to β sheet forming homooligopeptide films (121, 122) and solutions (122) and were able to detect the onset of β -structure formation. They have also measured the VCD for nonaqueous solutions of 3_{10} -helical octapeptides (123) and polytyrosine (124). In aqueous solutions, VCD features characteristic of right-handed α helix, antiparallel β sheet, and extended helix have been reported for poly (L-lysine) by Yasui and Keiderling (125) and Paterlini, Freedman, and Nafie (126). The latter also reports a completely unordered state characterized by the absence of amide I' VCD, achieved at high salt concentrations. Keiderling et al. (127) have demonstrated that the characteristic α -helical or β -sheet VCD features can be observed in globular proteins.

Polavarapu, et al. (128) have identified a VCD band near 1200 cm^{-1} in phenylcarbinols that correlates with configuration. Wieser and co-workers (129, 130) have recently reported FTIR-VCD spectra of chiral methyloxetan molecules. In the area of theoretical calculations, Lowe, Stephens, and Segal (131, 132) have implemented the theory of Stephens (118) in calculations on *trans*-1,2-dideuteriocyclopropane, *trans*-1,2-dideuteriocyclobutane, and propylene oxide. For the latter two molecules, favorable agreement with experiment was found. The first application of VCD to kinetic analysis has also been reported for (1*R*, 2*R*)-dideuteriocyclobutane thermolysis (133).

ACKNOWLEDGMENTS

The authors wish to acknowledge support from the National Science Foundation and the National Institutes of Health for research in vibrational optical activity.

We also wish to thank Dr. T. A. Keiderling for sending us manuscripts in advance of publication and Mr. William M. Zuk for assistance in the preparation of the stereodiagrams.

REFERENCES

1. Salvadori, P. and Ciardelli, F. "An Introduction to Chiroptical Techniques: Basic Principles, Definitions and Applications," In "Optical Rotatory Dispersion and Circular Dichroism"; Ciardelli, F.; Savadori, P., Eds.; Heyden: London, 1973; pp. 3-24.
2. See articles in "Optical Activity and Chiral Discrimination," Mason, S. F., Ed.; Reidel: Dordrecht, 1979 and Barron, L. D. "Molecular Light Scattering and Optical Activity"; Cambridge: London, 1982.
3. Hsu, E. C.; Holzwarth, G. *J. Chem. Phys.* 1973, 59, 4678.
4. Holzwarth, G.; Hsu, E. C.; Mosher, H. S.; Faulkner, T. R.; Moscovitz, A. *J. Am. Chem. Soc.* 1974, 96, 251.
5. Stephens, P. J.; Clark R. "Vibrational Circular Dichroism: The Experimental Viewpoint," In "Optical Activity and Chiral Discrimination"; Mason S. F., Ed.; Reidel: Dordrecht, 1979, pp. 263-287.
6. Nafie, L. A.; Diem, M. *Acc. Chem. Res.* 1979, 12, 296.
7. Keiderling, T. *Appl. Spectrosc. Rev.* 1981, 17, 189.
8. Nafie, L. A. "Infrared and Raman Vibrational Optical Activity," In "Vibrational Spectra and Structure," Vol. 10; Durig, J. R., Ed.; Elsevier, Amsterdam, 1981, pp. 153-255.
9. Barron, L. D.; Bogaard, M. P.; Buckingham, A. D. *J. Am. Chem. Soc.* 1973, 95, 603.
10. Barron, L. D.; Buckingham, A. D. *Ann. Rev. Phys. Chem.* 1975, 26, 381; Barron, L. D. "Rayleigh and Raman Scattering of Polarized Light," In "Molecular Spectroscopy"; Vol. 4; Barrow, R. F.; Long, D. A.; Sheridan, J., Eds.; The Chemical Society: London, 1976, pp. 96-124.
11. Barron, L. D. "Raman Optical Activity," In "Advances in Infrared and Raman Spectroscopy," Vol. 4; Clark, R. J. H.; Hester, R. E., Eds.; Heyden: London, 1978, pp. 271-331.
12. Barron, L. D. "Raman Optical Activity," In "Optical Activity and Chiral Discrimination"; Mason, S. F., Ed.; Reidel: Dordrecht, 1979, pp. 219-262.
13. Barron, L. D. *Acc. Chem. Res.* 1980, 13, 90.
14. Barron, L. D.; Vrbancich, J. "Natural Vibrational Raman Optical Activity," In "Topics in Current Chemistry," Vol. 123; Boschke, F. L., Ed.; Springer: Berlin, 1984, pp. 151-182.
15. Nafie, L. A. "Experimental and Theoretical Advances in Vibrational Optical Activity," In "Advances in Infrared and Raman Spectroscopy," Vol. 11; Clark, R. J. H.; Hester, R. E., Eds.; Wiley-Heyden: New York, 1984, pp. 49-93.
16. Faulkner, T. R.; Marcott, C.; Moscovitz, A.; Overend, J. *J. Am. Chem. Soc.* 1977, 99, 8160.
17. Nafie, L. A.; Freedman, T. B. *J. Chem. Phys.* 1983, 78, 7108.
18. Nafie, L. A. *J. Chem. Phys.* 1983, 79, 4950.
19. Chabay, I.; Holzwarth, G. *Appl. Opt.* 1975, 14, 454.
20. Nafie, L. A.; Keiderling, T. A.; Stephens, P. J. *J. Am. Chem. Soc.* 1976, 98, 2715.

21. Clark, R.; Stephens, P. J. *Proc. Soc. Photo. Instr. Eng.* **1977**, *112*, 127.
22. Su, C. N.; Heintz, V. J.; Keiderling, T. A. *Chem. Phys. Lett.* **1980**, *73*, 157.
23. Nafie, L. A.; Vidrine, D. W. "Double Modulation Fourier Transform Spectroscopy," In "Fourier Transform Infrared Spectroscopy," Vol. 3; Ferraro, J. R.; Basile, L. J., Eds.; Academic: New York, **1982**, pp. 83-123.
24. Lipp, E. D.; Zimba, C. G.; Nafie, L. A. *Chem. Phys. Lett.* **1982**, *90*, 1.
25. Lipp, E. D.; Nafie, L. A. *Appl. Spectrosc.* **1984**, *38*, 20.
26. Polavarapu, P. L. *Appl. Spectrosc.* **1984**, *38*, 26.
27. Boucher, H.; Brocki, T. R.; Moskovits, M.; Bosnich, B. *J. Am. Chem. Soc.* **1977**, *99*, 6870.
28. Hug, W.; Surbeck, H. *Chem. Phys. Lett.* **1979**, *60*, 186.
29. Hug, W. *Appl. Spectrosc.* **1981**, *35*, 115.
30. Barron, L. D.; Torrance, J. F. *Chem. Phys. Lett.* **1983**, *102*, 285.
31. Nafie, L. A. *Chem. Phys. Lett.* **1983**, *102*, 287.
32. Holzwarth, G.; Chabay, I. *J. Chem. Phys.* **1972**, *57*, 1632.
33. Faulkner, T. R. Ph.D. Thesis, University of Minnesota, 1976.
34. Sugeta, H.; Marcott, C.; Faulkner, T. R.; Overend, J.; Moscovitz, A. *Chem. Phys. Lett.* **1976**, *40*, 397.
35. Schellman, J. A. *J. Chem. Phys.* **1973**, *58*, 2882; **1974**, *60*, 343.
36. Moskovits, M.; Gohin, A. *J. Phys. Chem.* **1982**, *86*, 3947.
37. Abbate, S.; Laux, L.; Overend, J.; Moscovitz, A. *J. Chem. Phys.* **1981**, *75*, 3161.
38. Freedman, T. B.; Nafie, L. A. *J. Phys. Chem.* **1984**, *88*, 496.
39. Nafie, L. A.; Walnut, T. H. *Chem. Phys. Lett.* **1977**, *49*, 441.
40. Walnut, T. H.; Nafie, L. A. *J. Chem. Phys.* **1977**, *67*, 1491; Walnut, T. H.; Nafie, L. A. *J. Chem. Phys.* **1977**, *67*, 1501.
41. Nafie, L. A.; Polavarapu, P. L. *J. Chem. Phys.* **1981**, *75*, 2935.
42. Freedman, T. B.; Nafie, L. A. *J. Chem. Phys.* **1983**, *78*, 27; *J. Chem. Phys.*, **1983**, *79*, 1104.
43. Nafie, L. A.; Freedman, T. B., *J. Phys. Chem.* **1986**, *90*, 763.
44. Polavarapu, P. L. *Mol. Phys.* **1983**, *49*, 645.
45. Barnett, C. J.; Drake, A. F.; Kuroda, R.; Mason, S. F. *Mol. Phys.* **1980**, *41*, 455.
46. Havel, H. Ph.D. Thesis, University of Minnesota, 1981.
47. Prasad, P. L.; Nafie, L. A. *J. Chem. Phys.* **1979**, *70*, 5582.
48. Nafie, L. A.; Freedman, T. B. *J. Chem. Phys.* **1981**, *75*, 4847.
49. Polavarapu, P. L. *J. Chem. Phys.* **1982**, *77*, 2273.
50. Keiderling, T. A.; Stephens, P. J. *J. Am. Chem. Soc.* **1977**, *99*, 8061.
51. Su, C. N.; Keiderling, T. A. *J. Am. Chem. Soc.* **1980**, *102*, 511.
52. Marcott, C.; Blackburn, C. C.; Faulkner, T. R.; Moscovitz, A.; Overend, J. *J. Am. Chem. Soc.* **1978**, *78*, 5262.
53. Nakao, Y.; Sugeta, H.; Kyogoku, Y. *Chem. Lett.* **1984**, 623.
54. Mori, N.; Omura, S.; Kobayashi, N.; Tsuzuki, Y. *Bull. Chem. Soc. Jpn.* **1965**, *38*, 2149.
55. Nafie, L. A. *Appl. Spectrosc.* **1982**, *36*, 489.
56. Narayanan, U.; Keiderling, T. A. *J. Am. Chem. Soc.* **1983**, *105*, 6406.

57. Freedman, T. B.; Balukjian, G. A.; Nafie, L. A. *J. Am. Chem. Soc.* **1985**, *107*, 6213.
58. Pultz, V. M. Ph.D. Thesis, University of Minnesota, 1983.
59. Su, C. N.; Keiderling, T. A. *Chem. Phys. Lett.* **1981**, *77*, 494.
60. Polavarapu, P. L.; Michalska, D. F.; Neergaard, J. R.; Smith, H. E. *J. Am. Chem. Soc.* **1984**, *106*, 3378.
61. Hug, W.; Kamatari, A.; Srinivasan, K.; Hansen, H.-J.; Sliwka, H.-R. *Chem. Phys. Lett.* **1980**, *76*, 469.
62. Heintz, V. J.; Keiderling, T. A. *J. Am. Chem. Soc.* **1981**, *103*, 2395.
63. Polavarapu, P. L.; Michalska, D. F. *J. Am. Chem. Soc.* **1983**, *105*, 6190.
64. Annamalai, A.; Keiderling, T. A.; Chickos, J. S. *J. Am. Chem. Soc.* **1984**, *106*, 6254; **1985**, *107*, 2285.
65. Polavarapu, P. L.; Nafie, L. A. *J. Chem. Phys.* **1980**, *73*, 1567.
66. Polavarapu, P. L.; Diem, M.; Nafie, L. A. *J. Am. Chem. Soc.* **1980**, *102*, 5449.
67. Marcott, C.; Scanlon, K.; Overend, J.; Moscovitz, A. *J. Am. Chem. Soc.* **1981**, *103*, 483.
68. Singh, R. D.; Keiderling, T. A. *J. Am. Chem. Soc.* **1981**, *103*, 2387.
69. Singh, R. D.; Keiderling, T. A. *J. Chem. Phys.* **1981**, *74*, 5347.
70. Laux, L.; Pultz, V.; Abbate, S.; Havel, H. A.; Overend, J.; Moscovitz, A.; Lightner, D. A. *J. Am. Chem. Soc.* **1982**, *104*, 4276.
71. Laux, L. Ph.D. Thesis, University of Minnesota, 1982.
72. Freedman, T. B.; Young, D.; Kallmerten, J.; Nafie, L. A., unpublished results.
73. Barron, L. D.; Clark, B. P. *J. Chem. Soc. Perkins Trans. 2* **1979**, 1164.
74. Barron, L. D. *J. Chem. Soc. Perkins Trans. 2* **1977**, 1074.
75. Barron, L. D.; Torrance, J. F.; Vrbancich, J. J. *Raman Spectrosc.* **1982**, *13*, 171.
76. Barron, L. D.; Clark, B. P. *J. Raman Spectrosc.* **1982**, *13*, 155.
77. Freedman, T. B.; Kallmerten, J.; Zimba, C. G.; Zuk, W. M.; Nafie, L. A. *J. Am. Chem. Soc.* **1984**, *106*, 1244.
78. Keiderling, T. A.; Stephens, P. J. *J. Am. Chem. Soc.* **1979**, *101*, 1396.
79. Barnett, C.; Drake A. F.; Mason, S. F. *J. Chem. Soc. Chem. Commun.* **1980**, 43.
80. Polavarapu, P. L.; Nafie, L. A.; Benner, S. A.; Morton, T. H. *J. Am. Chem. Soc.* **1981**, *103*, 5349.
81. Su, C. N.; Keiderling, T. A.; Misiura, K.; Stec, W. J. *J. Am. Chem. Soc.* **1982**, *104*, 7343.
82. Diem, M.; Gotkin, P. J.; Kupfer, J. M.; Tindall, A. P.; Nafie, L. A. *J. Am. Chem. Soc.* **1977**, *99*, 8103.
83. Diem, M.; Gotkin, P. J.; Kupfer, J. M.; Nafie, L. A. *J. Am. Chem. Soc.* **1978**, *100*, 5644.
84. Diem, M.; Photos, E.; Khouri, H.; Nafie, L. A. *J. Am. Chem. Soc.* **1979**, *101*, 6829.
85. Diem, M.; Polavarapu, P. L.; Oboodi, M.; Nafie, L. A. *J. Am. Chem. Soc.* **1982**, *104*, 3329.
86. Lal, B. B.; Diem, M.; Polavarapu, P. L.; Oboodi, M.; Freedman, T. B.; Nafie, L. A. *J. Am. Chem. Soc.* **1982**, *104*, 3336.
87. Freedman, T. B.; Diem, M.; Polavarapu, P. L.; Nafie, L. A. *J. Am. Chem. Soc.* **1982**, *104*, 3343.
88. Nafie, L. A.; Oboodi, M. R.; Freedman, T. B. *J. Am. Chem. Soc.* **1983**, *105*, 7449.
89. Oboodi, M. R.; Lal, B. B.; Young, D. A.; Freedman, T. B.; Nafie, L. A. *J. Am. Chem. Soc.* **1985**, *107*, 1547.

90. Oboodi, M. R. Ph.D. Thesis, Syracuse University, 1983.
91. Aaron, H. S. "Conformational Analysis of Intramolecular Hydrogen-Bonded Compounds in Dilute Solution by Infrared Spectroscopy," In "Topics in Stereochemistry" Vol. 11; Allinger, N. L.; Eliel, E. L., Eds.; Wiley: New York, **1979**, pp. 1-52.
92. Chernovitz, A. Ph.D Thesis, Syracuse University 1986.
93. Zuk, W. M. Ph.D Thesis, Syracuse University 1986.
94. Singh, R. D.; Keiderling, T. A. *Biopolymers* **1981**, *20*, 237.
95. Schellman, J. A. "Optical Activity of Polypeptides in the Infrared: Symmetry Considerations," In "Peptides, Polypeptides and Proteins"; Blout, E. R.; Bovey, F. A.; Goodman, M.; Lotan, N., Eds.; Wiley: New York, **1974**, pp. 320-337.
96. Snir, J.; Frankel, R. A.; Schellman, J. A. *Biopolymers* **1975**, *14*, 173.
97. Lal, B. B.; Nafie, L. A. *Biopolymers* **1982**, *21*, 2161.
98. Sen, A. C.; Keiderling, T. A. *Biopolymers* **1984**, *23*, 1519.
99. Lipp, E. D.; Nafie, L. A. *Biopolymers* **1985**, *24*, 799.
100. Kauppinen, J. K.; Moffatt, D. J.; Mantsch, H. H.; Cameron, D. G. *Appl. Spectrosc.* **1981**, *35*, 271.
101. Chernovitz, A.; Freedman, T. B.; Nafie, L. A., unpublished results.
102. Mason, S. F. "Optical Activity and Molecular Dissymmetry in Coordination Compounds," In "Optical Rotatory Dispersion and Circular Dichroism"; Ciardelli, F.; Salvadori, P., Eds.; Heyden: London **1973**; pp. 196-239.
103. Young, D.; Nafie, L. A., unpublished results.
104. Young, D. A.; Freedman, T. B.; Lipp, E. D.; Nafie, L. A. *J. Am. Chem. Soc.* **1986**, *108*, 7255.
105. Cramer, R. E.; Huneke, J. T. *Inorg. Chem.* **1978**, *17*, 365.
106. Nakazawa, H.; Sakaguchi, U.; Yoneda, H. *J. Am. Chem. Soc.* **1982**, *104*, 3885.
107. Young, D. A. Ph.D. Thesis, Syracuse University 1986.
108. Young, D. A.; Lipp, E. D.; Nafie, L. A. *J. Am. Chem. Soc.* **1985**, *107*, 6205.
109. Herak, R.; Prelesnik, B.; Krstanovic, I. *Acta Cryst.* **1978**, *B34*, 91; Drew, M. G. B.; Dunlop, J. H.; Gillard, R. D.; Rogers, D. *J. Chem. Soc. Chem. Comm.* **1966**, 42.
110. Marcott, C.; Havel, H. A.; Overend, J.; Moscovitz, A. *J. Am. Chem. Soc.* **1978**, *100*, 7088.
111. Back, D. M.; Polavarapu, P. L. *Carbohydr. Res.* **1984**, *133*, 163.
112. Paterlini, M. G.; Freedman, T. B.; Nafie, L. A. *J. Am. Chem. Soc.* **1986**, *108*, 1389.
113. Moscovitz, A., private communication.
114. Freedman, T. B.; Nafie, L. A., unpublished results.
115. (a) Marcott, C.; Havel, H. A.; Hedland, B.; Overend, J.; Moscovitz, A. "A Vibrational Rotational Strength of Extraordinary Intensity. Azidomethemoglobin A," In "Optical Activity and Chiral Discrimination"; Mason, S. F., Ed.; Reidel: Dordrecht, **1979**, pp. 289-292. (b) Marcott, C. Ph.D. Thesis, University of Minnesota, 1979.
116. Freedman, T. B.; Nafie, L. A. *Chem. Phys. Lett.* **1986**, *126*, 441.
117. Stephens, P. J.; Lowe, M. *39th Symposium on Molecular Spectroscopy* **1984**, Columbus, OH, papers TF1-4.
118. Stephens, P. J. *J. Phys. Chem.* **1985**, *89*, 748.
119. Stephens, P. J.; Lowe, M. A. *Ann. Rev. Phys. Chem.* **1985**, *36*, 213.
120. Sen, A. C.; Keiderling, T. A. *Biopolymers* **1984**, *23*, 1533.

121. Narayanan, U.; Keiderling, T. A.; Bonora, G. M.; Toniolo, C. *Biopolymers* **1985**, *24*, 1257.
122. Narayanan, U.; Keiderling, T. A.; Bonora, G. M.; Toniolo, C. *J. Am. Chem. Soc.* **1986**, *108*, 2431.
123. Yasui, S. C.; Keiderling, T. A.; Bonora, G. M.; Toniolo, C. *Biopolymers* **1986**, *25*, 79.
124. Yasui, S. C.; Keiderling, T. A. *Biopolymers* **1986**, *25*, 5.
125. Yasui, S. C.; Keiderling, T. A. *J. Am. Chem. Soc.* **1986**, *108*, 5576.
126. Paterlini, M. G.; Freedman, T. B.; Nafie, L. A. *Biopolymers* **1986**, *25*, 1751.
127. Keiderling, T. A.; Yasui, S. C.; Sen, A. C.; Toniolo, C.; Bonora, G. M. In "Peptides: Structure and Function"; Deber, C. M.; Hruby, V. J.; Kopple, K. D., Eds.; Pierce Chemical Co. **1985**, pp. 167-172.
128. Polavarapu, P. L.; Fontana, L. P.; Smith, H. E. *J. Am. Chem. Soc.* **1986**, *108*, 94.
129. Shaw, R. A.; Ibrahim, N.; Nafie, L. A.; Rauk, A.; Wieser, H. In "1985 Conference on Fourier and Computerized Spectroscopy," Vol. 553; Grasselli, J. et al., Eds., SPIE: Bellingham, WA **1985**, pp. 433-434.
130. Shaw, R. A.; Ibrahim, N.; Wieser, H. In "41st Symposium on Molecular Spectroscopy," **1986**, Columbus, OH, Paper RC-3.
131. Lowe, M. A.; Segal, G. A.; Stephens, P. J. *J. Am. Chem. Soc.* **1986**, *108*, 248.
132. Lowe, M. A.; Stephens, P. J.; Segal, G. A. *Chem. Phys. Lett.* **1986**, *123*, 108.
133. Chickos, J. S.; Annamalai, T. A.; Keiderling, T. A. *J. Am. Chem. Soc.*, **1986**, *108*, 4398.

Chiral Crown Ethers

J. FRASER STODDART

Department of Chemistry, The University, Sheffield, United Kingdom

I. Prologue	207
II. Historical and General Background	209
III. Synthesis of Chiral Crown Ethers	229
A. Substituted All-Oxygen Crown Compounds	232
1. From Tartaric Acid Derivatives	232
2. From Carbohydrate Derivatives	236
3. From Resolved Hydrobenzoin and 2,3-Butanediol	239
4. From Precursors Derived from Lactic and Mandelic Acids	242
B. Fused-Ring All-Oxygen Crown Compounds	244
1. From (+)- <i>trans</i> -Cyclohexan-1,2-diol	244
2. From (+)- and (-)- <i>trans</i> -Bishydroxymethyltetrahydrofuran	244
3. From Carbohydrate Derivatives	244
4. From (<i>R</i>)- and (<i>S</i>)-Binaphthol and Related Compounds	254
5. From 9,9'-Spirobifluorene Derivatives	255
6. From Miscellaneous Chiral Sources	256
C. All-Oxygen Biscrown and Triscrown Compounds	258
D. All-Oxygen Macrobicyclic Compounds	260
E. Substituted Aza Crown Compounds	262
1. With Secondary and Tertiary Amine Functions in Chiral Macrocyclic Polyether Rings	264
2. Chiral Crown Ethers Containing Saturated Nitrogen Functions	265
3. From α -Amino Acid Derivatives	267
4. With Fused Pyridino Rings in Chiral Macrocyclic Polyethers	270
F. Aza Macrobicyclic and Macropolycyclic Compounds	270
G. Miscellaneous Compounds	273
IV. PROPERTIES	275
V. CONCLUDING REMARKS	278
Acknowledgments	279
References	279

I. PROLOGUE

The last two decades have witnessed dramatic developments in chemistry beyond the molecular level involving relatively low (ca. 200–2000) molecular

weight compounds. The fact that synthetic chemists have been turning their attention increasingly to the *extramolecular* aspects of the discipline (i.e., the effect of intermolecular interactions on properties and reactivity) has opened up challenging and exciting new areas for detailed stereochemical investigation. The conformational analysis of molecular complexes, especially the analysis of the intermolecular effects between receptor and small substrate molecules, promises to shed a great deal of light on our understanding of the nature of noncovalent bonds. In addition to elucidating the stereochemical principles that govern how a particular substrate interacts with a synthetic *molecular receptor*, the study of molecular complexes that maintain their structural integrity in solution is crucial to achieving a fundamental understanding of the phenomenon of molecular *complexation*.

Molecular complexation is a precondition for *receptor functions* such as substrate selection, substrate transportation, isomeric differentiation, and stereoselective catalysis. Although the investigation of such functions with synthetically derived compounds is a relatively new development in chemistry, they are well known and extensively studied functions in the biological domain. Evolution, gene expression, cell division, DNA replication, protein synthesis, immunological response, hormonal control, ion transportation, and enzymic catalysis are only some of the many examples where molecular complexation is a prerequisite for observing a biological process.

The recognition of a receptor function is the practical manifestation of successful *receptor design*. It follows that synthetic molecular receptors, in common with their natural counterparts, must be capable of recognizing other chemical species by achieving *complementarity* of steric and electronic shape, as well as, of course, size.

The noncovalent bonds that hold molecular complexes together are largely electrostatic in origin. They include the following interactions: pole–pole, pole–dipole, dipole–dipole, dipole–induced dipole, and induced dipole–induced dipole, that is, dispersion forces of the van der Waals–London type. Particular structural features and conditions lead to the recognition of important special cases such as hydrophobic interactions, hydrogen bonding, and charge transfer stabilization. They are all potentially available to the synthetic chemist for exploitation.

The binding forces that give rise to molecular complexes are no different from those present (i) in crystal lattices in the solid state and (ii) in solvating media in the solution state. We are familiar with the structural implications (e.g., clathrate formation) and practical applications (e.g., in chromatography), including chemical reactions themselves! It is the organization of binding sites within a molecular receptor that defines its special and unique function. This can be achieved within the context of relative structural rigidity or flexibility in the synthetic molecular receptor. Generally speaking, for a given constitutional

type, rigid receptors form strong complexes slowly, whereas flexible receptors form weak complexes quickly.

With the gift of hindsight, it is obvious that the majority of synthetic chemists would turn to macrocyclic compounds in the first instance for a ready source of molecular receptors. Indeed, this is exactly what has happened, although the most popular line (that concerned with macrocyclic polyethers) to date was to come on the scene serendipitously at just the right time. To their credit, synthetic chemists grasped the opportunity and wasted no time in developing the chemistry of the crown ethers.

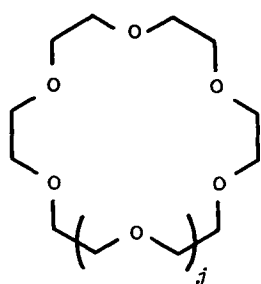
Soon thereafter, chirality was recognized as a necessary and indispensable part of synthetic receptor molecule design and function. Predictably, not only has nature's chiral pool been called upon to supply inexpensive and readily available sources of chirality, but the ability of the chemist to resolve optically active precursors from racemic modifications prepared in the laboratory has been exploited ingeniously in a number of different directions. The various elements of chirality: centers, axes, planes, as well as helices, have been incorporated into both axially symmetric and asymmetric receptors.

The functionality that is often necessary for a chiral crown ether to serve a particular purpose can usually be introduced by the synthetic chemist without too much difficulty. The practice here, however, can be very much more demanding on account of the promiscuous receptor properties of the compounds that have to be separated and isolated pure from reaction mixtures containing many components.

As with all activities in the extramolecular realm of chemistry, the art of designing and synthesizing chiral crown ethers should ideally be the first act in achieving, subsequently, some physical, chemical, or biological effect. In this review, we shall examine the ways in which chiral crown ethers can be made in the laboratory and then consider very briefly some of the uses they have found in different areas of physical, chemical, and biological science. First of all, however, a few introductory comments on the historical and general background to the development of crown ethers as synthetic molecular receptors will be made. For more details, the reader is referred to a number of monographs (1, 2), multiauthor works (3-8), and reviews (9-23).

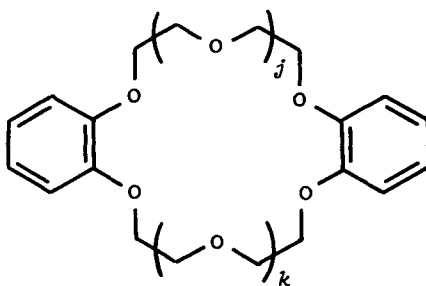
II. HISTORICAL AND GENERAL BACKGROUND

Since the accidental discovery (24) of dibenzo-18-crown-6, **3**, by Pedersen (25), a large number of macrocyclic polyethers have been reported in the literature (1-23). However, the most extensively studied of the so-called crown ethers is the parent macrocycle 1,4,7,10,13,16-hexaoxacyclooctadecane or 18-crown-6, **1**. It forms molecular complexes with a wide range of substrate species including



1 $j = 1$

2 $j = 2$



	j	k
3	1	1
4	0	5
5	1	5
6	3	3

(i) alkali metal (e.g., K^+), alkaline earth metal (e.g., Ba^{2+}), as well as the harder transition metal and post-transition metal cations (9–12, 25), (ii) nonmetal inorganic cations (9–12, 25, 26) such as NH_4^+ , $H_2NNH_3^+$, H_3O^+ , and $HONH_3^+$, (iii) neutral inorganic complexes (27) such as BF_3NH_3 and BH_3NH_3 , (iv) transition metal complexes (28) containing NH, OH, and CH acidic ligands (e.g., NH_3 , H_2O , and CH_3CN), (v) organic cations (9–12, 25, 26, 29, 32–36) such as PhN_2^+ , $MeNH_3^+$, $PhCH_2NH_3^+$, $PhCOCH_2NH_3^+$, $Ph_2SCH_3^+$, and $Ph_3PCH_3^+$, and (vi) neutral organic molecules (37–41) containing polar N–H (e.g., $PhNHNH_2$, $PhSONH_2$, and H_2NCSNH_2) and C–H (e.g., CH_3NO_2 , CH_3CN , $CH_3SO_2CH_3$, and $NCCH_2CN$) bonds. Molecular complexes involving cationic species have considerable strength (binding free energies = 5–15 kcal mol⁻¹ depending on the nature of the solvent) and a template effect (1,42,43) involving the cation—usually a metal ion—is often observed during the synthesis of 18-crown-6, **1**, and other crown ether derivatives. Molecular complexes involving neutral species are very much weaker (binding free energies = 0.5–5.0 kcal mol⁻¹ depending on the nature of the solvent). Apolar solvents (e.g., CH_2Cl_2 and $CHCl_3$) favor complexation. Polar solvents (e.g., MeOH and H_2O) destructure (e.g., by partial dissociation) molecular complexes and so disfavor complexation.

The X-ray crystal structures of 18-crown-6, **1**, in its uncomplexed form (44) and its molecular complexes with KSCN (45), NH_4Cl (46), BF_3NH_3 (27), *trans*- $Me_3PpCl_2NH_3$ (28), $PhCOCH_2NH_3PF_6$ (34), and $CH_3SO_2CH_3$ (39) are shown in Figure 1. Taken together with molecular mechanics calculations (33, 47), these X-ray crystallographic data reveal that 18-crown-6, **1**, has to undergo a considerable conformational change when it binds substrates. The potential ma-

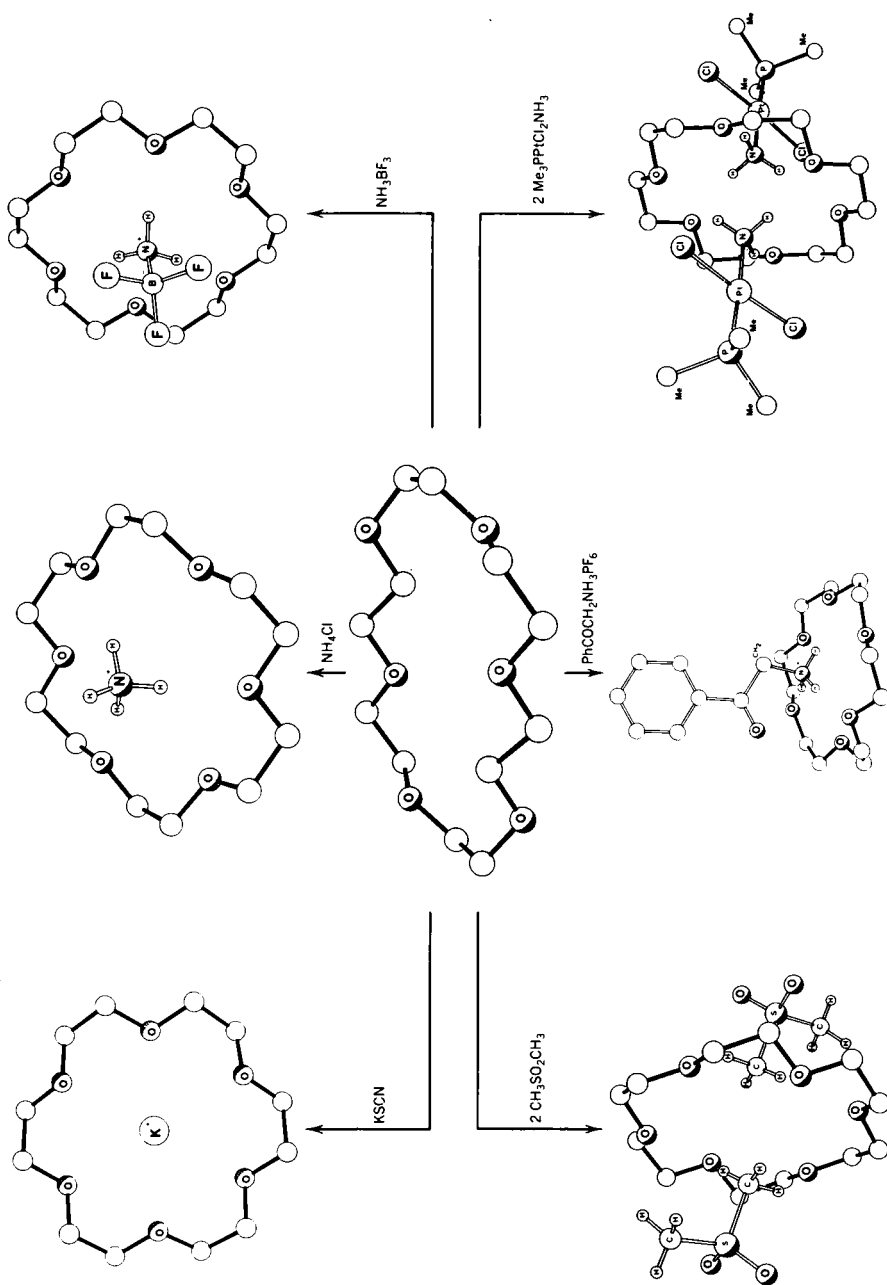
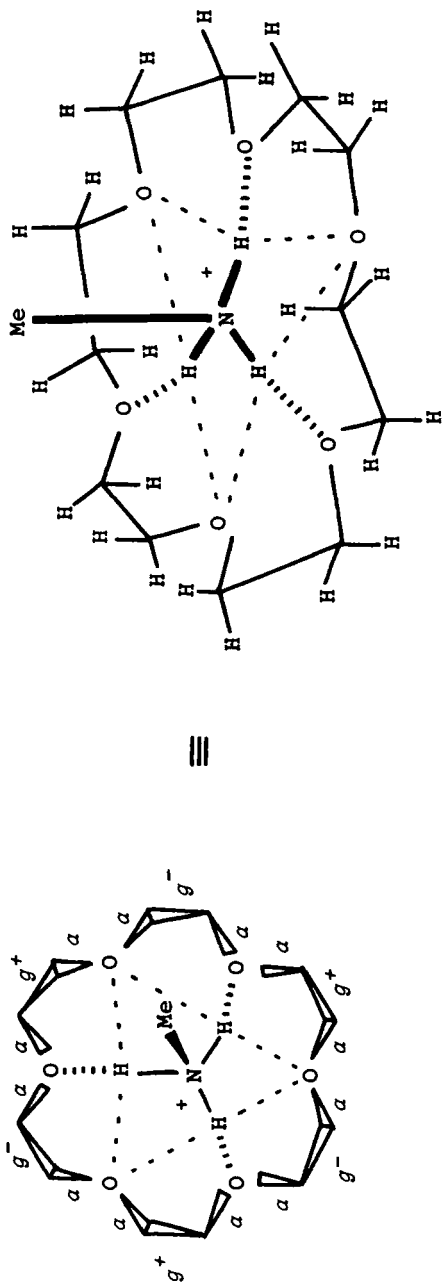


Figure 1. Framework representations of the X-ray crystal structures of 18-crown-6, 1, and its complexes with a wide range of substrates.

crocylic cavity of the free receptor is filled by two inward-pointing methylene groups and two of the six oxygen atoms have their electron pairs directed away from the center of the macrocycle. Nonetheless, 18-crown-6, **1**, forms complexes (Figure 1) with a wide range of substrates and in so doing it usually adopts a nearly ideal "crown" conformation in which the six oxygen atoms are oriented towards the principal axis of the macrocycle. In this ubiquitous "all-gauche" conformation with approximate D_{3d} symmetry, the sequence of torsional angles (O—C, C—C, C—O) in the symmetrically independent portions of the ring reads $ag^+a\ ag^-a$. Whereas the torsional angles about the anti (*a*) C—O bonds are close to the expected 180° , those about the gauche (*g*) C—C bonds are usually opened out a little to $65\text{--}70^\circ$. Clearly, the K^+ ion in **1**- K^+ is best located at the center of the ring on both steric and electronic grounds. However, all the other substrates illustrated in Figure 1 are obliged to form face-to-face complexes with 18-crown-6, **1**. Charged (e.g., NH_4^+ and $PhCOCH_2NH_3^+$) and highly polar (e.g., BF_3NH_3) substrates form only 1:1 complexes since presumably (32) the docking of a second substrate molecule to the opposite face of the macrocycle is discouraged by electrostatic repulsion between the two substrate molecules. However, neutral substrates (e.g., *trans*- $Me_3PPtCl_2NH_3$ and $CH_3SO_2CH_3$)—and even charged substrates (e.g., $Ph_2SCH_3^+$ and $Ph_3PCH_3^+$) where the formal positive charge is not associated directly with the binding site (i.e., the CH_3 groups) on the substrate—very often form 2:1 complexes.

In the binding of substrates with $-NH_3^+$ or $-CH_3$ centers to 18-crown-6, **1**, the three trigonally disposed N—H or C—H acidic hydrogen atoms are available for $[X-H \cdots O]$ hydrogen bonding (where $X = N^+, N$, or C) to three alternate oxygen atoms on the macrocyclic ring. This tripod arrangement, associated with the three-point binding model first proposed by Cram (30, 48–53), is illustrated diagrammatically in Figure 2 for the 1:1 complex **1**- $MeNH_3^+$. Lehn (54) has expressed the opinion, which is supported by calculations, that the binding is essentially electrostatic in nature with the formal positive charge on the $-NH_3^+$ group located on the three *hydrogen* atoms: Thus, the interaction with the ring oxygen atoms involves two arrays of three linear (strong) and six bent (weak) $[N-H^+ \cdots O]$ hydrogen bonds. Cram and co-workers (53) have estimated that a third of the total binding free energy arises from the weaker interactions. The space-filling representations (Figure 3) of the X-ray crystal structure (26) of **1**- $MeNH_3^+$ bears witness to the elegance of the match between the receptor and its substrate. One overwhelming message that emerges from the structural information encapsulated in Figures 1–3 is the preference for the C—C bond in $-OCH_2CH_2O-$ units to adopt an "all-gauche" conformation even in the absence of a bound substrate. It seems extremely likely that the helicity associated with such a gauche effect augments (43) the template effect during the synthesis of 18-crown-6, **1**, and other crown ether derivatives.



(a)

(b)

Figure 2. A diagrammatic representation of the face-to-face complex between 18-crown-6, 1, and the MeNH_3^+ ion.

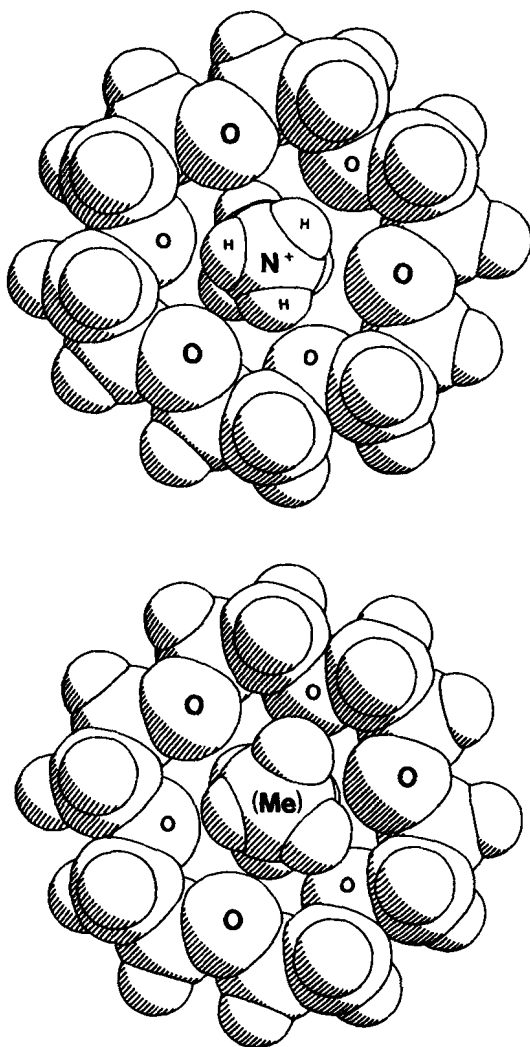


Figure 3. Space-filling representations of the X-ray crystal structure of 1-McNH₃⁺.

The observation (55) that the strengths of complexation of alkali metal and substituted ammonium ions in solution are dramatically impaired in the case of stereoisomerically related 18-crown-6 derivatives by introducing either conformational or configurational impediments that disfavor or even prevent the formation of the "all-gauche" conformation by the macrocyclic ring, raises (56–60) the issue of the importance of directionality in dictating the strengths of

noncovalent bonding interactions. Inspection of the X-ray crystal structures of the face-to-face complexes illustrated in Figure 1 reveals that, in *all* the examples cited, the hydrogen bonding involves the nearer triangular trio of oxygen atoms on the complexed face of the macrocycle, leaving those located on the opposite side to participate in interactions that are formally electrostatic in nature. This particular geometry of binding corresponds to the so-called (26, 32, 52) *perching* arrangement. It is characterized (32, 56–62) by a consistent tendency for the $[X-H \cdots O]$ hydrogen bonds to approach the accepting oxygen atoms trigonally rather than tetrahedrally. By contrast, the angles of approach (θ_X) of the $X \cdots O$ vectors to the respective COC planes show a consistent tendency towards tetrahedral ($\theta_X = \text{ca. } 55^\circ$) geometry. An idealized model for a perching substituted ammonium ion complexed to one face of 18-crown-6 **1** is illustrated in Figure 4. This arrangement, in which the nitrogen atom on the $-\text{NH}_3^+$ center lies somewhere between 0.9 and 1.2 \AA above the mean plane of the six oxygen atoms, is by far the most common. However, the other extreme situation, the so-called (26, 32, 52) *nesting* arrangement, has been observed (i) in the crys-

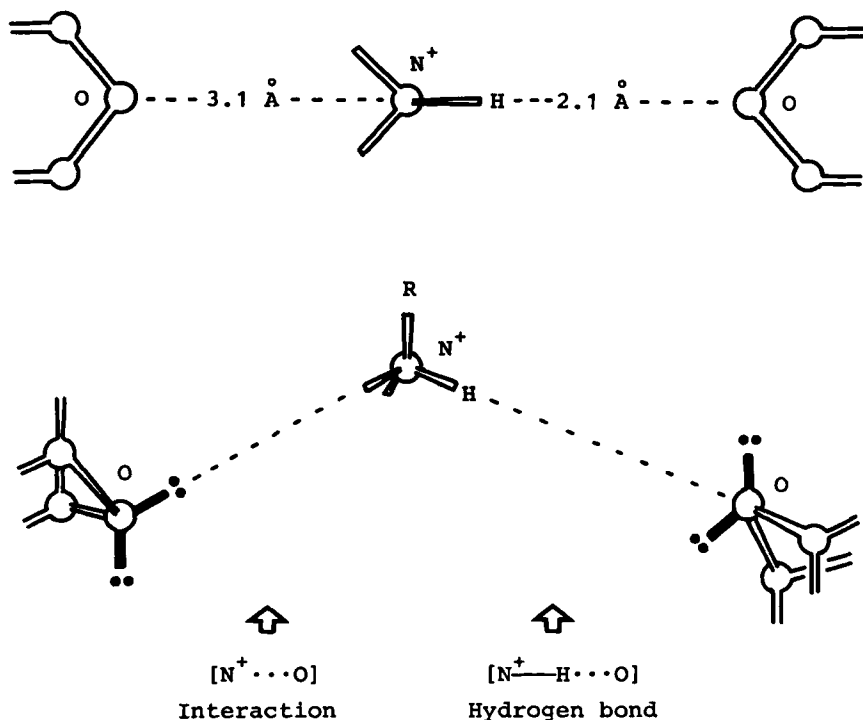


Figure 4. The stereoelectronic characteristics between a perching ammonium ion and 18-crown-6, **1**.

talline 1:1 complex formed (26) between H_2NNH_3^+ and 18-crown-6, **1**, and (ii) in the crystalline 2:1 complex formed (36) between $\text{Ph}_3\text{PCH}_3^+$ and 18-crown-6, **1**. In both cases, the binding centers (i.e., $-\text{NH}_3^+$ and $-\text{CH}_3$) on the substrate penetrate further towards the middle of the macrocyclic ring. The complex 1-HONH_3^+ provides a rare example, in the solid state at least, of an intermediate geometry of binding that is between the nesting and perching arrangements. Although the stereochemical features of the primary binding sites in 18-crown-6, **1**, are now well defined in structural terms, the implications for binding strengths are less clear and much fundamental work remains to be done.

Apart from metal ion complexation (3–12), the receptor properties of the homologous series of $3n$ -crown- n ethers ($n = 1, 2, 3, 4$, etc.) has been little investigated. An interesting exception is provided by 21-crown-7, **2**, which forms a crystalline 1:1 complex with *p*-methoxyphenyldiazonium tetrafluoroborate (63). The X-ray crystal structure (Figure 5) of $2\text{-}p\text{-MeOC}_6\text{H}_4\text{N}_2^+$ reveals (64) that the positively charged diazonium group is fully inserted into the hole of the receptor in accordance with earlier predictions (29, 30, 65) for 1-ArN_2^+ complexes. Indeed, X-ray crystallography has also confirmed (66) that 1-PhN_2^+ has a very similar structure to that shown for $2\text{-}p\text{-MeOC}_6\text{H}_4\text{N}_2^+$ in Figure 5. In solution, the complexation of arenediazonium salts by 18-crown-6, **1**, is highly sensitive (67) to both steric (e.g., substituents in the ortho positions to the diazonium group prevent complexation) and electronic factors (e.g., substituents on the aromatic ring that assist in delocalization of the positive charge on the diazonium group weaken complexation).

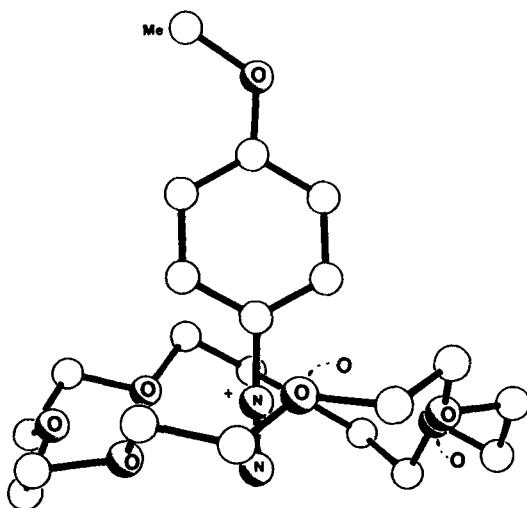
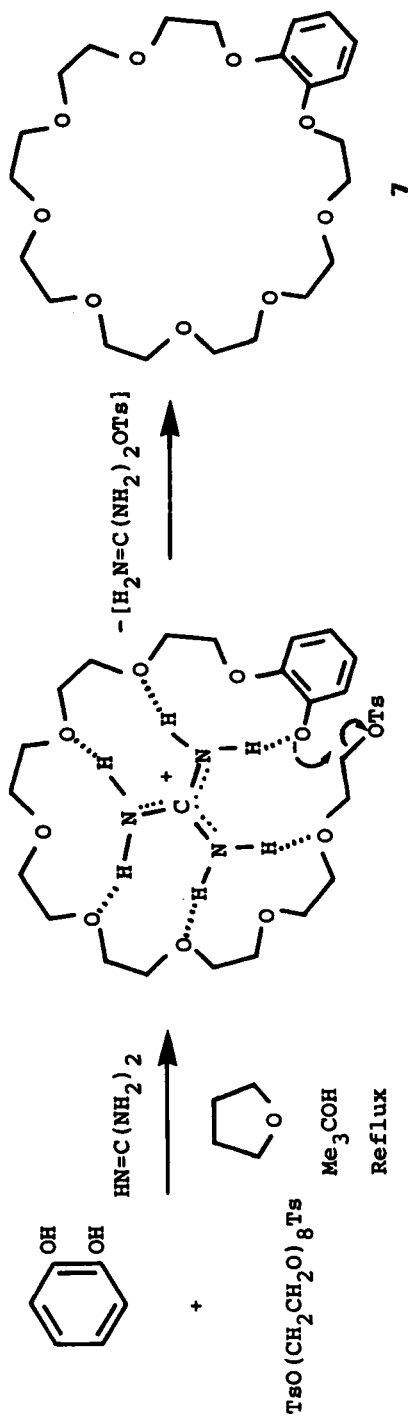


Figure 5. A framework representation of the X-ray crystal structure of $2\text{-}p\text{-MeOC}_6\text{H}_4\text{N}_2^+$.



Scheme 1.

Success in complexing larger organic cations through encirclement or encapsulation by crown ether receptors is enhanced when benzo rings are fused on to the $3n$ -crown- n framework, as in 3–6. Three examples are worthy of brief consideration in the context of this review.

An early suggestion (29) that the guanidinium ion can act as a template during the synthesis (Scheme 1) of benzo-27-crown-9, **7**, from catechol and octaethylene glycol bistosylate has received strong support from the isolation and characterization (68) of a crystalline 1:1 complex between **7** and guanidinium perchlorate. The dibenzo-27-crown-9, **4**, and dibenzo-30-crown-10, **5**, (*p* 210) derivatives also afford crystalline 1:1 complexes with the same substrate. The X-ray crystal structure of $7\text{-H}_2\text{N}=\text{C}(\text{NH}_2)_2\text{ClO}_4$, which is reproduced in Figure 6, shows that the molecular complex is stabilized in a highly efficient manner by six approximately linear $[\text{N}-\text{H} \cdots \text{O}]$ hydrogen bonds involving all three $-\text{NH}_2$ groups in the substrate and six of the nine oxygen atoms in the receptor. Benzo-27-crown-9, **7**, also forms a very similar 1:1 complex with uronium nitrate in the solid state (69). Both guanidinium and uronium salts can be extracted from their aqueous solutions into organic solvents containing crown ether receptors such as **4**, **5**, and **7**.

The discovery (70) that $[\text{Pt}(\text{bipy})(\text{NH}_3)_2]^{2+}$ is encapsulated in both the solid and solution states by the constitutionally symmetrical dibenzo-30-crown-10 derivative **6** (*p* 210) has led (71) to the realization that this easily accessible

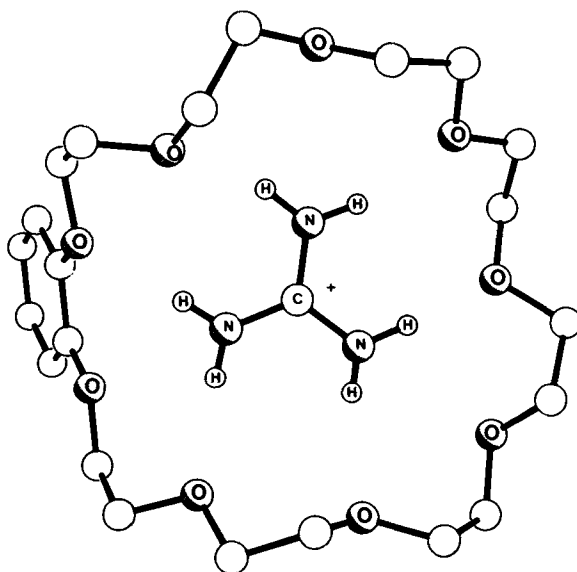
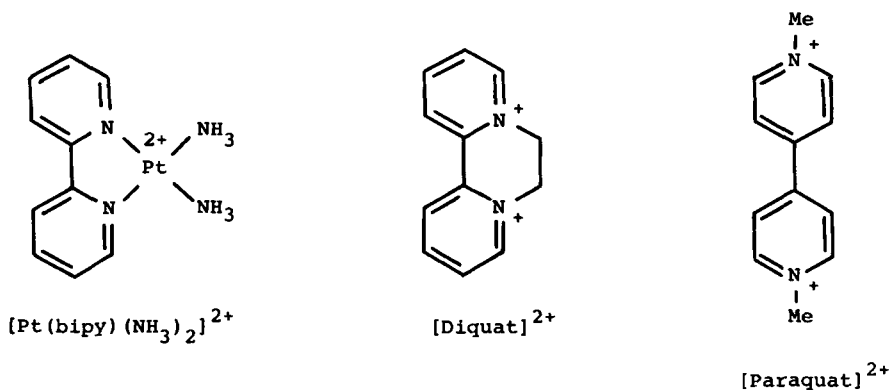


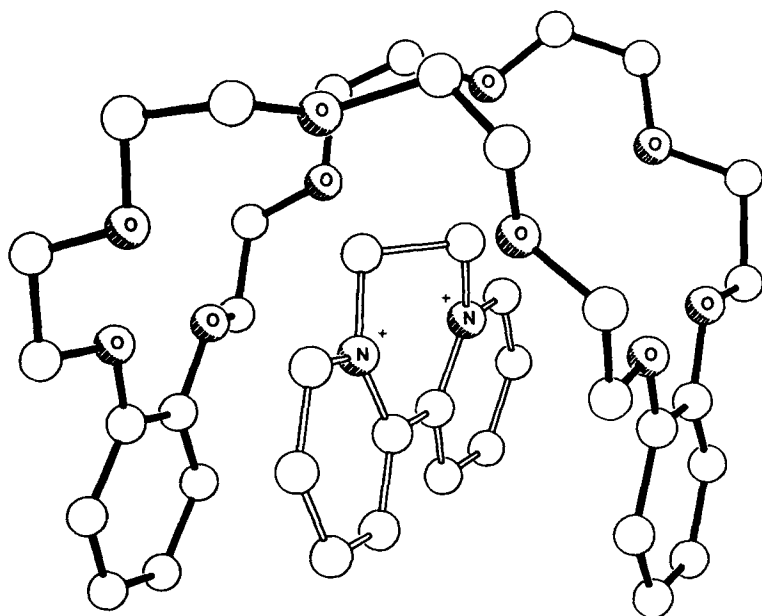
Figure 6. A framework representation of the X-ray crystal structure of $7\text{-H}_2\text{N}=\text{C}(\text{NH}_2)_2^+$.

(25) crown ether derivative provides an excellent molecular receptor for the bipyridinium herbicide, $[\text{Diquat}]^{2+}$. Although **6** does *not* complex with the sister herbicide of $[\text{Diquat}]^{2+}$, namely, $[\text{Paraquat}]^{2+}$, the constitutionally isomeric bismetaphenylene-32-crown-10, **8**, and bisparaphenylene-34-crown-10, **9**, derivatives are strikingly successful (72) in binding $[\text{Paraquat}]^{2+}$ as well as $[\text{Diquat}]^{2+}$. Whereas Diquat salts are extracted into organic solvents from their aqueous solutions by all three [**6**, **8**, and **9**] crown ether derivatives, only **8** and **9** will transport Paraquat salts from aqueous solutions into organic solvents.

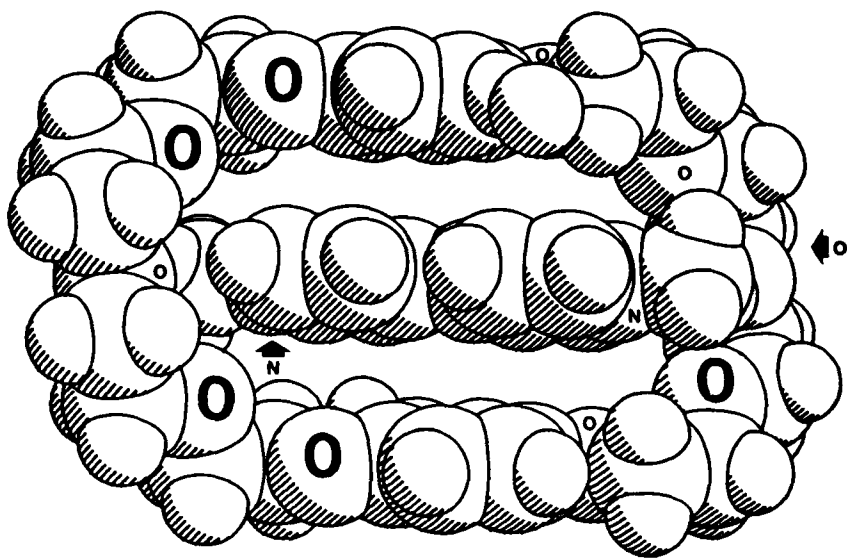
The X-ray crystal structures (Figure 7) of **6**- $[\text{Diquat}]^{2+}$ and **9**- $[\text{Paraquat}]^{2+}$ demonstrate that complex formation is aided not only by $[\text{C}-\text{H} \cdots \text{O}]$ hydrogen bonding and $[\text{N}^+ \cdots \text{O}]$ electrostatic interactions but also by charge transfer stabilization between the π electron rich aromatic rings in the molecular receptors and the π electron deficient bipyridinium rings in the substrates.

The introduction of nitrogen-containing functions (e.g., NMe) into the crown ether constitution has a profound effect (73) on both the structures and strengths of molecular complexes with organic substrates.





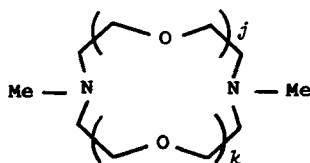
(a)



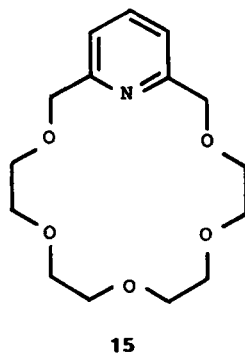
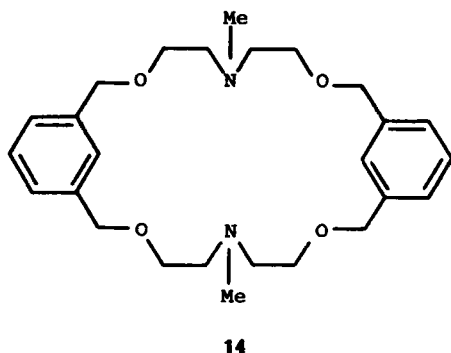
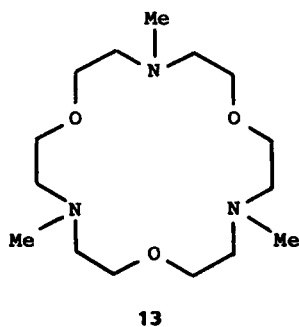
(b)

Figure 7. Model representations of the X-ray crystal structures of (a) 6-[Diquat]²⁺ and (b) 9-[Paraquat]²⁺.

As far as RNH_3^+ ions are concerned, the strengths of the complexes with 18-crown-6, **1**, in methanol decrease (74) in the order $\text{NH}_4^+ > \text{RNH}_3^+ > \text{R}_2\text{NH}_2^+ > \text{R}_3\text{NH}^+$ to the extent that **1** does not bind to R_4N^+ ions (75), cf. the complexation (36) of the $\text{Ph}_3\text{PCH}_3^+$ ion by 18-crown-6, **1**. However, the *N,N'*-dimethyl-1,7-diaza-12-crown-4 derivative **10** complexes just as well with dialkylammonium ions as with primary alkylammonium ions (76). This is presumably because only two-point binding is possible between the substrates and the receptor **10**, given its considerably smaller ring size of 12. The X-ray crystal structure (Figure 8) of **10**- $\text{PhCH}_2\text{NH}_3\text{SCN}$ not only supports this hypothesis but also reveals (59, 77) that the complex utilizes two $[\text{N}^+-\text{H} \cdots \text{NMe}]$ in preference to two $[\text{N}^+-\text{H} \cdots \text{O}]$ hydrogen bonds. The enhanced hydrogen-bonding ability of nitrogen over oxygen acceptors has been exploited in numerous different directions by Sutherland (73, 78) and Lehn (12-16, 79) using the *N,N'*-



	<i>j</i>	<i>k</i>
10	1	1
11	2	1
12	2	2



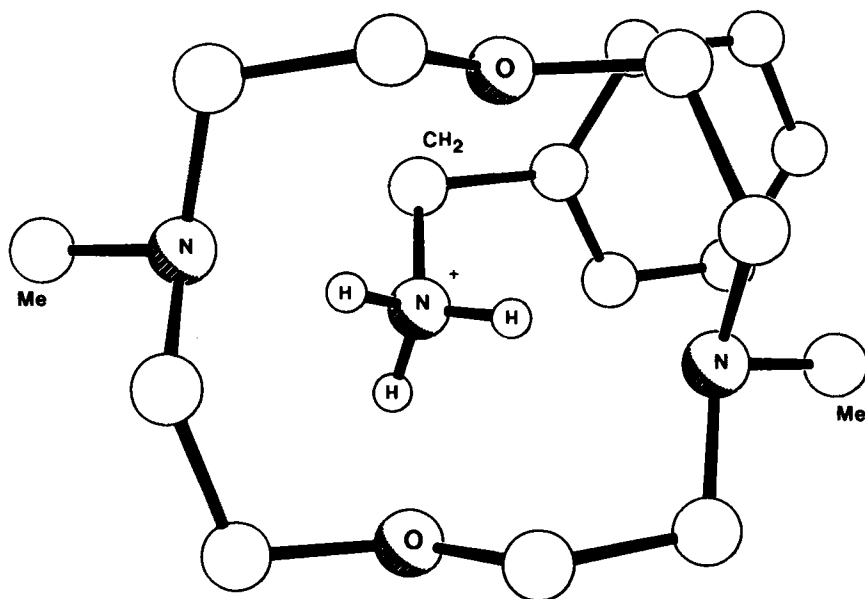


Figure 8. A framework representation of the X-ray crystal structure of **10**-PhCH₂NH₃SCN.

dimethyl-1,7-diaza-15-crown-5, **11**, *N,N'*-dimethyl-1,10-diaza-18-crown-6, **12**, and *N,N',N''*-trimethyl-1,7,13-triaza-18-crown-6, **13**, derivatives as points of departure for even larger receptor molecules, for example, the elaboration of cylindrical macropolycycles for substrate recognition at the constitutional level.

As with the all-oxygen crown ethers, interesting results emerge when the ring size is increased beyond 18. Thus, the diaza-24-crown-6 derivative **14** crystallizes with two equivalents of PhCH₂NH₃SCN to give a centrosymmetric structure (Figure 9) in which the substrate ions are located on opposite faces of the macrocycle such that the —NH₃⁺ centers are well separated from each other (80). Again, the atoms in the receptor molecule provide the acceptors for single [N⁺—H ··· NMe] hydrogen bonds involving each —NH₃⁺ group. The benzyl groups occupy the cavities defined by the remainder of the macrocycle and its associated aromatic rings.

Substitution of —CH₂OCH₂— fragments in 18-crown-6, **1**, by pyridine rings has provided (81) another valuable range of receptor molecules blessed not only with good hydrogen-bond acceptor atoms in the form of the *sp*² hybridized nitrogen atoms but also with built-in rigidity. The X-ray structure (Figure 10) of the stable crystalline 1 : 1 complex formed between the monopyrido-18-crown-6 derivative **15** and *t*-butylammonium perchlorate confirms that the Me₃CNH₃⁺ ion forms hydrogen bonds with two ether oxygen atoms and the pyridyl nitrogen

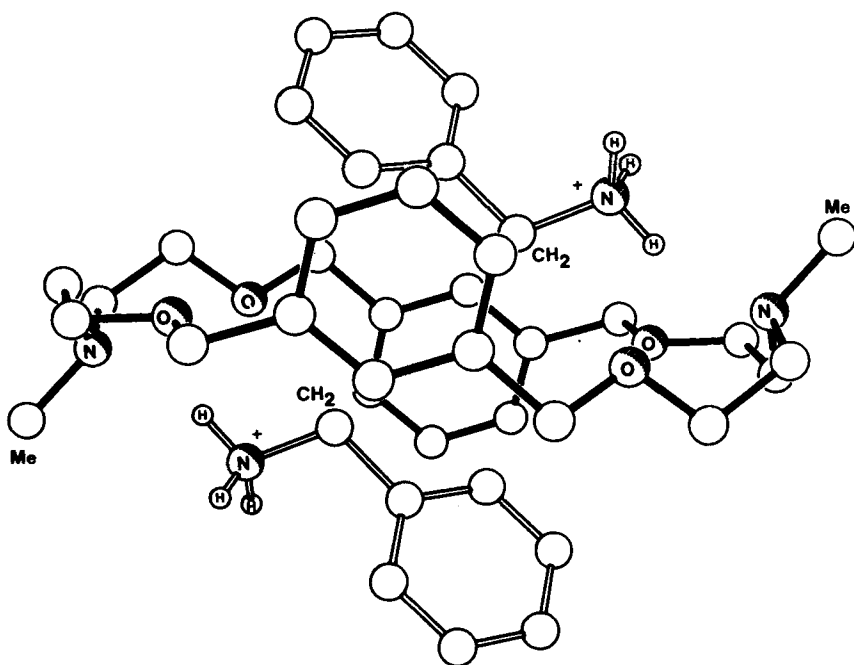


Figure 9. A framework representation of the X-ray crystal structure of 14-(PhCH₂NH₃⁺)₂.

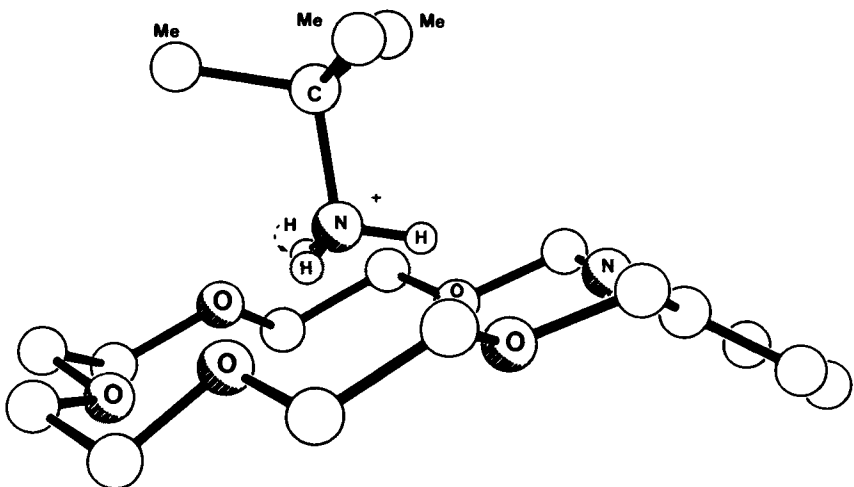
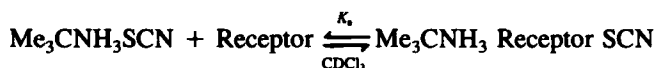


Figure 10. A framework representation of the X-ray crystal structure of 15-Me₃CNH₃⁺.

atom rather than with three ether oxygen atoms (82). This choice of superstructure is entirely in accord with a comparative analysis (83) of the free energies of complexation of $\text{Me}_3\text{CNH}_3\text{SCN}$ in CDCl_3 solutions by a range of 18-crown-6 derivatives containing either two or three pyridine rings.

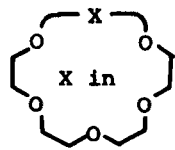
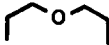
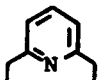
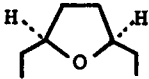
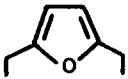
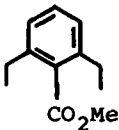
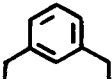

The dependence of the stabilities of complexes formed with $\text{Me}_3\text{CNH}_3^+$ ions on the constitutions of a range of 18-crown-6 derivatives has been investigated by a two-phase extraction procedure using CDCl_3 and D_2O . An ^1H NMR spectroscopic method can be employed to measure the extent of transfer of $\text{Me}_3\text{CNH}_3\text{SCN}$ from the D_2O layer into the CDCl_3 layer containing the receptor compound and so obtain a stability constant (K_a) and a derived free energy of complexation (ΔG°) in CDCl_3 for the equilibrium:

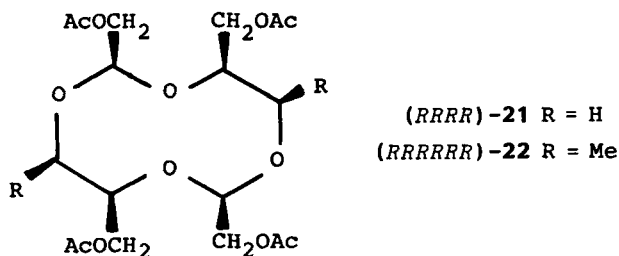


The K_a and ΔG° values listed in Table 1 for the various 18-crown-6 derivatives **15–20** demonstrate how constitutional modifications of 18-crown-6, **1**, can influence dramatically the complexing abilities of this receptor type to $\text{Me}_3\text{CNH}_3^+$ ions. In **15**, the stronger hydrogen-bonding potential of the pyridyl nitrogen atom is reflected in its K_a value being higher than that for **1**. The relative magnitudes of the K_a values for **16** and **17** reflect the fact that, while tetrahydrofuranyl oxygen atoms are more basic than “ordinary” ether oxygen atoms, furanyl oxygen atoms are considerably less basic. Steric factors associated with increased rigidity in receptors **15–17** compared with **1** may also be dictating better cooperativity in the binding of $\text{Me}_3\text{CNH}_3^+$ ions. Clearly, however, the rigid *m*-xylyl units present in **18** and **19** are a major impediment to complex formation, even when a binding site is provided in the form of a CO_2Me group. Not surprisingly, replacement of one of the oxygen atoms in **1** by a CH_2 group to afford **20** has a devastating effect on its complexing ability. No less than half the energy of complexation is sacrificed. The importance of constitutional factors in dictating the complexing efficiencies of molecular receptors of the crown ether type cannot be overstated.

The first reports of synthetic chiral saturated heterocycles with obvious similarities to crown ethers and aza-crown compounds relied on natural products as starting materials. In 1968, D-ribose and 6-deoxy-D-allose were employed (84) in the synthesis of the 10-crown-4 derivatives, (*RRRR*)-**21** and (*RRRRR*)-**22**. No molecular complexes involving these chiral tetraoxacyclodecanes have been characterized. However, this is hardly surprising in view of the interruption of the almost essential bismethylenedioxy repeating units present in most crown compounds by two acetal linkages in these carbohydrate-derived medium-sized

Table 1
The Dependence of the Stabilities of Complexes Formed with Me₃CNH₃SCN on the
Constitutions of a Range of 18-Crown-6 Derivatives in CDCl₃ at 25 °C

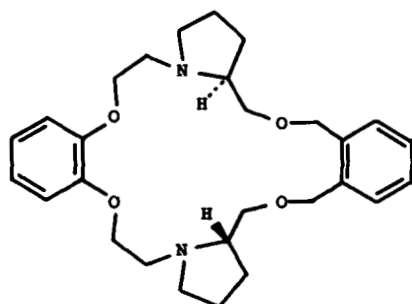
		K_a (l mol ⁻¹)	$-\Delta G^\circ$ (kcal mol ⁻¹)
	1	3,000,000	8.80
	15	5,800,000	9.20
	16	4,180,000	9.01
	17	209,000	7.24
	18	55,600	6.50
	19	3,300	4.78
	20	1,650	4.38



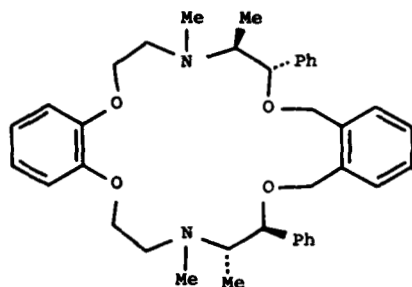
ring compounds. The synthesis of two chiral diaza-crown compounds, LL-23 and DD-24, from L-proline and D- ψ -ephedrine, respectively, as the chiral precursors were reported (85) in 1972. This time, the two chiral diaza-20-crown-6 derivatives were found to form complexes with alkali metal and alkaline earth metal cations in neutral media.

The first chiral crown ethers to exhibit chiral recognition towards enantiomeric substrates were described by Cram (86) in 1973. They [e.g., (*S*)-25 and (*SS*)-26] were prepared from optically pure 2,2'-dihydroxy-1,1'-binaphthyl, which can be obtained after resolution of the binaphthol by a number of different methods (87). The isolation of optically pure enantiomers of this diol reflects its axis of chirality resulting from hindered rotation about its naphthalene-naphthalene bond. Both the binaphthyl-20-crown-6 (*S*)-(25) and the bisbinaphthyl-22-crown-6 (*SS*)-(26) derivatives bear some structural resemblance to 18-crown-6, 1. However, the fact that the bismethylenedioxy repeating unit is perturbed by binaphthyl residues and some of the aliphatic oxygen atoms are necessarily replaced by less basic aryl oxygen atoms plays havoc with the strengths of complexes formed with primary alkylammonium ions. Nonetheless, a chloroform solution of the chiral receptor molecule (*SS*)-26 is capable (48), at -14°C of extracting twice as much of the (*R*)-enantiomer as of the (*S*)-enantiomer from (*RS*)-PhCHMeNH₃PF₆ dissolved in a 2.5 *M* aqueous solution of NaPF₆.

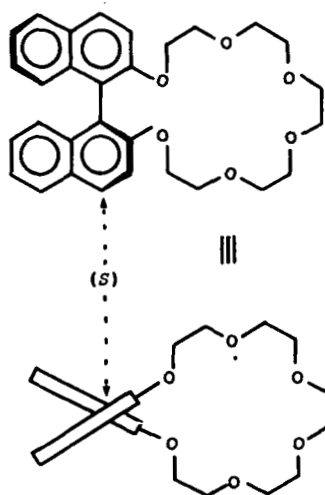
D-Mannitol and L-tartaric acid served as precursors to the first chiral 18-crown-6 derivatives reported (88) in 1975. In the D-mannitol series, the 1,2:5,6-di-*O*-isopropylidene derivative was the key intermediate in the synthesis of the 18-crown-6 derivatives DD-27 to DD-30. The key intermediate in the synthesis of LL-31 to LL-34 was 1,4-di-*O*-benzyl-L-threitol, which can be synthesized from L-tartaric acid in five steps. Simultaneously with the publication of these results, Lehn and co-workers (89) described the preparation of the chiral 18-crown-6 derivatives LL-35 containing four carboxamide groups from L-tartaric acid via its bis (*N,N*-dimethylamide). While LL-35 was reported (89) to change its specific optical rotation on addition of metal (e.g., Na⁺, K⁺, Rb⁺) and NH₄⁺ ions, DD-27 and LL-34 exhibited (90) enantiomeric differentiation [(*R*):(*S*) = 62:38



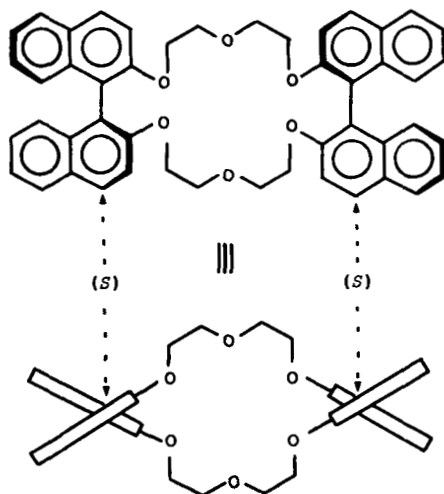
LL-23



DD-24



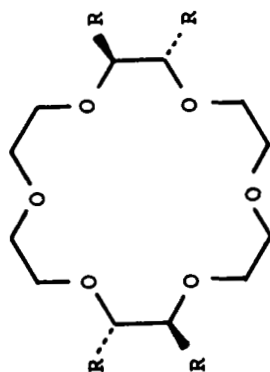
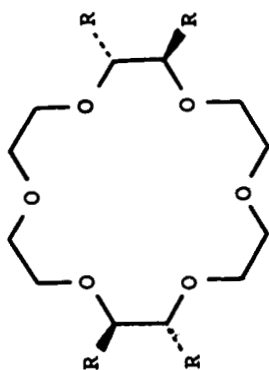
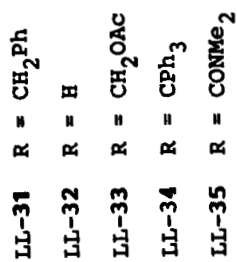
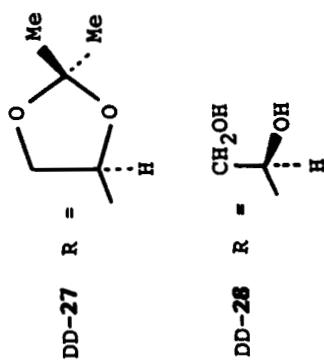
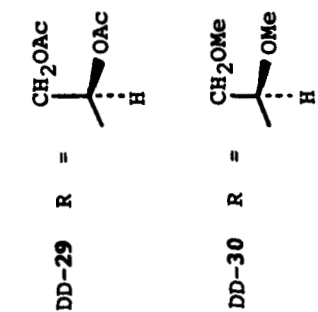
(S)-25



(SS)-26

for DD-27 and (*R*):(*S*) = 40:60 for LL-34] in complexation equilibrium experiments with (*RS*)-PhCHMeNH₃PF₆ similar to that described previously for the receptor (*SS*)-26.

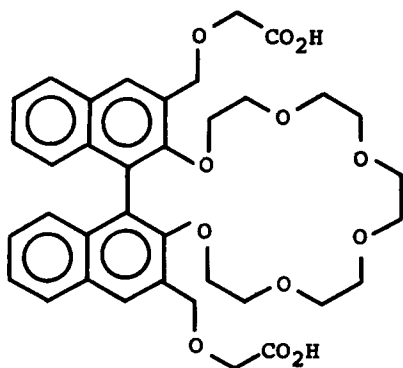
We shall now consider the synthesis of chiral crown ethers from the viewpoints of strategies and some recent accomplishments. For a detailed discussion of the earlier work on the synthesis of chiral crown ethers from natural product precursors, the reader is referred to reviews (91, 92) that appeared in the literature in 1981 and 1982.



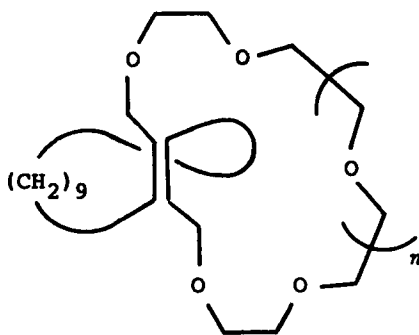
III. SYNTHESIS OF CHIRAL CROWN ETHERS

The various strategies available for the synthesis of crown ethers have been analyzed (12, 17–19, 43) and reviewed (1–10, 20) at considerable length. In principle, the problem of introducing chirality into crown compounds can be tackled in three different ways.

1. Racemic modifications may be resolved. There are very few examples of this approach having been employed successfully. The racemic cyclic ether (*RS*)-**36**, which contains two $\text{CH}_2\text{OCH}_2\text{CO}_2\text{H}$ arms attached to the 3 and 3' positions on the axially chiral binaphthyl units, has been resolved (48–50, 93, 94) to optical purity in both its enantiomers by liquid–liquid chromatography using a chiral stationary phase of either (*R*)- or (*S*)-valine adsorbed on diatomaceous earth. Very recently, the optical resolution of crown ethers (*RS*)-**37** and (*RS*)-**38**, incorporating the elements of planar chirality in the form of a *trans*-doubly bridged ethylene unit, has been achieved (95) by HPLC on (+)-poly(triphenylmethyl methacrylate).
2. Enantioselective synthesis, starting from prochiral or racemic precursors (involving kinetic resolution in the latter case) could, in principle, be utilized. No examples of this kind of approach yielding positive results are known to the reviewer.
3. Stereospecific synthesis, starting from chiral precursors, has been exploited in many different ways (91, 92). Apart from the usual demands incurred during synthetic work, symmetry considerations (49, 50, 56–59, 91) impose an additional constraint upon the design and synthesis of chiral crown compounds. Generally speaking, it is desirable to prepare



(*RS*)-**36**



(*RS*)-**37** $n = 1$

(*RS*)-**38** $n = 2$

macrocyclic polyethers in which the two faces are homotopic. With this arrangement, we can ensure that complexation involving facial binding of a substrate to the macrocyclic ring leads to the formation of only *one* complex. This is most easily accomplished by selecting chiral precursors containing C_2 symmetry and then bringing about macrocyclic ring formation (usually involving the making of C—O or C—N bonds) in the

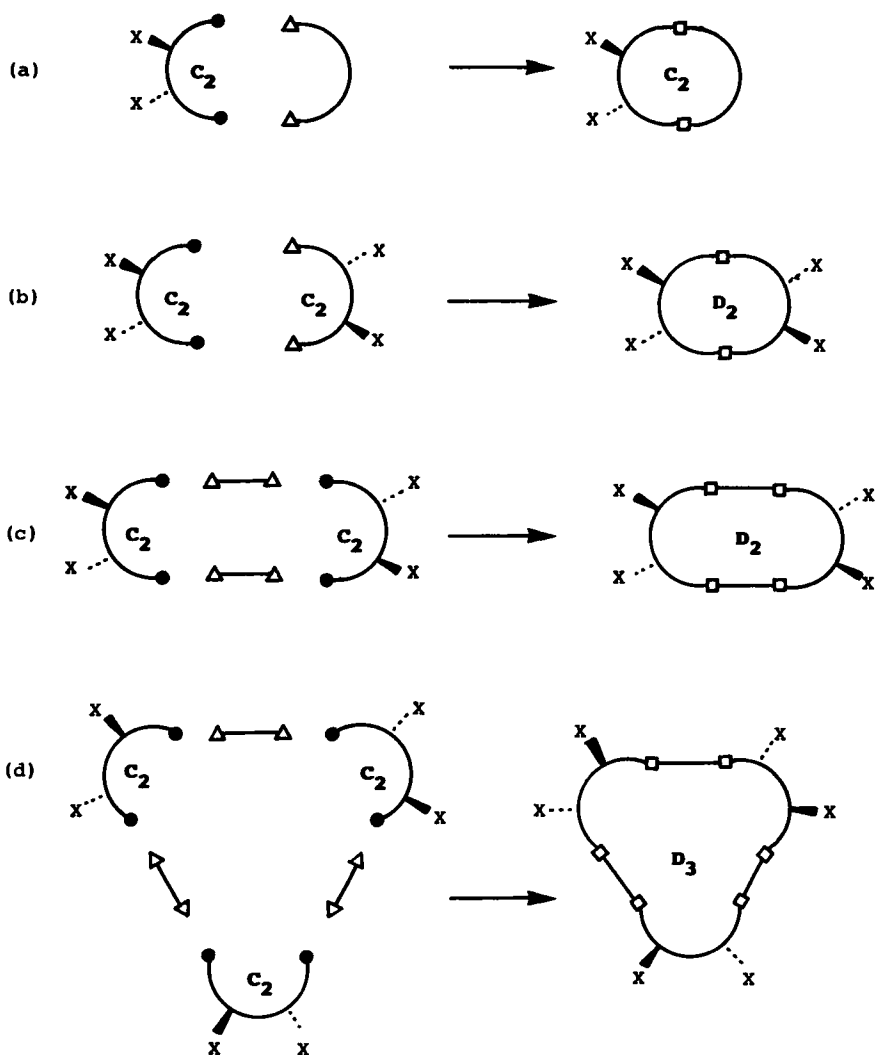


Figure 11. Some synthetic strategies leading to chiral crown compounds with homotopic faces starting from chiral precursors with C_2 symmetry.

conventional manner. Figure 11 outlines some of the synthetic strategies available to the bench chemist for the construction of chiral molecular receptors with homotopic faces. Examples of macrocycles with C_2 , D_2 , and D_3 symmetries are cited. Although less easy to accomplish, macrocycles with homotopic faces and the same range of symmetries can be fashioned (Figure 12) out of asymmetric precursors. Finally, asymmetric precursors can afford (Figure 13) either asymmetric or axially symmetric macrocycles with heterotopic faces. The synthetic strategies outlined in Figures 11–13 only give a flavor for what is possible. Many additional variations can be imagined and proposed. In the remainder of this section, numerous examples of the synthetic strategies shown in Figures 11–13 will be described.

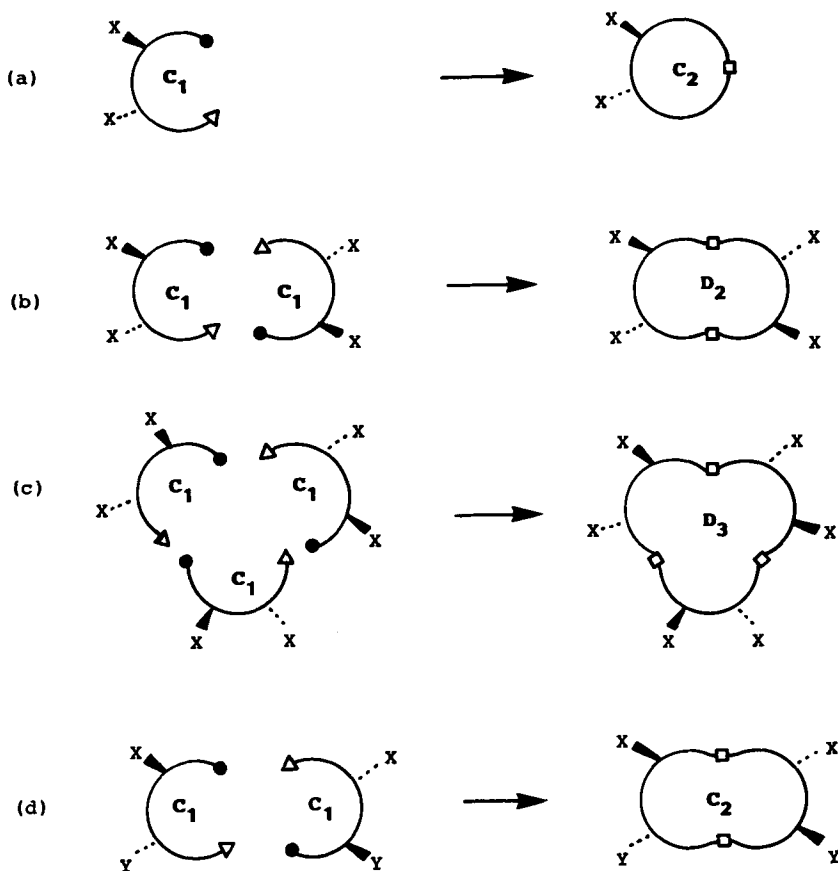


Figure 12. Some synthetic strategies leading to chiral crown compounds with homotopic faces starting from asymmetric precursors.

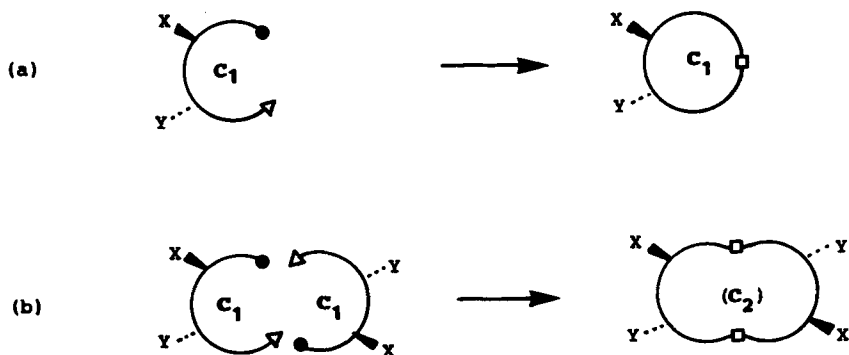


Figure 13. Two synthetic strategies leading to chiral crown compounds with heterotopic faces starting from asymmetric precursors. Note that, although the product obtained in (b) has C_2 symmetry, the symmetry element does not exchange the environment of the two faces.

A. Substituted All-Oxygen Crown Compounds

The chiral 1,2-diols that have been incorporated into crown ether derivatives that carry substituents but have no fused rings associated with the elements of chirality in the macrocycles are listed in Figure 14. We shall now examine some of the ways in which these chiral building blocks have been used.

1. From Tartaric Acid Derivatives

The need to synthesize chiral 18-crown-6 derivatives led Lehn and co-workers (89, 96) to identify L-tartaric acid as a suitable precursor (Figure 14). Not only does it contain a chiral substituted ethylene glycol unit of known absolute configuration, but it is also readily available in optically pure form. Further, its incorporation into the 18-crown-6 constitution affords side chains directly attached to the aliphatic carbon atoms on the macrocyclic ring with functionality that can be easily modified chemically. A one-step synthesis of a bistartaro-18-crown-6 derivative LL-35 by a modified Williamson ether synthesis (97), which relies on alkylation of the dithallium alcoholate of the bis(*N,N*-dimethylamide) of L-tartaric acid with the appropriate diiodide, 1,5-diiodo-3-oxapentane, has been devised (Scheme 2). It gives the same yield (20%) as the alternative two-step routes shown in the scheme. A very low yield (1%) of the tristartaro-27-crown-9 derivative was also obtained in the one-step procedure. A slightly better yield of this 27-crown-9-hexacarboxamide was obtained (96, 98) by a planned synthetic route. The 27-crown-9-hexacarboxylic acid, obtained on hydrolysis of the hexacarboxamide, forms complexes with guanidinium and imidazolium ions as well as with substituted ammonium ions. The tetracarboxamide LL-35 was

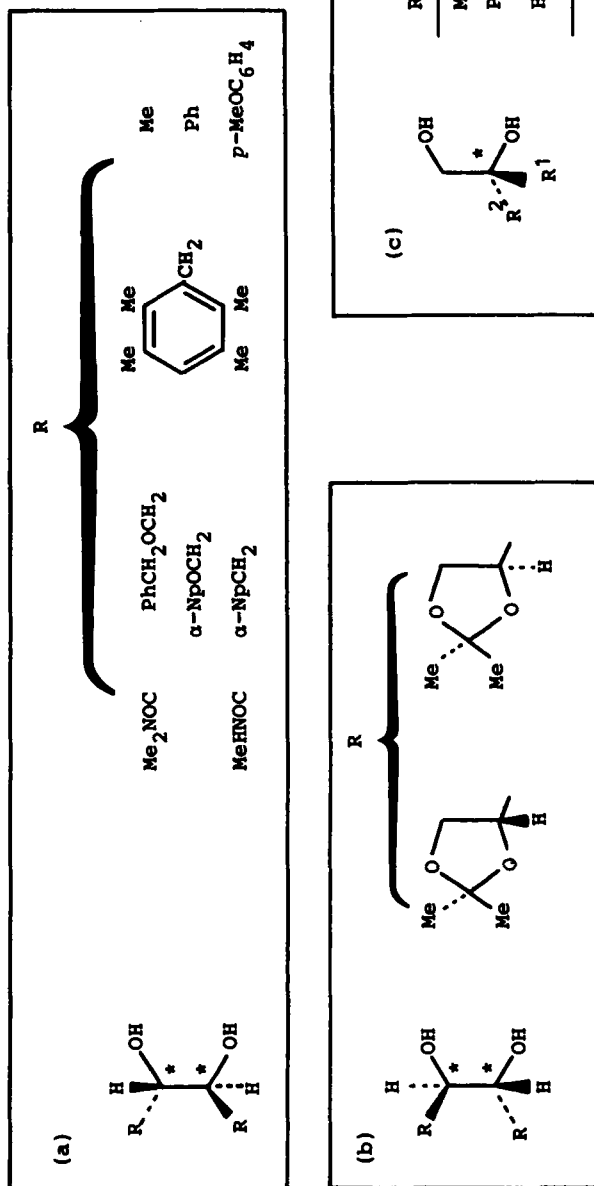
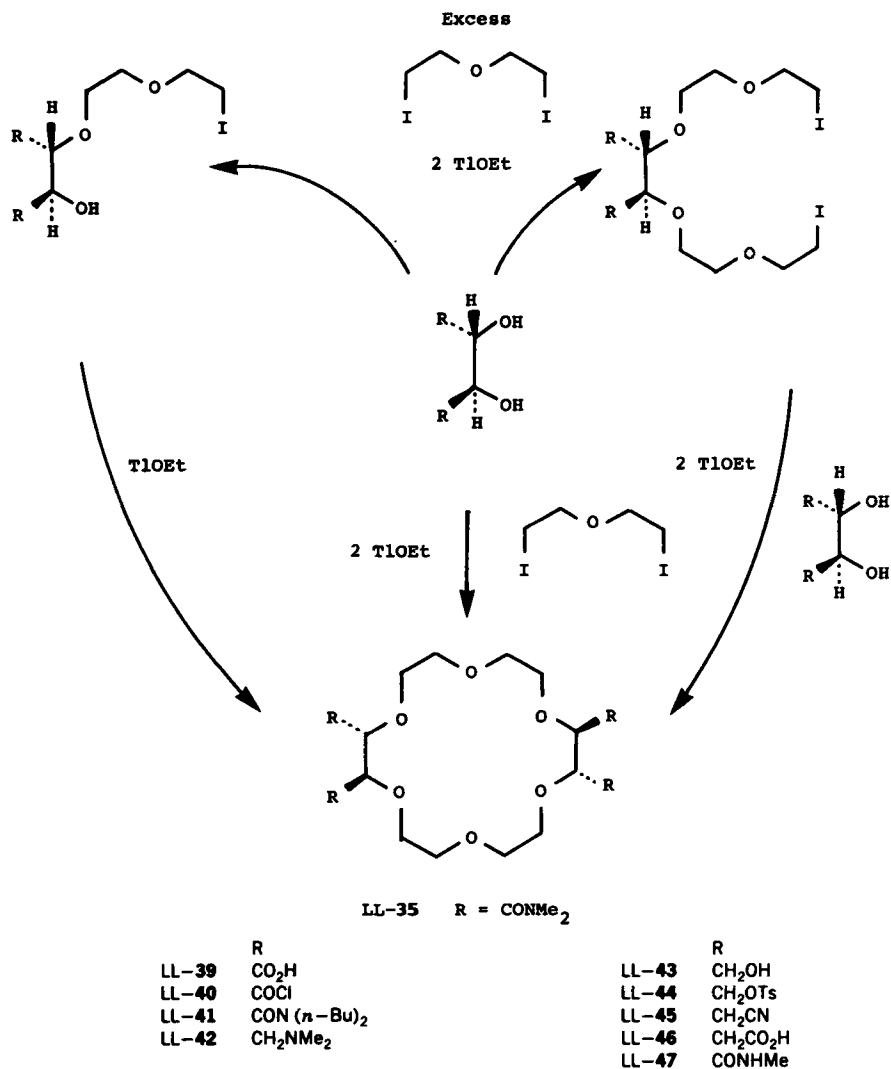


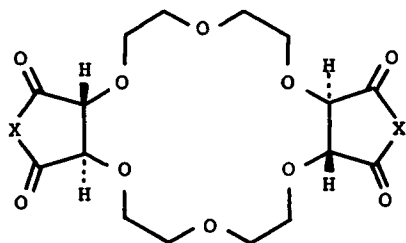
Figure 14. Chiral 1,2-diols that have been incorporated into monocyclic crown compounds. Listed under (a) are precursors with C_2 symmetry obtained from L-tartaric acid and L-threitol, as well as from (SS)-hydrobenzoin as its *p*-methoxy analog, under (b) are precursors with C_2 symmetry obtained from D-mannitol and L-iditol, and under (c) are asymmetric precursors obtained from (S)-lactic acid, (S)-mandelic acid, and L-glyceraldehyde dithioethylacetal.



Scheme 2. Different synthetic approaches to the bistartaro-18-crown-6 derivative LL-35.

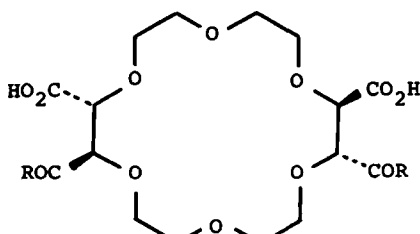
readily converted (96, 98) by conventional means into a wide range of derivatives where, for example, R is CO₂H; COCl; CON(*n*-Bu)₂; CH₂NMe₂; CH₂OH; CH₂OTs; CH₂CN; CH₂CO₂H (LL-39 to LL-46) rather than the CONMe₂ group defined in Scheme 2 for LL-35. The tetraacid chloride LL-40 was a key compound in the synthetic elaboration (98-100) of a range of bistartaro-18-crown-6 derivatives. The bistartaro-18-crown-6 derivative LL-47 where R = CONHMe was

obtained (96) from *L-N,N'*-dimethyltartaramide using a procedure identical to that described in Scheme 2 for the preparation of LL-35. Both LL-47 and LL-39 undergo ready cyclization to afford the bisimide LL-48 and the dianhydride LL-49, respectively. Reaction of LL-49 with aromatic amines such as aniline gives (101, 102) a mixture of the constitutional isomers LL-50 and LL-51 that can be separated chromatographically because the latter is much more polar than the former. Interestingly, however, if the reaction is performed in the presence of triethylamine then only one isomer—the more polar one, LL-51—is formed. The structural assignments to LL-50 and LL-51 have been confirmed by X-ray crystallography.

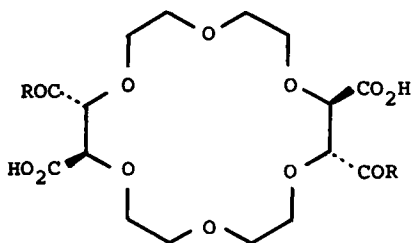


LL-48 X = NMe

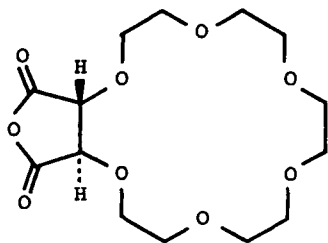
LL-49 X = O



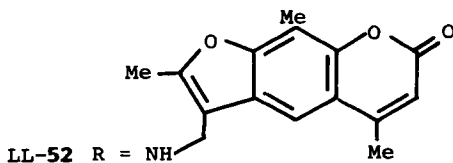
LL-50 R = NHPh



LL-51 R = NHPh



L-53



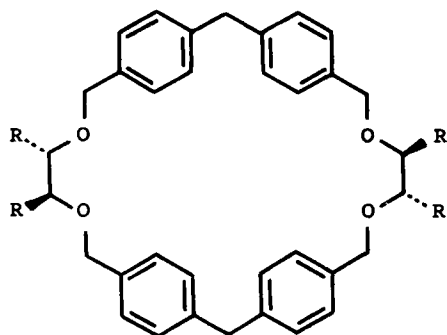
LL-52 R = NH

This remarkable regioselective opening of the anhydride rings in LL-49 has been applied (103) to the synthesis of DNA intercalating crown ether molecules. Thus, the bispsoralen-18-crown-6 derivative LL-52 was obtained in good yield from the reaction of the 18-crown-6 dianhydride LL-49 with 4'-aminomethyl-4,5',8-trimethylpsoralen in the presence of triethylamine in dichloromethane. The monotartaro-18-crown-6 anhydride L-53 (104) has been used (103) in the synthesis of the corresponding monopsoralen-18-crown-6 derivative.

The bishallium salt of L-tartaric acid bisdimethylamide has also been employed (105) in the synthesis of the chiral macrocyclic tetracarboxylic acid LL-56. Nitrosation of the macrocyclic tetramide LL-54, obtained from a (2 + 2)-cyclization of the bishallium salt with 4,7-bisbromomethyldiphenylmethane, afforded the macrocyclic tetranitroso-amide LL-55 that was treated sequentially with aqueous base and acid to give LL-56. The diphenylmethane units act as more or less rigid apolar shaping components with the polar binding L-tartaric acid residues to bind large substrate molecules such as acetylcholine and methylviologen, that is, Paraquat.

2. From Carbohydrate Derivatives

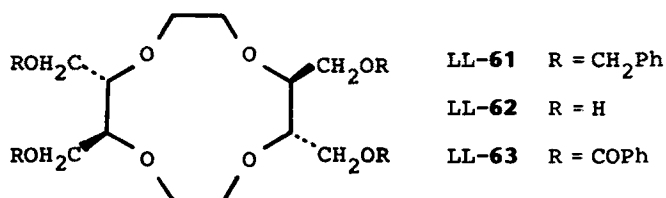
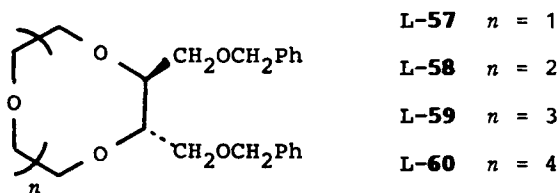
Among the 1,4-di-*O*-substituted-L-threitol derivatives (Figure 14a) the one that has found most use in chiral crown ether synthesis is the 1,4-dibenzyl ether. Not only has it provided (88, 106, 107) a ready entry into the chiral tetrasubstituted 18-crown-6 derivatives LL-31 to LL-34, but it has also proved to be a useful chiral precursor for the preparation of chiral disubstituted 9-crown-3 (107), 12-crown-4 (108), 15-crown-5 (108), and 18-crown-6 (109) derivatives L-57, L-58, L-59, and L-60, respectively. In the preparation of L-58 the base-promoted cyclization with triethylene glycol ditosylate is best carried out (108) with a



LL-54 R = CONHMe

LL-55 R = CON(NO)Me

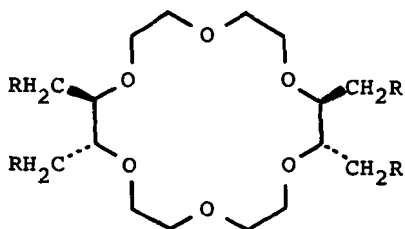
LL-56 R = CO₂H



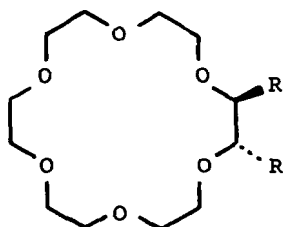
mixture of lithium and sodium hydrides. Presumably, the Li^+ ions act as a template for formation of the 12-membered ring. These reports illustrate the use of two procedures for extending the two hydroxyl groups in 1,4-di-*O*-benzyl-L-threitol by $-\text{CH}_2\text{CH}_2\text{OH}$ units. They involve either (i) alkylation of the diol with $\text{ClCH}_2\text{CH}_2\text{OTHP}$, followed by acid-catalyzed deprotection (108) or (ii) alkylation with $\text{BrCH}_2\text{CO}_2\text{H}$, followed by LiAlH_4 reduction (109). The former procedure was employed (108) in the preparation of the chiral tetrasubstituted 12-crown-4 derivatives LL-61 to LL-63.

The 1,4-ditosylate of 2,3-*O*-isopropylidene-L-threitol served (110) as a key intermediate in the preparation of the chiral 1,2-diols (Figure 14a), which were employed along with diethylene glycol bistosylate in the base-promoted synthesis of the three tetrasubstituted 18-crown-6 derivatives LL-64 to LL-66. 1,4-Dideoxy-1,4-diiodo-2,3-*O*-isopropylidene-L-threitol has played (111, 112) an analogous role in the preparation of the chiral disubstituted 18-crown-6 derivative L-67 whereas L-60 provided (111–113) the starting point for the synthesis of L-68 to L-70. These chiral 18-crown-6 derivatives, carrying thiol-containing side arms, have been employed to study (111, 112, 114) regioselective transacylations of amino acid ester salts and as enzyme models (113) for the synthesis of peptides.

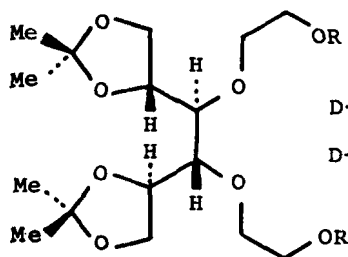
A base-promoted (2 + 2) cyclization between 1,2:5,6-di-*O*-isopropylidene-D-mannitol (Figure 14b) and diethylene glycol ditosylate had previously been applied (88, 106, 107) successfully to the preparation of the chiral 18-crown-6 derivative DD-27 (p. 228), whence DD-28 to DD-30 can be obtained. However,

LL-64 R = O α -NpLL-65 R = α -Np

LL-66 R =

L-67 R = CH₂CH₂CH₂SHL-68 R = CH₂SHL-69 R = CH₂OCH₂CH₂SHL-70 R = CH₂(OCH₂CH₂)₂SH

homologous chiral disubstituted 9-crown-3 and hexasubstituted 27-crown-9 derivatives were also isolated in somewhat smaller yields after chromatographic separation of the products. This problem can be circumvented by a chain extending the diol and then carrying out a (1 + 1) cyclization between the half-crown diol D-71 and its derived half-crown ditosylate D-72. This can be accomplished by a simple procedure (115), whereby the diol is converted into its diallyl ether, which is then subjected to ozonolysis followed by a reductive workup with sodium borohydride. The ditosylate D-72 is also a useful precursor for the synthesis of chiral diaza crown ethers. This (1 + 1) cyclization approach to the formation of chiral macrocyclic polyethers has been used (116) to incorporate two 1,2:5,6-di-*O*-isopropylidene-L-iditol (Figure 14b) residues into a chiral tetrasubstituted 18-crown-6 derivative.

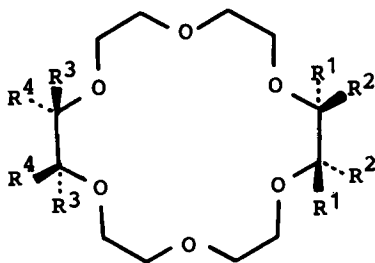


D-71 R = H

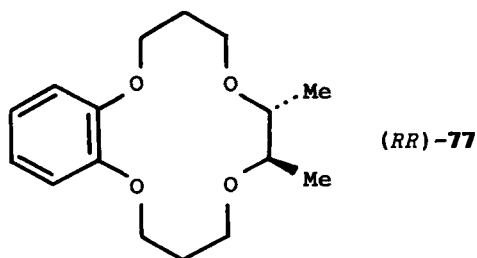
D-72 R = Ts

3. From Resolved Hydrobenzoins and 2,3-Butanediol

Both the (*RR*)- and (*SS*)-enantiomers of hydrobenzoin (Figure 14a) have been made to react (110, 117, 118) successfully in a (2 + 2) cyclization with ethylene glycol ditosylate in the presence of bases (e.g., NaOH in dioxane or NaH in *N,N'*-dimethylformamide) to give the enantiomeric tetraphenyl-18-crown-6 derivatives (*RRRR*)-**73** and (*SSSS*)-**73**. The corresponding optically pure tetra-anisyl, tetra- α -naphthyl, and tetra- β -naphthyl-18-crown-6 derivatives **74**, **75**, and **76**, respectively, have also been prepared in similar fashion (119). It should be noted that (*RRRR*)- and (*SSSS*)-**73** have also been obtained as a result of a base-promoted (1 + 1) cyclization (120) between the chiral extended diol and

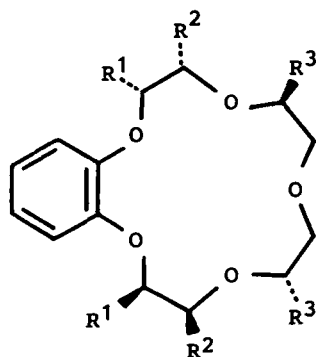


	R ¹	R ²	R ³	R ⁴
(<i>RRRR</i>)- 73	Ph	H	Ph	H
(<i>SSSS</i>)- 73	H	Ph	H	Ph
(<i>RRRR</i>)- 74	<i>p</i> -MeOC ₆ H ₄	H	<i>p</i> -MeOC ₆ H ₄	H
(<i>SSSS</i>)- 74	H	<i>p</i> -MeOC ₆ H ₄	H	<i>p</i> -MeOC ₆ H ₄
(<i>RRRR</i>)- 75	α -Np	H	α -Np	H
(<i>SSSS</i>)- 75	H	α -Np	H	α -Np
(<i>RRRR</i>)- 76	β -Np	H	β -Np	H
(<i>SSSS</i>)- 76	H	β -Np	H	β -Np

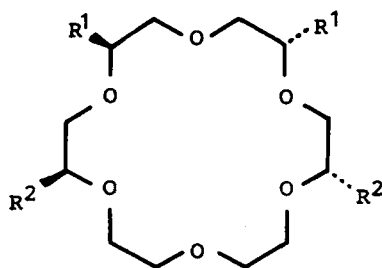


its derived ditosylate after chromatographic resolution (118) of the dibenzoate of racemic bis(2-hydroxyethoxy)-1,2-diphenylethane on cellulose acetate.

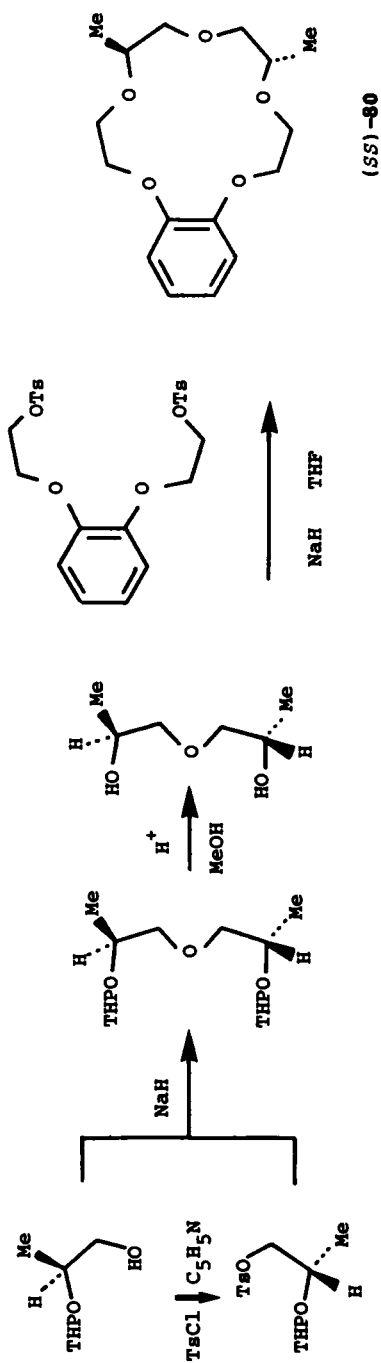
A chiral benzo-14-crown-4 derivative (*RR*)-77 has been prepared (121) from (2*R*,3*R*)-2,3-butanediol by applying to the chiral diol a chain extension procedure that involves (i) addition of acrylonitrile to both hydroxyl groups, (ii)



	R ¹	R ²	R ³
(<i>RR</i>)-78	Me	H	H
(<i>SS</i>)-79	H	Me	H
(<i>SS</i>)-80	H	H	Me



	R ¹	R ²
(<i>SS</i>)-81	Me	H
(<i>SS</i>)-82	H	Me
(<i>SSSS</i>)-83	Me	Me



Scheme 3.

methanolysis of the dinitrile, (iii) reduction of the diester, and (iv) conversion to the ditosylate for base-promoted (1 + 1) cyclization with catechol to afford (*RR*)-77. Catalytic hydrogenation of the benzo ring gave a single cyclohexano product that was assumed (121) to be the *cis* isomer.

4. From Precursors Derived from Lactic and Mandelic Acids

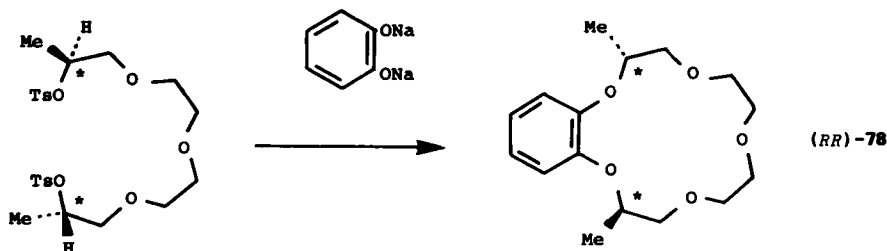
The incorporation of two asymmetric precursors into chiral crown ethers with C_2 symmetry must be carried out with total constitutional and stereochemical control during the reaction sequence. This has been accomplished elegantly during the synthesis of the three chiral benzo-15-crown-5 derivatives (*RR*)-78, (*SS*)-79, and (*SS*)-80 from (*S*)-lactic acid (122, 123).

The kind of approach that must be employed is illustrated in Scheme 3 for the synthesis of (*SS*)-80 starting from the 2-tetrahydropyranyl (THP) ether of (*S*)-propylene glycol (Figure 14c), which can be obtained (124) in two steps from ethyl (*S*)-lactate.

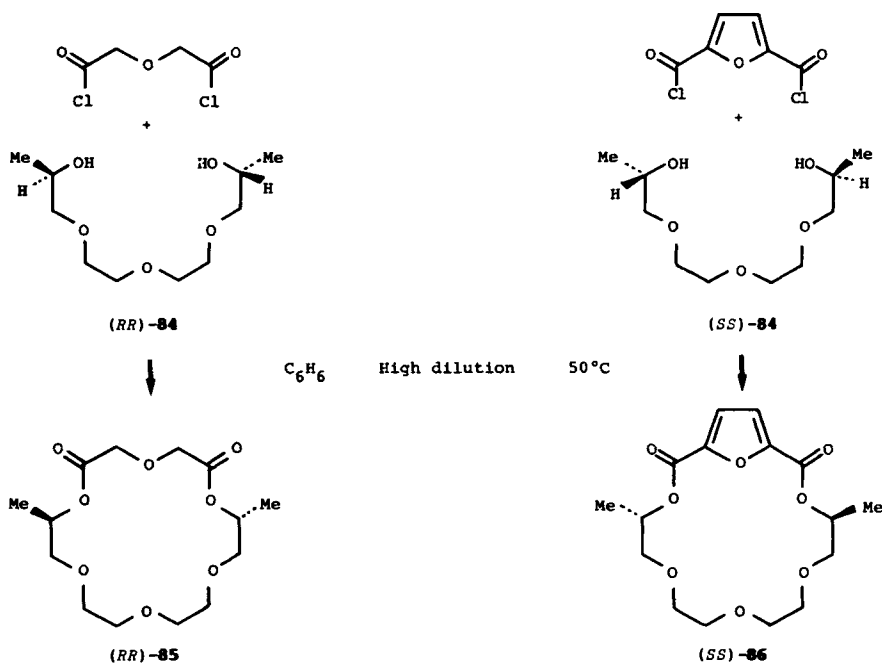
The synthesis of (*RR*)-78 involves in the final (1 + 1) cyclization step (see Scheme 4) a rare example of an inversion of configuration at both chiral centers in the (*SS*)-ditosylate precursor during its successive alkylations of the dianion derived from catechol. The (*5R,15R*)-5,15-dimethylbenzo-15-crown-5 derivative (*RR*)-78 is believed (123) to be optically pure.

Using very similar synthetic strategies, the chiral dimethyl-18-crown-6 derivatives (*SS*)-81 and (*SS*)-82 and the chiral tetramethyl-18-crown-6 derivative (*SSSS*)-83 have been made (125) in good yields from ethyl (*S*)-lactate as the chiral synthon.

The chiral dimethyl derivatives (*RR*)-84 and (*SS*)-84 of tetraethylene glycol have been employed (126) in the preparation of chiral macrocyclic polyether diesters such as (*RR*)-85 and (*SS*)-86. The reactions of the chiral diols with the appropriate diacid chlorides generally proceed (Scheme 5) in good yield in warm benzene under high dilution conditions.



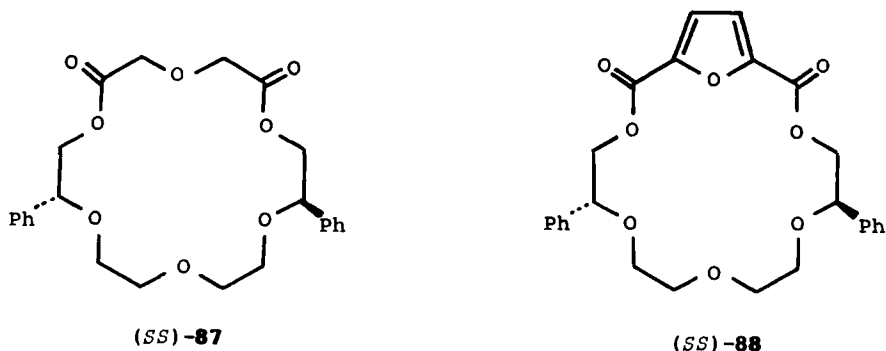
Scheme 4. Note the inversion of configuration at the chiral centers (*) of the (*SS*)-ditosylate during its (1 + 1) cyclization with disodium catecholate.



Scheme 5.

The chiral diphenyl-substituted polyether-diesters (*SS*)-87 and (*SS*)-88 were obtained (127) in similar fashion from the appropriate (*SS*)-diphenyl derivative of tetraethylene glycol synthesized stereospecifically from (*S*)-mandelic acid.

Chiral 18-crown-6 derivatives incorporating both one and two L-glyceraldehyde dithioethylacetal residues have also been reported (128) recently. Also, a benzo-18-crown-6 ring has been appended (129) to the C-5 and C-6 positions of 1,2-*O*-isopropylidene-3-*O*-methyl- α -D-glucofuranose.



B. Fused-Ring All-Oxygen Crown Compounds

In this section, we shall examine the various approaches by which crown compounds that have their chiral elements associated in some way with fused ring systems can be constructed. A selection of the wide and growing range of saturated chiral diols—many of them derived from readily available carbohydrates—which have been incorporated, as relatively inexpensive sources of chirality, into crown ether derivatives are displayed in Figure 15. It may be noted that the saturated chiral diols rely for their chirality on centers of the classical type (C*abcd)—not so the chiral dihydroxy compounds associated with the unsaturated systems listed in Figure 16. These examples reveal that axes and planes of chirality join with less conventional chiral centers (C*aaaa) in being sources of chirality in optically active crown ethers.

1. From (+)-*trans*-Cyclohexane-1,2-diol

The syntheses of (+)-*trans,anti,trans*-dicyclohexano-18-crown-6, (+)-*trans*-cyclohexano-15-crown-5, and (+)-*trans*-cyclohexano-18-crown-6 (115) from (+)-*trans*-cyclohexane-1,2-diol (Figure 15) have been described. They involve base-promoted cyclizations with the appropriate ditosylates after chain extension of the chiral diol using the allylation–ozonolysis–reduction procedure.

2. From (+)- and (–)-*trans*-2,5-bis(Hydroxymethyl)tetrahydrofuran

The (–)-*trans,trans*- and (–)-*cis,trans*-isomers of the bistetrahydrofuranodibenzo-18-crown-6 derivatives, (SSSS)-**89** and (RSSS)-**90** have been prepared (130) by reaction of the ditosylates, obtained from (–)-*trans*- (Figure 15) and *cis*-2,5-bis(hydroxymethyl)tetrahydrofurans with (i) catechol and base in a (2 + 2) cyclization in the case of (SSSS)-**89** and with (ii) a monoprotected catechol (the THP ether) using a stepwise procedure to introduce first the *cis*-diol unit and then finally the (–)-*trans* diol unit into (RSSS)-**90**.

3. From Carbohydrate Derivatives

Closely related to the synthetic work reported in the previous section is the incorporation (131) of a 2,5-anhydro-3,4-di-*O*-methyl-D-mannitol residue (Figure 15) into the 18-crown-6 derivative D-**91**. Other derivatives of D-mannitol that have been built into crown ether receptors include 1,4:3,6-dianhydro-D-mannitol (132), 1,3:4,6-di-*O*-methylene-D-mannitol (133, 134), and 1,3:4,6-di-*O*-benzylidene-D-mannitol (134). Examples of chiral crown compounds containing these residues include DD-**92**, DD-**93**, D-**94**, and D-**95**. Although not derived from carbohydrates—but rather (135) from the terpene, (+)-pulegone—

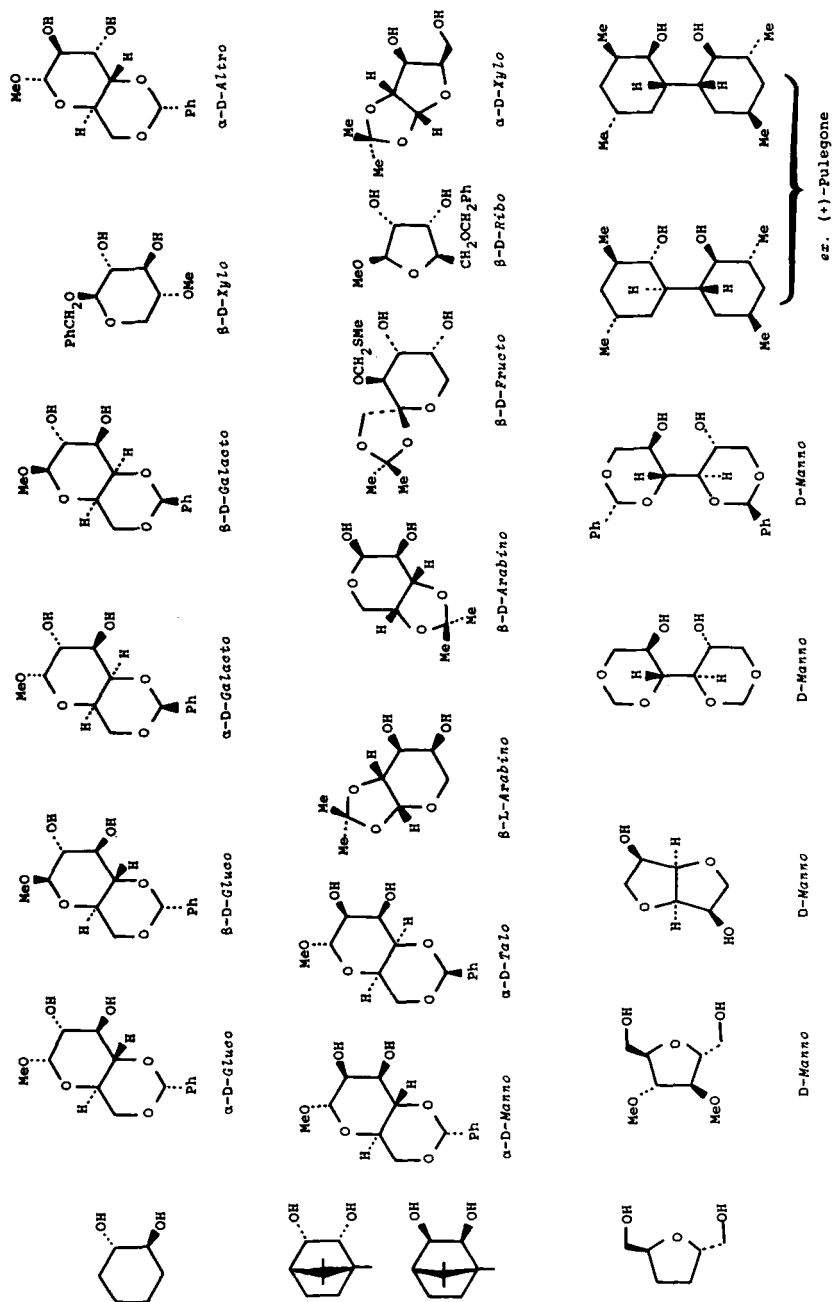


Figure 15. Saturated chiral diols that have been incorporated into fused-ring all-oxygen crown compounds.

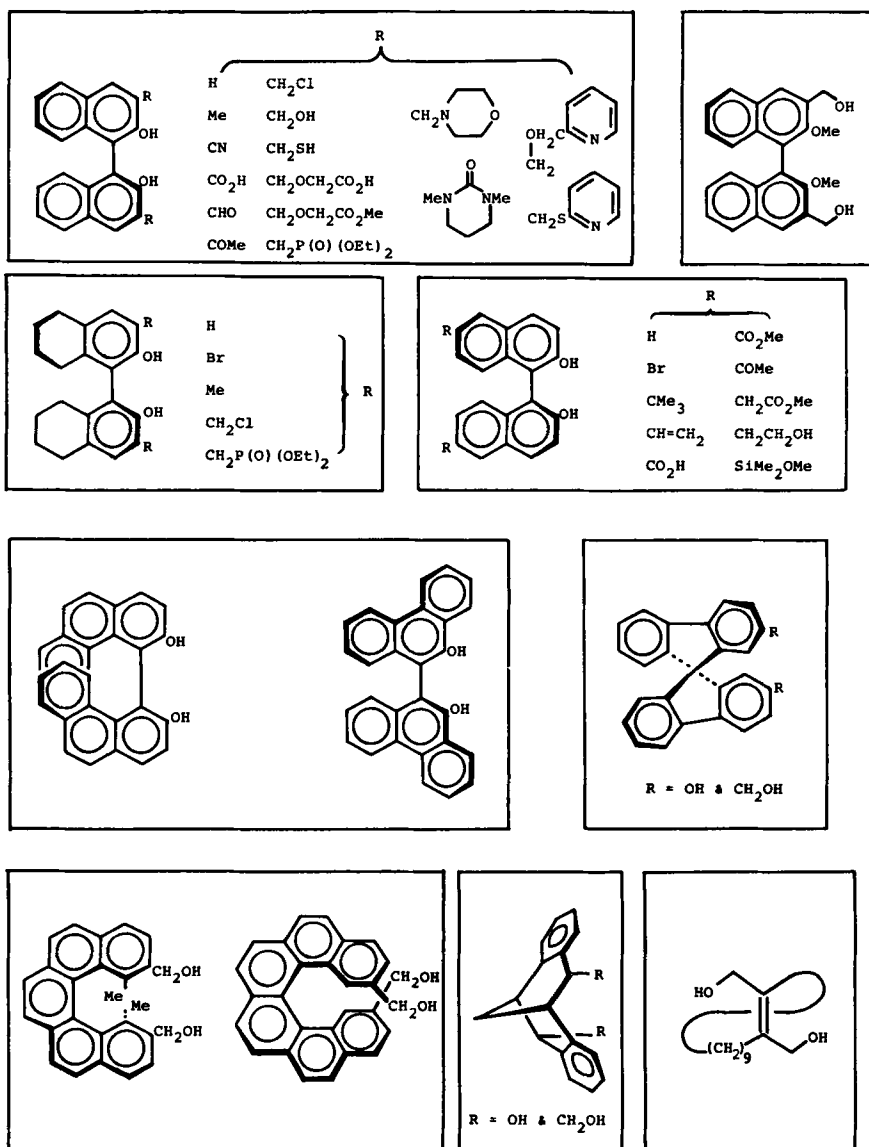
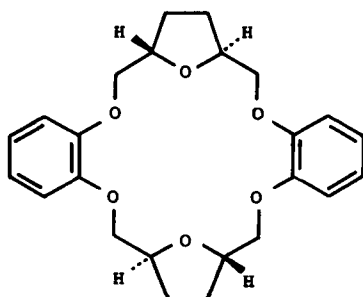
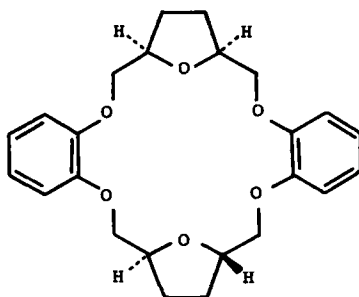


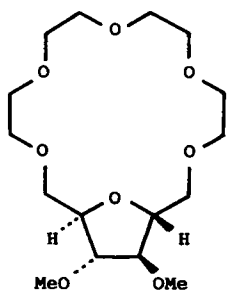
Figure 16. Unsaturated chiral dihydroxy compounds that have been incorporated into fused-ring all-oxygen crown compounds.



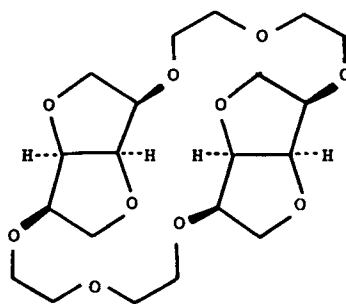
(SSSS)-89



(RSSS)-90



D-91

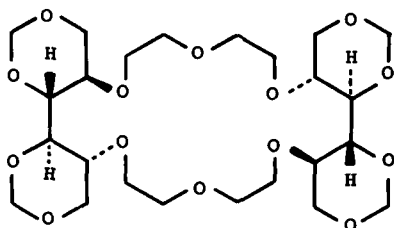


DD-92

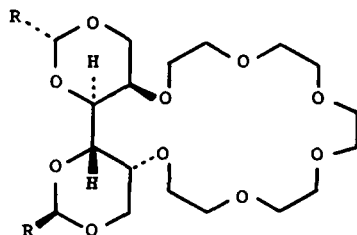
the 20 crown-6 derivatives (+)-96 and (-)-97 bear some resemblance to D-94 and D-95.

The way of designing and synthesizing a chiral 20-crown-6 derivative DDD-98 incorporating *two* 1,2-*O*-isopropylidene-D-mannitol residues and *one* 1,3:4,6-di-*O*-methylene-D-mannitol residue starting from appropriately constructed mono- and di-extended diacetone mannitol units is outlined (136) in Scheme 6. It relies on the local C_2 symmetry of all the carbohydrate residues and the C_2 symmetry present in the final product. By developing a strategy not dissimilar to that described in Scheme 3, dithiol-bearing chiral 18-crown-6 derivatives (+ +)-L-99 and (- -)-L-100 have been prepared (114) from 1,4-di-*O*-benzyl-L-threitol and (+)-(1*R*,2*R*,3*S*,4*S*)-camphane-2,3-diol and (-)-(1*R*,2*S*,3*R*,4*S*)-camphane-2,3-diol (Figure 15), respectively.

For the most part, the asymmetric 18-crown-6 derivatives 101-107 incorporating methyl 4,6-*O*-benzylidene- α (or) β -D-glucopyranoside residues (Fig-

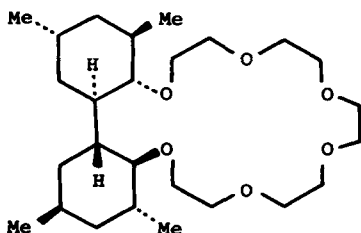


DD-93

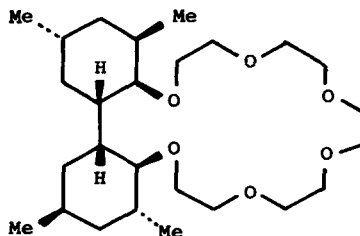


D-94 R = H

D-95 R = Ph

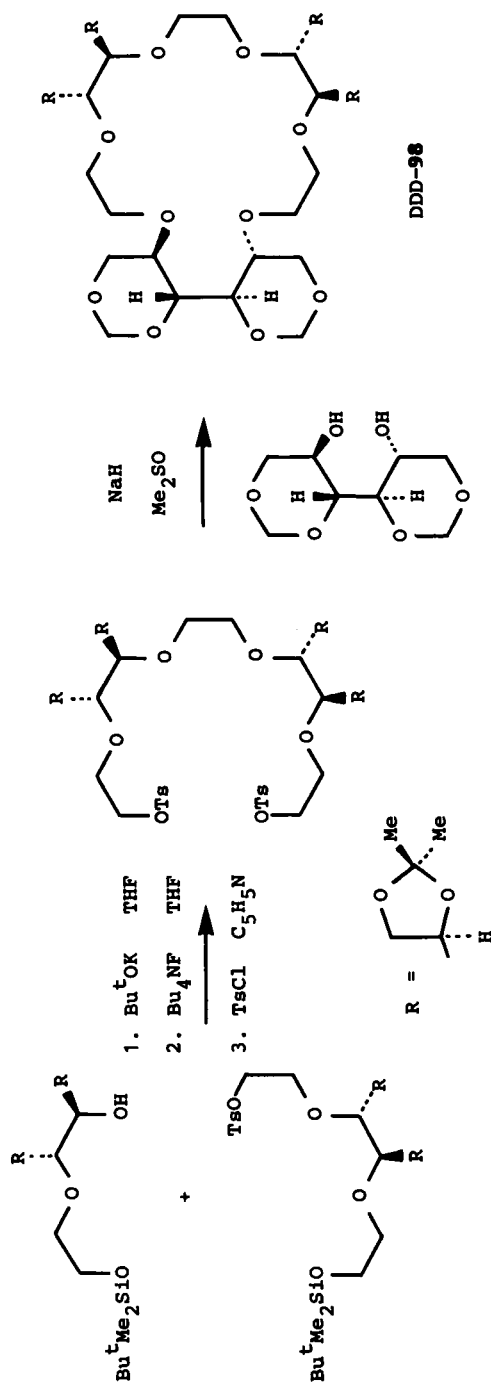


(+)-96

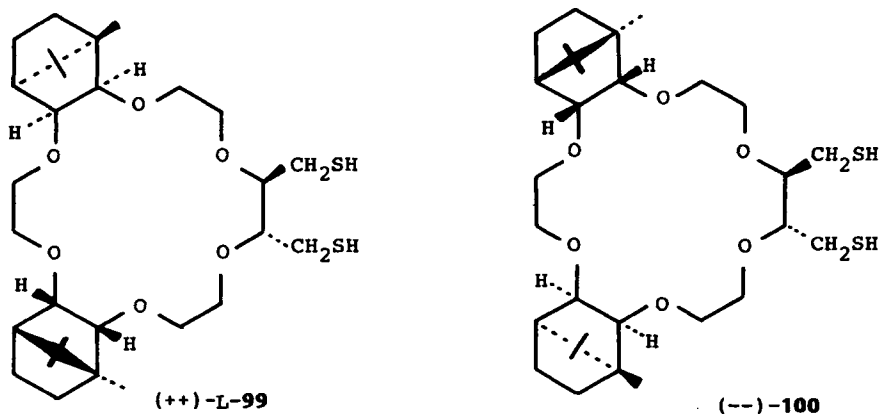


(-)-97

ure 17) have been synthesized (137–141) by standard procedures involving either double chain extensions of the diol and base-promoted cyclizations with triethylene glycol ditosylate or direct base-promoted cyclization of the diols with pentaethylene glycol ditosylate. A few analogous asymmetric 12-crown-4 and 15-crown-5 derivatives (141, 142) have been reported as well as some benzo-18-crown-6 and benzo-24-crown-8 derivatives (129). The incorporation of a 3,4-*O*-isopropylidene- β -D-arabinopyranose unit into a benzo-18-crown-6 macrocycle provides (129) a unique example of a macrocyclic polyether containing an anomeric carbon atom. The substituted pentosides shown in Figure 15 with the β -D-xylo, β -L-arabino, and β -D-ribo configurations have all been incorporated (128) into 18-crown-6 derivatives. Finally, macrocycles of the $3n$ -crown- n ($n = 3$ –7) type have been fused (143) on to the 1,2-*O*-isopropylidene-3-*O*-(methylthiomethyl)- β -D-fructopyranose residue (Figure 15). When a chiral residue with C_2 symmetry is condensed in a constitutionally symmetrical manner within a macrocycle that also contains an asymmetric unit, only one asymmetric crown ether derivative is obtained (137, 138), for example the 18-crown-6 compounds 108–112 listed in Figure 17 containing 1,2:5,6-di-*O*-isopropylidene-D-mannitol residues as well as methyl 4,6-*O*-benzylidene-D-glucopyranoside units.



Scheme 6. The preparation of a "three-residue" 20-crown-6 derivative DDD-98 from carbohydrate units with C_2 symmetry.

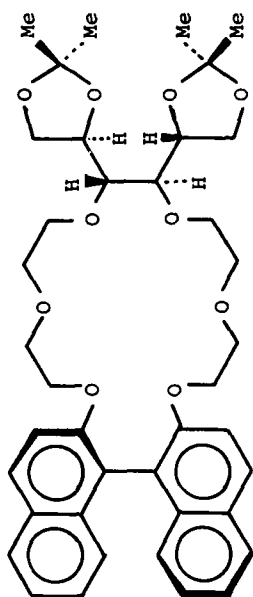


The incorporation of two nonidentical chiral residues, each supporting C_2 symmetry, into a macrocyclic polyether affords a chiral crown compound with C_2 symmetry provided its structure is constitutionally symmetrical. Thus, base-promoted reaction of the half-crown diol prepared from (*S*)-binaphthol with the half-crown ditosylate D-72 synthesized from diacetone-mannitol affords (144) the 20-crown-6 derivative (*S*)-D-113 with C_2 symmetry. When D-72 is condensed in like fashion with (*RS*)-binaphthol, then the diastereoisomeric 20-crown-6 derivative (*R*)-D-114 can be separated chromatographically from (*S*)-D-113. In this manner, (*RS*)-binaphthol is resolved by the carbohydrate unit during the synthesis.

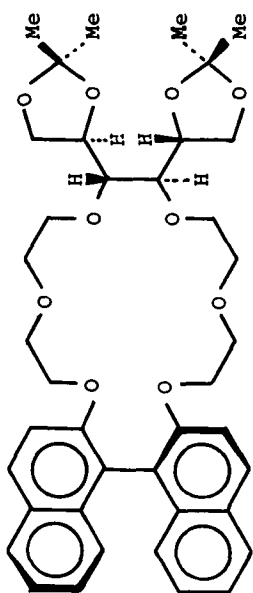
When an asymmetric half-crown diol reacts, in the presence of base, with its derived (asymmetric) half-crown ditosylate, two constitutional isomers, that is, the 2,3:2'3' isomer and the 2,3:3'2' isomer, can, in principle, result (145)

R = H	Glycosidic configurations	R =
α -D-101	α -D-Gluco	α -D-108
β -D-102	β -D-Gluco	β -D-109
α -D-103	α -D-Galacto	α -D-110
β -D-104	β -D-Galacto	β -D-111
α -D-105	α -D-Manno	α -D-112
α -D-106	α -D-Talo	
α -D-107	α -D-Altro	

Figure 17. Some asymmetric 18-crown-6 derivatives based on methyl 4,6-*O*-benzylidene-D-glycopyranosidic units.



(R)-D-114



(S)-D-113

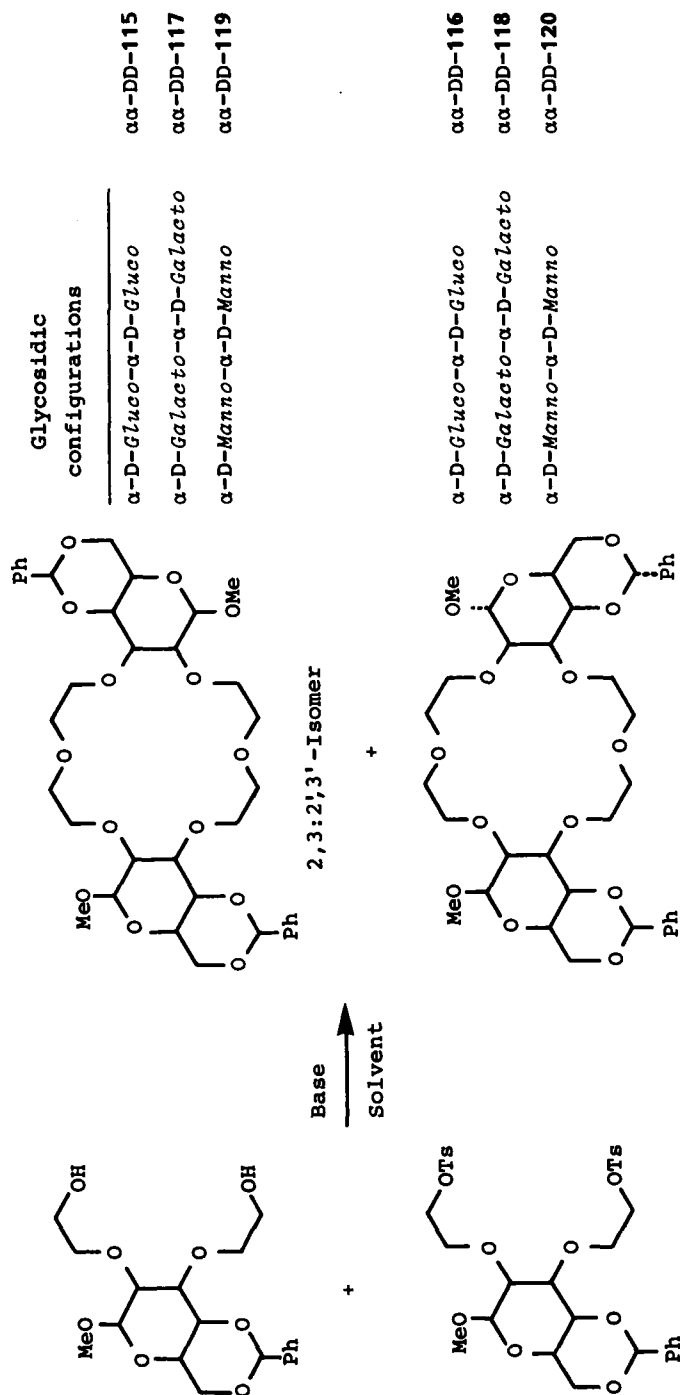
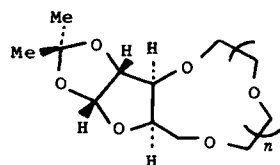
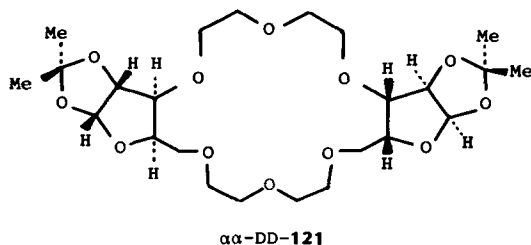


Figure 18. The preparation of constitutionally isomeric α-α-DD-bisglycosido-18-crown-6 derivatives with gluco, galacto, and manno configurations.

as shown in Figure 18. The isomers $\alpha\alpha$ -DD-115 and $\alpha\alpha$ -DD-116, containing two α -D-gluco residues, and the isomers $\alpha\alpha$ -DD-117 and $\alpha\alpha$ -DD-118, containing two α -D-galacto residues, have been prepared in this manner. Although, in each case, both isomers have C_2 symmetry, the 2,3:2',3' isomers have heterotopic faces and the 2,3:3',2' isomers have homotopic faces. Thus it is possible to make constitutional assignments by recording spectra of 1:1 complexes formed with primary alkyl ammonium salts in CD_2Cl_2 at low temperatures. The 2,3:2',3' isomers were identified positively as a result of the unequally populated diastereomeric complexes obtained from two of the compounds. The other two compounds each afforded a single complex and so it was concluded they corresponded to the 2,3:3',2' isomers. The $\alpha\alpha$ -DD-bisglucosido-18-crown-6 **115**, **116** (141, 146–149) and $\alpha\alpha$ -DD-bisgalactosido 18-crown-6 **117**, **118** (141, 147–149) derivatives, as well as the $\alpha\alpha$ -DD-bismannosido-18-crown-6 derivatives **119**, **120** (141, 147), have been obtained from (2 + 2) cyclizations of the appropriate protected glycosides with diethylene glycol ditosylate. Conditions have been found (146) that permit the isolation and characterization of intermediates leading to $\alpha\alpha$ -DD-118 and $\alpha\alpha$ -DD-120. In these intermediates ^{13}C NMR spectroscopy reveals that the C-3 and C-3' positions of the two glycosidic units are linked by a polyether chain. The identities of $\alpha\alpha$ -DD-118 and $\alpha\alpha$ -DD-120 as 2,3:3',2' isomers are thus established. The constitutional assignment to the compound corresponding to formula $\alpha\alpha$ -DD-115 has been confirmed (150) by X-ray crystallography. De-*O*-benzylidenation of $\alpha\alpha$ -DD-115 (147, 148), $\alpha\alpha$ -DD-116 (149), and $\alpha\alpha$ -DD-117 (151) have been effected as a prerequisite to making a range of chemically modified bisglycosido-18-crown-6 derivatives. One other example of the incorporation of two carbohydrate residues into a chiral crown ether is worthy of mention. 1,2-*O*-Isopropylidene- α -D-xylofuranose (Figure 15) undergoes (128) a base-promoted reaction with diethylene glycol ditosylate to give the bisxylo-20-crown-6 derivative $\alpha\alpha$ -DD-121 in addition to the xylo-10-crown-3 derivative α -D-122 resulting from (1 + 1) cyclization. The xylo-19-crown-6 derivative α -D-123 has also been prepared (128) and subjected to acid hydrolysis to afford the free xylofuranose derivative.



α -D-122 $n = 1$

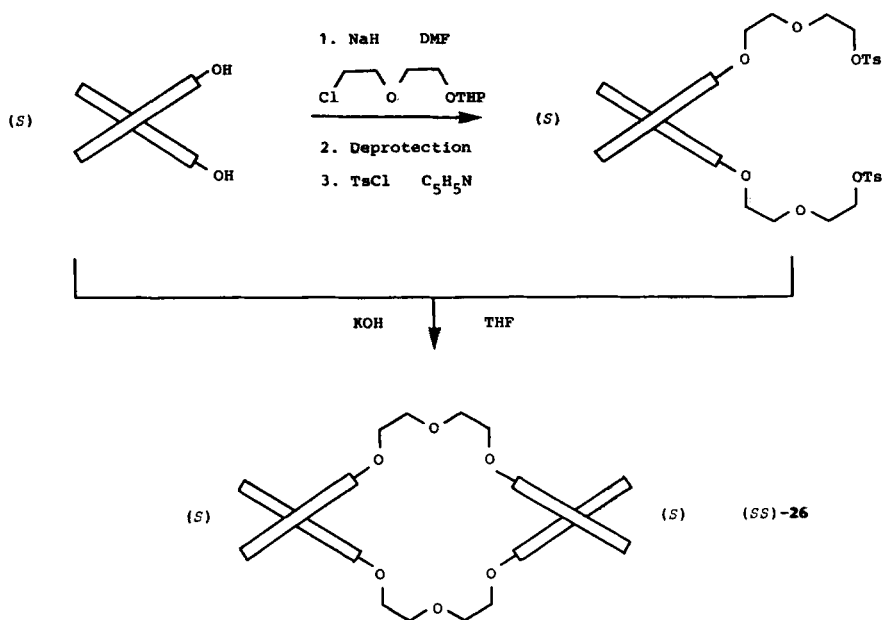
α -D-123 $n = 4$

4. From (*R*)- and (*S*)-Binaphthols and Related Compounds

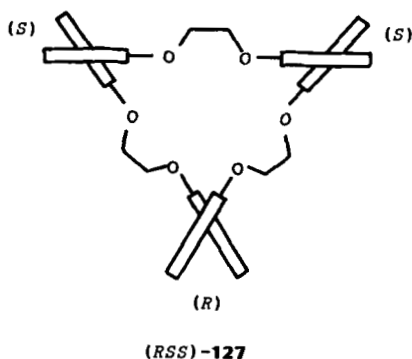
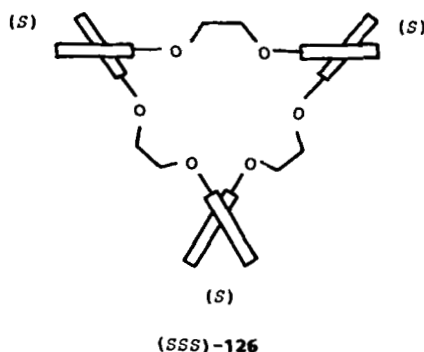
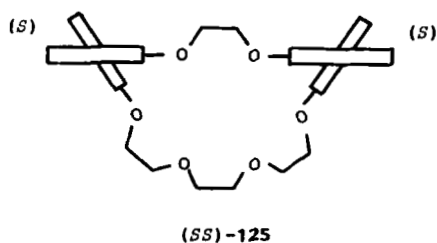
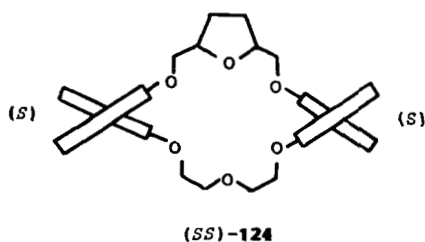
A number of methods have been described (152) for the preparation of the bisbinaphthyl-22-crown-6 derivative (*SS*)-**26** and its enantiomer. The best method is outlined in Scheme 7, starting from (*S*)-binaphthol.

The monobenzhydryl derivative of (*S*)-binaphthol has played an important role, not only in the synthesis of chiral bisbinaphthyl crown ether derivatives, for example, (*SS*)-**124**, containing two different bridges between the two binaphthyl units, but also in the provision of an entry into the constitutionally isomeric derivative (*SS*)-**125**. Rational stepwise syntheses of macrocycles containing three binaphthyl units have been devised and applied to the synthesis of (*SSS*)-**126** and (*RSS*)-**127**. Clearly, in all these procedures, the C_2 symmetry of the chiral building block restricts the number of products (to one!) and defines the symmetries of the macrocycles formed.

Similar preparative procedures were employed (153) to introduce chiral di-substituted binaphthol units (Figure 16) such as (*R*)-3,3'-dimethyl-2,2'-dihydroxy-1,1'-dinaphthyl and chiral ditetralol units (Figure 16) into a range of macrocycles. The high chiral recognition (154, 155) shown by the dimethyl substituted derivative (*RR*)-**128** merits giving it special mention. Also, a wide range of chiral macrocyclic polyethers, for example, (*R*)-**129**, shaped by one



Scheme 7.

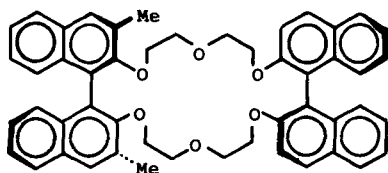
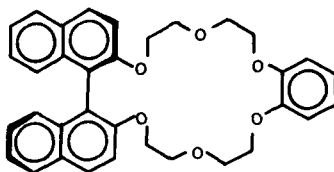
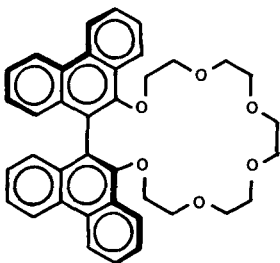
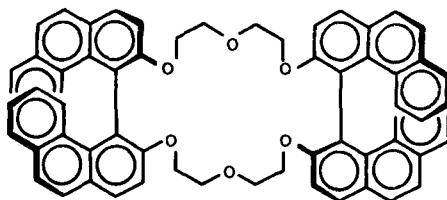


rigid binaphthyl unit have been reported (86, 156). Chiral crown ethers in which a single polyether chain connects the 3,3' positions of a 1,1'-binaphthyl unit have also been synthesized (157). In all cases, oxygen-containing substituents (e.g., OMe and OH) are located at the 2,2' positions (cf. Figure 16).

Very recently, chiral crown ethers incorporating 9,9'-biphenanthryl (158) and 4,4'-biphenanthryl (159) moieties have been prepared from the corresponding optically active 10,10'-dihydroxy and 3,3'-dihydroxy derivatives, respectively. Both 20-crown-6 macrocycles, for example, (S)-130, containing one chiral unit and 22-crown-6 macrocycles, for example, (RR)-131, containing two chiral units are known.

5. From 9,9'-Spirobifluorene Derivatives

Prelog and co-workers (160, 161) chose 9,9'-spirobifluorene as a starting material for synthesizing chiral crown ethers since (i) it has a more rigid carbon skeleton than the 1,1'-binaphthyl unit, and (ii) it can be substituted easily in the 2 and 2' positions by electrophilic reagents. Thus, the 2,2'-diacetyl derivative (Figure 19) obtained after a Friedel-Crafts on 9,9'-spirobifluorene can be con-

**(RR) - 128****(R) - 129****(S) - 130****(RR) - 131**

verted into diphenol (*RS*)-**132**, which, on reacting as its potassium salt with α,ω -dihalogeno-polyethers, affords the 17-crown-4, (*RS*)-**133**, 20-crown-5, (*RS*)-**134**, and 23-crown-6, (*RS*)-**135** derivatives. On the other hand, oxidation of 2,2'-diacetyl-9,9'-spirobifluorene gives the 2,2'-dicarboxylic acid that can be resolved as its diastereoisomeric camphanic acid esters. Subsequently, functional group manipulation leads to the enantiomeric 2,2'-bisbromomethyl derivatives, which can be reacted with appropriate α,ω -dihydroxy polyethers in the presence of base to yield the chiral [(*R*) and (*S*)] 19-crown-4, **136**, 22-crown-5, **137**, and 25-crown-6, **138**, derivatives [only the (*R*) isomers are shown in Figure 19].

Very recently, the synthesis of a series of chiral poly(9,9'-spirobifluorene)crown ethers [e.g., (*SS*)-**139**, (*SSSS*)-**140**, (*SSSSSS*)-**141**, and (*SSSSSSSS*)-**142**] with 26-, 52-, 78-, and 104-membered rings have been described (162). The last three are rare examples of compounds with C_4 , C_6 , and C_8 symmetries, respectively. They were isolated chromatographically from a reaction mixture consisting of (*S*)-2,2'-bisbromomethyl-9,9'-spirobifluorene, ethylene glycol, KO t -Bu, and CsI in toluene.

6. From Miscellaneous Chiral Sources

Three examples of novel sources of chirality developed by researchers at Osaka University are worthy of special mention in the context of chiral crown ethers.

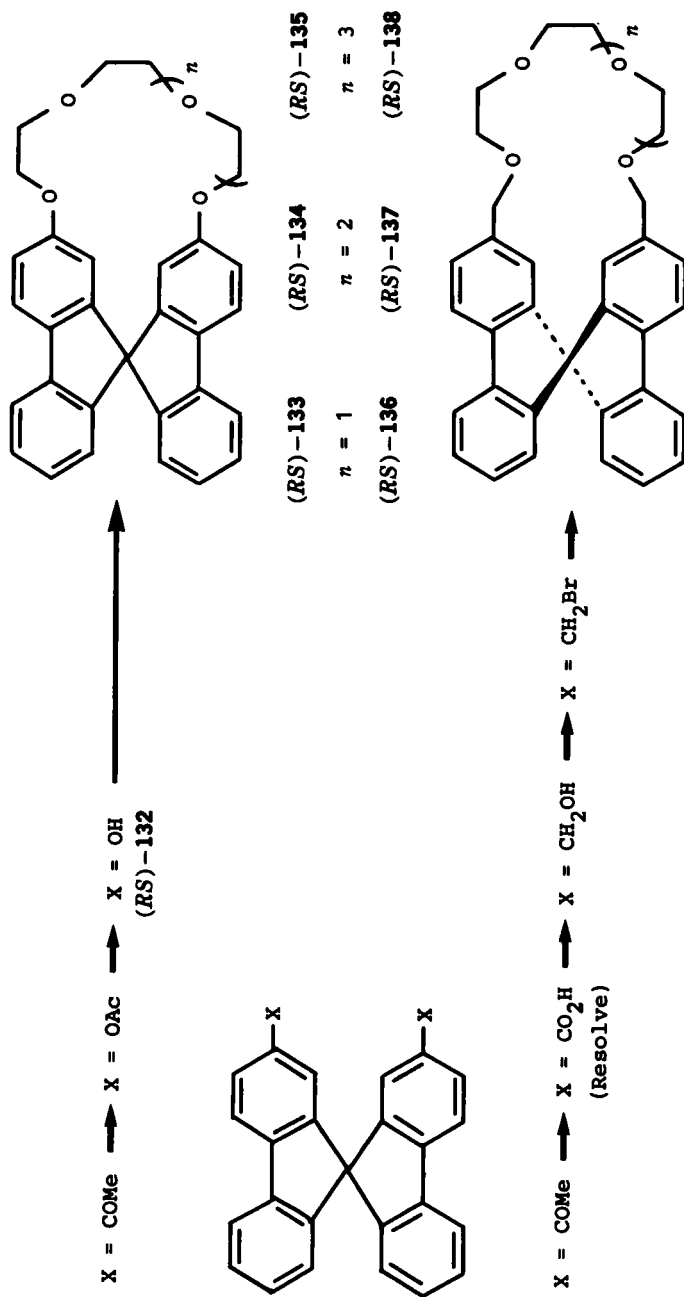
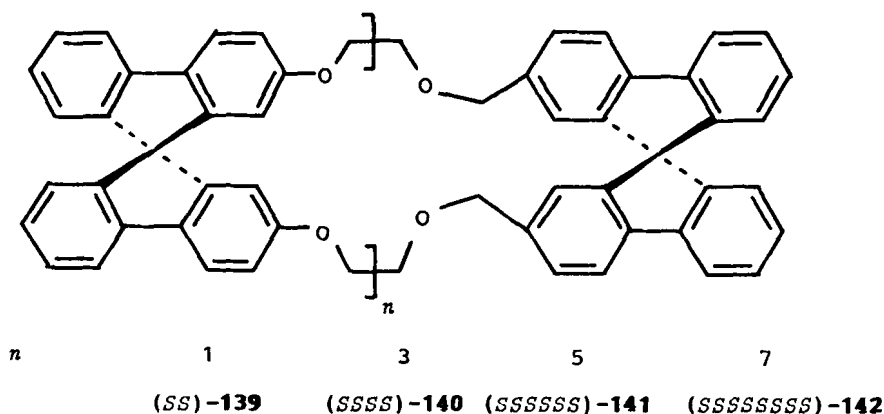


Figure 19. The synthesis of crown compounds containing racemic and chiral 9,9'-spirobifluorene units.

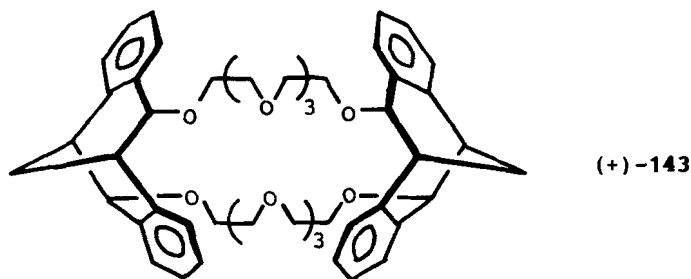


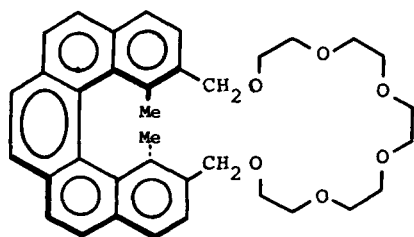
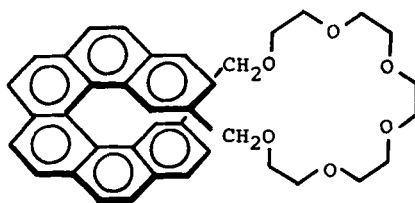
They are all characterized by C_2 symmetry: one exhibits planar chirality and another relies on helicity as the source of chirality.

The chiral 5,6,11,12-tetrahydro-5,11-methanodibenzo[*a,e*]cyclooctene sub-unit (Figure 16) has been incorporated (163) singly and doubly into macrocyclic polyethers containing from 5 to 10 oxygen atoms. The 36-crown-10 derivative (+)-143 constitutes the most spectacular example described so far. The crown ethers (*RS*)-37 and (*RS*)-38 incorporating a trans-doubly bridged ethylene framework (95) as a source of planar chirality have already been mentioned as candidates for resolution by chiral HPLC. Optically pure (*R*)- and (*S*)-38 have been isolated and characterized. Two novel chiral crown ethers, (*M*)-144 and (*M*)-145, incorporating helicene units (Figure 16), have been obtained (164) by synthesis of their racemic modifications and optical resolution by HPLC on (+)-poly(triphenylmethyl methacrylate).

C. All-Oxygen Biscrown and Triscrown Compounds

A number of chiral crown compounds containing more than one macrocyclic polyether ring have been described in the literature. They have been derived



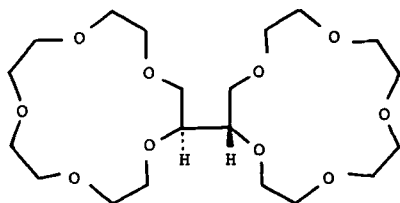
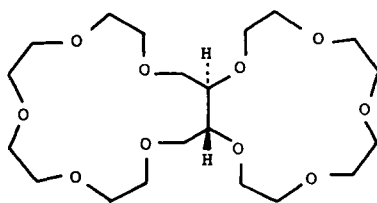
**(M)-144****(M)-145**

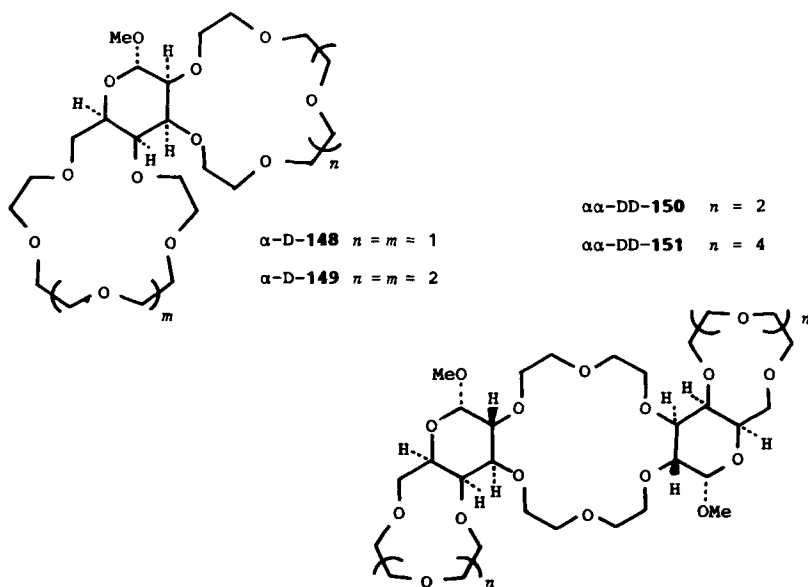
from both natural and laboratory sources of chirality. Examples of the former include L-threitol, and substituted D-talopyranose residues. An example of the latter is provided by the binaphthyl unit.

A base-promoted reaction between L-threitol and tetraethylene glycol ditosylate afforded (165) the chiral bis(15-crown-5) derivative **L-146** as well as the trans-fused bicyclic system **L-147** containing 15-crown-5 and 17-crown-5 rings. These constitutional isomers, which were separated chromatographically, were characterized by preparing **L-147** unequivocally by a stepwise route from 2,3-*O*-isopropylidene-L-threitol.

The 15-crown-5 and 18-crown-6 derivatives incorporating a methyl 4,6-*O*-benzylidene- α -D-talopyranoside residue have been de-*O*-benzylideneated (142) and converted into the biscrown ethers α -D-**148** and α -D-**149**, respectively. Using a similar approach, the triscrown ethers $\alpha\alpha$ -DD-**150** and $\alpha\alpha$ -DD-**151** have been prepared (151) from the 2,3:2',3'-isomer $\alpha\alpha$ -DD-**117** of the bisgalactosido-18-crown-6 derivative.

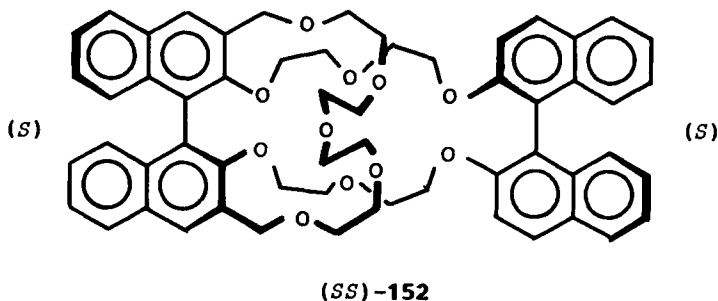
Although a large number of biscrown ethers based on the binaphthyl nucleus have been synthesized (157) many of these have only been isolated and characterized as their racemic modifications. An exception is provided (157) by (*SS*)-**152**, obtained from the chiral bisbinaphthyl-22-crown-6 derivative in which one of the binaphthyl units carries chloromethyl groups (in the 3 and 3' positions) capable of reacting, in the presence of base, with tetraethylene glycol.

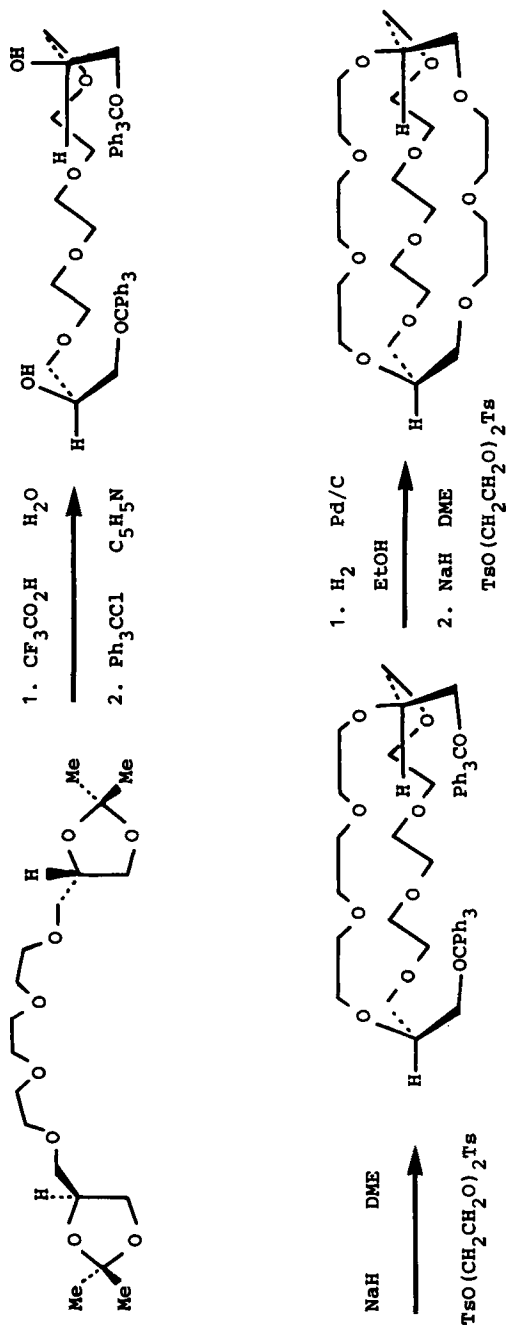
**L-146****L-147**



D. All-Oxygen Macrobicyclic Compounds

The naturally occurring sources of chirality (e.g., carbohydrates and tartaric acid) provide the most straightforward entries into chiral macrobicyclic compounds. The first example to be reported in the literature (166) is outlined in Scheme 8. The stereospecific synthesis, starting from 2,3-*O*-isopropylidene-D-glycerol, proceeds via an acyclic polyether. Following hydrolysis of the acetone protecting groups, selective tritylation of the primary hydroxyl groups provides the key to the stepwise insertion of the other two polyether chains into the chiral bicyclic triacontane derivative DD-153 with out-in (\rightleftharpoons in-out) topology





DD-153

Scheme 8.

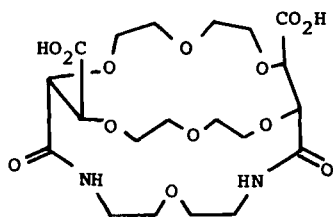
characterizing the two stereogenic centers. The corresponding achiral macrobicyclic polyethers with in-in (\Rightarrow out-out) topologies have recently been prepared stereospecifically (167) from 2,3-*O*-isopropylidene-D-glycerol and 2,3-di-*O*-benzyl-L-glycerol.

The bistartaro-18-crown-6 dianhydride LL-49 provides (102) a facile entry into chiral macrobicyclic compounds. For example, when LL-49 was treated in dichloromethane with $\text{H}_2\text{NCH}_2\text{CH}_2\text{OCH}_2\text{CH}_2\text{NH}_2$ in the presence of triethylamine, a 1:1 mixture of the bridged macrocycles LL-154a and LL-154b were obtained. They were separated by HPLC and their constitutions were assigned by synthesizing LL-154a independently from LL-49 via an unambiguous stepwise route.

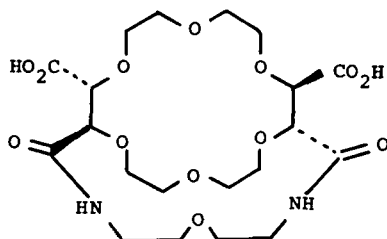
Novel macrobicyclic compounds have been prepared (151) from the tetraol obtained on de-*O*-benzylidenation of the bisgalactosido-18-crown-6 derivative $\alpha\alpha$ -DD-117 in Figure 18. Selective tritylation of the two hydroxymethyl groups of the tetraol, followed by a base-promoted reaction with pentaethylene glycol ditosylate afforded $\alpha\alpha$ -DD-155 with a polyether chain bridging the 4 and 4' positions of the D-galactopyranosidic rings across presumably the β face of the molecule.

E. Substituted Aza Crown Compounds

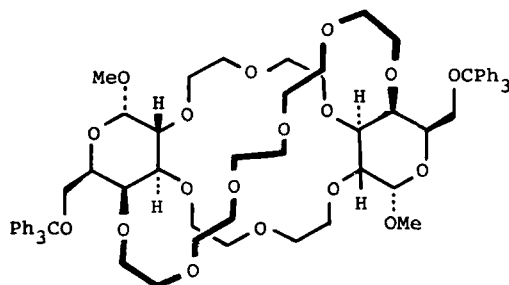
Nitrogen atoms have been incorporated into chiral macrocyclic polyethers in a variety of different ways. One of the most straightforward approaches is the



LL-154a



LL-154b

 $\alpha\alpha$ -DD-155

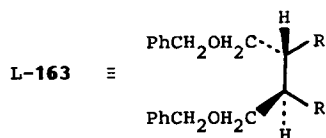
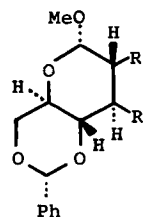
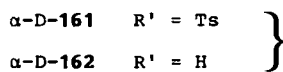
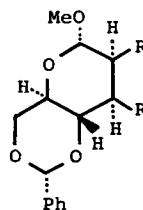
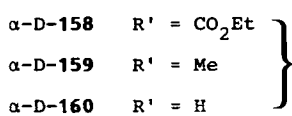
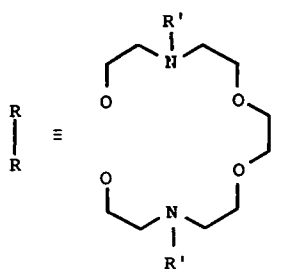
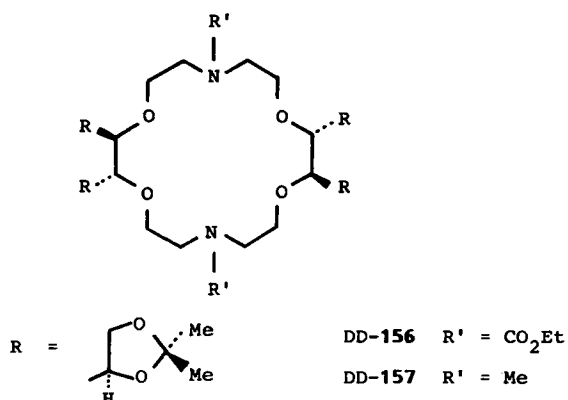


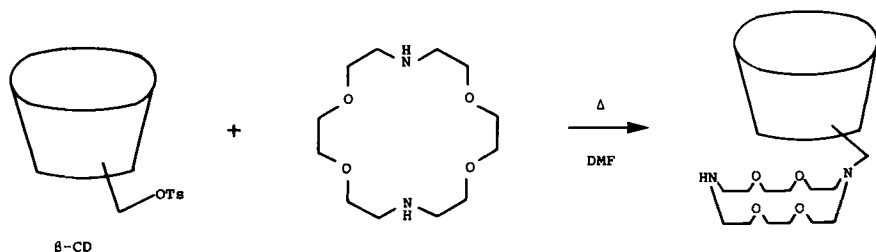
Figure 20. Chiral diaza-18-crown-6 derivatives containing secondary and tertiary amino functions.

replacement of ether oxygen atoms by secondary and tertiary amine functions. In some cases, the chirality is located in other positions of the macrocyclic rings. In other cases, it is attached as a side arm to one of the ring nitrogen atoms. Although not strictly aza crown compounds, macrocycles with nitrogen atoms sited in appended residues and chains will be discussed in this section. Perhaps most fascinating of all are aza crown ethers, which rely upon α -amino acids and their derived amino alcohols as sources of chirality. Some of these contain fused pyrido ring systems as, of course, do other chiral macrocycles where the chirality arises from other sources.

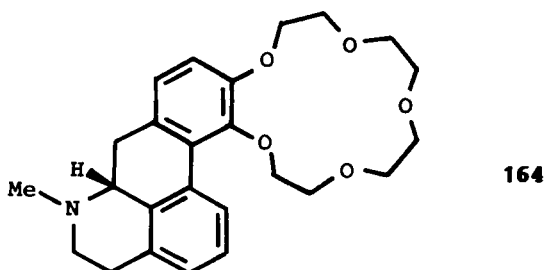
1. With Secondary and Tertiary Amine Functions in Chiral Macrocyclic Polyether Rings

The diaza crown ether analog DD-156 and DD-157 (Figure 20) of DD-27 have been synthesized (168) by a route that involves transformation of the ditosylate DD-72 into the corresponding half-crown bisurethane via the bisazide and derived diamine. A base-promoted reaction between the half-crown bisurethane and the ditosylate DD-72 yields the macrocyclic bisurethane DD-156, which affords the N,N' -dimethyl derivative DD-157 on reduction. A similar approach was employed (169) in the preparation of the diaza analog α -D-158 and α -D-159 (Figure 20) of the α -D-mannosido-18-crown-6 derivative α -D-105 shown in Figure 17. The corresponding chiral diaza-18-crown-6 derivative α -D-160 with secondary amine functions (Figure 20) has been obtained from the appropriate half-crown ditosylate and $(\text{H}_2\text{NCH}_2\text{CH}_2\text{OCH}_2)_2$ using potassium fluoride on alumina to promote macrocycle formation. The same compound results (170) from reductive deprotection of the N,N -ditosylate, α -D-161. In the α -D-glucosido series, the diaza-18-crown-6 derivative α -D-162 (Figure 20) has been prepared (171) by the bisamide route popularized by Lehn (12) in his syntheses of macrodiazabicyclic polyethers, i.e., the cryptands with nitrogen bridgeheads. This synthetic methodology has also afforded (109) the diaza-18-crown-6 derivative L-163 incorporating one 1,4-di-*O*-benzyl-L-threitol unit.

A novel diaza crown ether capped β -cyclodextrin has been prepared (172) as outlined in Scheme 9. It should be noted that the cap is attached to the face of



Scheme 9. Note that β -cyclodextrin (β -CD) contains seven α -1,4-linked D-glucopyranose residues in a cyclic array.

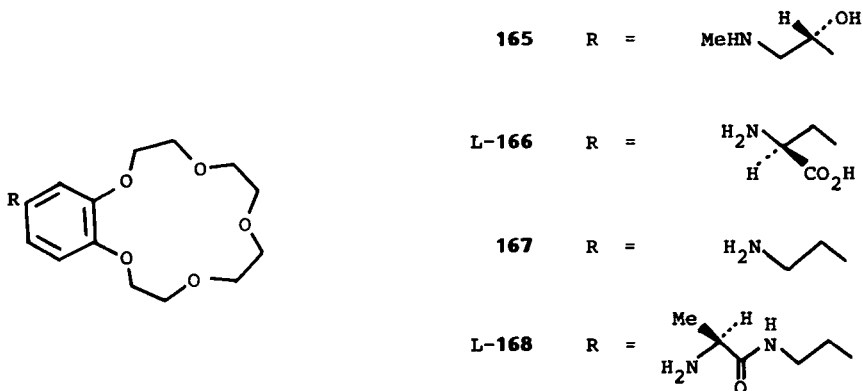


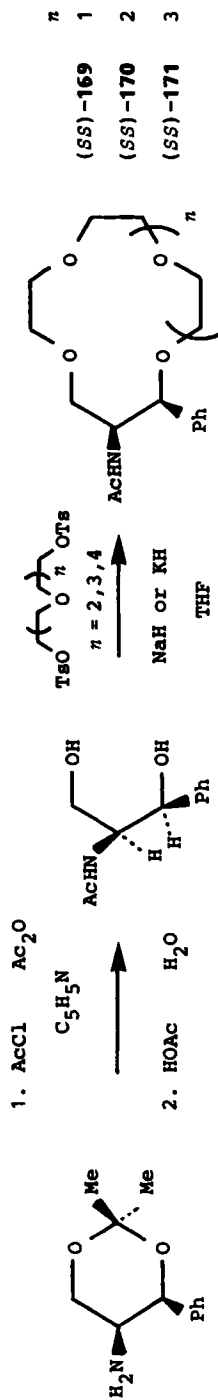
β -cyclodextrin which carries the primary hydroxyl groups of the D-glucopyranose residues.

2. Chiral Crown Ethers Containing Saturated Nitrogen Functions

A number of benzo-15-crown-5 derivatives are known where chirality is associated with side chains or fused ring systems. For example, base-promoted reactions of 1,11-dichloro-3,6,9,-trioxaundecane with apomorphine and adrenaline have afforded the benzo-15-crown-5 derivatives **164** and **165**, respectively (173). In the latter case, a dibenzo-30-crown-10 derivative of unspecified constitution was also isolated.

Employing similar reaction procedures and conditions, the corresponding benzo-15-crown-5 derivatives **L-166** and **167** have been derived from L-Dopa (**174**) and dopamine (**175**), respectively. In the case of **L-166**, it was established that the cesium carbonate promoted reaction proceeds without any racemization. In the case of **167**, condensation with suitably protected α -amino acids, for example, L-alanine, leads to the formation of peptide-functionalized crown ethers, for example, **L-168**. Also, a polypeptide carrying benzo-15-crown-5 poly-





Scheme 10

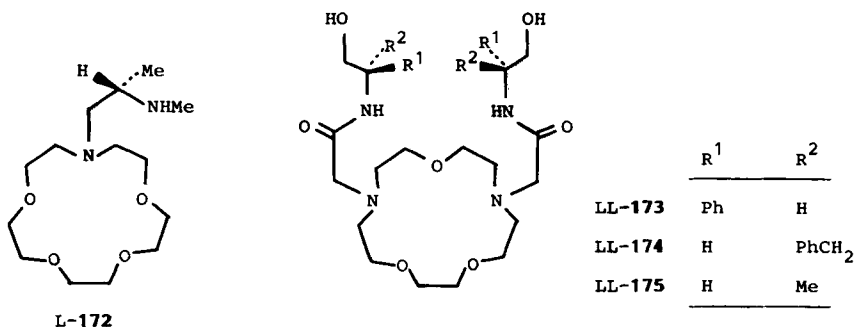
mer chain has been prepared (176) by condensing 45% debenzylated poly-(γ -benzyl-L-glutamate) with 4-hydroxymethylbenzo-15-crown-5.

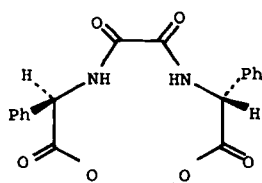
Recently, commercially available (4*S*,5*S*)-5-amino-2,2-dimethyl-4-phenyl-1,3-dioxane has been successfully employed (177) in the synthesis (Scheme 10) of the chiral 13-crown-4, (*SS*)-169, 16-crown-5, (*SS*)-170, and 19-crown-6, (*SS*)-171, derivatives.

3. From α -Amino Acid Derivatives

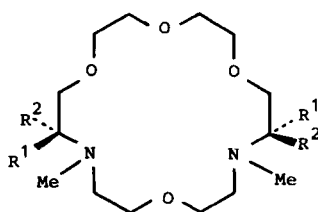
Chirality derived from the readily accessible α -amino acids has been incorporated into the side chains of aza and diaza macrocyclic polyethers. A number of procedures suitable for peptide synthesis have proved (178) to be unsuitable for acylating the relatively unreactive secondary amine groups of aza crown ethers. Eventually, it was discovered that mixed anhydrides of diphenylphosphinic acid and alkoxycarbonyl-L-alanine derivatives do yield amides, which can be reduced to the corresponding amines, e.g., L-172. By contrast, the corresponding bisamides of diaza-15-crown-5 derivatives could not be reduced and so an alternative approach, involving the use of chiral *N*-chloroacetamido alcohols derived from α -amino acids, has been employed (178) in the synthesis of chiral receptors, such as LL-173 to LL-175, based on this constitution.

After the early report by Wudl and Gaeta (85) of the use of two L-proline residues during the preparation of the macrocyclic ring of LL-23, it was a number of years before methods were developed for incorporating α -amino acids and their derived amino alcohols into chiral diaza crown ethers. Chiral macrocycles, for example, DD-176, containing two D-phenylglycine residues, and two ester and two amide linkages, can be made (179) in three steps starting from the benzyloxycarbonyl derivative of this α -amino acid. The amino alcohols derived from D-phenylglycine, L-phenylalanine, and L-valine are alkylated selectively (178, 180) with diethylene glycol ditosylate at their primary hydroxyl groups to afford acyclic triether diamines, which can then be made to react with





DD-176

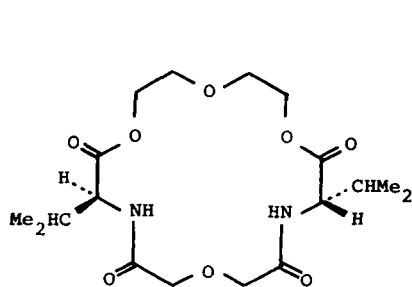


	R ¹	R ²
DD-177	H	Ph
LL-178	CH ₂ Ph	H
LL-179	CHMe ₂	H

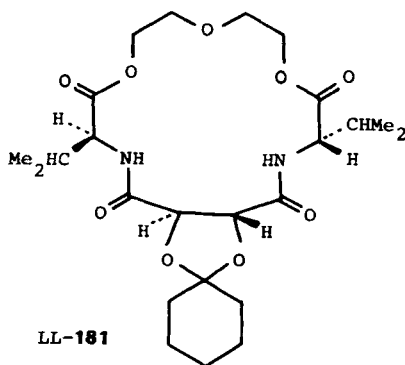
diglycolyl chloride to give the corresponding cyclic bisamides. Reduction, followed by Eschweiler-Clarke methylation, leads to the isolation of the chiral diaza crown ether derivatives DD-177, LL-178, and LL-179, respectively.

Chiral diester diamide macrocycles such as LL-180 have been synthesized (181) from esters of L-valine by, first of all, forming acyclic bisamides and then hydrolyzing the ester functions prior to template-promoted cyclization with cesium carbonate (182) and the appropriate dibromide. L-Tartaric acid has also been incorporated into a macrocycle, i.e., LLL-181, of this type.

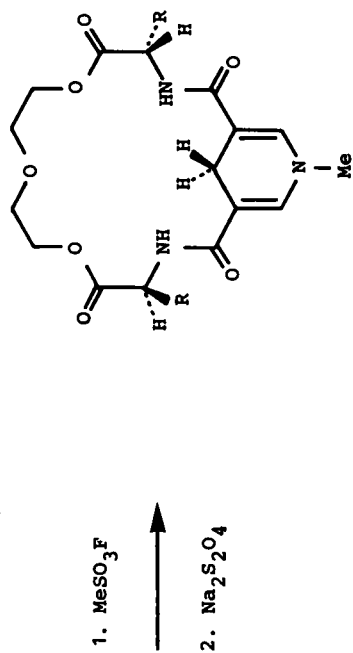
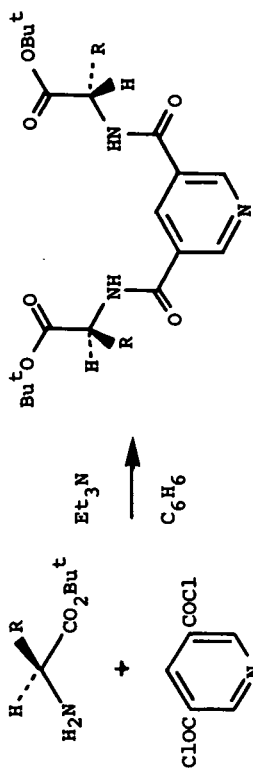
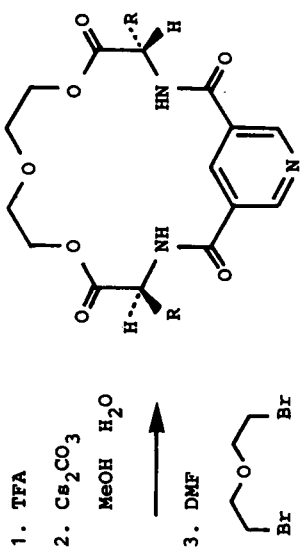
The pyridine ring has also been introduced (181, 183) into diester diamide macrocycles as a means of preparing (Scheme 11) chiral bridged 1,4-dihydropyridines for the reduction of activated carbonyl compounds. The starting point, along with the *t*-butyl esters of L-alanine and L-valine, is the diacid chloride of pyridine-3,5-dicarboxylic acid. The acyclic diesters are hydrolyzed prior to being converted to their di-cesium salts for template-assisted ring closure with 1,5-dibromo-3-oxopentane. Methylation gives the pyridinium salts, which are reduced with sodium dithionite to the desired macrocycles, LL-182 and LL-183, respectively, containing 1,4-dihydropyridine residues.



LL-180



LL-181



L-182 $\text{R} = \text{Me}$
 L-183 $\text{R} = \text{CHMe}_2$

Scheme 11

4. With Fused Pyridino Rings in Chiral Macrocyclic Polyethers

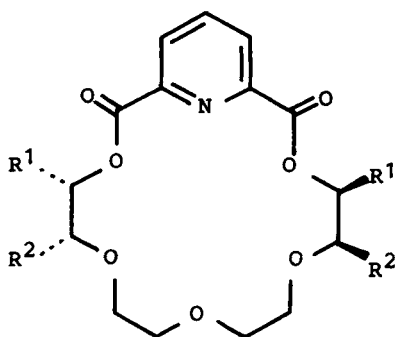
The pyridine subcycle unit has been introduced into a wide range of 18-crown-6 derivatives. For example, reaction of 2,6-pyridinedicarbonyl chloride with the dimethyl substituted tetraethylene glycol (*SS*)-**84**, derived from (*S*)-lactic acid, afforded (126) the chiral macrocyclic polyether diester (*SS*)-**184**. A similar preparative approach (127) gave (*SS*)-**185**, where the source of the chirality is (*S*)-mandelic acid.

The reaction sequence outlined in Scheme 12 illustrates how macrocyclic polyether-thiono diesters such as (*RR*)-**186** can be prepared (184) from *O,O*-dimethyl 2,6-pyridinedicarbothiolate and (*RR*)-**84**. Potassium thiocyanate forms a 1:1 crystalline complex with (*RR*)-**186** and presumably the potassium ion serves as a template for the (1 + 1) cyclization. Raney nickel desulfurization of (*RR*)-**186** yields the chiral pyridino-18-crown-6 derivative (*RR*)-**187**.

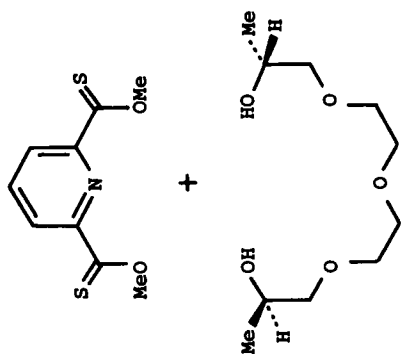
In a few cases, two pyridine rings have been incorporated into 18-crown-6 derivatives. Examples are provided by LL-**188** (89) and DD-**189** (168) that contain, as their sources of chirality, the bis(*N,N*-dimethylamide) of L-tartaric acid and the 1,2:5,6-di-*O*-isopropylidene derivative of D-mannitol, respectively.

F. Aza Macrobicyclic and Macropolycyclic Compounds

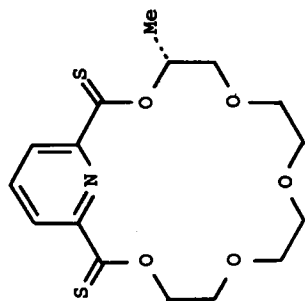
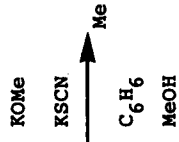
Chiral diaza-macrobicyclic polyethers derived from carbohydrates have been prepared (185) in high yield from diaza-18-crown-6 derivatives (e.g., α -D-**159** in Figure 20) by quaternizing them under high pressure and then demethylating (Scheme 13). Only one diastereoisomer of α -D-**190** was isolated: The same compound was obtained in much poorer yield by an alternative method starting from α -D-**160** (Figure 20) through reaction with diglycolic acid dichloride to afford a bisamide that was reduced to afford α -D-**190**. Other chiral diaza-macrobicyclic polyethers, based on the [2.2.1] and [2.2.2]cryptand constitutions



	R ¹	R ²
(<i>SS</i>)- 184	Me	H
(<i>SS</i>)- 185	H	Ph

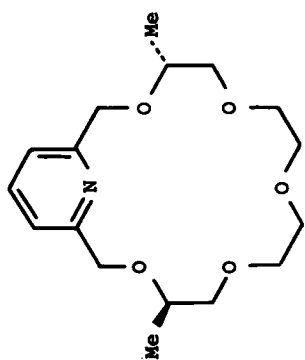
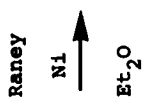


(*RR*)-**84**

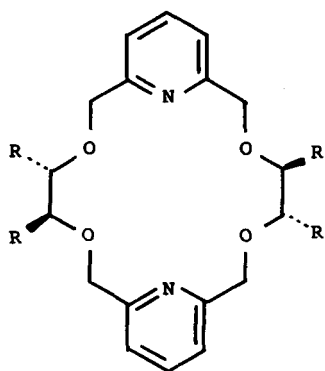
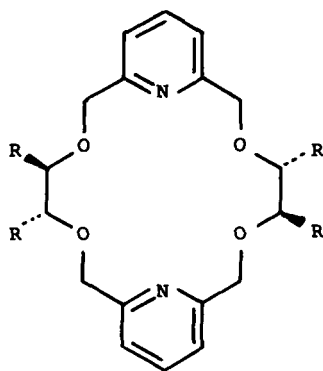


(*RR*)-**186**

Scheme 12



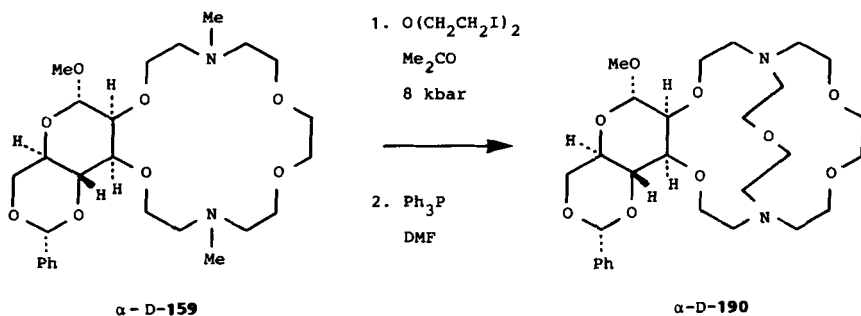
(*RR*)-**187**

LL-188 $R = \text{CONMe}_2$ DD-189 $R =$

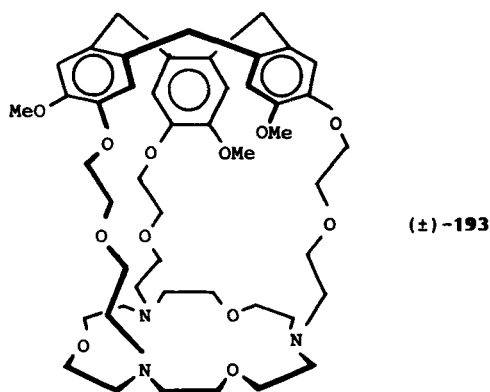
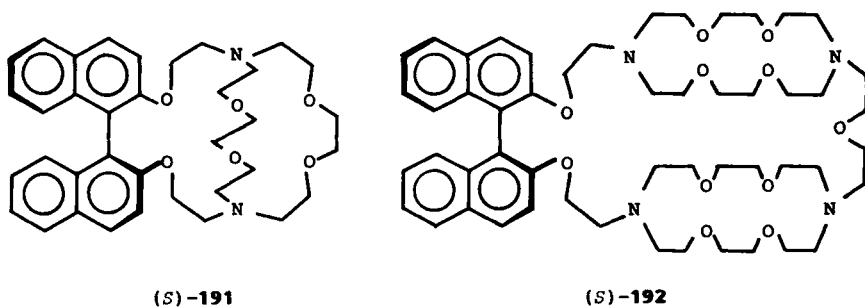
have been prepared that incorporate methyl 4,6-*O*-benzylidene- α -D-glucopyranoside (185) and α -D-galactopyranoside (185) residues, and a methyl 4,6-*O*-[(*S*)-phenylethylidene]- α -D-mannopyranoside unit (186).

The first optically active macrobicycles and macropolycycles were reported by Lehn and co-workers (187) in 1974. Employing the synthetic methodology developed in Strasbourg for the preparation of cryptands, chiral molecular receptors, such as (*S*)-191 and (*S*)-192, have been isolated and characterized.

Fascinating macrocyclic receptor cages based on a triaza-18-crown-6 derivative (79) and on a rigid cyclotrivierylene unit (188) can be synthesized (189) by connecting the two residues via three bridges in a single step. Macropolycycles, such as (\pm)-193 have been reported (189), and since the cyclotrivierylene unit is chiral and has been resolved (188), the preparation of optically active macrocyclic receptor cage molecules should be feasible (see below).



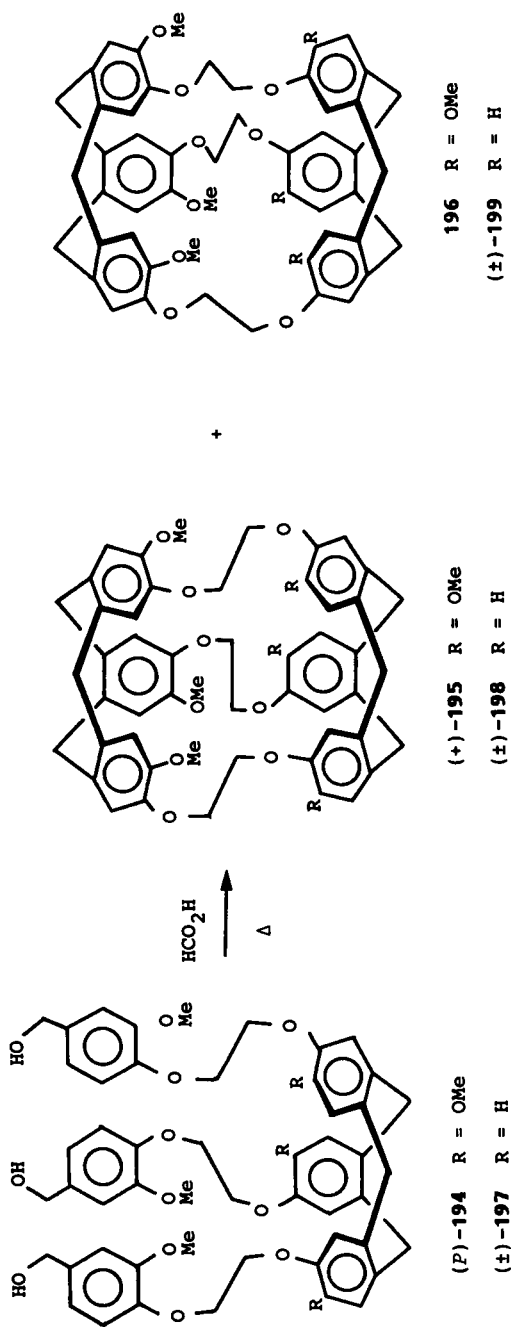
Scheme 13

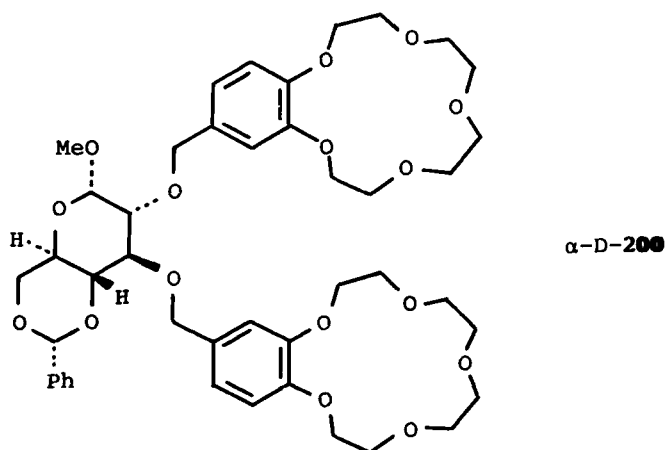


G. Miscellaneous Compounds

The synthesis of a chiral bis(cyclotrivenatryl) macrocage receptor (+)-**195** with D_3 symmetry has been achieved (190) by the stereospecific replication of (*P*)-**194** (Scheme 14). In so far as none of the meso isomer **196** was obtained, the intramolecular cyclization of (*P*)-**194** to give (+)-**195** provides a rare example of stereospecific replication. The corresponding intramolecular trimerization of the veratryl residues of the racemic precursor (±)-**197** proceeds (191a) with less stereospecificity to give (Scheme 14) a major isomer (±)-**198** and a minor isomer (±)-**199**. Compound **198** has been resolved and discriminates (by inclusion) between the enantiomers of CHBrClF, a neutral guest molecule (191b).

A range of benzo-15-crown-5 derivatives in which the crown ether is attached to a carbohydrate residue (e.g., 1,2:5,6-di-*O*-isopropylidene- α -D-glucopyranoside and - α -D-allofuranose, 1,2:3,4-di-*O*-isopropylidene- α -D-galactopyranoside, methyl 4,6-*O*-benzylidene- α -D-glucopyranoside, and 2,3,4,6-tetra-*O*-acetyl-D-glucopyranoside) through an ester, an ether, or a glycosidic linkage have been



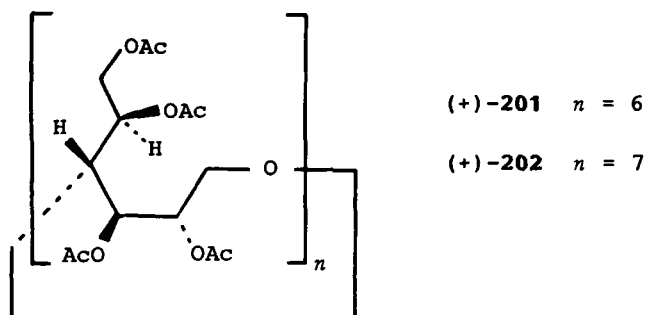


reported (192). The ether linkage has the attraction of hydrolytic stability relative to the other two types and it has been employed in the synthesis of the bisbenzo-15-crown-5 derivative **α-D-200**, emanating from a methyl 4,6-*O*-benzylidene- α -D-glucopyranoside unit (Figure 15). Acyclic polyether chains [$-\text{COCH}_2\text{O}(\text{CH}_2\text{CH}_2\text{O})_3\text{Me}$] have also been attached (193) via ester linkages to 1,2:5,6-di-*O*-isopropylidene- α -D-glucopyranose (one chain), 1,2-*O*-isopropylidene- α -D-glucopyranose (three chains), and methyl 4,6-*O*-benzylidene- α -D-glucopyranoside (two chains).

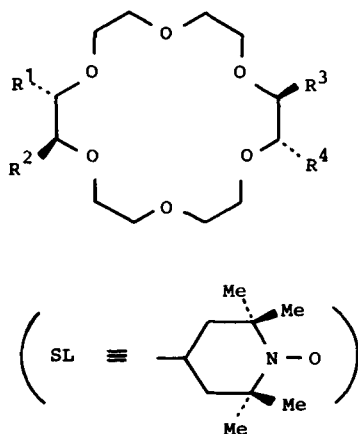
Finally, the chiral macrocyclic peracetylated polyhydroxy polyethers (+)-**201** and (+)-**202** have been prepared (194) recently by treatment of α - and β -cyclodextrins, respectively, with diethylborane and 9-borabicyclo[3.3.1]nonan-9-yl methanesulfonate as catalyst.

IV. PROPERTIES

The properties of chiral crown ethers in solution both in their free state and as their complexes with a wide range of substrates have been reviewed exten-



sively (7, 8, 17–19, 38, 48–52, 56–60, 91) during the last decade. Their chiroptical behavior, which has been assessed by circular dichroism measurements, as well as by specific rotation changes, has been investigated (89, 96, 115, 122–125, 161, 187, 188, 190, 195, 196) with particular reference to the effect their complexation with Groups IA and IIA metal cations has on this valuable physical probe. The most useful spectroscopic technique for studying the conformational properties of chiral crown ethers and their complexation properties has proved to be (mainly ^1H , but also some ^{13}C) NMR spectroscopy (96, 120, 132, 134, 166, 187). The dynamic aspects (132, 133, 136, 138–140, 168, 178, 180, 197, 198) of the technique have provided useful kinetic data on complexation–decomplexation rates, which have been employed along with thermodynamic data obtained from equilibration experiments (29, 48–53, 55–60, 88, 107, 128, 131, 133, 135–140, 142–145, 147–149, 157, 168, 199, 200) to ascertain the extent of the dependence of complexation strengths upon the configurations and conformations of chiral crown ether receptors (55–60, 131, 135, 138, 140, 145, 199, 200). EPR spectroscopy on chiral spin-labeled crown ethers has also been used (210) to follow the effects of K^+ ion binding, pH, solvent, and temperature upon the conformations adopted by LL-203, LL-204, and LL-205.



	R^1	R^2	R^3	R^4
LL-203	COOH	CONH-SL	CONH-SL	COOH
LL-204	COOH	CONH-SL	COOH	CONH-SL
LL-205	CONH-SL	CONH-SL	CONH-SL	CONH-SL

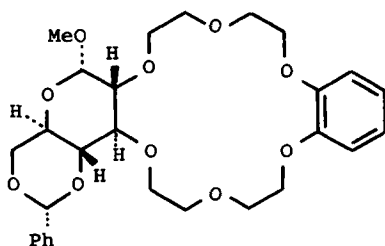
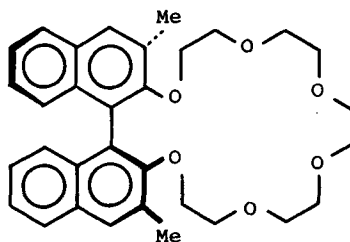
In the solid state, X-ray crystallography has provided (32, 62) valuable structural information on a wide variety of chiral crown ethers and their complexes with a range of substrates. These include

- The 18-crown-6 derivatives (obtained from L-tartaric acid) such as LL-35 with K^+ ions (202), LL-39 with the H_3O^+ cation (203) and the $^+H_3NCH_2CH_2NH_3^+$ dication (204), and LL-50 with Ca^{2+} cations and LL-51 with Sr^{2+} cations (101).
- The 18-crown-6 derivative (*RRRR*)-73 [obtained from (*RR*)-hydrobenzoin] with BH_3NH_3 (118).
- The 18-membered ring macrocyclic polyether diester (*SS*)-184 [containing a pyridino subunit and derived from (*S*)-lactic acid] with both enantiomers [i.e., (*R*) and (*S*)] of the $\alpha-C_{10}H_7CHMeNH_3^+$ cation (205).
- The 18-crown-6 derivatives (obtained from the methyl 4,6-*O*-benzylidene- α -D-glycopyranosides) such as α -D-206 with both KI (206) and KSCN (207), $\alpha\alpha$ -DD-115 (Figure 18) in its free form (150), and α -D-103 (Figure 17), α -D-105 (Figure 17), and $\alpha\alpha$ -DD-119 (Figure 18) with BH_3NH_3 (208).
- The 20-crown-6, 22-crown-6, and 30-crown-10 derivatives (incorporating D-mannitol residues) such as DD-92 and D-94 with BH_3NH_3 (208), D-94 with $Me_2CHNH_3^+$ cations (134), D-95 with $PhCH_2NH_3^+$ cations (134), DD-93 with H_2O (209), DD-92 both free and as a 1:1:1 complex with the (*S*)- $PhCHMeNH_3^+$ cation and H_2O (134).
- The 22-crown-5 derivative (*R*)-137 in Figure 19 (incorporating a 9,9'-spirobifluorene residue) with NH_4^+ cations (160) as well as the larger 26-crown-4 derivative (*SS*)-139 with benzene (162).
- The 20-crown-6 derivative (*S*)-207 (61), which contains a 3,3'-dimethyl-1,1'-dinaphthyl unit bound to the polyether macrocycle through its 2,2' positions, both in its free form and bound to $Me_3CNH_3^+$ cations.
- The 22-crown-6 derivative (*SS*)-129 [incorporating (*S*)-binaphthyl units] with the (*R*)- $PhCH(CO_2Me)NH_3^+$ cation (210).
- The free macropolycyclic receptor (*SS*)-208 consisting of two 1,1'-tetralyl units bridged by four polyether chains between their 2 and 3 positions (211).

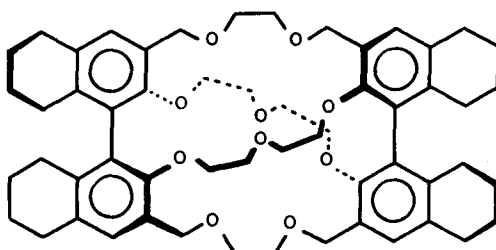
Chiral crown ethers have been employed extensively (48–53, 56–60, 86, 90, 93–95, 107, 110, 116, 117, 128, 143, 144, 152–155, 158–161, 163, 164, 212–227) for enantiomeric recognition of racemic primary alkyl ammonium cations including those associated with amino acid ester salts. Resolutions have been effected employing both bulk and chromatographic procedures.

Finally, chiral crown ethers have been utilized successfully both as enzyme mimics and as enzyme analogs. Important examples in the literature include

- Hydride transfer reactions (99, 181, 183, 228).

 α -D-206

(S)-207



(SS)-208

- Acyl transfer reactions (100, 111-114, 229, 230).
- Michael addition reactions (231).
- Ammonia borane (118, 208) and borohydride (232) reductions.

These exciting developments have been summarized at length in a number of recent review articles (19, 51, 54, 233, 234). They serve to raise expectations that useful artificial enzymes can be designed and constructed in chemical laboratories.

V. CONCLUDING REMARKS

By choosing to survey the field of chiral crown ethers at the level of their chemical production, it has been possible to expose the wide range of structural types that have been prepared and characterized to date. Clearly, the properties of some have been investigated and exploited by their makers to a much larger

extent than others at this time. However, as this relatively new branch of chemical science gains in maturity, so a more balanced appraisal of the relationship between receptor function and receptor structure will emerge. The quest for fundamental understanding of this relationship through detailed investigation of the chemistry of the noncovalent bond places intermolecular conformational analysis right at the forefront as a topic for contemporary stereochemical investigation.

ACKNOWLEDGMENTS

I am indebted to The Leverhulme Trust for the award of a Research Fellowship that made the writing of this review possible. I thank Dr. D. J. Williams (Imperial College London) and Mr. R. Zarzycki for their kind assistance in producing the computer drawn X-ray diagrams.

REFERENCES

1. Gokel, G. W.; Korzeniowski, S. H. In "Macrocyclic Polyether Synthesis"; Springer-Verlag: Berlin, 1982.
2. Hiraoka, M. In "Crown Compounds. Their Characteristics and Applications"; Elsevier: Amsterdam and New York, 1982.
3. Izatt, R. M.; Christensen, J. J., Eds., In "Synthetic Multidentate Macrocyclic Compounds"; Academic: New York, 1978.
4. Melson, G. A., Ed., In "Coordination Chemistry of Macrocyclic Compounds"; Plenum: New York, 1979.
5. Izatt, R. M.; Christensen, J. J., Eds., In "Progress in Macrocyclic Chemistry"; Wiley-Interscience: New York, 1979; Vol. 1 and 1981; Vol. 2.
6. Patai, S., Ed., In "The Chemistry of the Functional Groups. Supplement E. The Chemistry of Ethers, Crown Ethers, Hydroxyl Groups, and their Sulphur Analogues," Part 1; Wiley: Chichester, 1980.
7. Vögtle, F., Ed., "Host-Guest Chemistry I and II," In "Topics in Current Chemistry 98 and 101"; Springer-Verlag: Berlin, 1981 and 1982. See also Vögtle, F.; Weber, E., Eds., In "Host Guest Complex Chemistry. Macrocycles. Synthesis, Structures, Applications"; Springer-Verlag: Berlin, 1985.
8. Atwood, J. L.; Davies, J. E. D.; MacNicol, D. D., Eds., In "Inclusion Compounds," Vols. 1-3; Academic: London, 1984.
9. Truter, M. R.; Pedersen, C. J. *Endeavour* **1971**, *30*, 142.
10. Pedersen, C. J.; Frensdorff, H. K. *Angew. Chem. Int. Ed. Engl.* **1972**, *11*, 16.
11. Truter, M. R. *Structure and Bonding* **1973**, *16*, 71.
12. Lehn, J.-M. *Structure and Bonding* **1973**, *16*, 1.
13. Lehn, J.-M. *Acc. Chem. Res.* **1978**, *11*, 49.

14. Lehn, J.-M. *Pure Appl. Chem.* **1980**, *52*, 2303; Lehn, J.-M. *Pure Appl. Chem.* **1980**, *52*, 2441.
15. Lehn, J.-M. In "Frontiers of Chemistry"; Laidler, K. J., Ed.; Pergamon Press: Oxford, 1982, pp. 265-272.
16. Lehn, J.-M. *Science* **1985**, *277*, 849.
17. Hayward, R. C. *Chem. Soc. Rev.* **1983**, *12*, 285.
18. Hamilton, A. D. In "Comprehensive Heterocyclic Chemistry", Vol. 7; Katritzky, A. R.; Rees, C. W., Eds.; Pergamon Press: Oxford, 1984; Lwowski, W., Ed.; pp. 731-761.
19. Sirlin, C. *Bull. Soc. Chim. Fr., II* **1984**, *5*.
20. Bradshaw, J. S.; Stott, P. E. *Tetrahedron* **1980**, *36*, 461.
21. de Jong, F.; Reinhoudt, D. N. *Adv. Phys. Org. Chem.* **1980**, *17*, 279.
22. Cram, D. J. *Science*, **1983**, *219*, 1177.
23. Stoddart, J. F. *R. Soc. Chem. Ann. Rep. B* **1983**, **1984**, 353.
24. Pedersen, C. J. *Aldrichimica Acta* **1971**, *4*, 1.
25. Pedersen, C. J. *J. Am. Chem. Soc.* **1967**, *89*, 2495 and 7017; *Org. Synth.* **1972**, *52*, 66.
26. Trueblood, K. N.; Knobler, C. B.; Lawrence, D. S.; Stevens, R. V. *J. Am. Chem. Soc.* **1982**, *104*, 1355.
27. Colquhoun, H. M.; Jones, G.; Maud, J. M.; Stoddart, J. F.; Williams, D. J. *J. Chem. Soc., Dalton Trans.* **1984**, 63; see also Alston, D. R.; Stoddart, J. F.; Wolsteholme, J. B.; Allwood, B. L.; Williams, D. J. *Tetrahedron* **1985**, *41*, 2923.
28. Colquhoun, H. M.; Lewis, D. F.; Stoddart, J. F.; Williams, D. J. *J. Chem. Soc., Dalton Trans.* **1983**, 607; Colquhoun, H. M.; Stoddart, J. F.; Williams, D. J. *Angew. Chem. Int. Ed. Engl.* **1986**, *25*, 487.
29. Kyba, E. P.; Helgeson, R. C.; Madan, K.; Gokel, G. W.; Tarnowski, T. L.; Moore, S. S.; Cram, D. J. *J. Am. Chem. Soc.* **1977**, *99*, 2564; see also Madan, K., Cram, D. J. *J. Chem. Soc., Chem. Commun.* **1975**, 427.
30. Cram, D. J.; Cram, J. M. *Acc. Chem. Res.* **1978**, *11*, 8.
31. Bartsch, R. A. In "Progress in Macrocyclic Chemistry," Vol. 2; Izatt, R. M.; Christensen, J. J., Eds.; Wiley-Interscience: New York, 1981; pp. 1-39.
32. Goldberg, I. In "Inclusion Compounds," Vol. 2; Atwood, J. L.; Davies, J. E. D.; MacNicol, D. D., Eds.; Academic Press: London, 1984; pp. 261-335.
33. Bovill, M. J.; Chadwick, D. J.; Sutherland, I. O.; Watkin, D. J. *Chem. Soc., Perkin Trans. 2* **1980**, 1529.
34. Maud, J. M.; Stoddart, J. F.; Williams, D. J. *Acta Crystallogr., Sect. C* **1985**, *41*, 137.
35. Allwood, B. L.; Crosby, J.; Pears, D. A.; Stoddart, J. F.; Williams, D. J. *Angew. Chem. Int. Ed. Engl.* **1984**, *23*, 977; Pears, D. A.; Stoddart, J. F.; Crosby, J.; Allwood, B. L.; Williams, D. J. *Acta Crystallogr., Sect. C* **1986**, *42*, 804.
36. Allwood, B. L.; Colquhoun, H. M.; Crosby, J.; Pears, D. A.; Stoddart, J. F.; Williams, D. J. *Angew. Chem. Int. Ed. Engl.* **1984**, *23*, 824.
37. Pedersen, C. J. *J. Org. Chem.* **1971**, *36*, 1690.
38. Vögtle, F.; Weber, E. In "The Chemistry of the Functional Groups. Supplement E. The Chemistry of Ethers, Crown Ethers, Hydroxyl Groups, and Their Sulphur Analogues," Part 1; Patai, S., Ed.; Wiley: Chichester, 1980; pp. 59-156; Vögtle, F.; Sieger, H.; Müller, W. M. *Top. Curr. Chem.* **1981**, *98*, 107.
39. Bandy, J. A.; Truter, M. R.; Vögtle, F. *Acta Crystallogr., Sect. B* **1981**, *37*, 1568.

40. de Boer, J. A. A. Reinhoudt, D. N.; Harakema, S.; Hummel, G. J.; de Jong, F. *J. Am. Chem. Soc.* **1982**, *104*, 4073.
41. Elbasyouy, A.; Brügge, H. J.; Deuten, K. von; Dickel, M.; Knöchel, A.; Koch, K. U.; Kopf, J.; Melzer, D.; Rudolph, G. *J. Am. Chem. Soc.* **1983**, *105*, 6568.
42. Greene, R. N. *Tetrahedron Lett.* **1972**, 1793.
43. Laidler, D. A.; Stoddart, J. F. In "The Chemistry of the Functional Groups. Supplement E. Their Chemistry of Ethers, Crown Ethers, Hydroxyl Groups, and Their Sulphur Analogues," Part 1; Patai, S., Ed.; Wiley: Chichester, 1980; pp. 1-57.
44. Dunitz, J. D.; Seiler, P. *Acta Crystallogr., Sect. B* **1974**, *30*, 2739.
45. Seiler, P.; Dobler, M.; Dunitz, J. D. *Acta Crystallogr., Sect. B* **1974**, *30*, 2744.
46. Pears, D. A.; Stoddart, J. F.; Fakley, M. E.; Allwood, B. L.; Williams, D. J. in preparation; see also Nagano, O.; Kobayashi, A.; Sasaki, I.; *Bull. Chem. Soc. Jpn.* **1978**, *51*, 790.
47. Wipff, G.; Weiner, P.; Kollman, P. A. *J. Am. Chem. Soc.* **1982**, *104*, 3249; Wipff, G.; Kollman, P. A.; Lehn, J.-M. *J. Mol. Struct.* **1983**, *93*, 153; Weiner, P. K.; Profeta Jr., S.; Wipff, G.; Havel, T.; Kuntz, I. D.; Langridge, R.; Kollman, P. A. *Tetrahedron* **1983**, *39*, 1113; Uiterwijk, J. W. H. M.; Harkema, S.; van de Waal, B. W.; Gobel, F.; Nibbeling, H. T. M. *J. Chem. Soc., Perkin Trans. 2* **1983**, 1843; Kollman, P. A. *Acc. Chem. Res.* **1985**, *18*, 105.
48. Cram, D. J.; Cram, J. M. *Science* **1974**, *183*, 803.
49. Cram, D. J.; Helgeson, R. C.; Sousa, L. R.; Timko, J. M.; Newcomb, M.; Moreau, P.; de Jong, F.; Gokel, W. C.; Hoffman, D. H.; Domeier, L. A.; Peacock, S. C.; Madan, K.; Kaplan, L. *Pure Appl. Chem.* **1975**, *43*, 327.
50. Cram, D. J. In "Applications of Biomedical Systems in Chemistry," Vol. V; Jones, J. B.; Sih, C. J.; Perlman, D., Eds.; Wiley-Interscience: New York, 1976; pp. 815-873.
51. Cram, D. J. In "Structural and Dynamic Chemistry, Proceedings of Symposium"; Ahlberg, P.; Sundeloef, L. O. Eds., Almqvist & Wiksell: Stockholm, 1978; pp. 41-56.
52. Cram, D. J.; Trueblood, K. N.; *Top. Curr. Chem.* **1981**, *98*, 43.
53. Timko, J. M.; Moore, S. S.; Walba, D. M.; Hiberty, P. C.; Cram, D. J. *J. Am. Chem. Soc.* **1977**, *99*, 4207.
54. Lehn, J.-M. *Pure Appl. Chem.* **1979**, *51*, 979.
55. Coxon, A. C.; Laidler, D. A.; Pettman, R. B.; Stoddart, J. F. *J. Am. Chem. Soc.*, **1978**, *100*, 8260.
56. Stoddart, J. F. *Chem. Soc. Rev.* **1979**, *8*, 85.
57. Stoddart, J. F. In "Enzymic and Non-Enzymic Catalysis"; Dunnill, P.; Wiseman, A.; Blakebrough, N., Eds.; Ellis-Horwood: Chichester, 1980; pp. 84-110.
58. Stoddart, J. F. In "Bioenergetics and Thermodynamics: Model Systems"; Braibanti, A., Ed.; Reidel: Dordrecht, 1980; pp. 43-62.
59. Stoddart, J. F. In "Lectures in Heterocyclic Chemistry," Vol. 5; Castle, R. N.; Schneller, S. W., Eds.; 1980; pp. S47-S60.
60. Crawshaw, T. H.; Laidler, D. A.; Metcalfe, J. C.; Pettman, R. B.; Stoddart, J. F.; Wolstenholme, J. B. In "Chemical Approaches to Understanding Enzyme Catalysis"; Green, B. S.; Ashani, Y.; Chipman, D., Eds.; Elsevier: Amsterdam, 1982; pp. 49-65.
61. Goldberg, I. *J. Am. Chem. Soc.* **1980**, *102*, 4106.
62. Goldberg, I. In "The Chemistry of Functional Groups. Supplement E. The Chemistry of Ethers, Crown Ethers, Hydroxyl Groups, and Their Sulphur Analogues," Part 1; Patai, S., Ed.; Wiley: Chichester, 1980; pp. 175-214.

63. Krane, J.; Skjetne, T. *Tetrahedron Lett.* **1980**, 1775.
64. Groth, P. *Acta Chem. Scand., Ser. A* **1981**, 35, 541.
65. Gokel, G. W.; Cram, D. J. *J. Chem. Soc., Chem. Commun.* **1973**, 481.
66. Haymore, B. L., unpublished results, 1982 quoted in ref. 32.
67. Izatt, R. M.; Lamb, J. D.; Rossiter, B. E.; Izatt, N. E.; Christensen, J. J.; Haymore, B. L. *J. Chem. Soc., Chem. Commun.* **1978**, 386.
68. Uiterwijk, J. W. H. M.; Harkema, S.; Geevers, J.; Reinhoudt, D. N. *J. Chem. Soc., Chem. Commun.* **1982**, 200; de Boer, J. A. A.; Uiterwijk, J. W. H. M.; Geevers, J.; Harkema, S.; Reinhoudt, D. N. *J. Org. Chem.* **1983**, 48, 4821.
69. Uiterwijk, J. W. H. M.; Harkema, S.; Reinhoudt, D. N.; Daasvatn, K.; den Hertog, Jr., H. J.; Geevers, J. *Angew. Chem. Int. Ed. Engl.* **1982**, 21, 450.
70. Colquhoun, H. M.; Stoddart, J. F.; Williams, D. J.; Wolstenholme, J. B.; Zarzycki, R. *Angew. Chem. Int. Ed. Engl.* **1981**, 20, 1051; Colquhoun, H. M.; Doughty, S.; Maud, J. M.; Stoddart, J. F.; Williams, D. J.; Wolstenholme, J. B. *Israel J. Chem.* **1985**, 25, 15.
71. Colquhoun, H. M.; Goodings, E. P.; Maud, J. M.; Stoddart, J. F.; Wolstenholme, J. B.; Williams, D. J. *J. Chem. Soc., Chem. Commun.* **1983**, 1140; *J. Chem. Soc., Perkin Trans. 2* **1985**, 607; see also Allwood, B. L.; Kohnke, F. H.; Slawin, A. M. Z.; Stoddart, J. F.; Williams, D. J. *J. Chem. Soc., Chem. Commun.* **1985**, 311; Kohnke, F. H.; Stoddart, J. F. *J. Chem. Soc., Chem. Commun.* **1985**, 314; Kohnke, F. H.; Stoddart, J. F.; Allwood, B. L.; Williams, D. J. *Tetrahedron Lett.* **1985**, 26, 1681; Kohnke, F. H.; Stoddart, J. F. *Tetrahedron Lett.* **1985**, 26, 1685; Allwood, B. L.; Kohnke, F. H.; Stoddart, J. F.; Williams, D. J. *Angew. Chem. Int. Ed. Engl.* **1985**, 24, 581; Allwood, B. L.; Colquhoun, H. M.; Doughty, S. M.; Kohnke, F. H.; Slawin, A. M. Z.; Stoddart, J. F.; Williams, D. J.; Zarzycki, R. *J. Chem. Soc., Chem. Commun.*, in preparation.
72. Allwood, B. L.; Shahriari-Zavareh, H.; Stoddart, J. F.; Williams, D. J. *J. Chem. Soc., Chem. Commun.*, in preparation; Colquhoun, H. M.; Stoddart, J. F.; Williams, D. J. *New Sci.*, Feature Article, 1 May 1986, No. 1506, 44.
73. Leigh, S. J.; Sutherland, I. O. *J. Chem. Soc., Perkin Trans. 1* **1979**, 1089; Hodgkinson, L. C.; Sutherland, I. O. *J. Chem. Soc., Perkin Trans. 1* **1979**, 1908; Hodgkinson, L. C.; Johnson, M. R.; Leigh, S. J.; Spencer, N.; Sutherland, I. O.; Newton, R. F. *J. Chem. Soc., Perkin Trans. 1* **1979**, 2193.
74. Izatt, R. M.; Izatt, N. E.; Rossiter, B. E.; Christensen, J. J.; Haymore, B. L. *Science* **1978**, 199, 994.
75. Roland, B.; Smid, J. *J. Am. Chem. Soc.* **1983**, 105, 5269.
76. Metcalfe, J. C.; Stoddart, J. F.; Jones, G. *J. Am. Chem. Soc.* **1977**, 99, 8317; see also Krane, J.; Aune, O. *Acta Chem. Scand. B* **1980**, 34, 397.
77. Metcalfe, J. C.; Stoddart, J. F.; Jones, G.; Hull, W. E.; Atkinson, A.; Kerr, I. S.; Williams, D. J. *J. Chem. Soc., Chem. Commun.* **1980**, 540.
78. Johnson, M. R.; Sutherland, I. O.; Newton, R. F. *J. Chem. Soc., Chem. Commun.* **1979**, 309; Mageswaran, R.; Mageswaran, S.; Sutherland, I. O. *J. Chem. Soc., Chem. Commun.* **1979**, 722; Jones, N. F.; Kumar, A.; Sutherland, I. O. *J. Chem. Soc., Chem. Commun.* **1981**, 990; Sutherland, I. O. *Heterocycles* **1984**, 21, 235; *Chem. Soc. Rev.* **1986**, 15, 63.
79. Lehn, J.-M. *Pure Appl. Chem.* **1977**, 49, 857; Kotzyba-Hibert, F.; Lehn, J.-M.; Vierling, P. *Tetrahedron Lett.* **1980**, 21, 941; Lehn, J.-M.; Vierling, P. *Tetrahedron Lett.* **1980**, 21, 1323; Kintzinger, J.-P.; Kotzyba-Hibert, F.; Lehn, J.-M.; Pagelot, A.; Saigo, K. *J. Chem. Soc., Chem. Commun.* **1981**, 833; Kotzyba-Hibert, F.; Lehn, J.-M.; Saigo, K. *J. Am. Chem. Soc.* **1981**, 103, 4266; Pascard, C.; Riche, C.; Cesario, M.; Kotzyba-Hibert, F.; Lehn, J.-M. *J. Chem. Soc., Chem. Commun.* **1982**, 557.

80. Bovill, M. J.; Chadwick, D. J.; Johnson, M. R.; Jones, N. F.; Sutherland, I. O.; Newton, R. F. *J. Chem. Soc., Chem. Commun.* **1979**, 1065.
81. Timko, J. M.; Helgeson, R. C.; Newcomb, M.; Gokel, G. W.; Cram, D. J. *J. Am. Chem. Soc.* **1974**, *96*, 7097.
82. Maverick, E.; Grossenbacher, L.; Trueblood, K. N. *Acta Crystallogr., Sect. B* **1979**, *35*, 2233.
83. Newcomb, M.; Gokel, G. W.; Cram, D. J. *J. Am. Chem. Soc.* **1974**, *96*, 6810; Newcomb, M.; Timko, J. M.; Walba, D. M.; Cram, D. J. *J. Am. Chem. Soc.* **1977**, *99*, 6392.
84. Stoddart, J. F.; Szarek, W. A. *Canad. J. Chem.* **1968**, *46*, 3061; Ritchie, R. G. S.; Stoddart, J. F.; Vyas, D. M.; Szarek, W. A. *Carbohydr. Res.* **1974**, *32*, 279.
85. Wudl, F.; Gaeta, F. *J. Chem. Soc., Chem. Commun.*, **1972**, 107.
86. Kyba, E. P.; Siegel, M. G.; Sousa, L. R.; Sogah, G. D. Y.; Cram, D. J. *J. Am. Chem. Soc.* **1973**, *95*, 2691; Kyba, E. P.; Koga, K.; Sousa, L. R.; Siegel, M. G.; Cram, D. J. *J. Am. Chem. Soc.* **1973**, *95*, 2692.
87. Jacques, J.; Fouquey, C.; Viterbo, R. *Tetrahedron Lett.* **1971**, 4617; Pirkle, W. H.; Schreiner, J. L. *J. Org. Chem.* **1981**, *46*, 4988; Fujimoto, Y.; Iwadata, H.; Ikekawa, N. *J. Chem. Soc., Chem. Commun.* **1985**, 1333; Wu, S.-H.; Zhang, L.-Q.; Chen, C.-S.; Girdukas, G.; Sih, C. J. *Tetrahedron Lett.* **1985**, *26*, 4323.
88. Curtis, W. D.; Laidler, D. A.; Stoddart, J. F.; Jones, G. H. *J. Chem. Soc., Chem. Commun.* **1975**, 833.
89. Girodeau, J.-M.; Lehn, J.-M.; Sauvage, J.-P. *Angew. Chem. Int. Ed. Engl.* **1975**, *14*, 764.
90. Curtis, W. D.; Laidler, D. A.; Stoddart, J. F.; Jones, G. H. *J. Chem. Soc., Chem. Commun.* **1975**, 835.
91. Stoddart, J. F. In "Progress in Macrocyclic Chemistry," Vol. 2; Izatt, R. M.; Christensen, J. J., Eds.; Wiley-Interscience, New York, 1981, pp. 173-250.
92. Jolley, S. T.; Bradshaw, J. S.; Izatt, R. M. *J. Heterocyclic Chem.* **1982**, *19*, 3.
93. Helgeson, R. C.; Koga, K.; Timko, J. M.; Cram, D. J. *J. Am. Chem. Soc.* **1973**, *95*, 3021; see also Helgeson, R. C.; Timko, J. M.; Cram, D. J. *J. Am. Chem. Soc.* **1973**, *95*, 3023.
94. Timko, J. M.; Helgeson, R. C.; Cram, D. J. *J. Am. Chem. Soc.* **1978**, *100*, 2828.
95. Yamamoto, K.; Noda, K.; Okamoto, Y. *J. Chem. Soc., Chem. Commun.* **1985**, 1421.
96. Behr, J.-P.; Girodeau, J.-M.; Hayward, R. C.; Lehn, J.-M.; Sauvage, J.-P. *Helv. Chim. Acta* **1980**, *63*, 2096.
97. Kalinowski, H.-O.; Seebach, D.; Crass, G. *Angew. Chem. Int. Ed. Engl.* **1975**, *14*, 762; see also Menzies, R. C. *J. Chem. Soc.* **1947**, 1378.
98. Behr, J.-P.; Lehn, J.-M.; Vierling, P. *J. Chem. Soc., Chem. Commun.*, **1976**, 621; *Helv. Chim. Acta* **1982**, *65*, 1853; see also Lehn, J.-M.; Vierling, P.; Hayward, R. C. *J. Chem. Soc., Chem. Commun.*, **1979**, 296.
99. Behr, J.-P.; Lehn, J.-M. *J. Chem. Soc., Chem. Commun.* **1978**, 143; *Helv. Chim. Acta* **1984**, *63*, 2112.
100. Lehn, J.-M.; Sirlin, C. *J. Chem. Soc., Chem. Commun.* **1978**, 949.
101. Behr, J.-P.; Lehn, J.-M.; Moras, D.; Thierry, J. C. *J. Am. Chem. Soc.* **1981**, *103*, 701.
102. Behr, J.-P.; Burrows, C. J.; Heng, R.; Lehn, J.-M.; *Tetrahedron Lett.* **1985**, *26*, 215.
103. Basak, A.; Dugas, H. *Tetrahedron Lett.* **1986**, *27*, 3; see also Dugas, H.; Brunet, P.; Desroches, J. *Tetrahedron Lett.* **1986**, *27*, 7.
104. Frederick, L. A.; Fyles, T. M.; Malik-Diemer, V. A.; Whitfield, D. M. *J. Chem. Soc., Chem. Commun.* **1980**, 1211; Frederick, L. A.; Fyles, T. M.; Gurprasad, N. P.; Whitfield,

- D. M. *Can. J. Chem.* **1981**, *59*, 1724; see also Fyles, T. M.; Malik-Diemer, V. A.; Whitfield, D. M. *Can. J. Chem.* **1981**, *59*, 1734; Fyles, T. M.; Malik-Diemer, V. A.; McGavin, C. A.; Whitfield, D. M. *Can. J. Chem.* **1982**, *60*, 2259; Dulea, L. M.; Fyles, T. M.; Whitfield, D. M. *Can. J. Chem.* **1984**, *62*, 498; Fyles, T. M.; Whitfield, D. M. *Can. J. Chem.* **1984**, *62*, 507.
105. Dhaenens, M.; Lacombe, L.; Lehn, J.-M.; Vigneron, J. P. *J. Chem. Soc., Chem. Commun.* **1984**, 1097.
106. Coxon, A. C.; Curtis, W. D.; Laidler, D. A.; Stoddart, J. F. In "Asymmetry in Carbohydrates," Harmon, R. E., Ed.; Marcel Dekker, New York, 1979, pp. 167-197; *J. Carbohydr. Nucl. Nucl.* **1979**, *6*, 167.
107. Curtis, W. D.; Laidler, D. A.; Stoddart, J. F.; Jones, G. H. *J. Chem. Soc., Perkin Trans. I* **1977**, 1756.
108. Chênevert, R.; Voyer, N.; Plante, R. *Synthesis*, **1982**, 782.
109. Ando, N.; Yamamoto, Y.; Oda, J.; Inouye, Y. *Synthesis*, **1978**, 688.
110. Yamashita, J.; Minagawa, M.; Sonobe, A.; Ohashi, S.; Kawamura, M.; Shimizu, K.; Hashimoto, H. *Chem. Lett.* **1982**, 1409.
111. Matsui, T.; Koga, K. *Tetrahedron Lett.* **1978**, 1115.
112. Matsui, T.; Koga, K. *Chem. Pharm. Bull.* **1979**, *27*, 2295.
113. Sasaki, S.; Shionoya, M.; Koga, K. *J. Am. Chem. Soc.* **1985**, *107*, 3371.
114. Sasaki, S.; Koga, K. *Heterocycles* **1979**, *12*, 1305.
115. Hayward, R. C.; Overton, C. H.; Whitham, G. H. *J. Chem. Soc., Perkin Trans. I* **1976**, 2413.
116. Curtis, W. D.; Laidler, D. A.; Stoddart, J. F.; Wolstenholme, J. B.; Jones, G. H. *Carbohydr. Res.* **1977**, *57*, C17.
117. Dietl, F.; Merz, A.; Tomahogh, R. *Tetrahedron Lett.* **1982**, *23*, 5255.
118. Allwood, B. L.; Shahriari-Zavareh, H.; Stoddart, J. F.; Williams, D. J. *J. Chem. Soc., Chem. Commun.* **1984**, 1461.
119. Crosby, J.; Pears, D. A.; Shahriari-Zavareh, H.; Stoddart, J. F., unpublished results.
120. Merz, A.; Eichner, M.; Tomahogh, R. *Justus Liebigs Ann. Chem.* **1981**, 1774; see also Weber, G.; Sheldrick, G. M.; Burgemeister, Th.; Dietl, F.; Mannschreck, A.; Merz, A. *Tetrahedron* **1984**, *40*, 855; Blasius, E.; Raussch, R. A.; Andreetti, G. D.; Rebizant, J. *Chem. Ber.* **1984**, *117*, 1113.
121. Malpass, G. D.; Palmer, R. A.; Ghirardelli, R. G. *Tetrahedron Lett.* **1980**, *21*, 1489.
122. Mack, M. P.; Hendrixson, R. R.; Palmer, R. A.; Ghirardelli, R. G. *J. Am. Chem. Soc.* **1976**, *98*, 7830.
123. Mack, M. P.; Hendrixson, R. R.; Palmer, R. A.; Ghirardelli, R. G. *J. Org. Chem.* **1983**, *48*, 2029.
124. Ghirardelli, R. G. *J. Am. Chem. Soc.* **1973**, *95*, 4987.
125. Cooper, K. D.; Walborsky, H. M. *J. Org. Chem.* **1981**, *46*, 2110.
126. Jones, B. A.; Bradshaw, J. S.; Izatt, R. M. *J. Heterocycl. Chem.* **1982**, *19*, 551.
127. Bradshaw, J. S.; Jolley, S. T.; Izatt, R. M. *J. Org. Chem.* **1982**, *47*, 1229.
128. Alday, R.; Schröder, G. *Justus Liebigs Ann. Chem.* **1984**, 1036.
129. Cesare, P. D.; Gross, B. *Synthesis* **1979**, 458.
130. Nakazaki, M.; Naemura, K.; Makimura, M.; Matsuda, A.; Kawano, T.; Ohta, Y. *J. Org. Chem.* **1982**, *47*, 2429.

131. Haslegrave, J. A.; Stoddart, J. F.; Thompson, D. J. *Tetrahedron Lett.* **1979**, 2279.
132. Metcalfe, J. C.; Stoddart, J. F.; Jones, G.; Crawshaw, T. H.; Quick, A.; Williams, D. J. *J. Chem. Soc., Chem. Commun.* **1981**, 430; Metcalfe, J. C.; Stoddart, J. F.; Jones, G.; Crawshaw, T. H.; Gavuzzo, E.; Williams, D. J. *J. Chem. Soc., Chem. Commun.* **1981**, 432.
133. Laidler, D. A.; Stoddart, J. F. *Tetrahedron Lett.* **1979**, 453.
134. Fuller, S. E.; Stoddart, J. F.; Williams, D. J. *J. Chem. Soc., Chem. Commun.* **1982**, 1093; Fuller, S. E.; Mann, B. E.; Stoddart, J. F. *J. Chem. Soc., Chem. Commun.* **1982**, 1096.
135. Bell, T. W. *J. Am. Chem. Soc.* **1981**, 103, 1163.
136. Andrews, D. G.; Ashton, P. R.; Laidler, D. A.; Stoddart, J. F.; Wolstenholme, J. B. *Tetrahedron Lett.* **1979**, 2629.
137. Laidler, D. A.; Stoddart, J. F. *Carbohydrate Res.* **1977**, 55, C1.
138. Laidler, D. A.; Stoddart, J. F. *J. Chem. Soc., Chem. Commun.* **1977**, 481.
139. Pettman, R. B.; Stoddart, J. F. *Tetrahedron Lett.* **1979**, 457.
140. Pettman, R. B.; Stoddart, J. F. *Tetrahedron Lett.* **1979**, 461.
141. Hain, W.; Lehnert, R.; Röttele, H.; Schröder, G. *Tetrahedron Lett.* **1978**, 625.
142. Gruber, H.; Schröder, G. *Justus Liebigs Ann. Chem.* **1985**, 421.
143. Ellinghaus, R.; Schröder, G. *Justus Liebigs Ann. Chem.* **1985**, 418.
144. Curtis, W. D.; King, R. M.; Stoddart, J. F.; Jones, G. H. *J. Chem. Soc., Chem. Commun.* **1976**, 284.
145. Laidler, D. A.; Stoddart, J. F.; Wolstenholme, J. B. *Tetrahedron Lett.* **1979**, 465.
146. Hain, W.; Lehnert, R.; Walz, B.; Schröder, G. *Justus Liebigs Ann. Chem.* **1984**, 1046.
147. Töke, L.; Fenichel, L.; Bakó, P.; Szejtli, J. *Acta Chim. Acad. Sci. Hung.* **1978**, 98, 357.
148. Bakó, P.; Fenichel, L.; Töke, L.; Czugler, M. *Justus Liebigs Ann. Chem.* **1981**, 1163.
149. Bakó, P.; Fenichel, L.; Töke, L. *Acta Chim. Acad. Sci. Hung.* **1982**, 111, 297.
150. Czugler, M.; Bakó, P.; Fenichel, L.; Töke, L. *Cryst. Struct. Commun.* **1981**, 10, 511.
151. Walz, B.; Schröder, G. *Justus Liebigs Ann. Chem.* **1985**, 426.
152. Kyba, E. P.; Gokel, G. W.; de Jong, F.; Koga, K.; Sousa, L. R.; Siegel, M. G.; Kaplan, L.; Sogah, G. D. Y.; Cram, D. J. *J. Org. Chem.* **1977**, 42, 4173.
153. Cram, D. J.; Helgeson, R. C.; Peacock, S. C.; Kaplan, L. J.; Domeier, L. A.; Moreau, P.; Koga, K.; Mayer, J. M.; Chao, Y.; Siegel, M. G.; Hoffman, D. H.; Sogah, G. D. Y. *J. Org. Chem.* **1978**, 43, 1930.
154. Peacock, S. S.; Walba, D. M.; Gaeta, F. C. A.; Helgeson, R. C.; Cram, D. J. *J. Am. Chem. Soc.* **1980**, 102, 2043.
155. Lingenfelter, D. S.; Helgeson, R. C.; Cram, D. J. *J. Org. Chem.* **1981**, 46, 393.
156. Cram, D. J.; Helgeson, R. C.; Koga, K.; Kyba, E. P.; Madan, K.; Sousa, L. R.; Siegel, M. G.; Moreau, P.; Gokel, G. W.; Timko, J. M.; Sogah, G. D. Y. *J. Org. Chem.* **1978**, 43, 2758.
157. Koenig, K. E.; Helgeson, R. C.; Cram, D. J. *J. Am. Chem. Soc.* **1976**, 98, 4018; Helgeson, R. C.; Tarnowski, T. L.; Cram, D. J. *J. Org. Chem.* **1979**, 44, 2538.
158. Yamamoto, K.; Fukushima, H.; Okamoto, Y.; Hatada, K.; Nakazaki, M. *J. Chem. Soc., Chem. Commun.* **1985**, 1111; see also Yamamoto, K.; Fukushima, H.; Nakazaki, M. *J. Chem. Soc., Chem. Commun.* **1984**, 1490.
159. Yamamoto, K.; Noda, K.; Okamoto, Y. *J. Chem. Soc., Chem. Commun.* **1985**, 1065.

160. Prelog, V. *Pure Appl. Chem.* **1978**, 50, b93.
161. Prelog, V.; Bedekovic, D. *Helv. Chim. Acta* **1979**, 62, 2285.
162. Dobler, M.; Dumic, M.; Egli, M.; Prelog, V. *Angew. Chem. Int. Ed. Engl.* **1985**, 24, 792.
163. Naemura, K.; Fukunaga, R.; Yamanaka, M. *J. Chem. Soc., Chem. Commun.* **1985**, 1560.
164. Nakazaki, M.; Yamamoto, K.; Ikeda, T.; Kitsuki, T.; Okamoto, Y. *J. Chem. Soc., Chem. Commun.* **1983**, 787.
165. Bogatsky, A. V.; Lukyanenko, N. G.; Lobach, A. V.; Nazarova, N. Y.; Karpenko, L. P. *Synthesis*, **1984**, 139.
166. Gregory, B. J.; Haines, A. H.; Karntiang, P. *J. Chem. Soc., Chem. Commun.* **1977**, 918; Haines, A. H.; Karntiang, P. *J. Chem. Soc., Perkin Trans I* **1979**, 2577.
167. Allwood, B. L.; Fuller, S. E.; Ning, P. C. Y. K.; Slawin, A. M. Z.; Stoddart, J. F.; Williams, D. J. *J. Chem. Soc., Chem. Commun.* **1984**, 1356; Stoddart, J. F.; Fuller, S. E.; Doughty, S. M.; Ning, P. C. Y. K.; Williams, M. K.; Williams, D. J.; Allwood, B. L.; Slawin, A. M. Z.; Colquhoun, H. M. In "Organic Synthesis: An Interdisciplinary Challenge"; Streith, J.; Prinzbach, H.; Schill, G.; Eds.; Blackwell Scientific Publications: London, 1985; pp. 295-305.
168. Laidler, D. A.; Stoddart, J. F. *J. Chem. Soc., Chem. Commun.* **1976**, 979.
169. Pietraszkiewicz, M.; Jurczak, J. *J. Chem. Soc., Chem. Commun.* **1983**, 132.
170. Pietraszkiewicz, M.; Jurczak, J. *Tetrahedron* **1984**, 40, 2967.
171. Bakó, P.; Fenichel, L.; Töke, L. *Acta Chim. Acad. Sci. Hung.* **1984**, 116, 323.
172. Willner, I.; Goren, Z. *J. Chem. Soc., Chem. Commun.* **1983**, 1469.
173. Vögtle, F.; Jansen, B. *Tetrahedron Lett.* **1976**, 4895; see also Fenton, D. E.; Parkin D.; Newton, R. F. *J. Chem. Soc., Perkin Trans I* **1981**, 449.
174. Berthet, M.; Sonveaux, E. *J. Chem. Soc., Chem. Commun.* **1983**, 10.
175. Detellier, C.; Stover, H. D. H. *Synthesis* **1983**, 990.
176. Anzai, J.; Ueno, A.; Suzuki, Y.; Osa, T. *Makromol. Chem., Rapid Commun.* **1982**, 3, 55.
177. Chênevert, R.; Voyer, N. *Synthesis*, **1985**, 981.
178. Chadwick, D. J.; Cliffe, I. A.; Sutherland, I. O.; Newton, R. F. *J. Chem. Soc., Perkin Trans. I* **1984**, 1707.
179. Žinić, M.; Bosnić-Kasnar, B.; Kolbah, D. *Tetrahedron Lett.* **1980**, 21, 1365.
180. Chadwick, D. J.; Cliffe, I. A.; Sutherland, I. O.; Newton, R. F. *J. Chem. Soc., Chem. Commun.* **1981**, 992.
181. Talma, A. G.; Jouin, P.; de Vries, J. G.; Troostwijk, C. B.; Werumeus Buning, G. H.; Waninge, J. K.; Visscher, J.; Kellogg, R. M. *J. Am. Chem. Soc.* **1985**, 107, 3981.
182. van Keulen, B. J.; Kellogg, R. M.; Piepers, O. *J. Chem. Soc., Chem. Commun.* **1979**, 285; Buter, J.; Kellogg, R. M. *J. Org. Chem.* **1981**, 46, 4481; Kruizinga, W. H.; Kellogg, R. M. *J. Am. Chem. Soc.* **1981**, 103, 5183; Vriesema, B. K.; Buter, J.; Kellogg, R. M. *J. Org. Chem.* **1984**, 49, 110.
183. de Vries, J. G.; Kellogg, R. M. *J. Am. Chem. Soc.* **1979**, 101, 2759.
184. Jones, B. A.; Bradshaw, J. S.; Brown, P. R.; Christensen, J. J.; Izatt, R. M. *J. Org. Chem.* **1983**, 48, 2635.
185. Pietraszkiewicz, M.; Sławiński, P.; Jurczak, J. *J. Chem. Soc., Chem. Commun.* **1983**, 1184; *Tetrahedron* **1984**, 40, 2971.
186. Pietraszkiewicz, M.; Jurczak, J. *J. Carbohydr. Chem.* **1985**, 4, 429.
187. Dietrich, B.; Lehn, J.-M.; Simon, J. *Angew. Chem. Int. Ed. Engl.* **1974**, 13, 406.

188. Collet, A.; Jacques, J. *Tetrahedron Lett.* **1978**, 1265; Collet, A.; Gabard, J. *J. Org. Chem.* **1980**, *45*, 5400; Collet, A.; Gabard, J.; Jacques, J.; Cesario, M.; Guilhem, J.; Pascard, C. *J. Chem. Soc., Perkin Trans. 1* **1981**, 1630; Canceill, J.; Gabard, J.; Collet, A. *J. Chem. Soc., Chem. Commun.* **1983**, 122.
189. Canceill, J.; Collet, A.; Gabard, J.; Kotzyba-Hibert, F.; Lehn, J.-M. *Helv. Chim. Acta* **1982**, *65*, 1894.
190. Gabard J.; Collet, A. *J. Chem. Soc., Chem. Commun.* **1981**, 1137; see also Canceill, J.; Cesario, M.; Collet, A.; Guilhem, J.; Riche, C.; Pascard, C. *J. Chem. Soc., Chem. Commun.* **1986**, 339.
191. a) Canceill, J.; Lacombe, L.; Collet, A. *C. R. Acad. Sci., Ser. II* **1984**, 298, 39; Canceill, J. Cesario, M.; Collet, A.; Guilhem, J.; Pascard, C. *J. Chem. Soc., Chem. Commun.* **1985**, 361. b) Canceill, J.; Lacombe, L.; Collet, A. *J. Am. Chem. Soc.* **1985**, *107*, 6993.
192. Haines, A. H.; Hodgkinson, I.; Smith, C. *J. Chem. Soc., Perkin Trans. 1* **1983**, 311.
193. Haines, A. H.; Karntiang, P. *Carbohydr. Res.* **1980**, *78*, 205.
194. Bernabe, M.; Martin-Lomas, M.; Pendes, S.; Koster, R.; Dahlhoff, W. V. *J. Chem. Soc., Chem. Commun.* **1985**, 1001.
195. Kaneko, O.; Matsuura, N.; Kimura, K.; Shono, T. *Chem. Lett.* **1979**, 369.
196. Armstrong, D. W.; Ward, T. J.; Czech, A.; Czech, B. P.; Bartsch, R. A. *J. Org. Chem.* **1985**, *50*, 5556.
197. Pearson, D. P. J.; Leigh, S. J.; Sutherland, I. O. *J. Chem. Soc., Perkin Trans. 1* **1979**, 3113.
198. Pietraszkiewicz, M.; Stoddart, J. F. *J. Chem. Soc., Perkin Trans 2* **1985**, 1559.
199. Helgeson, R. C.; Weisman, G. R.; Toner, J. L.; Tarnowski, T. L.; Chao, Y.; Mayer, J. M.; Cram, D. J. *J. Am. Chem. Soc.* **1979**, *101*, 4928.
200. Bell, T. W.; Lein, G. M.; Nakamura, H.; Cram, D. J. *J. Org. Chem.* **1983**, *48*, 4728.
201. Dugas, H.; Keroack, P.; Ptak, M. *Can. J. Chem.* **1984**, *62*, 489.
202. Behr, J.-P.; Lehn, J.-M.; Dock, A. C.; Moras, D. *Nature (London)* **1982**, *295*, 526; Dock, A. C.; Moras, D.; Behr, J.-P.; Lehn, J.-M. *Acta Crystallogr., Sect. C* **1983**, *39*, 1001.
203. Behr, J.-P.; Dumas, P.; Moras, D. *J. Am. Chem. Soc.* **1982**, *104*, 4540.
204. Daly, J. J.; Schonholzer, P.; Behr, J.-P.; Lehn, J.-M. *Helv. Chim. Acta* **1981**, *64*, 1444.
205. Davidson, R. B.; Dalley, N. K.; Izatt, R. M.; Bradshaw, J. S.; Campana, C. F. *Israel J. Chem.* **1985**, *25*, 33.
206. Suwińska, K.; Pietraszkiewicz, M.; Lipkowski, J.; Jurczak, J.; Andreetti, G. D.; Bocelli, G. *J. Mol. Struct.* **1981**, *75*, 121.
207. Suwińska, K.; Andreetti, G. D. *J. Incl. Phenom.* **1983**, *1*, 71.
208. Shariari-Zavareh, H.; Stoddart, J. F.; Williams, M. K.; Allwood, B. L.; Williams, D. J. *J. Incl. Phenom.* **1985**, *3*, 355.
209. Fuller, S. E.; Stoddart, J. F.; Williams, D. J. *Tetrahedron Lett.* **1982**, 1835.
210. Goldberg, I. *J. Am. Chem. Soc.* **1977**, *99*, 6049.
211. Goldberg, I. *Acta Crystallogr., Sect. B* **1980**, *36*, 2104.
212. Tundo, P.; Fendler, J. H. *J. Am. Chem. Soc.* **1980**, *102*, 1760.
213. Bradshaw, J. S.; Jones, B. A.; Davidson, R. B.; Christensen, J. J.; Lamb, J. D.; Izatt, R. M.; Morin, F. G.; Grant, D. M. *J. Org. Chem.* **1982**, *47*, 3364.
214. Davidson, R. B.; Bradshaw, J. S.; Jones, B. A.; Dalley, N. K.; Christensen, J. J.; Izatt, R. M. *J. Org. Chem.* **1984**, *49*, 353.

215. Helgeson, R. C.; Timko, J. M.; Moreau, P.; Peacock, S. C.; Mayer, J. M.; Cram, D. J. *J. Am. Chem. Soc.* **1974**, *96*, 6762.
216. Newcomb, M.; Helgeson, R. C.; Cram, D. J. *J. Am. Chem. Soc.* **1974**, *96*, 7367.
217. Gokel, G. W.; Timko, J. M.; Cram, D. J. *J. Chem. Soc., Chem. Commun.* **1975**, 444.
218. Peacock, S. C.; Cram, D. J. *J. Chem. Soc., Chem. Commun.* **1976**, 282.
219. Kyba, E. P.; Timko, J. M.; Kaplan, L. J.; de Jong, F.; Gokel, G. W.; Cram, D. J. *J. Am. Chem. Soc.* **1978**, *100*, 4555.
220. Sousa, L. R.; Sogah, G. D. Y.; Hoffman, D. H.; Cram, D. J. *J. Am. Chem. Soc.* **1978**, *100*, 4569.
221. Peacock, S. C.; Domeier, L. A.; Gaeta, F. C. A.; Helgeson, R. C.; Timko, J. M.; Cram, D. J. *J. Am. Chem. Soc.* **1978**, *100*, 8190.
222. Sogah, G. D. Y.; Cram, D. J. *J. Am. Chem. Soc.* **1979**, *101*, 3035.
223. Newcomb, M.; Toner, J. L.; Helgeson, R. C.; Cram, D. J. *J. Am. Chem. Soc.* **1979**, *101*, 4941.
224. Thoma, A. P.; Viviani-Nauer, A.; Schellenberg, K. H.; Bedeković, D.; Pretsch, E.; Prelog, V.; Simon, W. *Helv. Chim. Acta* **1979**, *62*, 2303.
225. Bussmann, W.; Lehn, J.-M.; Oesch, U.; Plumere, P.; Simon, W. *Helv. Chim. Acta* **1981**, *64*, 657.
226. Prelog, V.; Mutak, S. *Helv. Chim. Acta* **1983**, *66*, 2274.
227. Yamaguchi, T.; Nishimura, K.; Shinbo, T.; Sugaira, M. *Chem. Lett.* **1985**, 1549.
228. Jouin, P.; Troostwijk, C. B.; Kellogg, R. M. *J. Am. Chem. Soc.* **1981**, *103*, 2091; see also Mashraqui, S. H.; Kellogg, R. M. *J. Am. Chem. Soc.* **1983**, *105*, 7792.
229. Chao, Y.; Cram, D. J. *J. Am. Chem. Soc.* **1976**, *98*, 1015; Chao, Y.; Weisman, G. R.; Sogah, G. D. Y.; Cram, D. J. *J. Am. Chem. Soc.* **1979**, *101*, 4948.
230. Cram, D. J.; Katz, H. E. *J. Am. Chem. Soc.* **1983**, *105*, 135.
231. Cram, D. J.; Sogah, G. D. Y. *J. Chem. Soc., Chem. Commun.* **1981**, 625; *J. Am. Chem. Soc.* **1985**, *107*, 8301.
232. Shida, Y.; Ando, N.; Yamamoto, Y.; Oda, J.; Inouye, Y. *Agric. Biol. Chem.* **1979**, *43*, 1797.
233. Kellogg, R. M. *Angew. Chem. Int. Ed. Engl.* **1984**, *23*, 782; *Recherche* **1984**, *15*, 819.
234. Stoddart, J. F. In "The Chemistry of Enzyme Action"; Page, M. I., Ed., Elsevier: Amsterdam, 1984, pp. 529-561.

SUBJECT INDEX

- Absolute asymmetric synthesis, 82
- Achirotopic carbon atoms, 6
- Acoustic properties, 65
- Acrylate polymerization, 89
- Acyl transfer reactions, 278
- Addition polymerization, 87
- Adjacent reentry, 62
- Adrenaline, 265
- (L-Alaninato)*bis*(acetylacetonato)Co(III), 190
- L-Alanine, 161, 165
 - macrocyclic derivatives, 268
- L-Alanine-*N*-*d*₃, 170, 172
- L-Alanylglycine, 176
- Aldehydes, 97
- Alkenyl ethers, 89
- All-gauche conformation, 212, 214
- All-oxygen crown compounds, 232, 245, 246
- L-Allothreonine, 167, 175
- Amino acid ester salts, regioselective trans-acylations, 237
- Amino acids, 161
 - poly-L-, 12
 - rotameric distribution, 161, 174
- Amino acid side-chain VCD, 173
- L-Amino acid transition metal complexes, 165
- (4*S*,5*S*)-5-Amino-2,2-dimethyl-4-phenyl-1,3-dioxane, macrocyclic derivatives, 267
- 4'-Aminomethyl-4,5',8-trimethylpsoralen, macrocyclic derivatives, 236
- Ammonia borane, 278
- 2,5-Anhydro-3,4-di-*O*-methyl-D-mannitol, macrocyclic derivatives, 244
- Anisotropy ratio, 121, 136
- Apocholic acid, 82, 86
- Apomorphine, 265
- APT (Atomic Polar Tensor) model for VCD, 131
- Asymmetric carbon atoms, 6, 106
- Asymmetric catalyst, 79
- Asymmetric copolymerization, 82
- Asymmetric first-order Markov chain, 79
- Asymmetric growth, 79
- Asymmetric inclusion polymerization, 81
- Asymmetric induction:
 - through bond, 82
 - conformational, 61
 - through space, 82
 - and stereoregularity, 79
- Asymmetric initiation, 78
- Asymmetric polymerization, 78
 - of benzofuran, 80
 - of methyl sorbate, 80
 - of α - and β -naphthofuran, 80
 - of 1,3-pentadiene, 80, 82
 - selective, 74
 - solid state, 83
- Asymmetric syntheses, 78
- Atactic (definition), 8
- Atactic polymers, 59, 73
- Atactic poly(methyl methacrylate), ¹H NMR spectrum, 28
- Atactic polypropylene, 92
- Atomic polar tensor, 131
- Aza crown compounds, 224, 262, 264
- Aza macrobicyclic compounds, 270
- Aza macrocyclic polyethers, 267
- Aza macropolycyclic compounds, 270
- Azidomethemoglobin A, 198
- Benzo-15-crown-5 derivatives, 265, 273
- Benzo-18-crown-6 derivatives, 248
- Benzo-24-crown-8 derivatives, 248
- Benzo-27-crown-9, 218
- Benzofuran, asymmetric polymerization, 80
- Bernoulli distribution, 59, 89
- Bernoulli trial process, 21, 33
- (*RS*)-Binaphthol, macrocyclic derivatives, 250
- Binaphthols, (*R*) and (*S*), macrocyclic derivatives, 254
- (*S*)-Binaphthyl, 277
- Binaphthyl-20-crown-6 derivatives, 226

- 4,4'-Biphenanthryl, macrocyclic derivatives, 255
- 9,9'-Biphenanthryl, macrocyclic derivatives, 255
- Bisbinaphthyl-22-crown-6 derivatives, 226, 254
- Bis Cu(II) amino acid complexes, 182
- $\alpha\alpha$ -DD-Bisgalactosido-18-crown-6 derivatives, 253, 259, 262
- $\alpha\alpha$ -DD-Bisglucosido-18-crown-6 derivatives, 253
- $\alpha\alpha$ -DD-Bismannosido-18-crown-6 derivatives, 253
- Bismetaphenylene-32-crown-10 derivatives, 219
- Bisparaphenylene-34-crown-10 derivatives, 219
- Bis(L-prolinato)Cu(II), 183
- Bistartaro-18-crown-6 derivative, 232
- Bistartaro-18-crown-6 dianhydride, 262
- Bis(L-threoninato)Cu(II), 183
- Bisxylo-20-crown-6 derivative, 253
- Bond-dipole theory of VCD, 129
- Borohydride reductions, 278
- (+)-3-Bromocamphor, 153, 157
- (+)-*p*-Bromophenylethylamine, 144
- (2*R*,3*R*)-2,3-Butanediol, macrocyclic derivatives, 240
- 1-*sec*-Butylbutadiene, 74
- 2-*sec*-Butylbutadiene, 74
- (-)-(1*R*,2*S*,3*R*,4*S*)-Camphane-2,3-diol, macrocyclic derivatives, 247
- (+)-(1*R*,2*R*,3*S*,4*S*)-Camphane-2,3-diol, macrocyclic derivatives, 247
- (+)-Camphor, 153, 157
- Carbohydrate derivatives, 244
- Carbohydrates, 193, 244
- ¹³C Chemical shift, 53
- CD curves, 85
- CF (Charge Flow) models of VCD, 129
- Chains:
- with correlated rotations, 55
 - with independent rotations, 55
- Characteristic ratio, 54, 62
- Charge flow, 129
- Charge flow model, 139, 141
- Charge transfer, 219
- CHBrClF, 273
- Chemical shift of methyl carbons in polypropylene, 59
- Chiral allenes, 197
- Chiral azides, 197
- Chiral benzo-14-crown-4 derivatives, 240
- Chiral bisbinaphthyl-22-crown-6 derivative, 259
- Chiral catalysts, 72, 90
- Chiral crown compounds, 258
- Chiral 18-crown-6 derivatives, 232, 243
- Chiral crown ether receptors, 276
- Chiral crown ethers, 209, 227, 255, 277, 278
- properties, 275
 - synthesis, 229
- Chiral diaza crown ethers, 238, 268
- Chiral diaza macrobicyclic polyethers, 270
- Chiral diester diamide macrocycles, 268
- Chiral environment, 79
- Chiral macrobicyclic compounds, 260
- Chiral macrocycles, 264
- Chiral macrocyclic polyether diesters, 242
- Chiral macrocyclic polyethers, 238, 254, 262
- Chiral mixing of inherently achiral vibrations, 157
- Chiral perturbations, 128
- Chiral poly(9,9'-spirobifluorene)crown ethers, 256
- Chiral styrene-methyl methacrylate copolymers, 16
- Chiral tartaric acid, 68
- Chiral 5,6,11,12-tetrahydro-5,11-methano-dibenzo[a,e]cyclooctene, macrocyclic polyethers, 258
- Chirality, 115
- of atactic polymers, 81
 - degradation, 73
 - of isotactic chain, 98
 - in macromolecular systems, 66
 - number in ROA, 122
 - in polymers, 66
 - prediction, 67
 - of rigid polymers, 66
- Chiroptical behavior, of chiral crown ethers, 276
- Chirotopic carbon atoms, 6, 68
- (*R*)-(+) -1-Chloro-phenylethane, 143
- β -Chlorovinyl ethers, 89
- Chromatographic resolution, polymers as chiral support for, 86
- CH stretching VCD, 136, 161, 182, 185
- Cryptochirality, 106

- Circular dichroism measurements, 276
Circularly polarized radiation, 115
Co(III) alanine complexes, 188
Complexation-decomplexation rates, 276
Configuration, 103
Configurational defects, 58
 in isotactic polypropylene, 90
Configurational effect, in VCD spectra, 188
Conformation, 42, 60, 103
 of atactic polymers, 58
 of semirigid polymers, 95
Conformational analysis, 42
 in disordered state, 53
 of molecular complexes, 208
 of polymers, 42
Conformational asymmetric induction, 61
Conformational asymmetric polymerization
 of triphenylmethyl methacrylate, 83
Conformational energy map of isotactic
 polypropylene, 49
Conformations, disordered, 52, 56
Conformation transition, 86
Constant or alternate presentation, 88
Copolymers, 71
 optically active, 85
2D-Correlated spectroscopy, 42
C=O stretching VCD, 134, 137, 179
Co(III) tris(ethylenediamine) complexes, 184
Coupled oscillator models, 145, 181, 199
 degenerate, 133
 of VCD, 195
 for VOA, 126
Coupled oscillator theory, 151
Coupling of achiral oscillators, 126, 199
CP-MAS NMR spectroscopy, 42, 63
CP-MAS spectrum of syndiotactic polypropylene, 63
18-Crown-6, 209–211, 226
18-Crown-6 complexes, 212, 213, 215
9-Crown-3 derivatives, 236
12-Crown-4 derivatives, 236
15-Crown-5 derivatives, 236
18-Crown-6 derivatives, 236
Crown compounds:
 all-oxygen, 232, 245, 246
 aza, 262
Crown ethers, 209, 222, 224
 aza, 267
 chiral, 209, 227, 255, 275, 277, 278
 diaz, 267
 resolution, 229
3*n*-Crown-*n* ethers, 216
Cryptochirality, 66, 68, 106
Cryptochiral polymers, 96
Crystalline gels, 52
Crystalline polymers, 46
Crystallinity bands, 65
Cyclic model, 67
Cyclic monomer, 69
Cyclic olefins, 10
 α -Cyclodextrin, 275
 β -Cyclodextrin, 264, 265, 275
(+)-*trans*-Cyclohexane-1,2-diol, macrocyclic derivatives, 244
(+)-*trans*-Cyclohexano-14-crown-5, 244
(+)-*trans*-Cyclohexano-18-crown-6, 244
(+)-(2*R*)-Cyclohexanone-*d*₁, 159
(-)-Cyclohexanone-2,6-*d*₂, 159
(-)-*trans*-(2*S*,6*S*)-Cyclohexanone-*d*₂, 159
Cyclophosphamides, 160
Cyclotrimeratrylene, 272
L-Cysteine, 166
L-Cysteine.DCl, 174

Degenerate Coupled Oscillator Model, 133
Delocalizable electron density, 132
6-Deoxy-D-allose, macrocyclic derivatives, 224
Deoxycholic acid, 82, 86
Deuterated phenylethanes, 139
(+)-(R)-2,2'-Diamino-1,1'-binaphthyl, 158
1,4:3,6-Dianhydro-D-mannitol, macrocyclic derivatives, 244
Diastereoface differentiation, 75
Diastereotopic methylene protons, 31, 35
Diastereic centers, 6
Diaz macrocyclic polyethers, 264, 267
Dibenzo-18-crown-6, 209
Dibenzo-27-crown-9 derivatives, 218
Dibenzo-30-crown-10 derivatives, 218, 265
2,3-Di-*O*-benzyl-L-glycerol, macrocyclic derivatives, 262
1,3:4,6-Di-*O*-benzylidene-D-mannitol, macrocyclic derivatives, 244
1,4-Di-*O*-benzyl-L-threitol, macrocyclic derivatives, 226, 247, 264
1,4-Di-*O*-benzyl-L-threitol derivatives, 237
(+)-*trans,anti,trans*-Dicyclohexano-18-crown-6, 244

- 1,4-Dideoxy-1,4-diiodo-2,3-*O*-isopropylidene-L-threitol, macrocyclic derivatives, 237
- trans*-1,2-Dideuteriocyclobutane, 147
- 2,2'-Dihydroxy-1,1'-binaphthyl, optically pure, macrocyclic derivatives, 226
- 1,2:5,6-Di-*O*-isopropylidene- α -D-allofuranose, macrocyclic derivatives, 273
- 1,2:3,4-Di-*O*-isopropylidene- α -D-galactopyranoside, macrocyclic derivatives, 273
- 1,2:5,6-Di-*O*-isopropylidene- α -D-glucofuranose, macrocyclic derivatives, 273, 275
- 1,2:5,6-Di-*O*-isopropylidene-L-itol, macrocyclic derivatives, 238
- 1,2:5,6-Di-*O*-isopropylidene-D-mannitol, macrocyclic derivatives, 237, 248, 270
- Diisotactic polymers, 8
- erythro*-Diisotactic structures, 8, 69
- threo*-Diisotactic structures, 8, 69
- Dimethylallene, 14, 73
- 1,3-Dimethylallene, 14
- (*R*)-3,3'-Dimethyl-2,2'-dihydroxy-1,1'-dinaphthyl, macrocyclic derivatives, 254
- 1,3:4,6-Di-*O*-methylene-D-mannitol, macrocyclic derivatives, 244, 247
- Dimethylketene, 15
- Dimethyl malate, 136
- 3,7-Dimethyl-1-octene, 77
- (+)-*N,N*-Dimethyl(1-phenylethyl)amine, 142
- Dimethyl tartrate, 133
- Dioxa[3.2.1]bicyclooctane, 13
- Dioxa[3.2.2]bicyclooctane, 73
- Dipolar moment, 53
- Dipole strength, 123
- [Diquat]²⁺, 219
- Disordered conformations, 52, 56
- Dispersive grating spectrometer, 119
- 1,4-Disubstituted butadienes, 11
- Disubstituted ethylenes, 25
- 1,2-Disubstituted ethylenes, 8
- Disubstituted olefins, 88, 100
- Disyndiotactic polymers, 8
- DNA intercalating crown ether molecules, 236
- L-Dopa, 265
- Dopamine, 265
- Double helix, 52
- Double-modulation FTIR spectroscopy, 119
- Drude equation, one-term, 84
- Dyads, 18
- (Meso) Dyads, 7
- (Racemic) Dyads, 7
- Dynamic dependence of VOA, 116
- Dynamic polarization model of VCD, 129
- Elastic and inelastic neutron scattering, 65
- Elastic properties, 65
- Electric dipole moment operator, 124
- Electric dipole transition moment, 123, 125, 188, 192
- Electric and magnetic dipole transition moments, 133
- Electric quadrupole moment operator, 125
- Electric quadrupole optical activity tensor, 124
- Electronic current density, 118, 200
- Electron microscopy, 62
- Electrooptic modulator in ROA, 120
- Enantioasymmetric polymerization, 74
- Enantioface differentiation, 75
- Enantiogenic polymerization, 78
- Enantiomeric differentiation, 226
- Enantioselective synthesis, 229
- Enantiosymmetric polymerization, 74
- Enantiotopic bonds, 7
- Enantiotopic faces, 87
- End-to-end distance, 53, 54, 62
- Enzyme analogs, 277
- Enzyme mimics, 277
- Enzyme models, 237
- D- ψ -Ephedrine, macrocyclic derivatives, 226
- Epimerization, 23
- equilibrium, 53
- of polypropylene, 59
- of propylene oligomers, 59
- cis*-2,3-Epoxybutane, 13, 107
- trans*-2,3-Epoxybutane, 13
- (+)-*trans*-2,3-Epoxybutane, 73
- (*S*)-(−)-Epoxypropane, 147
- Equivalence principle, 50
- Equivalent methylene protons, 31
- Ethylenebis(1-indenyl)titanium dichloride, 92
- Ethyl (*S*)-lactate, macrocyclic derivatives, 242

- Experimental parameters for ROA, 120
Extramolecular chemistry, 208
- Face-to-face complexes, 212
Fermi resonance in CH stretching VCD, 152
Finite chain:
 with identical terminal groups model, 67
 with nonidentical terminal groups model, 67
First-order Markov process, 23
Fischer projection, 4, 67
 horizontal (or rotated), 5
Fixed partial charge, *see* FPC (Fixed Partial Charge) model
Flexible polymers, 67
Fourier self-deconvolution, 178
Fourier transform infrared, 119
FPC (Fixed Partial Charge) model, 139, 145, 159, 200
 of VCD, 129
Free energy of complexation, 224
Free energy minimum, 53
Freely jointed chain, 54
Freely rotating chain, 55
FTIR (Fourier Transform Infrared), 119
FT-IR interferometers, 64
FTIR-VCD spectrometer, 119
- γ -Effect, 59, 63
Gauche effect, 212
Generalized Models for ROA, 132
L-Glyceraldehyde dithioethylacetal, 243
Glycyl-L-alanine, 176
 ΔG° values, 224
- Head-to-head sequences, 3
Head-to-head, tail-to-tail polymers, 17
Head-to-head, tail-to-tail polypropylene, 17
Head-to-tail sequences, 3
Helical conformations, 46
Helicenes, 258
 α -Helix, 48, 201
Helix-coil transition, 86
Helix sense inversion, 56
Hemiisotactic polymers, 17, 23
Hemiisotactic polypropylene, 18, 39
Hemitactic polymers, 17, 23
Heptad, 40
3,5,7,9,11,13,15-Heptamethylheptadecane, 39
Heterotactic polymer, 20
Hexad, 18
2,4,6,8,10,12-Hexamethyltridecane, 39
Higher-order Markov chains, 33
High resolution NMR spectroscopy of solid polymers, 63
Horizontal (or rotated) Fischer projection, 5
Hydride transfer reactions, 277
Hydrobenzoin, (*RR*) and (*SS*), 239
(*RR*)-Hydrobenzoin, 277
Hydrogen-bonded rings, 195
Hydrogen bonding, 212, 215, 219, 221
Hydrogen-bonding to chloride, VCD, 186
 π -Hydrogen bonding in VCD, 143
Hydrogen bonds, 212, 215, 222
 α -L-Hydroxy acids, 165
4-Hydroxymethylbenzo-15-crown-5, macrocyclic derivatives, 267
trans-2,5-bis(Hydroxymethyl)tetrahydrofuran, (+) and (−), macrocyclic derivatives, 244
- Ideal copolymerization, 21
L-Iditol, macrocyclic derivatives, 233
Inclusion polymerization, 81, 82, 86
Infinite chain model, 7, 67
Inherently dissymmetric chromophore, 148
chiro-Inositol, 70
Intramolecular hydrogen bonding in VCD, 175
Intramolecular ring in VCD, 200
Intrinsically chiral polymers, 106
Intrinsic contributions to VOA, 125
Intrinsic rotational strength, 136
IR (Infrared) photoelastic modulator, 119
IR spectroscopy, 62
IR spectrum of isotactic crystalline polypropylene, 65
Isochronous nuclei, 28
(+)-Isomenthone, 150
Isonitriles, polymerization, 60
Isoprene-pentadiene, block copolymer, optically active, 81
3,4-*O*-Isopropylidene- β -D-arabinopyranose, macrocyclic derivatives, 248
1,2-*O*-Isopropylidene- α -D-glucofuranose, macrocyclic derivatives, 275

- 2,3-*O*-Isopropylidene-D-glycerol, macrocyclic derivatives, 260, 262
- 1,2-*O*-Isopropylidene-3-*O*-methyl- α -D-glucopyranose, macrocyclic derivatives, 243
- 1,2-*O*-Isopropylidene-3-*O*-(methylthiomethyl)- β -D-fructopyranose, macrocyclic derivatives, 248
- 2,3-*O*-Isopropylidene-L-threitol, macrocyclic derivatives, 259
- 1,2-*O*-Isopropylidene- α -D-xylofuranose, macrocyclic derivatives, 253
- Isotactic polybutene, 47
- Isotactic polyethylidene, 9
- Isotactic poly(isopropyl vinyl ether), 48
- Isotactic polymers, 4, 5, 73
- Isotactic poly(methyl methacrylate), 52
- Isotactic poly(4-methylpentene), 48
- Isotactic poly(*m*-methylstyrene), 48
- Isotactic poly(*o*-methylstyrene), 47
- Isotactic polypropylene, 5, 47, 56, 91
- Isotactic polystyrene, 47, 52
- Kinetic resolution, 229
- K_a values, 224
- S-Lactic acid, 136, 161, 165
- Lactic acids, macrocyclic derivatives, 242, 270, 277
- Linear repetition groups, 47
- Line group symmetry, 67
- Liquid crystals, 60, 72
- LMO (Localized Molecular Orbital) model of VCD, 130, 161
- Localized molecular orbital model, 130, 161
- Macroconformation, 61
- Macrocyclic compounds, 209, 260
- Macrocyclic polyethers, 209, 230, 258
- Magic-angle spectroscopy, 42, 63
- Magnetic dipole moment operator, 124
- Magnetic dipole optical activity tensor, 124
- Magnetic dipole transition moment, 123, 125, 171, 188, 192
- Mandelic acids, macrocyclic derivatives, 242
- D-Mannitol, macrocyclic derivatives, 226, 233, 244
- α -D-Mannosido-18-crown-6, macrocyclic derivatives, 264
- Markov chains, 33, 79
- first-order, 23
- second-order, 23, 93
- Markov scheme, symmetric, 90
- (-)-Menthone, 150
- Meso/racemic (or *m/r*) nomenclature, 7
- Methine VCD, 137
- p*-Methoxy-(*SS'*)-hydrobenzoin, macrocyclic derivatives, 233
- Methyl 4,6-*O*-benzylidene- α -D-galactopyranoside, macrocyclic derivatives, 272
- Methyl 4,6-*O*-benzylidene- α -D-glucopyranoside, macrocyclic derivatives, 247, 272, 273, 275, 277
- Methyl 4,6-*O*-benzylidene- β -D-glucopyranoside, macrocyclic derivatives, 247
- Methyl 4,6-*O*-benzylidene-D-glycopyranosides, macrocyclic derivatives, 248, 250
- Methyl 4,6-*O*-benzylidene- α -D-talopyranoside, macrocyclic derivatives, 259
- 2-Methylbutyl isocyanate, 74
- 3-Methylcyclohexanone, 153
- (+)-(3*R*)-Methylcyclohexanone, 152, 157
- Methylene protons, 31, 35
- Methylene stretching VCD, 151
- α - and β -Methyl-D-glucoside, 194
- (*S*)-4-Methylhexene, 85
- Methyl 3-hydroxybutyrate, 136
- Methylisopropylketene, 15
- Methyl lactate, 136
- Methyl methacrylate, optically active oligomers, 96
- Methyl 3, *d*₁-methacrylate, 26
- 3-Methyloxetane, 12
- trans*-2-Methylpentadiene, asymmetric polymerization, 82
- Methylpentamethyleneketenes, 15
- (*S*)-3-Methyl-1-pentene, 77
- 4-Methylpentene, 85
- Methyl 4,6-*O*-[(*S*)-phenylethylidene]- α -D-mannopyranoside, macrocyclic derivatives, 272
- Methyl propenyl ether, 26
- Methyl sorbate, asymmetric polymerization, 80
- Methyl stretching VCD, 142, 195
- Michael addition reactions, 278
- Microconformation, 61

- Microtacticity, 7, 18
Mid-infrared VCD, 143, 193, 195
Mirror glide plane, 67
Mirror symmetry elements, 67
Molecular complexation, 208
Molecular complexes, 209, 210, 219
 conformational analysis, 208
Molecular dynamics, 64
Molecular mechanics calculations, 43, 210
Molecular orbital models for VCD, 131
Molecular receptors, 208, 209
Monopsoralen-18-crown-6 derivative, 236
4-Monosubstituted butadienes, 11
Monotartaro-18-crown-6 anhydride, 236
Morphology, 65
Multichannel detection system for ROA, 120
- α - and β -Naphthofuran, asymmetric polymerization, 80
Nesting arrangement, 215
Neutron scattering, 62, 105
NH stretching VCD, 182, 185
NMR spectroscopy, 64
 contribution to macromolecular stereochemistry, 27
 quantitative, 30
 of solid polymers, 63
¹³C NMR spectroscopy, 276
2D-NMR spectroscopy, 42
¹H NMR spectroscopy, 276
¹³C NMR spectrum:
 of poly(methyl methacrylate), 33
 of polypropylene, 36
 of poly(vinyl alcohol), 40
Non-Born-Oppenheimer effects in VCD, 118, 201
Noncovalent bonding interactions, 215
Noncovalent bonds, 208
Nonideal copolymerization, 23
Nonintrinsically chiral polymers, 106
Non-Markov processes, 23, 33
Nonselective polymerization, 74
Nonsymmetric Bernoulli process, 23
Nonsymmetric Markov chains, 23
(+)-Nopinone, 153, 157
Normal coordinate analysis, 128, 139, 152
N-Substituted Nylon-1, 60
Nylon-1, *N*-substituted, 60
- OH stretching VCD, 134
Oligo(methyl methacrylate), optically active, 96
One-term Drude equation, 84
Optical activity:
 of isotactic polypropylene, 95
 of rigid polymers, 94
Optically active copolymers, 85
Optically active isonitriles, 73
Optically active isoprene-pentadiene block copolymer, 81
Optically active oligomers of methyl methacrylate, 96
Optically active oligomers of trityl methacrylate, 96
Optically active polychloral, 95
Optically active polyiminomethylenes, 95
Optically active poly-2-methylpentadiene, 82
Optically active polymers, 65
 methods of synthesis, 72
ORD curves, 84
Oxiranes, polymerization, 76, 77
- [Paraquat]²⁺, 219
Pentad, 18
1,3-Pentadiene, 11
 asymmetric polymerization, 80, 82
 radical asymmetric polymerization, 81
2,3-Pentadiene, 14, 73
Pentamethyleneketene, 15
Peracetates of sugars, 196
Perching arrangement, 215
Perfect nuclear following, 129
 contribution to VCD, 173
Perhydrotriphenylene, 81
Persistence length, 95
L-Phenylalanine, macrocyclic derivatives, 267
 α -Phenylethane derivatives, 142
(*R*)-(+)-1-Phenylethanethiol, 143
 α -Phenylethanol, VCD of, 140
(*R*)-1-Phenylethanol, 141, 143
(+)- α -Phenylethylamine, 144
(+)- α -Phenylethyl isocyanate VCD, 140
D-Phenylglycine, macrocyclic derivatives, 267
Planar chirality, 258
Point group symmetry, 67
Polarizability tensor, 124

- Polarization measurements in ROA, 120
Poly(1-alkylbutadienes), 70
Polyalkylisocyanates, 60
Polyalkyloxiranes, 69
Polyallenes, 14
Polyamino acids, 69
Poly-L- α -amino acids, 12, 98
Polyaziridines, 69
Poly(γ -benzyl-L-glutamate), 177
Polybutadiene, 10
1,2-Polybutadiene, syndiotactic, 5
Polybutene, isotactic, 47
Polychloral, optically active, 84, 95
Polycondensation, 12
Poly(2,3-epoxybutane), 70
Polyethylene, 55, 66
 monocrystals, 61
 random coil, stochastic achirality, 66
Polyethylenes, 9
Polyfluoromethylene, 9, 26
Polyhexadiene, 70
Polyiminomethylenes, 60
 optically active, 95
Polyisobutene, 52
Polyisocyanates, 95
cis-1,4-Polyisoprene, 11
trans-1,4-Polyisoprene, 11
Poly(isopropyl vinyl ether), isotactic, 48
Polyketenes, 14
Polymer chirality, 66
Polymer conformations, 46
Polymerization:
 addition, 87
 asymmetric, 74, 78, 82
 of chiral α -olefins, 73
 conformationally asymmetric, of triphenylmethyl methacrylate, 83
 enantioasymmetric, 74
 enantioselective, 78
 of enantiomerically pure monomers, 72
 enantiosymmetric, 74
 inclusion, 81, 82, 86
 nonselective, 74
 of partially resolved mixture of enantiomers, 77
 of (+)-propylene oxide, 72
 of racemic monomers, 74
 stereoselective, 74, 76
 stereoselective, 74, 75, 76
 stereospecific, 75
Polymers:
 conformational analysis, 42
 morphology, 61
 nonintrinsically chiral, 106
Poly(α -methyl- α -ethylpropiolactone), 27
Poly(4-methyl-1-hexene), 75
Poly(methyl methacrylate), 93
 atactic, 28
 isotactic, 52
 NMR analysis, 31
 ^1H NMR spectra, 32
 ^{13}C NMR spectrum, 33
Poly(2-methylpentadiene), optically active, 82
1,4-*trans*-Poly(2-methylpentadiene), 86
Poly((*S*)-3-methyl-1-pentene), 75
 as chiral support, 87
Poly(4-methylpentene), isotactic, 48
Poly(α -methyl- α -propylpropiolactone), 27
Poly(*m*-methylstyrene), isotactic, 48
Poly(*o*-methylstyrene), isotactic, 47
Polymethyltetramethylene, 26
1,4-*trans*-Polypentadiene, 26
Poly(phenylene oxide), 63
Polypropylene, 34
 atactic, 92
 epimerization, 59
 isotactic, 5, 47, 56, 90, 91
 conformational energy map, 49
 IR spectrum, 65
 optical activity, 95
 methyl carbons, chemical shift, 59
 NMR analysis, 34
 ^{13}C NMR spectrum of, 28, 36
 pentads in, 37
 steric purity, 58
 syndiotactic, 48, 57, 89, 92
 CP-MAS spectrum, 63
 energy map, 50, 57
Poly(propylene oxide), 12
Polysorbates, 27, 70
Polystyrene, isotactic, 47, 52
Polythiiranes, 69
Poly(triphenylmethyl methacrylate), 60, 87
 stationary phase for HPLC, 229
Poly(trityl methacrylate), *see*
 Poly(triphenylmethyl methacrylate)
Poly(vinyl alcohol), ^{13}C NMR spectrum, 40
Poly(vinyl isobutyl ether), 98
Primary binding sites, 216

- Principle of equivalence, 46
Principle of minimum conformational energy, 46
Prochirality, 7
L-Proline, macrocyclic derivatives, 226
Propylene-1-*d*₁, 8, 89
Propylene-1,2,3,3,3-*d*₅, 35
Propylene-2,3,3,3-*d*₄, 35
Propylene oligomers, epimerization, 59
Propylene oxide, 147
Prostereoisomerism, 7
Pseudoasymmetric atoms, 6, 68
(+)-Pulegone, 153, 157, 244
- Racemic mixtures, 72
Racemic modifications, 229
Radical asymmetric polymerization of pentadiene, 81
Radius of gyration, 53, 62
Raman atomic polar tensor model, 157
Raman optical activity, *see* ROA (Raman Optical Activity)
Raman resonant spectroscopy, 64
Raman spectroscopy, 64
Random coil, 53, 61
Random-coil conformation, 66
Receptor design, 208
Receptor functions, 208
Receptor molecule, 222
Reflection, 67
Regioselective transacylations of amino acid ester salts, 237
Resolution:
 of crown ethers, 229
 of optical antipodes, 72
2D-Resolved spectroscopy, 42
Rheology, 65
D-Ribose, macrocyclic derivatives, 224
Rigid helix, 61
Rigid rod conformation, 60, 61
Ring current mechanism, 197, 200
 of VCD, 182, 192
Ring-opening polymerization, 12
ROA (Raman Optical Activity), 116
 chirality number, 122
 electrooptic modulator, 120
 experimental parameters, 120
 generalized models, 132
 intensity, 124
 of low-frequency skeletal motions, 153
 measurement, 120
 multichannel detection system, 120
 polarization measurements, 120
 scanning grating monochromators, 120
 two group model, 128
Rotameric distribution in amino acids, 161, 174
Rotation, 67
Rotational isomeric state (RIS) model, 45
Rotational strength, 123
Rules for vibrationally generated current in VCD, 200
- Scanning grating monochromators for ROA, 120
Screw axis, 67
Second-order Markov chains, 23, 93
L-Serine, 174, 175
Solid state physics, 65
Specific heat, 65
Specific rotation changes, 276
Spectroscopy, NMR, 42
9,9'-Spirobifluorene, macrocyclic derivatives, 255
(+)-(5*S*)-1,6-Spiro[4,4]nonadiene, 158
Stabilities of complexes, 224
Stability constant, 224
Stationary chiral phases, 86
Stereochemical applications of VOA, 132
Stereochemical nomenclature, 100, 101
Stereoelective polymerization, 74, 76
Stereogenic carbon atoms, 6, 68
Stereoisomeric centers, 6
Stereoregular symmetric growth, 78
Stereoselective polymerization, 74, 75, 76
Stereosequence nomenclature, 18
Stereosequences:
 number, 20
 quantitative relationships, 21
Stereospecificity of vibrational optical activity, 122
Stereospecific polymerization, 75
Stereospecific synthesis, 229
Steric purity of polypropylene samples, 58
Steroids, 137
Stochastic achirality of random coil polyethylene, 66
Structural dependence of VOA, 116
Styrenes, 85
Substituted benzalacetone, 70

- Sugars, 194
 peracetates, 196
Symmetric Bernoulli scheme, 90
Symmetric Markov scheme, 90
Symmetry, 229
Symmetry properties of dyads, tetrads, hexads, 20
Syndiotactic phenol-acetaldehyde polymers, 17
Syndiotactic 1,2-polybutadiene, 5
Syndiotactic polyethylidene, 9
Syndiotactic polymers, 4, 5, 73
Syndiotactic polypropylene, 48, 57, 89, 92
 energy map, 50
- cis*-Tactic polymers, 10
trans-Tactic polymers, 10
Tail-to-tail sequences, 3
D-Talopyranose, macrocyclic derivatives, 259
Tartaric acid, 68, 136
L-Tartaric acid, macrocyclic derivatives, 226, 232, 233, 268, 270, 277
2,3,4,6-Tetra-O-acetyl-D-glucopyranose, macrocyclic derivatives, 273
Tetrad, 18
Tetraphenyl-18-crown-6 derivatives, 239
Theoretical models for VOA, 122
Theta conditions, 54
Thiiranes, polymerization, 76, 77
Three-point binding model, 212
L-Threitol, macrocyclic derivatives, 233, 250, 259
L-Threonine, 167, 175
Through bond asymmetric induction, 82
Through space asymmetric induction, 82
Time-averaged structure, 67
Titanium trichloride, 110
Topology in polymers, 94
Torsion angle convention, 44, 102
Trans disubstituted cyclopropanes, 144
Transition metal complexes, VCD, 182
Translation, 67
Triads, 18
Triaza-18-crown-6, 272
2,2,2-Trifluoro-1-phenylethanol, 141
(*S*)-(+) -2,2,2-Trifluoro-1-phenylethanol, 142
meso-Trihydroxyglutaric acid, 68
Triphenylmethyl methacrylate:
 conformational asymmetric polymerization, 83
 optically active oligomers, 96
 polymerization, 61, 63
Tristartaro-27-crown-9 derivative, 232
Tritactic polymers, 11
Trityl methacrylate, *see* Triphenylmethyl methacrylate
Two group model of ROA, 128
Two-state mechanism, 93
Two-state model, 92
Type of addition, 87
- Undecad, 18, 40
Unperturbed conditions, 54
Urethane amino acid derivatives, 178
- L-Valine, macrocyclic derivatives, 267, 268
VCD (Vibrational Circular Dichroism), 115
 of alanyl peptides, 176
 in amide vibrations, 177
 Atomic Polar Tensor model, 131
 bias, 161
 bond-dipole theory, 129
 Charge Flow models, 129
 of chiral $\text{CH}_2\text{CH}_2\text{C}^*\text{H}$ fragment, 148
 of chiral ring molecules, 144
 coupled oscillator model, 195
 due to hydrogen-bonding to chloride, 186
 dynamic polarization model, 129
 Fixed Partial Charge model, 129
 in α -helix, 177
 π -hydrogen bonding in, 143
 instrumentation, 119
 intensity, 123
 intramolecular hydrogen bonding, 175
 intramolecular ring, 200
 Localized Molecular Orbital model, 130
 marker band, 160, 195
 in methine bending modes, 175
 molecular orbital models, 131
 non-Born-Oppenheimer effects, 118, 201
 observed bias, 181
 perfect nuclear following, contribution to, 173
 in polypeptides, 177
 as probe of molecular self-association, 200

- ring current mechanism, 182, 192
- rules for vibrationally generated current, 200
- in transition metal complexes, 182
- vibrational ring current model, 130
- Vibration modes, 105
- Vibrational circular dichroism, *see* VCD (Vibrational Circular Dichroism)
- Vibrationally induced electronic currents, 132, 133, 137, 145, 188, 195
- Vibrational optical activity, *see* VOA (Vibrational Optical Activity)
- Vibrational Ring Current Model of VCD, 130, 132, 143, 159, 171
- Vibrational spectroscopy, 64
- Vicinal effect in VCD spectra, 188
- N*-Vinylcarbazole, 85
- Vinylchrysene, 85
- Vinylidene monomers, 97
- Vinylnaphthalene, 85
- Vinyl polymerization, stereospecific, 75
- Vinyl polymers, disordered conformations, 56
- VOA (Vibrational Optical Activity), 115, 116
 - coupled oscillator models, 126
 - dynamic dependence, 116
 - intrinsic contributions, 125
 - stereochemical applications, 132
 - stereospecificity, 122
 - structural dependence, 116
 - theoretical models, 122
- X-ray crystallography, 277
- Xylo-10-crown-3 derivative, 253
- Xylo-19-crown-6 derivative, 253
- Zigzag projection, 4, 67

CUMULATIVE INDEX, VOLUMES 1-17

	VOL.	PAGE
Absolute Configuration of Planar and Axially Dissymmetric Molecules (<i>Krow</i>)	5	31
Absolute Stereochemistry of Chelate Complexes (<i>Saito</i>)	10	95
Acetylenes, Stereochemistry of Electrophilic Additions (<i>Fahey</i>)	3	237
Aldol Condensations, Stereoselective (<i>Evans, Nelson and Taber</i>)	13	1
Alkaloids, Asymmetric Catalysis by (<i>Wynberg</i>)	16	87
Aluminum Hydrides and Tricoordinate Aluminum Reagents, Asymmetric Reductions with Chiral Complex (<i>Haubenstock</i>)	14	231
Analogy Model, Stereochemical (<i>Ugi and Ruch</i>)	4	99
Asymmetric Reductions with Chiral Complex Aluminum Hydrides and Tricoordinate Aluminum Reagents (<i>Haubenstock</i>)	14	231
Asymmetric Synthesis, New Approaches in (<i>Kagan and Fiaud</i>)	10	175
Asymmetric Synthesis Mediated by Transition Metal Complexes (<i>Bosnich and Fryzuk</i>)	12	119
Atomic Inversion, Pyramidal (<i>Lambert</i>)	6	19
Atropisomerism, Recent Advances in (<i>Okii</i>)	14	1
Axially and Planar Dissymmetric Molecules, Absolute Configuration of (<i>Krow</i>)	5	31
Barriers, Conformational, and Interconversion Pathways in Some Small Ring Molecules (<i>Malloy, Bauman, and Carriera</i>)	11	97
Barton, D. H. R., and Hassel, O.-Fundamental Contributions to Conformational Analysis (<i>Barton, Hassel</i>)	6	1
Bicyclic Compounds, Walk Rearrangements in [n.1.0] (<i>Klärner</i>)	15	1
Carbene Additions to Olefins, Stereochemistry of (<i>Closs</i>)	3	193
Carbenes, Structure of (<i>Closs</i>)	3	193
sp ² -sp ¹ Carbon-Carbon Single Bonds, Rotational Isomerism about (<i>Karabatsos and Fenoglio</i>)	5	167
Carbonium Ions, Simple, the Electronic Structure and Stereochemistry of (<i>Buss, Schleyer and Allen</i>)	7	253
Chelate Complexes, Absolute Stereochemistry of (<i>Saito</i>)	10	95
¹³ C Chemical Shifts in Aliphatic Molecular Systems, Substituent Effects on Dependence on Constitution and Stereochemistry (<i>Duddeck</i>)	16	219
Chirality, On Factoring Stereoisomerism and (<i>Hirschmann and Hanson</i>)	14	183
Chirality Due to the Presence of Hydrogen Isotopes at Noncyclic Positions (<i>Arigoni and Eliel</i>)	4	127
Chiral Crown Ethers (<i>Stoddart</i>)	17	207
Chiral Lanthanide Shift Reagents (<i>Sullivan</i>)	10	287
Chiral Monolayers at the Air-Water Interface (<i>Stewart and Arnett</i>)	13	195

	VOL.	PAGE
Chiral Organic Molecules with High Symmetry, The Synthesis and Stereochemistry of (<i>Nakazaki</i>)	15	199
Chiral Organosulfur Compounds (<i>Mikolajczyk and Drabowicz</i>)	13	333
Chiral Solvating Agents, in NMR (<i>Pirkle and Hoover</i>)	13	263
Classical Stereochemistry, The Foundations of (<i>Mason</i>)	9	1
Conformational Analysis, Applications of the Lanthanide-induced Shift Technique in (<i>Hofer</i>)	9	111
Conformational Analysis, The Fundamental Contributions of D. H. R. Barton and O. Hassel (<i>Barton, Hassel</i>)	6	1
Conformational Analysis of Intramolecular Hydrogen-Bonded Compounds in Dilute Solution by Infrared Spectroscopy (<i>Aaron</i>)	11	1
Conformational Analysis of Six-membered Rings (<i>Kellie and Riddell</i>)	8	225
Conformational Analysis and Steric Effects in Metal Chelates (<i>Buckingham and Sargeson</i>)	6	219
Conformational Analysis and Torsion Angles (<i>Bucourt</i>)	8	159
Conformational Barriers and Interconversion Pathways in Some Small Ring Molecules (<i>Malloy, Bauman and Carreira</i>)	11	97
Conformational Changes, Determination of Associated Energy by Ultrasonic Absorption and Vibrational Spectroscopy (<i>Wyn-Jones and Pethrick</i>)	5	205
Conformational Changes by Rotation about sp^2 - sp^3 Carbon-Carbon Single Bonds (<i>Karabatsos and Fenoglio</i>)	5	167
Conformational Energies, Table of (<i>Hirsch</i>)	1	199
Conformational Interconversion Mechanisms, Multi-step (<i>Dale</i>)	9	199
Conformations of 5-Membered Rings (<i>Fuchs</i>)	10	1
Conjugated Cyclohexenones, Kinetic 1,2 Addition of Anions to, Steric Course of (<i>Toromanoff</i>)	2	157
Crystals as Probes for the Direct Assignment of Absolute Configuration of Chiral Molecules, A Link Between Macroscopic Phenomena and Molecular Chirality (<i>Addadi, Berkovitch-Yellin, Weissbuch, Lahav, and Leiserowitz</i>)	16	1
Crystal Structures of Steroids (<i>Duax, Weeks and Rohrer</i>)	9	271
Cyclobutane and Heterocyclic Analogs, Stereochemistry of (<i>Moriarty</i>)	8	271
Cyclohexyl Radicals, and Vinylic, The Stereochemistry of (<i>Simamura</i>)	4	1
Double Bonds, Fast Isomerization about (<i>Kalinowski and Kessler</i>)	7	295
Electronic Structure and Stereochemistry of Simple Carbonium Ions, (<i>Buss, Schleyer and Allen</i>)	7	253
Electrophilic Additions to Olefins and Acetylenes, Stereochemistry of (<i>Fahey</i>)	3	237
Enzymatic Reactions, Stereochemistry of, by Use of Hydrogen Isotopes (<i>Arigoni and Eliel</i>)	4	127
1,2-Epoxides, Stereochemistry Aspects of the Synthesis of (<i>Berti</i>)	7	93
EPR, in Stereochemistry of Nitroxides (<i>Janzen</i>)	6	177
Ethylenes, Static and Dynamic Stereochemistry of Push-Pull and Strained (<i>Sandström</i>)	14	83

	VOL.	PAGE
Five-Membered Rings, Conformations of (<i>Fuchs</i>).....	10	1
Foundations of Classical Stereochemistry (<i>Mason</i>)	9	1
Geometry and Conformational Properties of Some Five- and Six-Membered Heterocyclic Compounds Containing Oxygen or Sulfur (<i>Romers</i> , <i>Altona</i> , <i>Buys</i> and <i>Havinga</i>).....	4	39
Hassel, O. and Barton, D. H. R.-Fundamental Contributions to Conformational Analysis (<i>Hassel</i> , <i>Barton</i>)	6	1
Helix Models, of Optical Activity (<i>Brewster</i>)	2	1
Heterocyclic Compounds, Five- and Six-Membered, Containing Oxygen or Sulfur, Geometry and Conformational Properties of (<i>Romers</i> , <i>Altona</i> , <i>Buys</i> and <i>Havinga</i>).....	4	39
Heterocyclic Four-Membered Rings, Stereochemistry of (<i>Moriarty</i>) ...	8	271
Heterotopism (<i>Mislow</i> and <i>Raban</i>).....	1	1
Hydrogen-Bonded Compounds, Intramolecular, in Dilute Solution, Conformational Analysis of, by Infrared Spectroscopy (<i>Aaron</i>) ...	11	1
Hydrogen Isotopes at Noncyclic Positions, Chirality Due to the Presence of (<i>Arigoni</i> and <i>Eliel</i>)	4	127
Infrared Spectroscopy, Conformational Analysis of Intramolecular Hydrogen-Bonded Compounds in Dilute Solution by (<i>Aaron</i>)	11	1
Intramolecular Hydrogen-Bonded Compounds, in Dilute Solution, Conformational Analysis of, by Infrared Spectroscopy (<i>Aaron</i>) ...	11	1
Intramolecular Rate Processes (<i>Binsch</i>).....	3	97
Inversion, Atomic, Pyramidal (<i>Lambert</i>).....	6	19
Isomerization, Fast, About Double Bonds (<i>Kalinowski</i> and <i>Kessler</i>)...	7	295
Ketones, Cyclic and Bicyclic, Reduction of, by Complex Metal Hydrides (<i>Boone</i> and <i>Ashby</i>)	11	53
Lanthanide-induced Shift Technique—Applications in Conformational Analysis (<i>Hofer</i>)	9	111
Lanthanide Shift Reagents, Chiral (<i>Sullivan</i>)	10	287
Mass Spectrometry and the Stereochemistry of Organic Molecules (<i>Green</i>)	9	35
Metal Chelates, Conformational Analysis and Steric Effects in (<i>Buckingham</i> and <i>Sargeson</i>)	6	219
Metal Hydrides, Complex, Reduction of Cyclic and Bicyclic Ketones by (<i>Boone</i> and <i>Ashby</i>)	11	53
Metallocenes, Stereochemistry of (<i>Schlogl</i>)	1	39
Metal Nitrosyls, Structures of (<i>Feltham</i> and <i>Enemark</i>).....	12	155
Molecular Mechanics Calculations—Application to Organic Chemistry (<i>Osawa</i> and <i>Musso</i>)	13	117
Monolayers, Chiral, at the Air-Water Interface (<i>Stewart</i> and <i>Arnett</i>)...	13	195
Multi-step Conformational Interconversion Mechanisms (<i>Dale</i>)	9	199

	VOL.	PAGE
Nitroxides, Stereochemistry of (<i>Janzen</i>)	6	177
Non-Chair Conformations of Six Membered Rings (<i>Kellie and Riddell</i>)	8	225
Nuclear Magnetic Resonance ^{13}C , Stereochemical Aspects of (<i>Wilson and Stothers</i>)	8	1
Nuclear Magnetic Resonance, Chiral Solvating Agents in (<i>Pirkle and Hoover</i>)	13	263
Nuclear Magnetic Resonance, for Study of Intra-Molecular Rate Processes (<i>Binsch</i>)	3	97
Nuclear Overhauser Effect, Some Chemical Applications of (<i>Bell and Saunders</i>)	7	1
Olefins, Stereochemistry of Carbene Additions to (<i>Closs</i>)	3	193
Olefins, Stereochemistry of Electrophilic Additions to (<i>Fahey</i>)	3	237
Optical Activity, Helix Models of (<i>Brewster</i>)	2	1
Optical Circular Dichroism, Recent Applications in Organic Chemistry (<i>Crabbé</i>)	1	93
Optical Purity, Modern Methods for the Determination of (<i>Raban and Mislow</i>)	2	199
Optical Rotatory Dispersion, Recent Applications in Organic Chemistry (<i>Crabbé</i>)	1	93
Organic Solid-State, Stereochemistry and Reactions (<i>Green, Arad-Yellin, and Cohen</i>)	16	131
Organosulfur Compounds, Chiral (<i>Mikolajczyk and Drabowicz</i>)	13	333
Overhauser Effect, Nuclear, Some Chemical Applications of (<i>Bell and Saunders</i>)	7	1
Phosphorus Chemistry, Stereochemical Aspects of (<i>Gallagher and Jenkins</i>)	3	1
Phosphorus-containing Cyclohexanes, Stereochemical Aspects of (<i>Maryanoff, Hutchins and Maryanoff</i>)	11	186
Piperidines, Quaternization Stereochemistry of (<i>McKenna</i>)	5	275
Planar and Axially Dissymmetric Molecules, Absolute Configuration of (<i>Krow</i>)	5	31
Polymer Stereochemistry, Concepts of (<i>Goodman</i>)	2	73
Polypeptide Stereochemistry (<i>Goodman, Verdini, Choi and Masuda</i>) ..	5	69
Pyramidal Atomic Inversion (<i>Lambert</i>)	6	19
Quaternization of Piperidines, Stereochemistry of (<i>McKenna</i>)	5	75
Radicals, Cyclohexyl and Vinylic, The Stereochemistry of (<i>Simamura</i>) ..	4	1
Reduction, of Cyclic and Bicyclic Ketones by Complex Metal Hydrides (<i>Boone and Ashby</i>)	11	53
Resolving-Agents and Resolutions in Organic Chemistry (<i>Wilen</i>)	6	107
Rotational Isomerism about $\text{sp}^2\text{-sp}^3$ Carbon-Carbon Single Bonds (<i>Karabatsos and Fenoglio</i>)	5	167
Small Ring Molecules, Conformational Barriers and Interconversion Pathways in Some (<i>Malloy, Bauman and Carreira</i>)	11	97

	VOL.	PAGE
Stereochemical Aspects of ^{13}C Nmr Spectroscopy (<i>Wilson and Stothers</i>)	8	1
Stereochemical Aspects of Phosphorus-containing Cyclohexanes (<i>Maryanoff, Hutchins and Maryanoff</i>)	11	186
Stereochemical Aspects of Vibrational Optical Activity (<i>Freedman and Nafie</i>)	17	113
Stereochemical Nomenclature and Notation in Inorganic Chemistry (<i>Sloan</i>)	12	1
Stereochemistry, Classical, The Foundations of (<i>Mason</i>)	9	1
Stereochemistry, Dynamic, A Mathematical Theory of (<i>Ugi and Ruch</i>)	4	99
Stereochemistry of Biological Reactions at Propochiral Centers (<i>Floss, Tsai, and Woodard</i>)	15	253
Stereochemistry of Chelate Complexes (<i>Saito</i>)	10	95
Stereochemistry of Cyclobutane and Heterocyclic Analogs (<i>Moriarty</i>)	8	271
Stereochemistry of Germanium and Tin Compounds (<i>Gielen</i>)	12	217
Stereochemistry of Linear Macromolecules (<i>Farina</i>)	17	1
Stereochemistry of Nitroxides (<i>Janzen</i>)	6	177
Stereochemistry of Organic Molecules, and Mass Spectrometry (<i>Green</i>)	9	35
Stereochemistry of Push-Pull and Strained Ethylenes, Static and Dynamic (<i>Sandström</i>)	14	83
Stereochemistry of Reactions of Transition Metal-Carbon Sigma Bonds (<i>Flood</i>)	12	37
Stereochemistry at Silicon (<i>Corriu, Guérin, and Moreau</i>)	15	43
Stereochemistry of Transition Metal Carbonyl Clusters (<i>Johnson and Benfield</i>)	12	253
Stereoisomeric Relationships, of Groups in Molecules (<i>Mislow and Raban</i>)	1	1
Stereoisomerism, On Factoring Chirality and (<i>Hirschmann and Hanson</i>)	14	183
Stereoselective Aldol Condensations (<i>Evans, Nelson and Taber</i>)	13	1
Steroids, Crystal Structures of (<i>Duax, Weeks and Rohrer</i>)	9	271
Structures, Crystal, of Steroids (<i>Duax, Weeks and Rohrer</i>)	9	271
Torsion Angle Concept in Conformational Analysis (<i>Bucourt</i>)	8	159
Ultrasonic Absorption and Vibrational Spectroscopy, Use of, to Determine the Energies Associated with Conformational Changes (<i>Wyn-Jones and Pethrick</i>)	5	205
Vibrational Spectroscopy and Ultrasonic Absorption, Use of, to Determine the Energies Associated with Conformational Changes (<i>Wyn-Jones and Pethrick</i>)	5	205
Vinylc Radicals, and Cyclohexyl, The Stereochemistry of (<i>Simamura</i>)	4	1
Wittig Reaction, Stereochemistry of (<i>Schlosser</i>)	5	1

